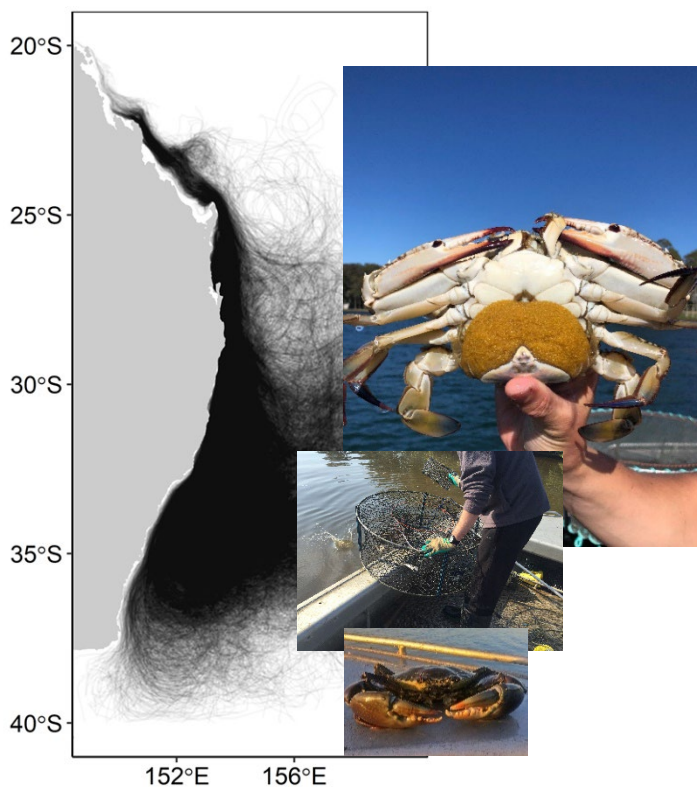


# Informing adaptive management of portunid fisheries in NSW



**Matthew D. Taylor**

**Daniel Hewitt**

**Roshan Hanemseth**

**Hayden Schilling**

**Samuel Nolan**

**Iain M. Suthers**

**Daniel D. Johnson**

**July 2023**

FRDC Project No **2017/006**

© 2023 Fisheries Research and Development Corporation.  
All rights reserved.

ISBN 978-1-76058-704-8

**Informing adaptive management of portunid fisheries in NSW  
2017/006**

2023

### **Ownership of Intellectual property rights**

Unless otherwise noted, copyright (and any other intellectual property rights, if any) in this publication is owned by the Fisheries Research and Development Corporation and NSW Department of Primary Industries

This publication (and any information sourced from it) should be attributed to **Taylor M.D., Hewitt D., Hanemseth R., Schilling H., Nolan S., Suthers I.M., Johnson D.D. (2023) Informing adaptive management of portunid fisheries in NSW. Final Report to the Fisheries Research and Development Corporation on project 2017/006, NSW Department of Primary Industries, Port Stephens. CC BY 3.0**

### **Creative Commons licence**

All material in this publication is licensed under a Creative Commons Attribution 3.0 Australia Licence, save for content supplied by third parties, logos and the Commonwealth Coat of Arms.



Creative Commons Attribution 3.0 Australia Licence is a standard form licence agreement that allows you to copy, distribute, transmit and adapt this publication provided you attribute the work. A summary of the licence terms is available from <https://creativecommons.org/licenses/by/3.0/au/>. The full licence terms are available from <https://creativecommons.org/licenses/by-sa/3.0/au/legalcode>.

Inquiries regarding the licence and any use of this document should be sent to: [frdc@frdc.com.au](mailto:frdc@frdc.com.au)

### **Disclaimer**

The authors do not warrant that the information in this document is free from errors or omissions. The authors do not accept any form of liability, be it contractual, tortious, or otherwise, for the contents of this document or for any consequences arising from its use or any reliance placed upon it. The information, opinions and advice contained in this document may not relate, or be relevant, to a readers particular circumstances. Opinions expressed by the authors are the individual opinions expressed by those persons and are not necessarily those of the publisher, research provider or the FRDC.

The Fisheries Research and Development Corporation plans, invests in and manages fisheries research and development throughout Australia. It is a statutory authority within the portfolio of the federal Minister for Agriculture, Fisheries and Forestry, jointly funded by the Australian Government and the fishing industry.

#### **Researcher Contact Details**

Name: Matthew D. Taylor  
Address: Port Stephens Fisheries Institute  
Taylors Beach Rd, Taylors Beach,  
NSW, 2316  
Phone: 02 4916 3937  
Email: [matt.taylor@dpi.nsw.gov.au](mailto:matt.taylor@dpi.nsw.gov.au)

#### **FRDC Contact Details**

Address: 25 Geils Court  
Deakin ACT 2600  
Phone: 02 6122 2100  
Email: [frdc@frdc.com.au](mailto:frdc@frdc.com.au)  
Web: [www.frdc.com.au](http://www.frdc.com.au)

In submitting this report, the researcher has agreed to FRDC publishing this material in its edited form.

# Contents

|   |              |
|---|--------------|
| <b>Contents</b> .....   | <b>iii</b>   |
| Tables .....  | viii         |
| Figures .....   | x            |
| <b>Acknowledgments</b> .....  | <b>xvii</b>  |
| <b>Executive Summary</b> .....  | <b>xviii</b> |
| Background and aims.....  | xviii        |
| Approach.....   | xix          |
| Key findings.....   | xix          |
| <b>Blue Swimmer Crab</b> .....  | <b>xix</b>   |
| <b>Giant Mud Crab</b> .....   | <b>xx</b>    |
| Implications.....   | xxi          |
| <b>Blue Swimmer Crab</b> .....  | <b>xxi</b>   |
| <b>Giant Mud Crab</b> .....   | <b>xxi</b>   |
| <b>Introduction</b> .....   | <b>22</b>    |
| Environmental influences on the population ecology of exploited portunid species .....                  | 22           |
| Estuarine and inshore crab fisheries within New South Wales .....                                       | 23           |
| Biology of Blue Swimmer Crab.....   | 26           |
| Influence of environmental variability on Blue Swimmer Crab .....                                       | 26           |
| Biology of Giant Mud Crab.....  | 28           |
| Influence of environmental variability on Giant Mud Crab .....  | 28           |
| <b>Objectives</b> .....   | <b>30</b>    |
| <b>Structure of this report</b> .....   | <b>31</b>    |
| <b>Design and evaluation of a novel research trap for surveying Blue Swimmer Crab populations</b> ..... | <b>32</b>    |
| Background and rationale .....  | 32           |
| Methods .....   | 33           |
| <b>Description of sampling gear</b> .....   | <b>33</b>    |
| <b>Sampling design and collection</b> .....   | <b>33</b>    |
| <b>Statistical analyses</b> .....   | <b>34</b>    |
| Results and Discussion .....  | 35           |
| <b>Total catch, size structure and selectivity among trap types and trawls</b> .....                    | <b>35</b>    |
| <b>Temporal comparison between trap types</b> .....   | <b>37</b>    |
| <b>Temporal variation in trap selectivity</b> .....   | <b>41</b>    |
| <b>Design considerations and potential biases</b> .....   | <b>42</b>    |
| <b>An automated image analysis system for estimating fecundity in portunid crabs</b> .....              | <b>44</b>    |
| Background and rationale.....   | 44           |
| Methods.....  | 44           |
| <b>Sample collection and processing</b> .....   | <b>44</b>    |
| <b>ZooSCAN approaches</b> .....   | <b>45</b>    |
| <b>Data analyses</b> .....  | <b>46</b>    |
| Results and Discussion .....  | 46           |

|  |            |
|--|------------|
| <b>Fishery independent survey of Blue Swimmer Crab – Description and data summary.....</b>         | <b>50</b>  |
| Background and study locations.....  | 50         |
| Survey design and approach.....  | 54         |
| <b>Supplementary sampling.....</b>   | <b>54</b>  |
| <b>Laboratory processing.....</b>  | <b>55</b>  |
| <b>Water quality monitoring.....</b>   | <b>56</b>  |
| Summary of broad trends in water quality, abundance, and size structure.....                       | 56         |
| <b>Water quality and flow throughout study period.....</b>   | <b>56</b>  |
| <b>Broad patterns in abundance and size structure.....</b>   | <b>61</b>  |
| <b>Latitudinal trends in the reproductive biology of female Blue Swimmer Crab in south-eastern</b> |            |
| <b>Australia.....</b>  | <b>67</b>  |
| Background and rationale.....  | 67         |
| Methods.....   | 68         |
| <b>Sampling and analysis.....</b>  | <b>68</b>  |
| Results.....   | 69         |
| <b>Patterns in reproductive development.....</b>   | <b>69</b>  |
| <b>Water temperature as a driver of variability in reproduction.....</b>                           | <b>70</b>  |
| Discussion.....  | 73         |
| <b>Relationship between GSI and HSI.....</b>   | <b>73</b>  |
| <b>Relationship between crab size and egg mass weight.....</b>                                     | <b>73</b>  |
| <b>Water temperature as a driver of variability in reproduction.....</b>                           | <b>74</b>  |
| <b>Potential impacts of tropicalisation.....</b>   | <b>75</b>  |
| <b>Study limitations and concluding remarks.....</b>   | <b>75</b>  |
| <b>Estuary-specific drivers of Blue Swimmer Crab abundance and distribution.....</b>               | <b>77</b>  |
| Background and rationale.....  | 77         |
| Methods.....   | 77         |
| <b>Sampling and analysis.....</b>  | <b>77</b>  |
| Results.....   | 79         |
| <b>Influence of environmental variables on abundance.....</b>                                      | <b>79</b>  |
| <b>Influence of environmental variables on location and distribution.....</b>                      | <b>82</b>  |
| Discussion.....  | 88         |
| <b>Influence of temperature on crab abundance and distribution.....</b>                            | <b>88</b>  |
| <b>Influence of conductivity and flow on crab abundance and distribution.....</b>                  | <b>89</b>  |
| <b>Reproductive cycles of Blue Swimmer Crab in relation to variation in temperature and</b>        |            |
| <b>conductivity.....</b>   | <b>91</b>  |
| Background and rationale.....  | 91         |
| Methods.....   | 91         |
| <b>Sampling and analysis.....</b>  | <b>91</b>  |
| Results.....   | 92         |
| <b>Size at maturity.....</b>   | <b>92</b>  |
| <b>Size at functional maturity and catches of ovigerous crabs.....</b>                             | <b>95</b>  |
| <b>Gonad and ovarian development.....</b>  | <b>99</b>  |
| Discussion.....  | 100        |
| <b>Spatial and temporal patterns.....</b>  | <b>100</b> |
| <b>Concluding comments.....</b>  | <b>101</b> |

|   |            |
|---|------------|
| <b>Long-term drivers of catch variability in Wallis Lake .....</b>                                | <b>103</b> |
| Background and rationale .....  | 103        |
| Data sources, approach and modelling .....  | 104        |
| <b>Hypotheses .....</b>   | <b>104</b> |
| <b>Data sources.....</b>  | <b>105</b> |
| <b>Predictability of fisheries productivity .....</b>   | <b>107</b> |
| Results.....  | 107        |
| <b>General observations on Wallis Lake fishery .....</b>  | <b>107</b> |
| <b>Freshwater flow .....</b>  | <b>108</b> |
| <b>Winter harvest .....</b>   | <b>109</b> |
| <b>Coastal temperature and wind .....</b>   | <b>111</b> |
| <b>Climatic indices .....</b>   | <b>114</b> |
| <b>Predictability.....</b>  | <b>114</b> |
| Discussion.....   | 117        |
| <b>Environmental and climatic influences .....</b>  | <b>117</b> |
| <b>Effects of winter fishing mortality.....</b>   | <b>119</b> |
| <b>Management implications and conclusion .....</b>   | <b>119</b> |
| <b>Oceanic connectivity and particle dispersal for Blue Swimmer Crab and Giant Mud Crab .....</b> | <b>120</b> |
| Background and rationale .....  | 120        |
| Data sources, approach and modelling .....  | 121        |
| <b>Oceanographic model and regional context.....</b>  | <b>121</b> |
| <b>Particle tracking .....</b>  | <b>122</b> |
| <b>Summary of model outputs .....</b>   | <b>124</b> |
| Results.....  | 124        |
| Discussion.....   | 133        |
| <b>Patterns in larval dispersal and connectivity .....</b>  | <b>133</b> |
| <b>Implications for management.....</b>   | <b>134</b> |
| <b>Model limitations and future research .....</b>  | <b>135</b> |
| <b>Environmental influence on spawning migrations in Giant Mud Crab .....</b>                     | <b>137</b> |
| Background and rationale .....  | 137        |
| Methods.....  | 138        |
| <b>Study systems .....</b>  | <b>138</b> |
| <b>Crab capture and tagging.....</b>  | <b>138</b> |
| <b>Tag programming and array design.....</b>  | <b>139</b> |
| <b>Data collection and storage .....</b>  | <b>140</b> |
| <b>Data analysis .....</b>  | <b>140</b> |
| Results.....  | 142        |
| Discussion.....   | 146        |
| <b>Environmental triggers of the female spawning migration.....</b>                               | <b>147</b> |
| <b>Potential influence of migration on future recruitment and fisheries catch .....</b>           | <b>148</b> |
| <b>Technical considerations and caveats .....</b>   | <b>148</b> |
| <b>Conclusions and future work .....</b>  | <b>149</b> |
| <b>Movement, habitat use, and behaviour of free-ranging Giant Mud Crab .....</b>                  | <b>150</b> |
| Background and rationale .....  | 150        |
| Methods .....   | 151        |

|   |            |
|---|------------|
| <b>Study site and array design</b> .....  | <b>151</b> |
| <b>Crab capture and tagging</b> .....   | <b>152</b> |
| <b>Tag programming</b> .....  | <b>152</b> |
| <b>Hyperbolic positioning</b> .....   | <b>153</b> |
| <b>Data processing</b> .....  | <b>153</b> |
| <b>Behavioural state classification</b> .....                                       | <b>154</b> |
| <b>Behavioural state dynamics</b> .....   | <b>155</b> |
| Results .....   | 156        |
| <b>Model selection and diagnostics</b> .....  | <b>156</b> |
| <b>Crab behavioural states</b> .....  | <b>157</b> |
| <b>Behavioural state dynamics</b> .....   | <b>159</b> |
| Discussion.....   | 161        |
| <b>Fine-scale movement and behaviour of Giant Mud Crab</b> .....                    | <b>161</b> |
| <b>Implications for fisheries management</b> .....                                  | <b>162</b> |
| <b>Technical considerations and caveats</b> .....                                   | <b>163</b> |
| <b>Conclusions</b> .....  | <b>164</b> |
| <b>Environmental drivers of variation in Giant Mud Crab harvest rates</b> .....     | <b>165</b> |
| Background and rationale.....   | 165        |
| Methods .....   | 166        |
| <b>Fishery observer program</b> .....   | <b>166</b> |
| <b>Environmental data</b> .....   | <b>166</b> |
| <b>Data processing and analysis</b> .....   | <b>169</b> |
| Results.....  | 169        |
| Discussion.....   | 170        |
| <b>Drivers of variation in Giant Mud Crab catch</b> .....                           | <b>170</b> |
| <b>Implications for management and assessment</b> .....                             | <b>180</b> |
| <b>Technical considerations and caveats</b> .....                                   | <b>180</b> |
| <b>Conclusions</b> .....  | <b>181</b> |
| <b>Testing broad-scale environment-catch relationships for Giant Mud Crab</b> ..... | <b>182</b> |
| Background and rationale.....   | 182        |
| Data sources, approach and modelling .....  | 182        |
| <b>Larval supply</b> .....  | <b>182</b> |
| <b>Larval settlement and recruitment</b> .....                                      | <b>183</b> |
| <b>Climate drivers</b> .....  | <b>183</b> |
| <b>Data sources</b> .....   | <b>184</b> |
| <b>Modeling approach</b> .....  | <b>186</b> |
| Results and discussion .....  | 187        |
| <b>Modelling outcomes</b> .....   | <b>187</b> |
| <b>Comparative importance of predictor variables</b> .....                          | <b>190</b> |
| <b>Conclusion and next steps</b> .....  | <b>192</b> |
| <b>General discussion and conclusions</b> .....                                     | <b>195</b> |
| Blue Swimmer Crab.....  | 195        |
| Giant Mud Crab.....   | 197        |
| <b>Implications</b> .....   | <b>201</b> |
| Blue Swimmer Crab.....  | 201        |
| Giant Mud Crab.....   | 202        |

**Recommendations and further development ..... 204**

**Extension and adoption ..... 205**

    Communication and coverage ..... 205

    Adoption ..... 207

**Blue Swimmer Crab ..... 207**

**Giant Mud Crab ..... 207**

**Project materials developed..... 208**

**References ..... 209**

## Tables

|  |     |
|--|-----|
| <b>Table 1</b> Summary of outcomes of the GLMMs comparing abundance of small (<60 mm CL) and large (>60 mm CL) crabs caught in small-mesh and large traps in each estuary during phase 2. Separate models were run for each estuary, crab size class combination. Significance levels are indicated as * < 0.05; ** < 0.01; *** < 0.001; “nd” no difference. NA denotes a model that did not converge properly .....   | 40  |
| <b>Table 2</b> Linear regression equations fit for the adjusted gonadosomatic index as a function of adjusted hepatosomatic index during ovarian development in mature females. * Indicates significant p-value ....   | 69  |
| <b>Table 3</b> Linear regression equations fit for the total weight of the egg mass (g) as a function of the total body weight (g) of the berried crabs by estuary. * Indicates significant p-value. ....  | 71  |
| <b>Table 4</b> Model selection table for Wallis Lake Blue Swimmer Crab abundance constructed with backwards stepwise selection. Linear and quadratic forms of temperature ( <i>Temp</i> <sup>2</sup> ) and conductivity ( <i>Cond</i> <sup>2</sup> ) were included to test for non-linearity. Models are presented in the order tested, and included random intercept effects for site (1 Site) and date (1 Date). ΔAIC shows the difference in AIC values from the best (lowest AIC) model. If two models were equivalent (<2 ΔAIC; shown in bold), the simpler model was retained in the selection process. The best model was M6 .....    | 80  |
| <b>Table 5</b> Model selection table for Port Stephens Blue Swimmer Crab abundance constructed with backwards stepwise selection. Linear and quadratic forms of temperature ( <i>Temp</i> <sup>2</sup> ) and conductivity ( <i>Cond</i> <sup>2</sup> ) were included to test for non-linearity. Models are presented in the order tested, and included random intercept effects for site (1 Site) and date (1 Date). ΔAIC shows the difference in AIC values from the best (lowest AIC) model. If two models were equivalent (<2 ΔAIC; shown in bold), the simpler model was retained in the selection process. The best model was M10 ..... | 81  |
| <b>Table 6</b> Model selection table for Wallis Lake Blue Swimmer Crab distance to sea ( <i>Distance</i> ) constructed with backwards stepwise selection where the least significant (highest P-value) term was removed in each step (‘:’ between two variables indicates an interaction term. Models are presented in the order tested, and included random intercept effects for each sample period (1 Period). ΔAIC shows the difference in AIC values from the best (lowest AIC) model. If two models were equivalent (<2 ΔAIC; shown in bold), the simpler model was retained in the selection process.....                             | 85  |
| <b>Table 7</b> Model selection table for Wallis Lake Blue Swimmer Crab interquartile spread ( <i>Spread</i> ) constructed with backwards stepwise selection where the least significant (highest P-value) term was removed in each step (‘:’ between two variables indicates an interaction term. Models are presented in the order tested, and included random intercept effects for each sample period (1 Period). ΔAIC shows the difference in AIC values from the best (lowest AIC) model. If two models were equivalent (<2 ΔAIC; shown in bold), the simpler model was retained in the selection process.....                          | 85  |
| <b>Table 8</b> Model selection table for Port Stephens Blue Swimmer Crab distance to sea ( <i>Distance</i> ) constructed with backwards stepwise selection where the least significant (highest P-value) term was removed in each step (‘:’ between two variables indicates an interaction term. Models are presented in the order tested, and included random intercept effects for each sample period (1 Period). ΔAIC shows the difference in AIC values from the best (lowest AIC) model. If two models were equivalent (<2 ΔAIC; shown in bold), the simpler model was retained in the selection process.....                           | 86  |
| <b>Table 9</b> Model selection table for Port Stephens Blue Swimmer Crab interquartile spread ( <i>Spread</i> ) constructed with backwards stepwise selection where the least significant (highest P-value) term was removed in each step (‘:’ between two variables indicates an interaction term. Models are presented in the order tested, and included random intercept effects for each sample period (1 Period). ΔAIC shows the difference in AIC values from the best (lowest AIC) model. If two models were equivalent (<2 ΔAIC; shown in bold), the simpler model was retained in the selection process.....                        | 87  |
| <b>Table 10</b> Results of the linear model predicting summer CPUE. ....   | 116 |
| <b>Table 11</b> Estuaries and embayments included in the study that support notable commercial and recreational harvest of Blue Swimmer Crab and Giant Mud Crab along eastern Australia.....   | 123 |
| <b>Table 12</b> Mean (± SD) northern/southern percentage particle contribution (%) to estuaries along eastern Australia.....   | 125 |
| <b>Table 13</b> Mean (± SD) percentage particle contribution (%) to estuaries along eastern Australia from each of the East Australian Current (EAC) regions. ....   | 131 |

|  |     |
|--|-----|
| <b>Table 14</b> Mean ( $\pm$ SD) percentage particle contribution (%) to estuaries along eastern Australia from Queensland (Queensland) or New South Wales (NSW).....  | 132 |
| <b>Table 15</b> Tagging and detection information for female Giant Mud Crab in Clarence River and Kalang River.....  | 139 |
| <b>Table 16</b> Oceanic detection information for female Giant Mud Crab obtained from IMOS ATF and NSW DPI Shark management strategy acoustic array. ....  | 145 |
| <b>Table 17</b> Biological and detection information for tagged Giant Mud Crab.....  | 154 |
| <b>Table 18</b> State-dependent parameter estimates for tagged Giant Mud Crab.....   | 158 |
| <b>Table 19</b> State transition probabilities of tagged Giant Mud Crab. Diagonal entries indicate the probability of staying in the same state (i.e., state-dwell probabilities).....   | 160 |
| <b>Table 20</b> Characteristics of study estuaries adapted from Roy <i>et al.</i> (2001), with areal coverage of mangrove, seagrass and saltmarsh for each study estuary also included (as reported in Creese <i>et al.</i> 2009).....                   | 167 |
| <b>Table 21</b> Number of observer trips ( $n$ ), traps deployed ( $n$ ) and total soak time (d; from left to right) in each estuary per month throughout the observer program (2018–2020). ....   | 168 |
| <b>Table 22</b> Summary of estuary-specific model smoothers for abundance (crabs trap <sup>-1</sup> ) and biomass (kg trap <sup>-1</sup> ) of Giant Mud Crab in southeast Australian estuaries. Bold values indicate statistical significance. ....      | 173 |
| <b>Table 23</b> Catch (kg d <sup>-1</sup> ) thresholds for estuaries included in modelling, reflecting the 75 <sup>th</sup> percentile of daily catches in each estuary. Records that reported values greater than this were not used in modelling. .... | 184 |
| <b>Table 24</b> Prediction error and correlation between observed and predicted daily catch (kg) from the test data set. ....  | 190 |
| <b>Table 25</b> Communication and coverage of project activities for the period from project commencement until the completion of the Final Report. ....   | 205 |

# Figures

**Figure 1** Map showing main estuaries for capture of Blue Swimmer Crab and Giant Mud Crab within New South Wales, with the main study estuaries indicated in black, and other estuaries that generally support good crab harvests (mentioned in the text) indicated in grey. The inset shows the location of the main map on the eastern Australian seaboard. .... 24

**Figure 2** New South Wales catch history for Blue Swimmer Crab and Giant Mud Crab since the 1998 fiscal year (upper panel), and the relative proportion of catch from each of the main estuaries for the 10 years prior to the 2021 fiscal year, for Blue Swimmer Crab (lower left panel) and Giant Mud Crab (lower right panel). Estuary names are shown in Figure 1. .... 25

**Figure 3** Conceptual model outlining the inter-relationships between different processes that were investigated in this project. .... 30

**Figure 4** Large-mesh collapsible trap common in New South Wales, Australia (left), with two entry funnels and a novel small-mesh collapsible trap with four entry funnels (right). .... 33

**Figure 5** Predicted crab abundance for the three gear types tested in Lake Macquarie and Port Stephens based upon generalised linear modelling. Predictions were made on the fixed effects only and the error bars therefore show 95% confidence intervals. Bars which do not share a common letter are statistically different (adjusted  $P < 0.05$ ). .... 36

**Figure 6** Comparison of kernel density estimate (KDE) probability density functions for all Blue Swimmer Crab captured in the phase 1, 3-way gear comparison. Note all estuaries and sexes were pooled due to low numbers of crabs in the beam trawl samples ( $n = 19$ ) compared to small-mesh ( $n = 141$ ) and large-mesh traps ( $n = 90$ ). .... 37

**Figure 7** Catch comparison rate (left column, a, c, e) and catch ratio rate (right column, b, d, f) for the different gear comparisons (black curve). a and b: Comparison of small-mesh traps and beam trawl. c and d: Comparison of large-mesh traps and beam trawl. e and f: Comparison of small-mesh traps and large-mesh traps. The circles represent the experimental rates with the circles scaled to the number of crabs observed in that length class. The grey ribbons represent the 95% confidence limits for the rate curves. The horizontal red dashed line shows the expected catch comparison rate in case of no difference in catch efficiency in the compared gears. In the right hand panels, dots outside the axis range (larger values) are partially visible on upper edges. .... 38

**Figure 8** Mean (+ standard error) Blue Swimmer Crab captured during each month across Port Stephens, Lake Macquarie and Wallis Lake in large-mesh and small-mesh traps. .... 39

**Figure 9** Catch comparison rate (left column, a, c) and catch ratio rate (right column, b, d) for the comparison between small and large-mesh traps (lines). a and b: Results from the estuary specific modelling with colours and line types represent the different estuaries. c and d: Results from global (pooled estuaries) model. The circles marks represent the experimental rates with the circles scaled to the number of crabs observed in that length class. The ribbons represent the 95% confidence limits for the rate curves. The horizontal red dashed line shows the expected catch comparison rate in case of no difference in catch efficiency in the compared gears. In the right hand panels, dots outside the axis range (larger values) are partially visible on upper edges .... 41

**Figure 10** Schematic of the ZooSCAN (left) processing methodology with the digitised image (middle) and enhanced image (right), processed using a custom macro in ImageJ (total number of eggs is 120). Counted eggs are highlighted in blue and debris that is automatically excluded from counts is highlighted in yellow within the red circle. .... 45

**Figure 11** Linear regression between egg counts derived from the manual microscope approach and the manual ZooSCAN approach (left panel), and automated ZooSCAN approach (right panel). The dashed blue line represents the 1:1 line and the red line represents the linear models described in the text ( $n = 10$ ). .... 47

**Figure 12** Processing times for the different egg counting methods examined, including manual microscope approach (red line), manual ZooSCAN approach (green line) and the automated ZooSCAN approach (blue line). .... 48

**Figure 13** Fitted model relating sampling effort of Blue Swimmer Crab egg masses with the probability that the estimated mean lies within the error threshold (i.e., the true mean estimated from the data,

±15%). The solid black curve indicates the fitted model, and the black dashed line indicates a curve segment that is extrapolated past the range of data simulated (confidence intervals are indicated as dotted red lines. Data points from simulations for each month are as indicated in figure legend (note that some data points overlap). Also indicated is the corresponding number of samples required to achieve an 80% (orange dashed line) and 90% (green dashed line) probability that egg count mean estimates lie within 15% of the actual mean..... 48

**Figure 14** Detail map of Wallis Lake showing sites targeted during the regular independent survey program (denoted as BSC.*n*), the inshore sub-program (teal polygon), and logger stations (denoted as LOG.*n*) where water quality was continually monitored during the program. Also indicated are emergent aquatic habitat types within the estuary (see legend) and marine park no-take zones (pink polygons). .. 51

**Figure 15** Detail map of Port Stephens showing sites targeted during the independent survey program (denoted as BSC.*n*, red circles for regular independent survey, green circles for Port Stephens sub-program), and logger stations (denoted as LOG.*n*) where water quality was continually monitored during the program. Also indicated are emergent aquatic habitat types within the estuary (see legend) and marine park no-take zones (pink polygons). ..... 52

**Figure 16** Detail map of Lake Macquarie showing sites targeted during the independent survey program (denoted as BSC.*n*), and logger stations (denoted as LOG.*n*) where water quality was continually monitored during the program. Also indicated are emergent aquatic habitat types within the estuary (see legend)..... 53

**Figure 17** Detail map of Botany Bay (left panel) and Lake Illawarra (right panel) showing additional sites targeted during the latitudinal sub-program (denoted as BSC.*n*). Also indicated are emergent aquatic habitat types within the estuary (see legend)..... 55

**Figure 18** Trace plot of water quality (conductivity, solid line; temperature, dotted line) and flow data over the study period summarised from loggers deployed within Wallis Lake including Wallis Is. (LOG.2), Green Pt. (LOG.5), Wallamba R. (LOG.1), lower Coolongolook R. (LOG.3), and the Wang Wauk flow gauge on the Coolongolook R. Also presented is data for the upper Coolongolook R. (originally LOG.4), which was discontinued in June 2019. Gaps in the trace indicate logger loss, theft or failure..... 58

**Figure 19** Trace plot of water quality (conductivity, solid line; temperature, dotted line) and flow data over the study period summarised from loggers deployed within Port Stephens including Pindimar (LOG.2), Lemon Tree Passage (LOG.3), Tilligerry Ck. (LOG.4), Myall R. (LOG.1), lower Karuah R. (LOG.5), and the Booral flow gauge on the Karuah R. Gaps in the trace indicate logger loss, theft or failure..... 59

**Figure 20** Trace plot of water quality (conductivity, solid line; temperature, dotted line) and flow data over the study period summarised from loggers deployed within Lake Macquarie including Warners Bay (LOG.1), Wangi Pt. (LOG.2), Bonnells Bay (LOG.3), Chain Valley Bay (LOG.4), and the Cooranbong flow gauge on Dora Ck. Gaps in the trace indicate logger loss, theft or failure..... 60

**Figure 21** Composite plot summarising all sampling data for the regular independent survey, presented as mean ± standard error (SE), grouped by estuary, site and month. Also overlaid is a conductivity and temperature trace for the reference station within each estuary (colour coded to the secondary y-axis). ..... 63

**Figure 22** Monthly sex-specific size structures for samples collected in Wallis Lake, expressed as kernel density estimates (including inshore samples [Insh.], not split by sex). Panel headers indicate sampling period (YYYYMM). Sample sizes are indicated in brackets, and the P-value from a K-S test of differences between male and female size structure is indicated in the legend panel. The green and blue vertical dashed lines indicate female size at maturity, and the MLS respectively. .... 64

**Figure 23** Monthly sex-specific size structures for samples collected in Port Stephens, expressed as kernel density estimates (including sanctuary zone samples [SZ], not split by sex). Panel headers indicate sampling period (YYYYMM). Sample sizes are indicated in brackets, and the P-value from a K-S test of differences between male and female size structure is indicated in the legend panel. The green and blue vertical dashed lines indicate female size at maturity, and the MLS respectively..... 65

**Figure 24** Monthly sex-specific size structures for samples collected in Lake Macquarie, expressed as kernel density estimates. Panel headers indicate sampling period (YYYYMM). Sample sizes are indicated in brackets, and the P-value from a K-S test of differences between male and female size structure is

indicated in the legend panel. The green and blue vertical dashed lines indicate female size at maturity, and the MLS respectively. .... 66

**Figure 25** Linear models illustrating the relationship between the adjusted gonadosomatic index and adjusted hepatosomatic index during ovarian development in mature females (pooled across estuaries) for A) Stage 1 ovaries (n = 48), B) Stage 2-3 ovaries (n = 62) and C) Stage 4-5 ovaries (n = 148). The solid black line represents the linear model, and the grey area represents the confidence interval (95%)..... 69

**Figure 26** Non-linear models illustrating the relationship between the total weight of the egg mass (g) and the total body weight (g) of berried crabs in Wallis Lake (WLL, n = 25), Port Stephens (PST, n = 18), Lake Macquarie (LMQ, n = 38), Botany Bay (BGR, n = 8) and Lake Illawarra (LIL, n = 24). The solid black line represents the non-linear model fit for each estuary and the grey area represents the confidence interval (95%). The dashed black line depicts a model fit for combined estuaries. .... 70

**Figure 27** Bar charts showing egg mass index (EMI) in Wallis Lake (WLL), Port Stephens (PST), Lake Macquarie (LMQ), Botany Bay (BGR) and Lake Illawarra (LIL) for each month with the sampling period (October 2019 – February 2020). The top of grey box indicates the mean, and the error bars indicate the standard error. .... 71

**Figure 28** Mean monthly water temperatures in Wallis Lake, Port Stephens Estuary, Lake Macquarie, Botany Bay and Lake Illawarra between October 2019 and February 2020. The water temperature in these estuaries peaked in the January and February sampling periods, with mean monthly temperatures in Wallis Lake = 27.3°C, Port Stephens = 26.6°C, Lake Macquarie = 27.2°C, Botany Bay = 24.6°C and Lake Illawarra = 24.8°C. The data was gathered using HOBO U24-002-C data loggers deployed at a depth of 1 m throughout the sampling period. Water temperatures in Lake Macquarie are influenced by the release of hot water by the Mannering Park Power Station and Eraring power station, two coal fired power stations situated on the shores of the estuary (Taylor *et al.* 2017e). .... 72

**Figure 29** Thermal performance curves from generalised additive models fit for the A) Gonadosomatic index, B) Hepatosomatic index and C) Total egg mass on mean monthly temperature in each estuary for the month prior to capture. The solid line depicts the fit of the model to the data and the dashed lines represent the confidence interval (95%). The ticks on the x-axis indicate the mean monthly temperatures of each sampling effort. .... 72

**Figure 30** Modelled relative Blue Swimmer Crab abundance (grey shading is standard error of prediction) in relation to temperature (a, b) and conductivity (c, d), for Wallis Lake (left panels) and Port Stephens (right panels). .... 80

**Figure 31** Monthly sex-specific spatial data for Blue Swimmer Crab samples collected in Wallis Lake, expressed as kernel density estimates. Panel headers indicate sampling period (YYYYMM). The vertical solid lines indicate the median distance-to-sea for female (black) and male (grey) crabs, and the vertical dashed lines indicate the lower and upper bounds for the interquartile range for each sex. .... 83

**Figure 32** Monthly sex-specific spatial data for Blue Swimmer Crab samples collected in Port Stephens, expressed as kernel density estimates. Panel headers indicate sampling period (YYYYMM). The vertical solid lines indicate the median distance-to-sea for female (black) and male (grey) crabs, and the vertical dashed lines indicate the lower and upper bounds for the interquartile range for each sex. .... 84

**Figure 33** Modelled Blue Swimmer Crab median distance to sea in Wallis Lake (grey shading and error bars indicate standard error of prediction) in relation to temperature (a), conductivity (b) and sex (c)... 87

**Figure 34** Modelled Blue Swimmer Crab interquartile range in Port Stephens (error bars show the standard error of the predictions) in relation to sex..... 88

**Figure 35** Comparison of fitted maturity ogives for Blue Swimmer Crab captured from Wallis Lake in 2018 using Frequentist and Bayesian approaches. The top left and right panels present histograms of A, B parameters, the lower left panel is the size at maturity and the lower right is the maturity ogive for size at 50% maturity. Actual data is indicated with light grey dots, dashed blue lines represent 95 % CI, and the intersection of the red lines is the size at which 50% of individuals are mature. .... 93

**Figure 36** Spatial and temporal breakdown of size-at-maturity for Blue Swimmer Crab for Wallis Lake and Port Stephens for 2018, 2019 and 2020 fishing seasons, modelled using the Frequentist approach. Actual data is indicated with light grey dots, dashed blue lines represent 95 % CI, and the intersection of the red lines is the size at which 50% of individuals are mature. .... 94

|   |     |
|---|-----|
| <b>Figure 37</b> Seasonally calculated $L_{50}$ ( $\pm$ 95% C.I.) for Blue Swimmer Crab in Wallis Lake plotted alongside seasonally averaged water temperature and conductivity (at the reference station) for the duration of the regular independent survey. ....   | 95  |
| <b>Figure 38</b> Proportion of mature female Blue Swimmer Crab recorded as ovigerous from Wallis Lake, Port Stephens, and Lake Macquarie. ....  | 96  |
| <b>Figure 39</b> The monthly proportion of mature and berried Blue Swimmer Crab per estuary across three seasons in Wallis Lake, Port Stephens, and Lake Macquarie. Also shown is the total number of mature Blue Swimmer Crab caught during each month (black dot). ....   | 96  |
| <b>Figure 40</b> Proportion of berried Blue Swimmer Crab caught across 5 (November 2018 to August 2019) or 7 sites (September 2019 to March 2021) in Wallis Lake, Port Stephens, and Lake Macquarie and the total number of ovigerous Blue Swimmer Crab caught during each month (black dot). ....  | 97  |
| <b>Figure 41</b> Size-structure of berried (ovigerous) Blue Swimmer Crab, and all female crabs, from Wallis Lake, Port Stephens and Lake Macquarie (data pooled across years). ....   | 98  |
| <b>Figure 42</b> Size-structure of recorded catches of berried Blue Swimmer Crab during the Wallis Lake regular independent survey and Wallis Lake observer survey for 2018 (November) – 2019 (October) and 2019 (November) – 2020 (March). ....  | 99  |
| <b>Figure 43</b> Categorical representation of ovary stages (expressed as the proportion of examined ovaries) for Blue Swimmer Crab across three estuaries. Also indicated is the total number of crabs that were processed for biological samples (excluding berried females) during each month (black dot). ....  | 100 |
| <b>Figure 44</b> Time series showing the commercial catch (in black) and catch per unit effort (dashed red; CPUE; kg scaled-fisher-day <sup>-1</sup> ) in Wallis Lake from July 1997 – February 2022. The top panel shows monthly catch and CPUE while the bottom panel shows the combined summer (January – April) catch and CPUE. Note the lower plot is truncated to only include 1998 – 2021 which included full summer periods. .... | 108 |
| <b>Figure 45</b> Relationship between the independent survey catch per unit effort (CPUE; crabs trap <sup>-1</sup> ) in Wallis Lake and the adjacent inshore area. The solid blue line shows the linear regression and the grey ribbon shows the 95% confidence interval. ....  | 109 |
| <b>Figure 46</b> Relationship between the change in summer (January – April) commercial CPUE (kg scaled fisher-day <sup>-1</sup> ; relative to previous summer) and the total catch taken the previous winter (June – November). The solid blue line shows the linear relationship with the grey ribbon showing the 95% confidence interval. ....   | 110 |
| <b>Figure 47</b> Proportion of the catch (by weight) which is made up of female Blue Swimmer Crab in the Wallis Lake fishery each month. The mean was calculated using data from July 2009 – June 2020. Error bars show 1 standard deviation around the mean. ....  | 111 |
| <b>Figure 48</b> Time series showing the interannual variations in Blue Swimmer Crab catch by month for each sex (July 2009 – June 2020). For example, the January panel shows the catch of male and female crabs in January each year. The dotted vertical black line shows when the minimum size limit increased from 60 to 65 mm CL. ....  | 112 |
| <b>Figure 49</b> Size structure of the Blue Swimmer Crab harvest each month, pooled across all years. The solid red line shows the female size structure while the dotted blue line shows the male size structure. Length represents carapace length. ....  | 113 |
| <b>Figure 50</b> Relationship between the summer (January – April) commercial CPUE and the mean Pacific Decadal Oscillation Index (PDO; November - January). The solid blue line shows the linear relationship with the grey ribbon showing the 95% confidence interval. ....   | 114 |
| <b>Figure 51</b> Simulated residuals for the linear model used to predict summer CPUE. The left panel shows no significant deviations from normality. The right panel shows no deviations in residuals distributions. ...   | 115 |
| <b>Figure 52</b> Hindcast predictions of summer (January – April) CPUE (kg scaled Fisher Day <sup>-1</sup> ) for Blue Swimmer Crab in Wallis Lake. The red line shows observed CPUE while the black line shows the predicted CPUE. The grey ribbon shows the 95% prediction interval using the linear model. Note we have predicted CPUE for 2022 but the observations are not yet available to compare. ....                             | 116 |
| <b>Figure 53</b> Visual representation of classification of above- and below-average seasons based upon the quadratic discrimination analysis using winter catch and the previous summer CPUE (kg scaled fisher day <sup>-1</sup> ). Panel A shows the outcomes of the discrimination analysis. Letters represent the predicted outcome   |     |

for the season (A = above average, B = below average) and colour represents whether the prediction was correct (black = correct, red = incorrect). The grey line shows the prediction boundary based upon the two variables. Panel B shows the performance of the predictions over time relative to the observed financial year catch. The dashed line represents the mean total catch..... 117

**Figure 54** Map of eastern Australia showing the release locations and range of east coast populations of a) Giant Mud Crab (dark green), b) Blue Swimmer Crab (blue) and c) an example of the structure of the EAC, including sea surface temperature (SST, °C) and the approximate locations of key oceanographic features, including: the EAC jet (~24–28°S); the EAC separation (28–31°S); and, mesoscale eddy field (south of 31°S; dashed box). Features are marked at their centre latitude. The dotted line represents the reduced boundaries of ozROMS that provided the velocity fields used in the simulations (Wijeratne *et al.* 2018) and the solid black line shows the 200 m isobath. .... 121

**Figure 55** Percentage contribution (%) of Blue Swimmer Crab particles to settlement at estuaries (indicated by the dotted line) from putative spawning latitudes (in 0.5° latitude bands) along eastern Australia. Note percentages are calculated for each estuary separately and cover the entire simulation period (2008–2017). The dashed line indicates the Queensland/NSW border (~28.2°S), and the area shaded red indicates the approximate location of the EAC separation (28–31°S) as simulated in ozROMS. .... 126

**Figure 56** Percentage contribution (%) of Giant Mud Crab particles to settlement at estuaries (indicated by the dotted line) from putative spawning latitudes (in 0.5° latitude bands) along eastern Australia. Note percentages are calculated for each estuary separately and cover the entire simulation period (2008–2017). The dashed line indicates the Queensland/NSW border (~28.2°S), and the area shaded red indicates the approximate location of the EAC separation (28–31°S) as simulated in ozROMS. .... 127

**Figure 57** Percentage contribution (%) of Blue Swimmer Crab particles to settlement at estuaries (indicated by rugs along y-axis) within the EAC jet (north of 28°S) or eddy-field (south of 31°S) from putative spawning latitudes (in 0.5° latitude bins) along eastern Australia. Note percentages are calculated for each region separately over the entire simulation period (2008–2017). .... 128

**Figure 58** Geographic distribution of Blue Swimmer Crab particles (km<sup>-2</sup>) tracked backwards-in-time from estuaries within the EAC jet (north of 28°S) or eddy-field (south of 31°S) when they reached their degree-days threshold (382.5 ± 50). The dashed red lines represent the approximate EAC separation (~28–31°S; as simulated in ozROMS) and the dashed black lines represent the reduced model domain used in our simulations. The solid black line represents the 200 m isobath, all particles offshore of this at the end of tracking are excluded from our analysis. Note counts are derived from the entire simulation period (2008–2017) and the log<sub>10</sub>-transformed colour scale. .... 129

**Figure 59** Percentage contribution (%) of Giant Mud Crab particles to settlement at estuaries (indicated by rugs along y-axis) within the EAC jet (north of 28°S), the EAC separation (~28–31°S) or the eddy-field (south of 31°S) from putative spawning latitudes (in 0.5° latitude bins) along eastern Australia. Note percentages are calculated for each region separately over the entire simulation period (2008–2017). 130

**Figure 60** Geographic distribution of Giant Mud Crab particles (km<sup>-2</sup>) tracked backwards-in-time from estuaries north of the EAC separation (north of 28°S), within the EAC separation (~28–31°S) or south of the EAC separation (south of 31°S) when they reached their degree-days threshold (535 ± 32). The dashed red lines represent the approximate EAC separation (as simulated in ozROMS) and the dashed black lines represent the reduced model domain used in our simulations. The solid black line represents the 200 m isobath, all particles offshore of this are excluded from our analysis. Note counts are derived from the entire simulation period (2008–2017) and the log<sub>10</sub>-transformed colour scale. .... 133

**Figure 61** Map of Clarence River (left panel) and Kalang River (right panel) showing linear array of receivers (red circles) and water quality loggers (purple circles)..... 138

**Figure 62** Example of interpolated female Giant Mud Crab tracks during spawning migration, showing daily distance to sea (km) and path for Clarence River (a and b) and Kalang River (c and d). Note differing x- and y-axis scales in (a) and (c) owing to different estuary lengths and tracking periods. .... 142

**Figure 63** Cumulative migration curve (solid black line) illustrating proportion of female Giant Mud Crab commencing spawning migration throughout the tracking period for each year (2018/19 and 2020/21) in Clarence River (a and b) and Kalang River (c and d). Red and blue lines indicate mean daily temperature

(°C) and conductivity ( $\text{mS cm}^{-1}$ ), respectively. Vertical dashed line indicates date of tagging. Note variable scales on x-axis as tagging was undertaken at different times in each estuary/year. .... 143

**Figure 64** Smooth estimated probabilities of triggering female Giant Mud Crab spawning migration for mean daily temperature (a; °C),  $\Delta$ -conductivity (b;  $\text{mS cm}^{-1}$ ) and lunar phase (c; rad). Shaded area indicates 95 % confidence intervals and rugs along x-axis indicate distribution of covariate values. .... 144

**Figure 65** Maps of oceanic detections of tagged female Giant Mud Crab (a) obtained from IMOS ATF and NSW DPI Shark Management strategy acoustic array and their relative position on the east Australian coast (b). Filled circles (●) indicate the location of receivers and empty circles (○) indicate the mouth of the estuary where the crab was tagged. .... 146

**Figure 66** Map of a) Fenninghams Island Creek showing the locations of receivers (●) and reference tags (▲) within the array, as well as the distribution of seagrass, mangrove and saltmarsh. Oyster farming infrastructure is indicated by the grey outline. The location of Fenninghams Island Creek and within Port Stephens (inset; Sanctuary Zones in red), and b) on the east Australian coast is indicated. .... 151

**Figure 67** State-dependent probability distributions (lines) and histograms of observations (grey bars) for a) step length (m), b) turning angle (radians) and c) acceleration ( $\text{m s}^{-2}$ ). Note x-axis on a) and c) has been truncated to aid visualization and excludes the upper ~3 % of observations. .... 158

**Figure 68** a) Example track from a tagged female Giant Mud Crab (ID: 7795) and b) the time-series of Viterbi-decoded behavioural states and the corresponding probabilities of c) State 1 (foraging; yellow) and d) State 2 (inactive; purple). .... 159

**Figure 69** Stationary state probabilities as function of the interaction between tide height (m) and  $\Delta$ -tide height ( $\text{m 15-min}^{-1}$ ) in tagged Giant Mud Crab. .... 160

**Figure 70** Stationary state probabilities ( $\pm$  95 % CI) as a function of a) tide height (m) and b)  $\Delta$ -tide height ( $\text{m 15-min}^{-1}$ ). .... 160

**Figure 71** Model diagnostics plots for the abundance model, including residual QQ-plot (top left), residuals vs. linear predictor (top right), histogram of residuals (bottom left) and observed vs. fitted values (bottom right). .... 171

**Figure 72** Model diagnostics plots for the biomass model, including residual QQ-plot (top left), residuals vs. linear predictor (top right), histogram of residuals (bottom left) and observed vs. fitted values (bottom right). .... 172

**Figure 73** Estimated partial effects ( $\pm$  95 % CI) of soak time (days) on abundance (crabs  $\text{trap}^{-1}$ ; dark blue) and biomass (kg  $\text{trap}^{-1}$ ; light blue) of Giant Mud Crab in southeast Australian estuaries. Rugs indicate the distribution of observations. .... 174

**Figure 74** Estimated partial effects ( $\pm$  95 % CI) of mean temperature (°C) during trap deployment on abundance (crabs  $\text{trap}^{-1}$ ; dark blue) and biomass (kg  $\text{trap}^{-1}$ ; light blue) of Giant Mud Crab in southeast Australian estuaries. Rugs indicate the distribution of observations. .... 175

**Figure 75** Estimated partial effects ( $\pm$  95 % CI) of mean river flow ( $\text{m}^3 \text{s}^{-1}$ ) in the 7 days prior to trap deployment on abundance (crabs  $\text{trap}^{-1}$ ; dark blue) and biomass (kg  $\text{trap}^{-1}$ ; light blue) of Giant Mud Crab in southeast Australian estuaries. Rugs indicate the distribution of observations. .... 176

**Figure 76** Estimated partial effects ( $\pm$  95 % CI) of mean wind speed ( $\text{km h}^{-1}$ ) during trap deployment on abundance (crabs  $\text{trap}^{-1}$ ; dark blue) and biomass (kg  $\text{trap}^{-1}$ ; light blue) of Giant Mud Crab in southeast Australian estuaries. Rugs indicate the distribution of observations. .... 177

**Figure 77** Estimated partial effects ( $\pm$  95 % CI) of lunar phase (radians) at trap deployment on abundance (crabs  $\text{trap}^{-1}$ ; dark blue) and biomass (kg  $\text{trap}^{-1}$ ; light blue) of Giant Mud Crab in southeast Australian estuaries. Note: 0 and  $2\pi$  radians = new moon;  $\pi$  = full moon. Rugs indicate the distribution of observations. .... 178

**Figure 78** Distribution of daily catch (kg) in each estuary. Dashed grey lines indicate the 75<sup>th</sup> percentile, catch records greater than this are assumed erroneous and are excluded from modelling (see Table 23). Note x-axes were truncated to show the majority of the data (3% of data exceeds 200 kg). .... 185

**Figure 79** a) Root mean square error (RMSE) and b) mean absolute error (MAE) of model predictions obtained via 10-fold cross-validation on our training data for varying numbers of variables used for node splitting ( $m_{\text{try}} \in [1, 9]$ ) and minimum sample size of leaf nodes ( $n_{\text{min}} \in [1, 2, 5, 10, 20, 50, 100]$ ). Each colour represents a different value for  $n_{\text{min}}$ . .... 188

**Figure 80** Observations versus predictions of daily catch (kg) from the test data. Points along the red line indicate perfect prediction. .... 189

**Figure 81** Comparison between mean ( $\pm$  SD) observed and predicted daily catch (kg) in a fishing year. Dashed red line indicates the long-term mean ( $\pm$  SD, dotted lines). .... 191

**Figure 82** Relative variable importance measured as the decrease in node impurity gained by inclusion of that variable. .... 192

**Figure 83** Partial dependence between predicted daily catch (kg) and a) net wind displacement, b) larval supply index, c) rescaled river flow, d), Tripole Index for the Interdecadal Pacific Oscillation (IPO) e) Southern Oscillation Index (SOI), f) Pacific Decadal Oscillation (PDO) Index and g) mean East Australian Current (EAC) separation latitude ( $^{\circ}$ ). Note all variables reflect the environmental conditions in the previous austral spring–summer period (September–February) when settlement and recruitment is assumed to occur. Smoothed (blue) lines are overlaid to aid interpretation. Panels are ordered by variable importance (top left – bottom right). .... 193

**Figure 84** Histogram of observations of net wind displacement in our training data ..... 194

**Figure 85** Targeted sampling for early benthic stage Giant Mud Crab within Port Stephens using fyke nets (red triangles) and opera house traps (green circles) in inter-tidal mangrove habitats. Three locations within the estuary were sampled during the pilot phase of this project in 2018, which are indicated in each panel, with the upper left panel showing the position of these locations within the broader estuary. .... 199

# Acknowledgments

The authors wish to acknowledge a number of people and organisations who supported the work that is captured in this report. The NSW Recreational Fishing Saltwater Trust (RFST, project DPIS046) provided cofunding alongside the Fisheries Research and Development Corporation (on behalf of the Australian Government) which supported the work herein. We acknowledge the NSW Department of Primary Industries Fisheries (NSW DPI-Fisheries) Executive (G. Allen, N. Moltschaniwskyj, D. McPherson, M. Lowry) and natural resource managers (D. Reynolds and B. van der Walt), the NSW Research Advisory Committee, the RFST Expenditure Committee, and Recreational Fishing NSW for supporting the concept and development of the initial application, and recommending the work for funding.

A very special acknowledgement goes to B. Leach, A/Technical Coordinator within Fisheries Research (NSW DPI-Fisheries) who filled the role of Project Technician on this program, and personally led the extensive field program. Without his commitment, initiative, attention to detail, wisdom, and dogged hard work, the project would never have been a success. The field program was also ably supported by J. McLeod, M. Burns, B. Kearney, T. New, D. Cruz, and C. Gallen. Various other aspects of the program were supported by E. Junk (preliminary evaluation of survey techniques for Blue Swimmer Crab), S. Morris (initial exploration of TropFishR functions for Blue Swimmer Crab length data) and J. Stewart (who provided commercially harvested length data for Blue Swimmer Crab that was collected by the Resource Assessment and Monitoring Program). Parts of the research were also supported by key industry personnel including Professional Fisherman's Association (PFA), P. Ragno, and J. Bowland.

The NSW Government Research Attraction and Acceleration Program grant awarded funding to the Sydney Institute of Marine Science which supported H. Schilling while working on this project, and the two University of NSW postgraduate students (R. Hanemseth and D. Hewitt) were supported by Australian Government Research Training Program scholarships.

# Executive Summary

This report describes new research by the NSW Department of Primary Industries and the University of NSW into Blue Swimmer Crab and Giant Mud Crab in south-eastern Australia. Over 3 years, data was collected through extensive field sampling and modelled alongside environmental and oceanographic variables to examine how crab populations respond to environmental variability, with a focus on their abundance, distribution and reproduction. Findings were then compiled to test whether the new knowledge could aid in predicting some of the variability observed in fisheries harvest for portunid species. The patterns resolved will aid future stock assessments, and inform management (including regulation, quota setting, and fisheries enhancement) of portunid fisheries in south-eastern Australia into the future.

## Background and objectives

The lifecycles of portunid crabs in south-eastern Australia, and the fisheries that exploit them, largely play out in estuarine and inshore coastal habitats. These habitats represent the interface between terrestrial and oceanographic influences, which creates a highly variable environment characterised by complex interactions between freshwater run-off, catchment-derived stressors, coastal winds, ocean currents, thermal and upwelling regimes, and anthropogenic impacts. Such variability has been shown to have considerable influence across the life-history of portunid species, as evidenced through numerous case studies (albeit conducted in other regions) over the past 3 decades. Freshwater inflow to estuaries leads to lower salinity which can impact spawning, through direct effects on maturation or driving migration by adult crabs to areas with more suitable conditions for egg development. Temperature and thermal cycles can influence egg production and timing of spawning and growth, which impacts the number of propagules available for settlement, and may lead to spatio-temporal mismatches in arrival of recruits to nurseries. Small-scale wind driven currents and broader oceanography can impact dispersive processes and contribute to spatial matches and mismatches in recruitment to nursery areas. Upwelling and sea-surface temperature can impact survival and development of planktonic larvae during pelagic larval stages, and anthropogenic impacts, such as adverse estuarine water quality from poor land-use practices, can impact behaviour, growth and survival through early life history. These myriad relationships can interact to impact spawning, dispersal, settlement, growth, recruitment and migration patterns, contributing to variable population abundance, and variation in exploitable biomass across seasonal and annual time scales. Existing work from elsewhere indicates that complex relationships exist between environmental variation, spawning, settlement, recruitment and catch, which have implications for the productivity of Blue Swimmer Crab and Giant Mud Crab fisheries. Broadly, this project aimed to investigate these relationships by evaluating the influence of key environmental variables on patterns in abundance, reproduction and dispersal in eastern Australian crabs, and integrate this new knowledge with patterns in commercial catch for the species. Consequently, the project sought to address several broad objectives:

1. Describe temporal and spatial patterns in settlement and juvenile habitat use, to determine if spawning, nursery habitat availability, or connectivity creates localised recruitment bottlenecks in NSW estuaries
2. Define and model links between environmental (physicochemical and oceanographic) variables and patterns in abundance, distribution, reproduction and dispersal, and potential effects on catch rates; and,
3. Use this information to develop an independent measure of recruitment, which links the effects of environmental variability on recruitment and current harvest, to future catch.

Pilot work during the very early stages of the project was largely unsuccessful in reliably capturing early life-history stages of Blue Swimmer Crab and Giant Mud Crab, so field sampling was refocussed to target later life history stages for these objectives.

## Approach

The core approach for Blue Swimmer Crab employed in this study was an independent survey in Wallis Lake (NSW largest Blue Swimmer Crab fishery), Lake Macquarie (NSW largest recreational fishery), and Port Stephens, that spanned the period from November 2018 – March 2021 (with the Wallis Lake survey extended to June 2021). Initially, a novel research trap design was developed for the independent surveys of Blue Swimmer Crab populations, incorporating smaller mesh sizes than conventional commercial round traps, and tested for efficacy and bias. Seven sites were sampled within each estuary using six small-mesh traps, with the exception of the period prior to May 2019, during which five sites were sampled using five large-mesh and five small-mesh traps. Sampling was conducted monthly within each estuary, with two nights sampled during each month, and crabs were measured and key reproductive variables quantified. The regular independent survey was supplemented by some additional sampling sub-programs, and a comprehensive array of temperature and conductivity loggers were deployed in the surveyed estuaries for the duration of sampling to measure environmental variables.

The core approach for Giant Mud Crab included a range of process studies examining the influence of key abiotic and habitat variables on the movement and abundance of crabs (primarily through acoustic telemetry in three estuaries, and observer surveys across 6 major estuaries). Sampling work for both species was integrated through statistical modelling, and complemented by modelling of the influence of oceanographic variables on the dispersal and distribution of crabs during their dispersive oceanic phase. The important relationships that were identified were further integrated for each species, through modelling of commercial catch along much broader time series, to establish their utility for forecasting of catch magnitude.

## Key findings

### Blue Swimmer Crab

Over 30,000 Blue Swimmer Crab were captured during the study, with most measured and released alive back into the water. There was substantial spatial and temporal variability observed within the time series of Blue Swimmer Crab abundance data. The greatest catch rates were observed in Wallis Lake, with seasonal peaks 3x and 5x that observed in Port Stephens and Lake Macquarie respectively. Size-structure data suggested that, for all estuaries, there was usually only a single major cohort moving through the fishery in any one summer-autumn period (although there were some exceptions to this). Temperature was highly influential on the abundance of Blue Swimmer Crab, which largely reflected a seasonal effect. Peak abundance of crabs occurred at conductivities around  $35 \text{ mS cm}^{-1}$ , with lower abundance at higher conductivities observed in Wallis Lake and Port Stephens, which likely reflected the crabs redistributing into (unmonitored) areas further up the estuary as they became increasingly marine. There was also a decline in abundance at lower conductivities, which reflected crabs moving closer to sea and into inshore areas.

Estimates of size-at-maturity for Blue Swimmer Crab ranged from ~51-52 mm Carapace Length (CL, with little variation between estuaries), and the smallest berried female observed was 47 mm CL (captured in Wallis Lake). The highest proportion of berried females were recorded from September to March in Lake Macquarie, with the proportion being generally lowest in the months with the highest catches of mature crabs (June-July). Similar peaks were observed in Port Stephens (September to February). In contrast, the

proportion of berried female Blue Swimmer Crab from Wallis Lake tended to have a sharp peak in September or October, and remained comparatively low in magnitude at other times. Overall, the proportions of mature crabs that were berried in Wallis Lake were considerably lower than Port Stephens and Lake Macquarie. There was a negative correlation between the gonadosomatic index (GSI, an index of gonadal development and reproductive investment) and hepatosomatic index (HSI, an index of energy storage) detected for females in the final stages of ovarian development. Egg mass increased logarithmically with body mass, accounting for up to 55% of total body mass, which was significantly larger than observed in other studies. Thermal performance curves showed a peak in individual reproductive output at a mean monthly temperature of 24.8°C, at which the individual egg mass weight reached a maximum and the HSI reached a minimum.

Oceanographic modelling indicated some broad-scale connectivity for Blue Swimmer Crab, and dispersal patterns suggested a minor north-to-south source-sink structure. Recruitment of ocean-spawned animals back to the estuary in which the mother grew up was dependent on the proximity of mesoscale oceanographic features of the EAC, but simulations showed that for most estuaries Blue Swimmer Crab young were most likely to self-recruit (i.e., recruit back to the same estuary from/in which their mother originally emigrated/spawned). Modelling of key variables against long-term commercial catch history indicated that winter and spring harvesting may impact the following summer harvest by removing the spawning stock biomass, and also that a basin-scale climatic index (Pacific Decadal Oscillation) positively correlated with summer catch rates. Using a long-term series of commercial catch data, these two variables were able to correctly predict above- or below- average summer catch ~85% of the time.

## **Giant Mud Crab**

The work presented in this report primarily targeted investigations of specific processes, at fine and broad scales, and are the first to describe aspects of the ecology and fishery for Giant Mud Crab in NSW in more than 20 years. At the fine scale, this included resolving activity patterns, their drivers and relationship with catch rates from commercial trapping. Within estuaries, acoustically tagged adult Giant Mud Crab displayed two clear behavioral states (inactive, and foraging). Crabs were most likely to forage during low, incoming tides, likely exploiting intertidal habitats (including vegetated habitats) as they were inundated, but small-scale variations in water temperature and diel periodicity were unimportant for crab activity patterns. Modelling of fine-scale data collected during an extensive observer survey indicated that soak time had little effect on catch rates, but temperature, river flow, wind speed and the lunar phase also influenced catch rates at varying degrees.

At the broad scale, process studies included identification of abiotic drivers of both spawning migrations in female crabs, and subsequent dispersal and recruitment patterns, as well as integrating these patterns to establish whether identified drivers could predict better- or worse-than-average commercial catch. Acoustically tagged female Giant Mud Crab displayed a strong inclination to emigrate from estuaries (a behaviour exhibited by 52% of tagged crabs), with the highest probability of migration associated with relatively low temperatures (<22°C), and when conductivity rapidly declined (< -10 mS cm<sup>-1</sup> d<sup>-1</sup>) following heavy rainfall. Emigration also coincided with larger tides associated with the new and full moon, and following heavy rainfall. Oceanic detections of 14 crabs (30% of 'successful' migrators) showed that once crabs emigrated from estuaries, they migrated north. The environmental triggers for these spawning migrations likely contribute to interannual variation in spawning patterns, and subsequent recruitment. Modelling of dispersal patterns from ocean spawning showed a clear north-south source-sink relationship for Giant Mud Crab, with recruits from the north of the species NSW distribution originating from Queensland waters. The EAC separation could act as a passive barrier to connectivity between waters to the north or south of this region. Drawing together variables that influenced spawning and recruitment in Giant Mud Crab supported predictive modelling of catch, correctly predicting above- or below- average catch years 86% of the time.

# Implications

## Blue Swimmer Crab

1. Based on connectivity patterns, Blue Swimmer Crab in NSW and Queensland appear to constitute demographically separate stocks, supporting the current assessment and management at the state level
2. The scale and spatial structure of the fishery-independent monitoring program for Blue Swimmer Crab designed and implemented within the current project is appropriate to provide information on relative abundance, size structures and mechanisms underlying changes in abundance
3. New modelling predicting relative strength of recruitment and catch provides an additional source of information to support quota setting for the commercial fishery. This modelling suggested that winter harvest may directly influence the following season catch due to disproportionately high impact on mated pre-spawning female crabs
4. The data collected on the biology of Blue Swimmer Crab may represent a useful proxy to understand the effects of further tropicalisation on reproduction of Blue Swimmer Crab in south-eastern Australia

## Giant Mud Crab

1. A comparatively high level of inter-jurisdictional connectivity for Giant Mud Crab, predominantly between Queensland and northern NSW, suggests that stock structure issues need to be acknowledged, to accommodate potential changes in productivity, and their implications, in different parts of the stock
2. Environmental processes influence catchability across a hierarchy of spatial and temporal scales which need to be considered when interpreting estimates of stock size and fishing mortality rates from stock assessments
3. Variability in environmental triggers for spawning migrations may contribute to interannual variation in spawning patterns, which may in turn impact fisheries productivity in this region
4. Above and below average years of Giant Mud Crab catch can be predicted from key stock and environmental variables with reasonable certainty, which will aid decision making and adaptive management of harvest levels

## Keywords

Independent surveys; Blue Swimmer Crab; Giant Mud Crab; reproduction; migration; dispersal; prediction; climate change; fecundity; fisheries

# Introduction

## Environmental influences on the population ecology of exploited portunid species

Crab species are important members of most aquatic ecosystems, and support extensive fisheries across estuarine, inshore and deep ocean habitats. Portunid crabs (members of the family Portunidae), are characterised by the flattening of their fifth pair of legs into paddles, and are thus specialised for swimming (Poore 2004). Many taxa within subfamily Portuninae grow to comparatively large sizes, which make them desirable targets of commercial and recreational fisheries. Well known exploited genera within Portuninae include *Callinectes* spp., *Portunus* spp., and *Scylla* spp., with harvested species commonly associated with estuarine and inshore coastal habitats (Stevens *et al.* 2020).

Estuarine and inshore coastal habitats are at the interface between terrestrial and oceanographic influences, and are often further impacted by populous urban communities with assemblages subjected to high fishing pressure (Taylor and Suthers 2021). This creates a highly variable environment characterised by complex interactions between freshwater run-off, catchment-derived stressors, coastal winds, ocean currents, thermal and upwelling regimes, and anthropogenic impacts. This variability has been shown to have considerable influence across the life-history of portunid species, as evidenced through numerous case studies conducted over the past 3 decades. For example, freshwater inflow to estuaries leads to lower salinity which can impact spawning, through direct effects on maturation or driving migration by adult crabs to areas with more suitable conditions for egg development (e.g., Turner *et al.* 2003). Temperature and thermal cycles can influence egg production and timing of spawning (e.g., Hamasaki 2002) and growth, which impacts the number of propagules available for settlement, and may lead to spatio-temporal mismatches in arrival of recruits to nurseries. Small-scale wind driven currents and broader oceanography can impact dispersive processes and contribute to spatial matches and mismatches in recruitment to nursery areas (e.g., Biermann *et al.* 2016). Upwelling and sea-surface temperature can impact survival and development of planktonic larvae during pelagic larval stages (e.g., Sulkin and Van Heukelem 1986; Andrade *et al.* 2017). Anthropogenic impacts, such as adverse estuarine water quality from poor land-use practices, can impact behaviour, growth and survival through early life history (e.g., Das and Stickle 1994). These myriad relationships can interact to impact spawning, dispersal, settlement, growth, recruitment and migration patterns, contributing to variable population abundance and variation in exploitable biomass across seasonal and annual time scales.

Measuring and quantifying the relationships between environmental variation and critical population processes is especially important for exploited species. Fishing pressure can heavily influence spawning stock biomass, which may act synergistically with influences of environmental variability on population processes, and lead to severe impacts on fast-growing crab species (Marks *et al.* 2021). For example, if environmental factors contribute to poor recruitment but fishing mortality is not adjusted accordingly, substantial declines can occur which impact the viability of exploited stocks (Johnston *et al.* 2011). Furthermore, many conventional stock assessment approaches assume that an exploited population persists in a steady-state—environmental variability can lead to violation of this assumption, thus reducing confidence in assessments, and the management decisions they inform.

Adaptive management provides a framework to maintain or improve fishery performance in the face of uncertainty arising from the effects of environmental variation (Norman-Lopez *et al.* 2011), but requires reliable and ongoing data streams to evaluate and inform decision making (Walters 2007). Given that many exploited portunid species display fast growth and short life-histories, data to

inform the adaptive management of such stocks may be required in close-to-real-time (e.g., monitoring early in a season to manage levels of fishing mortality later in the season, Caputi *et al.* 2014). Characterising how patterns in abundance, dispersal and reproduction may be affected by different environmental conditions and how they affect the pipeline of recruits, will support the development of longitudinal monitoring programs and independent surveys that can identify expected changes in stock biomass within a recruitment season or between recruitment years. However, fundamental research is required to characterise important relationships under local conditions, such that monitoring can be efficiently and effectively targeted at important processes or ecological bottlenecks. Such monitoring may range from simply remote logging of water quality through recruitment and/or reproductive periods, to more complex modelling of the impact of oceanography on dispersal patterns, or intensive fisheries-independent surveys of recruits or berried individuals. Regardless of the form that targeted monitoring may take, if designed appropriately the resultant data series will provide additional evidence to forecast current or future stock performance, aid decisions on catch quotas (Caputi *et al.* 2014), and identify recruitment bottlenecks that may be targeted by other means (such as aquaculture-based enhancement, e.g., Jenkins *et al.* 2017).

## Estuarine and inshore crab fisheries within New South Wales

Within New South Wales (NSW) Australia, commercial portunid fisheries primarily exploit Blue Swimmer Crab (*Portunus armatus*) and Giant Mud Crab (*Scylla serrata*), but other portunid and non-portunid crab species are also targeted (e.g., Spanner Crab *Ranina ranina*, and Ocean Sand Crab *Ovalipes australiensis*). Portunid crabs are mainly captured within estuaries in NSW, and the majority of catch across both species is taken north of latitude 34.5°S, although they are also taken from inshore waters in smaller numbers.

Generally, crabs are harvested using traps, but are also caught commercially using trawls, seines/hauls, and in mesh nets. The majority of commercial Blue Swimmer Crab catch within NSW is taken from Wallis Lake on the mid-north coast, but other estuaries supporting large catches include Port Stephens, Lake Illawarra, Tuggerah Lakes, and Camden Haven (Figure 1 and Figure 2). Lake Macquarie supports the largest recreational harvest for Blue Swimmer Crab (Ochwada-Doyle *et al.* 2014), but the species is also targeted recreationally across a large number of urban and regional estuaries.

Within NSW, Blue Swimmer Crab are managed through a range of controls. Commercial and recreational harvest is subject to a minimum legal size (MLS, 65 mm carapace length [CL] as of 2019 for commercial fisheries and 2021 for recreational fisheries), and there is a ban on retaining berried females. Harvest is also managed through share-linked quota (for commercial fishers), gear restrictions and spatial management (Johnston *et al.* 2021a). Additional controls on recreational harvest include gear restrictions and bag limits (Johnston *et al.* 2021a), but aquaculture-based enhancement has also been proposed to improved productivity in times and places that recruitment may be depressed (NSW Department of Primary Industries 2014; Junk *et al.* 2021). There are also other controls implemented at the estuary level, but fishing for the species is currently permitted all year round, within all estuaries.

Within NSW, Giant Mud Crab are captured almost exclusively from estuaries, and targeted using traps. Over the past 10 years, Macleay River, Wallis Lake and Clarence River (Figure 1) have supported the greatest cumulative commercial harvest, with Camden Haven and Tweed River also supporting reasonable harvests (Figure 2). The spread of harvest among these important estuaries is not as skewed toward Wallis Lake as for Blue Swimmer Crab (Figure 2). Giant Mud Crab are fished recreationally in most estuaries that support commercial harvest, and are also targeted in some Recreational Fishing Havens. Giant Mud Crab are managed using a similar suite of controls as for Blue

Swimmer Crab, including share-linked quota, gear restrictions, bag and possession limits, spatial closures, an MLS (85 mm CL), and a ban on retaining berried females (Saunders *et al.* 2021). Aquaculture-based enhancement is also identified as a future management approach for the species (NSW Department of Primary Industries 2014).

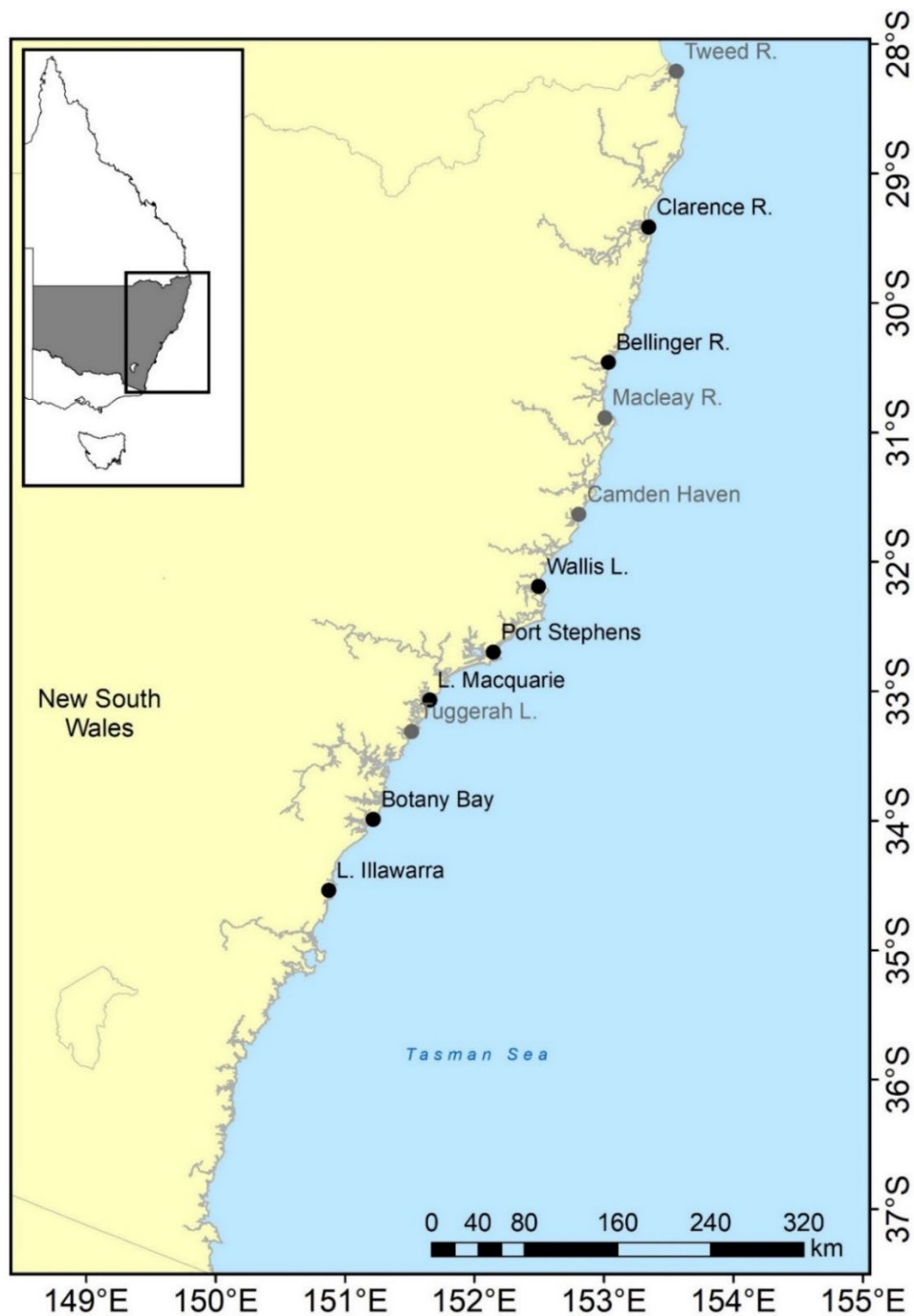


**Figure 1** Map showing main estuaries for capture of Blue Swimmer Crab and Giant Mud Crab within New South Wales, with the main study estuaries indicated in black, and other estuaries that generally support good crab harvests (mentioned in the text) indicated in grey. The inset shows the location of the main map on the eastern Australian seaboard.

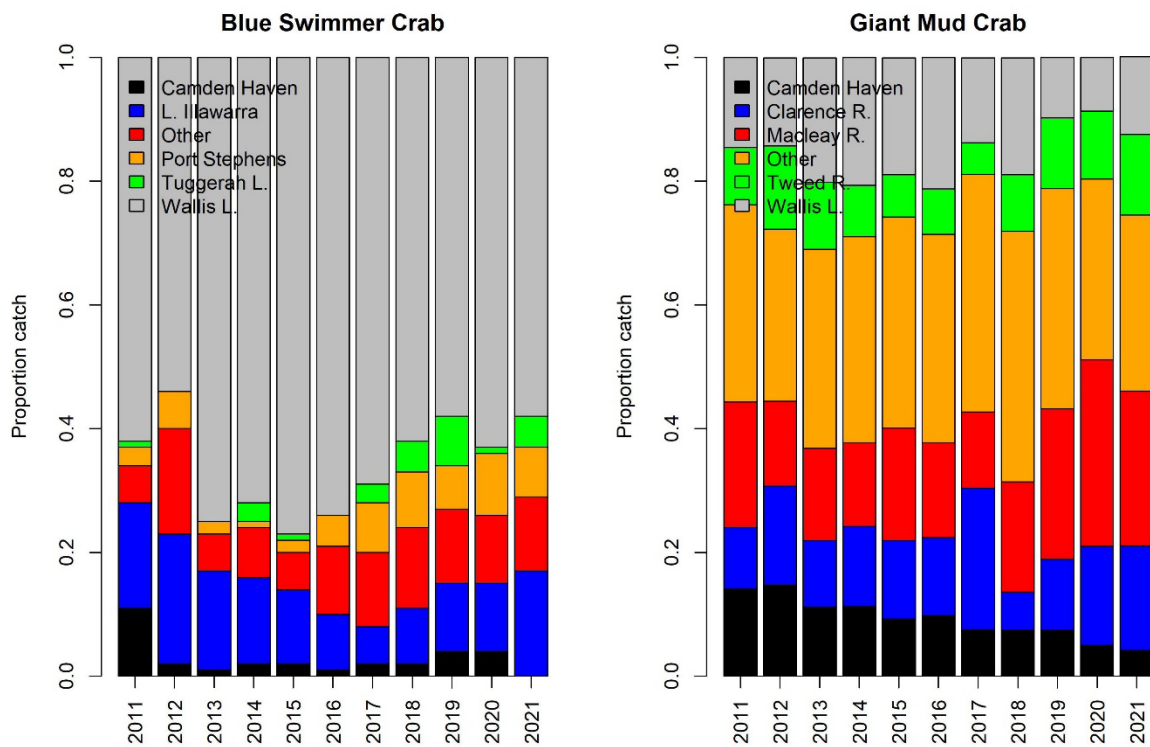
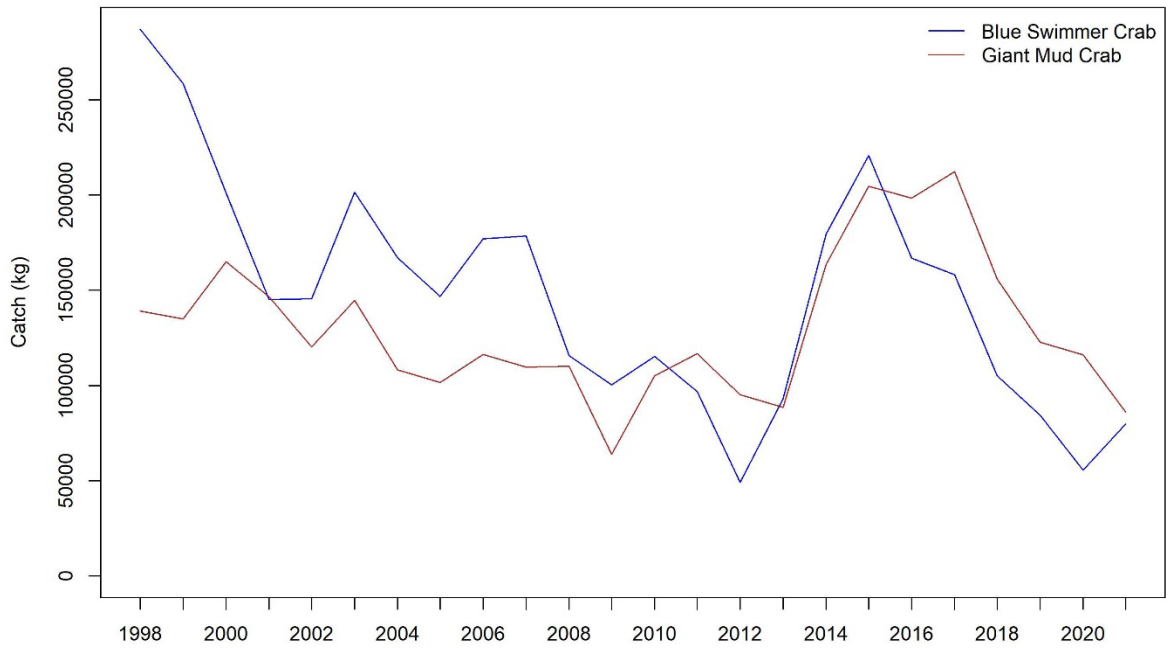


**Figure 2** New South Wales catch history for Blue Swimmer Crab and Giant Mud Crab since the 1998 fiscal year (upper panel), and the relative proportion of catch from each of the main estuaries for the 10 years prior to the 2021 fiscal year, for Blue Swimmer Crab (lower left panel) and Giant Mud Crab (lower right panel). Estuary names are shown in Figure 1.

Blue Swimmer Crab and Giant Mud Crab sustain comparatively similar levels of overall catch within NSW (Figure 2). However, these species are also similarly variable, with differences between peaks and troughs in the recent catch history being around 150-200 tonnes. Year-on-year variation is often

in the vicinity of ~40 tonnes, and the extent of variability is evident in the coefficient-of-variation in the annual catch over the 10 years to 2021—47% for Blue Swimmer Crab (on a mean of 118 t y<sup>-1</sup>) and 33% for Giant Mud Crab (on a mean of 142 t y<sup>-1</sup>). Alongside the interannual variation, spatial variation in catch among estuaries is also evident across years (Figure 2), and the months of peak catch also vary among years (data not shown). Standardised catch rates (as an index of stock biomass) are similarly variable for both Blue Swimmer Crab (Johnson 2020a), and Giant Mud Crab (Johnson 2020b). While there are fisheries-specific and market-based drivers that influence overall variability, consideration of the ecology and life history of both species also suggests that environmental variation is likely to impact a number of the critical processes outlined in the previous section, and contribute to the observed temporal and spatial variation in catch.

## Biology of Blue Swimmer Crab

There is been little published work on the ecology on Blue Swimmer Crab in south-eastern Australia, with a single study dealing with aspects of fisheries ecology for the species in this area which sampled a single estuary (Wallis Lake, Figure 1) over a single growth season (Johnson *et al.* 2010). This study estimated a length at maturity of 46 mm CL, and showed that ovigerous females were most abundant in late spring and early summer (although winter and early spring were not sampled) and that up to 3 broods of eggs could be produced every year. This study also suggested that crabs larger than 60 mm produced 76% of estimated total egg production.

Western Australian research has produced a more complete picture of reproductive and early life history processes, which complements the preliminary work of Johnson *et al.* (2010) in south-eastern Australia. In Western Australia, ovigerous females were found to be most abundant from November to July (de Lestang *et al.* 2003a), and Kangas (2000) suggested that the main hatching period extended from November to March. Kangas (2000) also suggested that spawning primarily took place in marine embayment's or inshore areas, but other work in Western Australia suggested spawning could also occur in estuaries (Gaughan and Potter 1994, found larvae in the Western Australian estuaries between September and April). Eggs hatch after about 15 days, and the larval phase consists of five stages spanning 26-45 days in duration, depending on temperature (Kangas 2000). Larvae are thought to drift in prevailing currents (and can move as far as 80 km out to sea) before returning to settle in shallow inshore waters at ~5-10 mm CW. Work on the species in Queensland suggests that onshore winds are potentially important for moving Blue Swimmer Crab toward inshore and estuarine habitats (Sumpton *et al.* 2003). It is important to point out that temperature may impact dispersal patterns (as the planktonic phase is faster at warmer temperature), as well as larval survival. In South Australia, Bryars and Havenhand (2006) found that larval survival was greatest between 22.5-25°C in a laboratory setting, that larval development was fastest between ~20-23°C, and the larvae will not survive past early zoea stage at temperatures less than 18°C. This study concluded that larval survival and postlarval settlement should be greatest during years with abnormally warm summers. This contrasts somewhat with the conclusions of Chandrapavan *et al.* (2019), which suggested that in Western Australia juvenile Blue Swimmer Crab may suffer heat stress at temperatures >24°C, and that temperatures exceeding 26°C may be detrimental for survival.

## Influence of environmental variability on Blue Swimmer Crab

The above summary highlights that environmental factors may influence Blue Swimmer Crab at many critical stages of its life cycle, which in turn may impact abundance and productivity (through influence on spawning, recruitment, growth and survival). Further to the work outlined above, there has been considerable contemporary research aimed at characterising the influence of

environmental factors on Blue Swimmer Crab. Again, much of this research is relevant to Western Australian stocks, and has been motivated by substantial declines in commercial landings of the species in several locations within this jurisdiction. Following these sharp declines and the fisheries closures that followed, comprehensive fisheries independent surveys were put in place, and have proceeded for ~2 decades. The data from these surveys (alongside data from other sources) have supported a comprehensive body of research into linkages between environmental variation and productivity of Blue Swimmer Crab, and provides some indication of potential relationships that may be relevant for the species in other locations.

The first of these recent studies examined factors that affected growth of Blue Swimmer Crab, specifically temperature, density dependence and primary productivity (Marks *et al.* 2019). This study identified an influence of primary productivity on crab productivity, whereby elevated chlorophyll-*a* led to improved larval growth and survival, which in turn led to elevated juvenile abundance. However, it was hypothesised that this in turn contributed to juvenile density dependence, which resulted in comparatively smaller adult crabs. Sea surface temperature (SST) was not found to influence crab growth in this study, presumably because other factors had an overbearing influence on crab size. It was suggested that density dependence may have been exacerbated by prior seagrass declines (which are important for juvenile foraging, Campbell *et al.* 2021), and that lower growth may have flow on effects for size-at-maturity, fecundity-at-age, and overall biomass.

Using the time series of independent survey data, Johnston and Yeoh (2021) found strong relationships between temperature and reproductive parameters in Western Australia Blue Swimmer Crab. Firstly, maturity occurred at smaller sizes at higher latitudes, but batch fecundity was higher at more southern latitudes. When modelled against temperatures between 16 and 21°C, both size at maturity and functional maturity (the smallest size observed for ovigery) formed tight positive relationships with temperature. Also, functional maturity converged on size-at-maturity in warmer waters, suggesting that reproduction commences as soon as maturity is reached. These patterns highlight the potential for spatial heterogeneity in reproductive strategies, that are primarily driven by temperature variation.

Further to analyses of fishery independent data, Johnston *et al.* (2021b) examined the influence of environmental variables on commercial trap fishery catch rates over an 18-year period. Environmental variables explained 3-26% of the variation in catch rates, but patterns were variable between different estuaries/embayment's. Wind speed influenced catch rates, potentially though effects on turbidity and plume size from baited traps. Freshwater influx had variable effects, with rainfall positively influencing catch rates in a marine embayment (potentially driven by egression from adjacent estuaries), and river flow negatively influencing catch rates in a riverine estuary. Temperature was found to contribute to increased catch rates, potentially due to increased metabolic demands for food (leading to increased activity and interest in trap baits). Southern locations showed a peak in catch at 22-23°C, whereas catch rates at the most northern location increased to the maximum temperature (30°C)—Blue Swimmer Crab show an increase in metabolic rate with temperature between 18°C and at least 29°C (Junk *et al.* 2021), which means other factors are likely to have contributed to the peak observed at southern locations.

In south-eastern Australia, Gillson *et al.* (2012) is the only study which seeks to establish broad-scale linkages between fishery-dependent catch or catch rates, and environmental variables. Gillson *et al.* (2012) found that the contribution of Blue Swimmer Crab to estuarine fisheries landings increased during dryer years, and that the contribution to coastal landings increased during wetter years. This suggests potential sensitivity to lower salinities in estuarine habitats under heavy inflow scenarios, resulting in emigration to inshore areas. This concurs with previous reports that Blue Swimmer Crab prefer higher salinity (Potter *et al.* 1983).

Overall, while there is a considerable body of research identifying the influence of environmental variables on various aspects of life history, reproduction, and productivity of Blue Swimmer Crab, much of the research points to considerable variation between regions, climatic zones, and estuaries. Consequently, although previous work conducted in regions other than south-eastern Australia provides a good foundation for defining potential relationships, the applicability of relationships among regions is uncertain. Thus, there is a clear need for fundamental research to further examine relationships in south-eastern Australia, especially in light of considerable variability in the catch of the species in this region (outlined in the previous section).

## **Biology of Giant Mud Crab**

As an important aquaculture species, various components of the Giant Mud Crab life-cycle and reproduction have been extensively studied, however similarly to Blue Swimmer Crab there is little information for south-eastern Australia. Large adult Giant Mud Crab (>150 mm CW) are primarily distributed in subtidal habitats, with peak abundances in summer (Hill *et al.* 1982). Length-at-maturity for female Giant Mud Crab is estimated to be ~138 mm CW in subtropical Australia (Heasman 1980), although there are no estimates published for south-eastern Australia. Spawning occurs from October to March in southern Queensland, and females undertake a spawning migration to oceanic areas presumably so the stenohaline larval stages are not exposed to brackish water (Hill 1994). It is thought that most females in the wild mate only once, but can spawn multiple times. Increased freshwater inflow increases Giant Mud Crab activity, and may influence migratory behaviour, but this has never been measured directly. Giant Mud Crab develop through five larval stages, and require high salinity water and temperatures >20°C for development, with an optimal temperature of 28-30°C (Nurdiani and Zeng 2007). The larval stage is up to 22 days, with another 10 days for development through megalopa into crablets. Early juveniles likely remain in their juvenile habitats until they are 3 months of age. The recent comprehensive review of Alberts-Hubatsch *et al.* (2016) concludes that knowledge of spawning behaviour of female Giant Mud Crab is vague, and that more knowledge on larval transport, settlement processes, habitat use, and recruitment mechanisms, is needed. This is partly because post-mating reproductive processes occur outside estuaries (in oceanic areas), and capture of mated female crabs in these areas is rare.

## **Influence of environmental variability on Giant Mud Crab**

Several studies have sought to quantify environmental factors that influence Giant Mud Crab (e.g., Loneragan and Bunn 1999; de Lestang *et al.* 2003a; Sumpton *et al.* 2003; Hay *et al.* 2005; Meynecke *et al.* 2010; Gillson *et al.* 2012), but similarly to Blue Swimmer Crab, patterns are geographically variable. As with many crab species, activity, feeding rate and metabolic rate, increase with water temperature for adult Giant Mud Crab (Hill 1980). But water temperature (and salinity) also has a substantial influence on growth and survival of larvae and juveniles (Alberts-Hubatsch *et al.* 2016). Larval Giant Mud Crab in Philippines did not survive well at salinity <25, and grew best at temperatures of 26°C or greater (Baylon 2010). Baylon (2010) also found little influence of temperature or salinity on juvenile stages (although crabs did not survive in salinities <5), however an earlier study on Australian Giant Mud Crab by Ruscoe *et al.* (2004) indicated that best growth in juveniles occurred at 30-32°C and at salinity between 10-20. Hill (1979a) reports adult crabs tolerating salinities as low as 2 for extended periods. The differences in tolerance and optima among geographic areas suggests potential for the presence of localised phenotypes (Alberts-Hubatsch *et al.* 2016). The intolerance of larvae to low salinities may underpin the coastal spawning strategy employed by this species in the wet tropics (where extreme freshwater inflow to estuaries occurs on

a seasonal basis), but there is also a secondary benefit of aiding dispersal (Hill 1994). Although there is some geographic variation in thermal and salinity optima for early life history stages, larger juveniles and adult Giant Mud Crab are euryhaline and tolerate a broad range of conditions (Alberts-Hubatsch *et al.* 2016).

The above environmental variables can exert a marked influence on catch. Temperature has a positive impact on catch in Giant Mud Crab (Meynecke *et al.* 2010; Alberts-Hubatsch *et al.* 2016), most likely due to the influence on activity rates noted above. Principally, research has also identified a positive relationship between catch and rainfall or freshwater inflow to estuaries on both a direct basis (i.e., where flow may influence aggregation and catchability of crabs, Loneragan and Bunn 1999), and on a lagged basis (e.g., where flows may influence earlier processes like spawning and recruitment). Using historic commercial fisheries data (from 1985 – 1997) for Giant Mud Crab, Meynecke *et al.* (2012b) found moderate ( $R^2 = \sim 0.3-0.4$ ) direct correlations between summer and autumn SST and catch per unit effort (CPUE) across most northern NSW estuaries. This study also found strong relationships ( $R^2 = \sim 0.5-0.7$ ) between CPUE in northern NSW estuaries and spring and summer rainfall two years prior. While it is tempting to attribute this to a potential spawning or early life history affect, Hill (1975) suggests that crabs may grow at such a rate as to reach a size equivalent to the NSW MLS within  $\sim 12$  months. Meynecke *et al.* (2012b) concludes by highlighting that the mechanisms underpinning how and why these variables might be linked to catch needed further research. Coupling this point with the fact that SST was taken from coastal areas to a distance of 20 km from the estuary (so was not estuary water temperature), and that only very old (pre-1997) and potentially unreliable catch data were used (crab species were not reliably separated in log-book reporting prior to 1997), means that relationships between environmental variables and Giant Mud Crab catch in NSW require further investigation.

Developing a mechanistic understanding of the relationships between temperature, flow, and later recruitment to the commercial fishery, presents a complex problem for Giant Mud Crab in NSW. Giant Mud Crab are an ocean spawning species, and the oceanography off northern NSW is dominated by a comparatively strong southward flowing current, the East Australia Current (Suthers *et al.* 2011). This suggests that southward dispersal of the ocean-spawned eggs and larvae is likely while crabs develop to settlement stage, creating potentially complex inter-estuarine and inter-jurisdictional source-sink relationships, with spawning stock originating from a different estuary to that which young crabs eventually recruit. Consequently, any investigation of lagged linkages between environmental variables and catch will require consideration of which location the recruits to a particular fishery may have originated from, and catch or catch indices in one estuary (the 'sink') may well be influenced by spawning stock biomass, mating patterns, and spawning cues, in an estuary further north (the 'source'). Quantifying these relationships is essential to model the mechanistic links between environmental variation on a temporal scale that is useful for management. However, these source-sink dynamics are completely unknown for Giant Mud Crab within NSW (and Blue Swimmer Crab as well).

# Objectives

The above background highlights the complex relationships between environmental variation, spawning, settlement, recruitment and catch, which have implications for the productivity of Blue Swimmer Crab and Giant Mud Crab fisheries (Figure 3). Broadly, the project aimed to investigate these relationships by evaluating the influence of key environmental variables on patterns in abundance, reproduction and dispersal in eastern Australian crabs, and integrating this new knowledge with patterns in commercial catch for the species. Following pilot field work, comprehensive literature reviews, and project planning, the project focussed on three broad objectives:

1. Describe temporal and spatial patterns in settlement and juvenile habitat use, to determine if spawning, nursery habitat availability, or connectivity creates localised recruitment bottlenecks in NSW estuaries
2. Define and model links between environmental (physicochemical and oceanographic) variables and patterns in abundance, distribution, reproduction and dispersal, and potential effects on catch rates; and,
3. Use this information to develop an independent measure of recruitment, which links the effects of environmental variability on recruitment and current harvest, to future catch.

As suggested by Objective 1, initially the project sought to examine these relationships through monitoring the abundance of early juvenile crabs. Pilot work during the very early stages of the project was largely unsuccessful in reliably capturing early life-history stages of Blue Swimmer Crab and Giant Mud Crab, so field sampling was refocussed to target later life history stages for the above objectives.

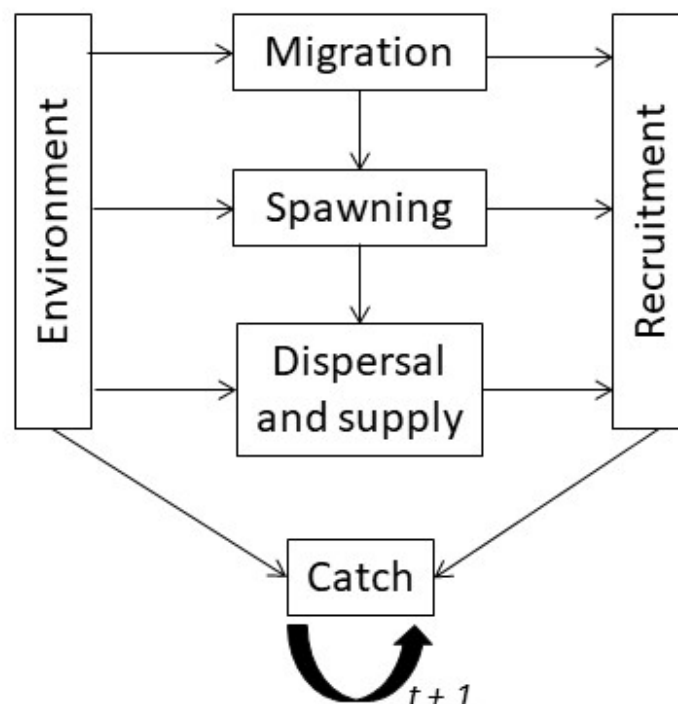


**Figure 3** Conceptual model outlining the inter-relationships between different processes that were investigated in this project.

Another objective (*Interpret patterns in recruitment limitation to target a large-scale release of Blue Swimmer Crab, and analyse post-release abundance patterns to better understand recruitment bottlenecks and improve modelled relationships*) was also proposed in the project application. Unfortunately, due to issues developing effective rearing techniques and expertise by aquaculture facilities within NSW, this objective could not be fulfilled by the project.

## **Structure of this report**

The project involved a large number of diverse project components, including pilot studies, field-based process-study components, modelling components and multi-year independent surveys. The report initially deals with pilot studies which informed the approaches taken during the field-based project components. Following this, a series of chapters outline the main survey program for Blue Swimmer Crab, with a unified methodology chapter for the regular fishery independent surveys and supplementary sampling that proceeded through the duration of the project, followed by analysis and modelling chapters that used this data. This is followed by a series of chapters reporting the process studies undertaken for Giant Mud Crab. The report concludes with a unified discussion of the main findings in the context of the core objectives for each study species, which supports the implications and recommendations that are put forward for management, and for future work, at the very end of the report.

# Design and evaluation of a novel research trap for surveying Blue Swimmer Crab populations

## Background and rationale

Effective sampling methods for free-ranging crab populations generally need to capture the desired size range of individuals, as well as support the derivation of estimates of relative abundance with reasonable accuracy and precision. However, no sampling method is perfect, and it is important to consider how different methods perform and elements of bias that may be specific for different sampling approaches. Crabs can be captured using a range of different approaches, such as cylindrical wire traps, beach seines, trawls, pots, gill nets and lift nets (Butcher *et al.* 2012). The nuances of these different gear types, configurations, and the mesh sizes used, mean that there is inevitably some selection for different life history stages, or exploitation of different behaviors to catch crabs.

For Blue Swimmer Crab, various studies have reported benthic trawling (Sumpton *et al.* 2003; Harris *et al.* 2012) as a suitable approach for surveying exploited crab populations. Beam trawling is often used in these surveys, as a precise estimate of swept area can be calculated, and the gear can capture both juveniles and adults (Bacheler *et al.* 2013). However, beam trawling is time, labour, and fuel intensive, and can have environmental impacts on sensitive habitats (McConnaughey *et al.* 2020). Also, nocturnal surveys are often required for Blue Swimmer Crab, which can exacerbate labor costs. Crab traps provide an alternate approach to efficiently capture crabs, but have their own set of biases—the sampled area may be uncertain due to variable bait plume dispersal; antagonistic behavior may impact trap efficiency; and catch saturation (i.e., declining catch rate as fishing time increases) can decouple catch and abundance. Nonetheless, traps still present a useful means of surveying crab populations, and are used in observer surveys of commercial fishing operations (Harris *et al.* 2012) or research surveys that are independent of commercial fishing effort (Scandol and Kennelly 2002). Various design specifications of traps can impact their size selectivity and efficacy. In particular, mesh size and escape gaps can be used to control size selectivity (e.g. Broadhurst *et al.* 2019). Furthermore, these variables can interact—crabs have been shown to be more motivated to find the entrance funnels of traps with smaller mesh size, as crabs are less able to access the bait by inserting their chelipeds through the mesh (Zhou and Shirley 1997), hence a greater number of funnels may improve efficacy. Thus, choosing appropriate design features that are most effective for the particular objectives under investigation is important when using traps in independent surveys.

Standard commercial traps are typically designed to avoid capture of smaller Blue Swimmer Crab, so may have limited suitability for juvenile surveys (Butcher *et al.* 2012; de Lestang *et al.* 2012; Broadhurst *et al.* 2020). Modifying the trap design with smaller mesh may improve selectivity for smaller (juvenile) crabs, where sampling of these size classes is important. Consequently, we developed a novel research trap design for independent surveys of Blue Swimmer Crab populations, incorporating smaller mesh sizes than conventional commercial round traps. To evaluate the efficacy of the new trap design relative to some existing survey methods, we evaluated the catch numbers and size structures alongside co-located samples obtained using beam trawls and standard commercial round traps. We also compared samples collected using the novel traps with commercial round traps across an entire fishing season, to ascertain how they perform as the size structure of the population changes through time.

## Methods

### Description of sampling gear

The new research traps were simply a “small-mesh trap” adapted from the standard commercial round traps (termed “large-mesh traps”) employed in commercial and recreational fisheries in south-eastern Australia (Leland *et al.* 2013). The traps were the same overall dimensions (900 mm diameter, 300 mm height) with two 10 mm stainless-steel rings to give structure to the trap. The research traps had a 25 mm diamond mesh of green-grey net (polyethylene [PE]) tied with chaff rope to the top and bottom ring. In addition, the research traps had four entry funnels instead of two (funnels were 300 x 200 mm on the outside and tapering to 200 x 50 mm). The large-mesh traps had a 55 mm diamond mesh of black net (polyethylene [PE]), and only two entry funnels, but the top and bottom ring were threaded through the mesh rather than tied with chaff rope (Figure 4). The beam trawl design employed is described in detail in Rotherham *et al.* (2008). This consisted of a stainless-steel beam trawl frame (3 x 0.8 m), and trawl body including a 3.7 m headrope, 4.1 m ground rope, with diamond-shaped 26 mm mesh made from twisted 3-strand ~1.1 mm diameter green PE.

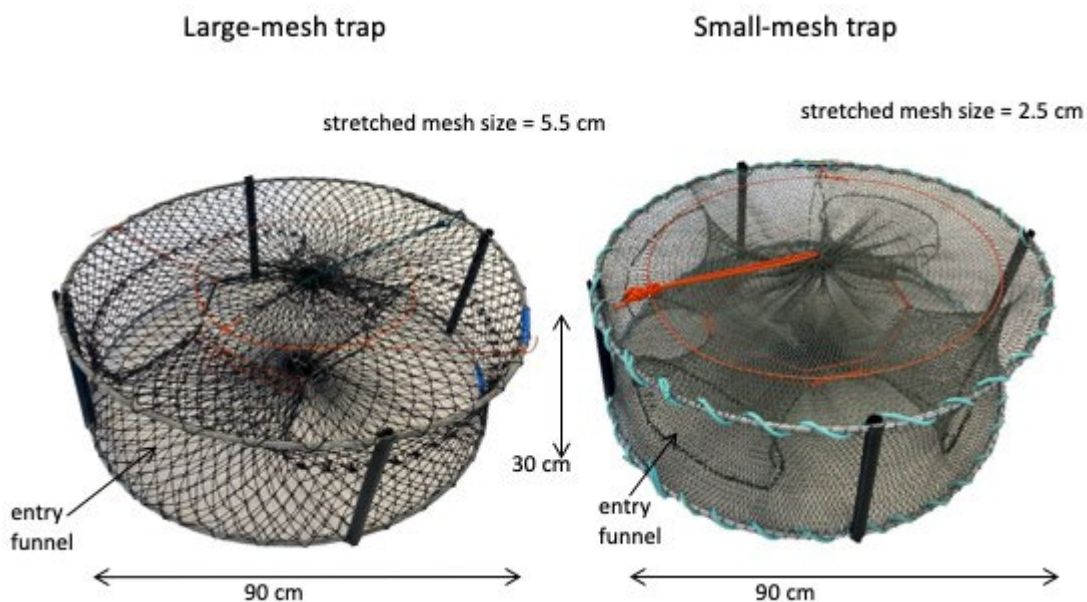


**Figure 4** Large-mesh collapsible trap common in New South Wales, Australia (left), with two entry funnels and a novel small-mesh collapsible trap with four entry funnels (right).

### Sampling design and collection

This study was conducted in Wallis Lake (32°18'S, 152°30'E), Port Stephens (32°44'S, 152°3'E) and Lake Macquarie (33°05'S, 151°35'E, Figure 1). Sampling was conducted in two phases. Phase 1 compared samples captured using the three different gears collected over four nights spread across two months (October and November 2018), in two estuaries (two nights in each of Lake Macquarie and Port Stephens). Phase 2 compared small-mesh and large-mesh traps at five sites within Wallis Lake, Lake Macquarie and Port Stephens estuary, for a period of 6 months (December to May, 2018-2019). Each estuary was sampled during two nights within each month.

For phase 1 sampling, five large-mesh traps, five small-mesh traps, and five trawl replicates (trawls were of 5-minutes duration at a speed of 1-2 knots, which covered the distance of ~150 m) were deployed within each of 4 sites within each estuary. Sampling occurred at depths of 2 – 4 m adjacent to shallow seagrass habitats, and different gears were fished simultaneously with traps deployed in the afternoon, trawling occurring in the evening, and traps collected the following day (i.e., ~18 h sets). Gear deployments were separated by >50 m. Traps were baited similarly, with two thawed Sea Mullet per trap, chopped in half, with the two tails placed inside a 20 x 20 cm bait bag of 1-cm mesh, and the two heads skewered on a metal hook, with the baits secured to the centre of the trap. GPS waypoints were used to mark the location (including start and finish for trawls) of each gear deployment. Traps were deployed and retrieved in the same order to ensure similar soak times. During phase 2, the same procedures were followed except that 4 large-mesh traps and 4 small-mesh traps were deployed at each site in three estuaries, and there was no trawling. Temperature and salinity were measured at each site to ensure that conditions were unlikely to impact on the main comparisons being made, and ranged from 17 – 25°C and 32 – 36 respectively.

Upon retrieval of gear, crabs were placed into an ice slurry for 30 seconds or less to calm them so that they could be identified and measured (Bellchambers and de Lestang 2005). Blue Swimmer Crab were counted and sexed, and carapace length (CL, the distance between the frontal notch and the posterior carapace margin) measured using vernier callipers and then released. Crabs were returned to the water at the location of capture following data collection.

## Statistical analyses

All statistical analyses were conducted in R v. 4.0.2 (R Core R Core Team 2022), and several approaches were used to evaluate efficacy of small-mesh traps, relative to large-mesh traps and beam trawl. Firstly, the total number of crabs captured using different gears at each site during phase 1 was evaluated using a generalised linear mixed model (GLMM) with a Poisson error distribution. This model included fixed factors of *estuary* (Lake Macquarie and Port Stephens) and *gear* (small-mesh traps, large-mesh traps and beam trawl) and an interaction term of *estuary:gear*. To account for dependency structure in the sampling we included random intercept effects of *site* (nested within estuary) and *date*. We note that trawls and traps have very different units of effort, but we considered a single trap or trawl a replicate “sampling unit”, as the sampling unit reflected how these gears are generally used. The model was fit using the glmmTMB package (Brooks *et al.* 2017), residuals and assumptions of the model were checked using the DHARMA package (Hartig 2020), and the pairwise comparisons were conducted using the emmeans package (Lenth 2021). The results of this model were visualised with marginal effects plots and post-hoc tests were conducted using adjusted P-values.

Due to the small number of crabs collected across beam trawl samples ( $n = 19$ ), length structures of crabs sampled during phase 1 were pooled and presented as kernel density estimates (KDE) by gear type, and differences in length structure were assessed visually. To compare the relative length-dependent catch efficiency of the three methods (beam trawl, small-mesh and large-mesh traps) we applied pairwise comparisons using the binomial generalised linear model (with a 3 degree polynomial for length) method of Herrmann *et al.* (2017). We calculated the length-dependent catch comparison ratios ( $cc_l$ ) and catch comparison rates ( $cr_l$ ) where  $l$  is a specific length class,  $cc_l$  is the ratio of crabs in a size class  $l$  caught in one type of gear compared to the total number of crabs in a size class  $l$  caught in both types of gear, and  $cr_l$  is a direct relative value of the catch efficiency between two gear types for length  $l$ . If the catch efficiency is equal to 1 then the efficiency of the gears is equal. A full description of the modelling can be found in Herrmann *et al.* (2017) and Savina *et al.* (2017), which fully derive the equations for comparable experiments. We applied a double-bootstrapping method (1000 replications, Herrmann *et al.* 2017; Savina *et al.* 2017) to calculate 95%

confidence intervals and incorporate the uncertainty in the estimation resulting from between-deployment (trawl or trap) variation in catch efficiency and availability of crabs, as well as uncertainty associated with the size structure of the catch across individual deployments. This procedure was implemented with the 'selfisher' R package (Brooks *et al.* 2022) and due to the double bootstrapping procedure inherently controlling for variation which would traditionally be simulated with a random effect of deployment/trap, we did not include any random effects. During this analysis we initially included *estuary* as a factor in the models but this was removed and the estuaries pooled as likelihood ratio tests showed the models including estuary gave no improvements over the simpler model for any of the pairwise comparisons ( $P > 0.6$ ).

Abundance data (number of crabs per trap) from Phase 2 was also analysed using GLMMs following the above method but with a negative binomial error distribution (which was found to be better than Poisson when the model residuals were inspected). Each estuary was analysed separately to simplify the interpretation. The GLMMs included *gear* (small-mesh trap and large-mesh traps) and *month* (December – May) as fixed factors and included random slope effects of *site* and *date* to account for dependency structure in the data collection. To account for sampling effort, the soak time of each trap was included in the models as an offset. As our hypothesis concerned the performance of gear type over the fishing season, the key term in the model was the interaction between *month* and *gear* which if significant would suggest the two gear types have differing efficiencies over the fishing season. This analysis was also repeated for abundance data split into size categories above and below 60 mm CL, to quantify the impacts of trap type on relative abundance above and below the size of full selectivity (~60 mm) for the large-mesh traps.

Catch selectivity of small and large-mesh traps over the 6-month fishing season was assessed in a similar way to the initial 2-month, 3-way gear comparison, through the use of binomial GLMMs. To assess if there was any variation in catch selectivity between months or estuaries, we conducted a model selection process starting with the base selectivity model (all estuaries and months pooled) and compared this to more complicated models including estuary and or month variables. As part of these hypothesis testing models, we incorporated random effects of *date* and *site* (nested within *estuary*) to account for dependency in sampling structure. The best performing model was then used to estimate the confidence intervals using the bootstrapping methods described above (after removing the random effects which the double bootstrapping naturally incorporates). As the major driver of temporal variability (within a fishing season) in sampling is likely to be the progression of size classes through the population, we considered the monthly size structure visually with KDE estimates produced for each gear type, in each estuary, each month.

## Results and Discussion

Overall, 7,768 Blue Swimmer Crab were caught across phase 1 and 2 of the sampling period. During phase 1, the small-mesh traps captured 434 Blue Swimmer Crab, the large-mesh traps captured 362 Blue Swimmer Crab individuals and the beam trawl captured 19 Blue Swimmer Crab individuals. During phase 2, 3,834 Blue Swimmer Crab were captured in the small-mesh traps, and 3,119 Blue Swimmer Crab were captured in the large-mesh traps.

### Total catch, size structure and selectivity among trap types and trawls

The abundance of crabs caught varied substantially among gears and estuaries (Figure 5). There were a greater number of crabs caught in Port Stephens than Lake Macquarie ( $\chi^2_1 = 6.778$ ,  $P = 0.009$ ), and there were differences in the number of crabs using different gears ( $\chi^2_2 = 51.529$ ,  $P << 0.001$ ). There

was no evidence of an interaction between estuary and gear ( $\chi^2_2 = 0.452$ ,  $P = 0.798$ ). Post-hoc tests revealed that more crabs were caught in small ( $P < 0.001$ ) and large ( $P < 0.001$ ) mesh traps compared to the beam trawl, but with no difference between the trap types ( $P = 0.117$ , Figure 5).

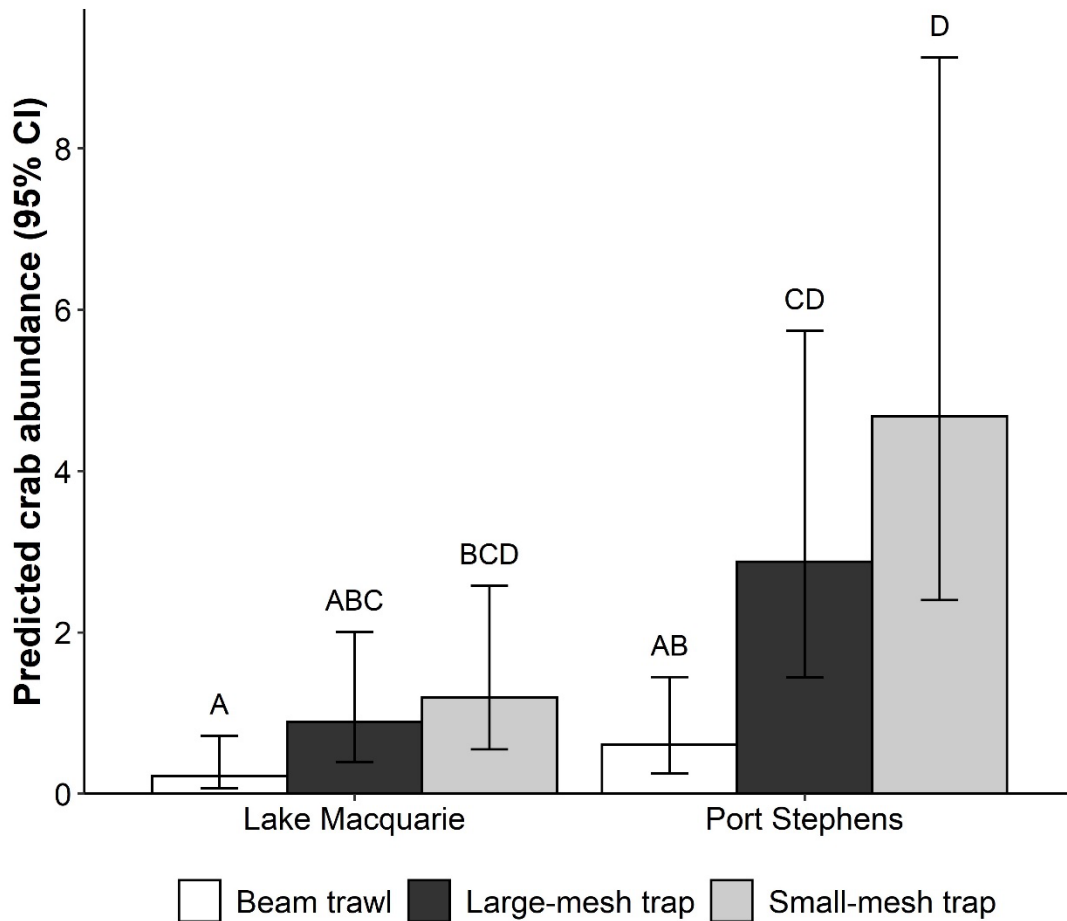


**Figure 5** Predicted crab abundance for the three gear types tested in Lake Macquarie and Port Stephens based upon generalised linear modelling. Predictions were made on the fixed effects only and the error bars therefore show 95% confidence intervals. Bars which do not share a common letter are statistically different (adjusted  $P < 0.05$ ).

There were minor differences between the length structure of crabs sampled by different gears, either when considering both sexes pooled (Figure 6), or male and female independently (data not shown). The overall size structure of crabs in Lake Macquarie appeared to be larger than Port Stephens. In Port Stephens, small-mesh traps appeared to capture more smaller crabs than large-mesh traps, and there was some evidence for multiple smaller modes that were not evident for large-mesh traps. In some instances, smaller size classes appeared to be better represented in beam trawl samples than small-mesh traps in terms of the percentage of the harvest within the gear type but this is likely due to the small sample numbers caught in beam trawls, potentially not being representative (Figure 6).

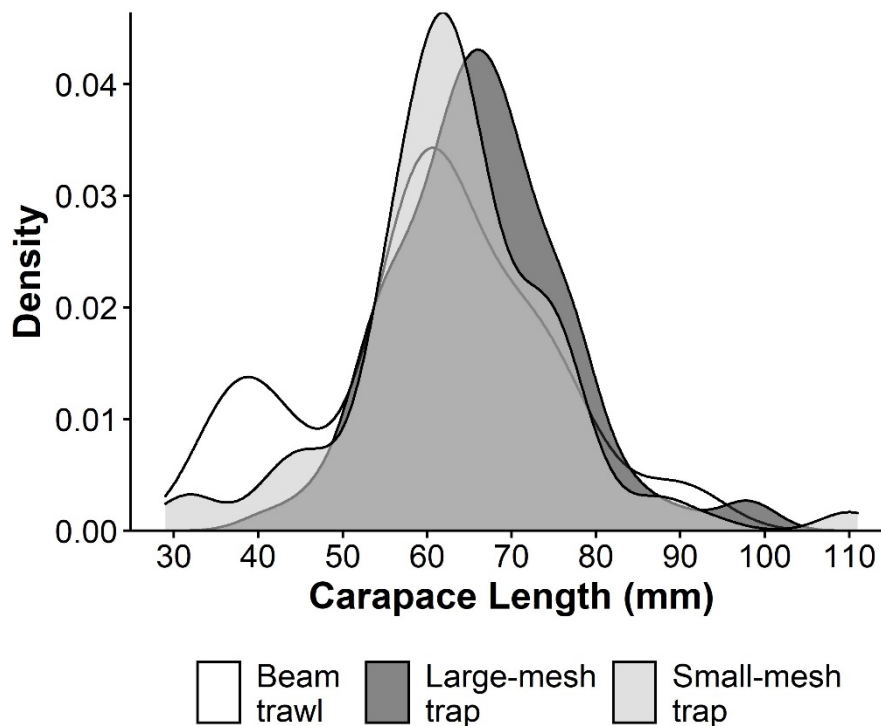


**Figure 6** Comparison of kernel density estimate (KDE) probability density functions for all Blue Swimmer Crab captured in the phase 1, 3-way gear comparison. Note all estuaries and sexes were pooled due to low numbers of crabs in the beam trawl samples ( $n = 19$ ) compared to small-mesh ( $n = 141$ ) and large-mesh traps ( $n = 90$ )

The pairwise comparisons of selectivity for phase 1 samples are visualised in Figure 7. When compared to both types of traps, beam trawls were found to catch fewer moderate size crabs. Small-mesh traps had a significantly higher catch comparison rate for crabs between 40 and 85 mm CL (*ccr* 95 % CI does not overlap 0.5; Figure 7a) while large-mesh traps had a significantly higher catch comparison rate for crabs between 53 and 82 mm CL (*ccr* 95 % CI does not overlap 0.5; Figure 7c). These patterns were reflected in the catch ratio rate with moderate sized crabs caught ~5x more in traps compared to the trawls (Figure 7b and Figure 7d). There was no evidence of differing selectivity between the two types of traps (95% CI of catch comparison rate overlaps 0.5 at all sizes) although there was a trend towards small-mesh traps being more efficient at sampling small (<50 mm CL) and large (>95 mm CL) crabs (Figure 7e). This was reflected in the catch ratio rate, with small traps likely to capture much greater numbers of small crabs (Figure 7f).

### Temporal comparison between trap types

The average number of individuals per trap varied among estuaries during phase 2, with the highest catches in Wallis Lake, followed by Port Stephens, and then Lake Macquarie. Small-mesh traps consistently captured a greater amount of crabs than large-mesh traps in Lake Macquarie ( $\chi^2_1 = 9.298$ ,  $P = 0.002$ ) and Wallis Lake ( $\chi^2_1 = 38.891$ ,  $P << 0.001$ ), but there was no difference between gears in Port Stephens ( $\chi^2_1 = 0.483$ ,  $P = 0.487$ ) and no significant interactions between Gear and Month for any estuary ( $P > 0.6$ ). Overall abundance varied through time for Port Stephens ( $\chi^2_5 = 373.313$ ,  $P << 0.001$ ), Lake Macquarie ( $\chi^2_5 = 66.434$ ,  $P << 0.001$ ) and Wallis Lake ( $\chi^2_5 = 21.947$ ,

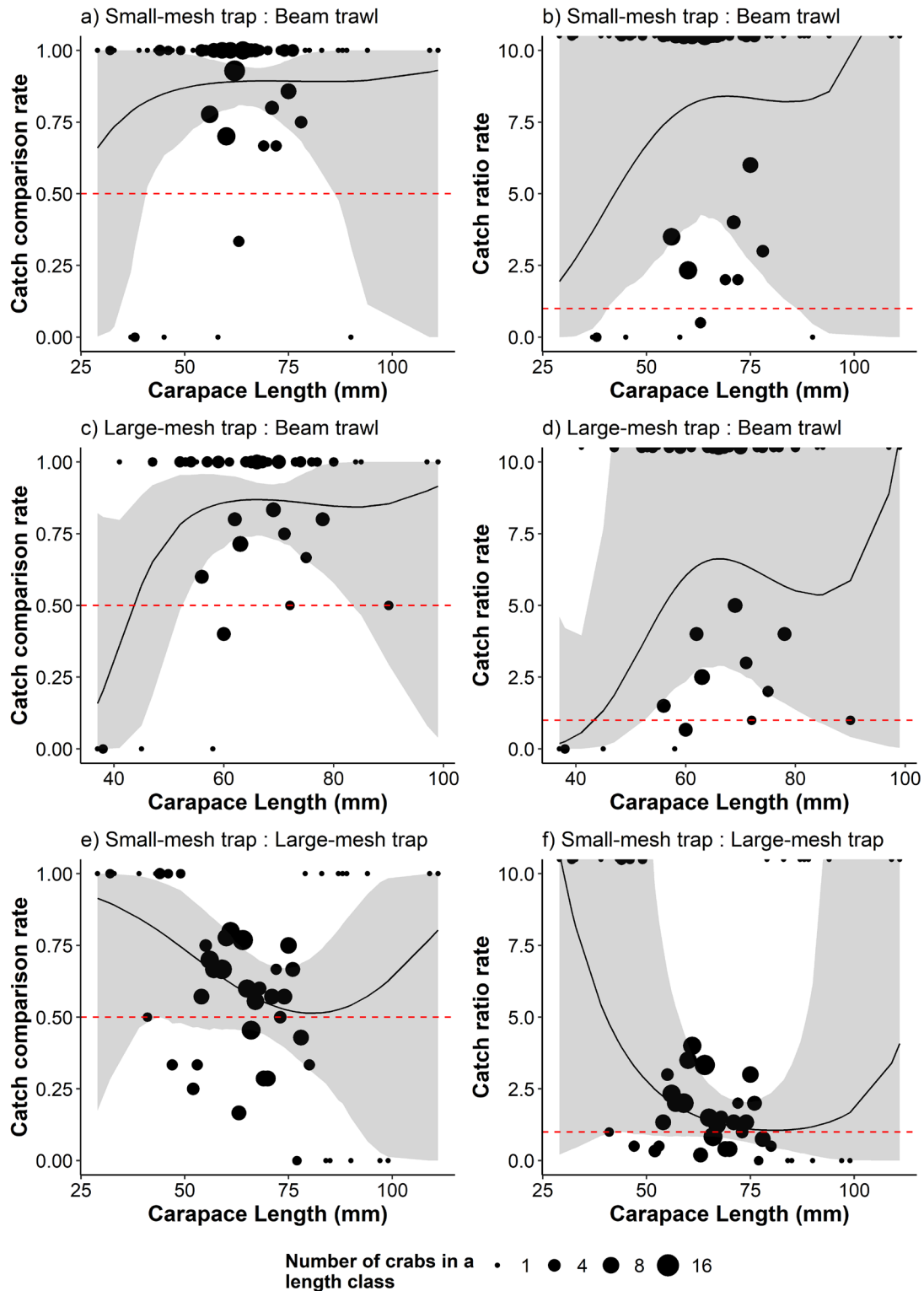


**Figure 7** Catch comparison rate (left column, a, c, e) and catch ratio rate (right column, b, d, f) for the different gear comparisons (black curve). a and b: Comparison of small-mesh traps and beam trawl. c and d: Comparison of large-mesh traps and beam trawl. e and f: Comparison of small-mesh traps and large-mesh traps. The circles represent the experimental rates with the circles scaled to the number of crabs observed in that length class. The grey ribbons represent the 95% confidence limits for the rate curves. The horizontal red dashed line shows the expected catch comparison rate in case of no difference in catch efficiency in the compared gears. In the right hand panels, dots outside the axis range (larger values) are partially visible on upper edges.

$P < 0.001$ , Figure 8), showing a minor downward trend through time in Port Stephens (Figure 8a), as opposed to clear peaks in Lake Macquarie (February and March, Figure 8b) and Wallis Lake (January and February, Figure 8c). Similar patterns were resolved when abundance data was split into groups above and below 60 mm CL (Table 1), with small-mesh traps catching a greater number of both small (<60 mm CL) and large (>60 mm CL) crabs in Wallis Lake, and small-mesh traps catching a greater number of large crabs in Lake Macquarie (very few small crabs were caught in this estuary). The small crab model in Lake Macquarie did not converge, likely due to the very low number of crabs (72 crabs over 472 traps). Again, there was no interaction between gear and month for any estuary ( $P > 0.5$ ).

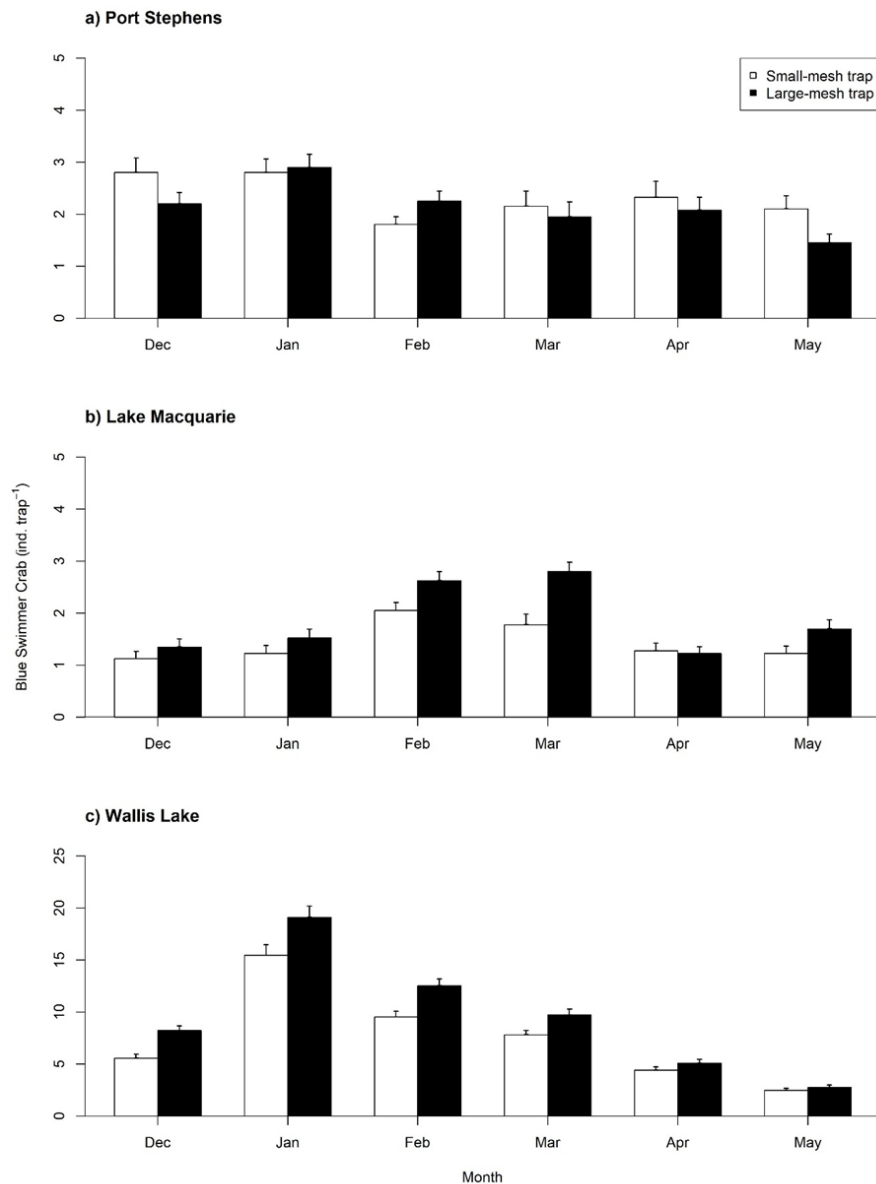


**Figure 8** Mean (+ standard error) Blue Swimmer Crab captured during each month across Port Stephens, Lake Macquarie and Wallis Lake in large-mesh and small-mesh traps

**Table 1** Summary of outcomes of the GLMMs comparing abundance of small (<60 mm CL) and large (>60 mm CL) crabs caught in small-mesh and large traps in each estuary during phase 2. Separate models were run for each estuary, crab size class combination. Significance levels are indicated as \* < 0.05; \*\* < 0.01; \*\*\* < 0.001; “nd” no difference. NA denotes a model that did not converge properly

| Estuary        | Small crabs  |   | Large crabs  |   |
|----------------|--|---|--|---|
|                | Gear   | Sampling period                         | Gear   | Sampling period                         |
| Wallis Lake    | Small-mesh > Large-mesh***<br>$\chi^2_1 = 25.421, P << 0.001$          | ***<br>$\chi^2_5 = 431.892, P << 0.001$ | Small-mesh > Large-mesh***<br>$\chi^2_1 = 21.084, P << 0.001$          | ***<br>$\chi^2_5 = 115.344, P << 0.001$ |
| Port Stephens  | Small-mesh = Large-mesh <sup>nd</sup><br>$\chi^2_1 = 18.78, P = 0.171$ | ***<br>$\chi^2_5 = 33.000, P << 0.001$  | Small-mesh = Large-mesh <sup>nd</sup><br>$\chi^2_1 = 3.135, P = 0.077$ | *<br>$\chi^2_5 = 11.235, P = 0.047$     |
| Lake Macquarie | NA   | NA                                      | Small-mesh > Large-mesh**<br>$\chi^2_1 = 7.635, P = 0.006$             | ***<br>$\chi^2_5 = 45.698, P << 0.001$  |

## Temporal variation in trap selectivity

Our model selection process identified that the most parsimonious model was the base selectivity model plus a fixed effect of estuary, suggesting that while the patterns of selectivity between the traps were similar between estuaries, there were still some differences between estuaries (Figure 9a). In all estuaries, small-mesh traps were more effective at sampling the smaller crabs and there was no indication of differing selectivity for larger crabs (Figure 9). While there was evidence for some progression through the size classes in the population over time, selectivity models which included month did not perform well, giving no indication that the selectivity of traps varied over the fishing season. When the three estuaries were pooled to estimate a global selectivity comparison of small- and large-mesh traps, the small-mesh traps were more efficient at catching crabs less than 47 mm CL (*ccr* 95% CI does not overlap 0.5), with some evidence that small traps also caught more crabs of all sizes (Figure 9c and Figure 9d).

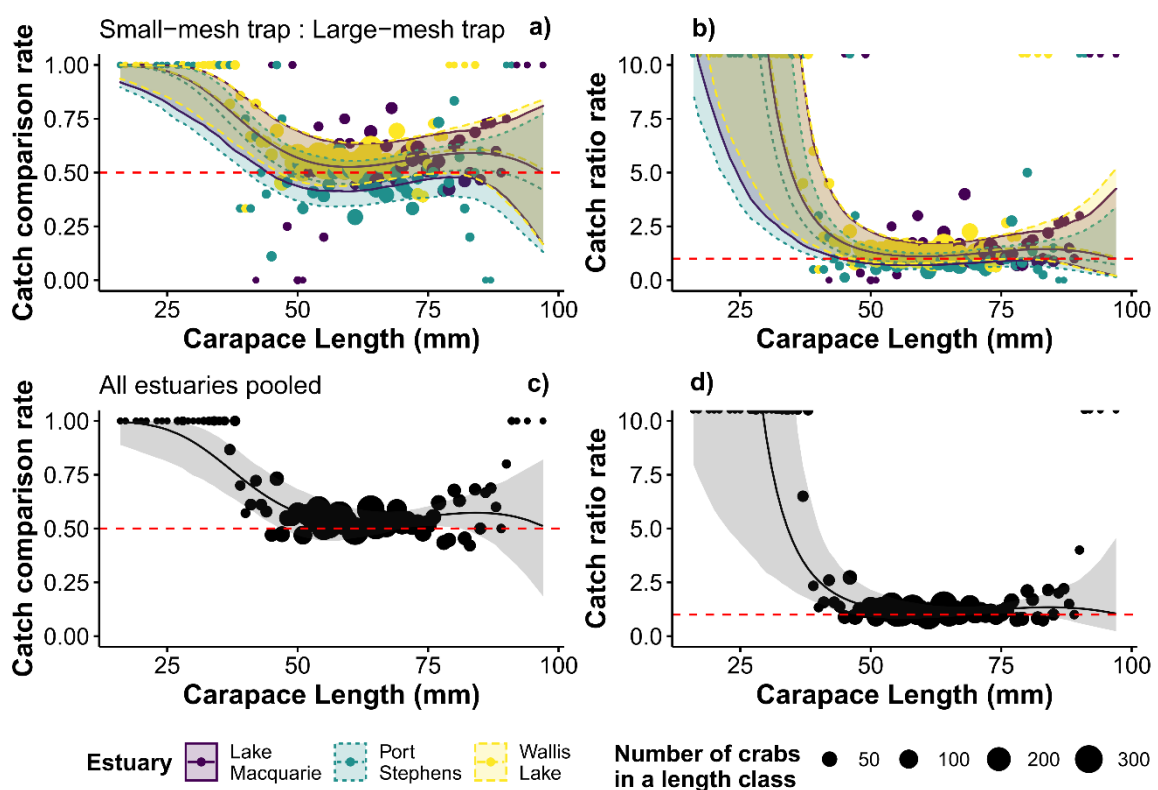


**Figure 9** Catch comparison rate (left column, a, c) and catch ratio rate (right column, b, d) for the comparison between small and large-mesh traps (lines). a and b: Results from the estuary specific modelling with colours and line types represent the different estuaries. c and d: Results from global (pooled estuaries) model. The circles marks represent the experimental rates with the circles scaled to the number of crabs observed in that length class. The ribbons represent the 95% confidence limits for the rate curves. The horizontal red dashed line shows the expected catch comparison rate in case of no difference in catch efficiency in the compared gears. In the right hand panels, dots outside the axis range (larger values) are partially visible on upper edges

## Design considerations and potential biases

Overall, the data presented here suggests the novel small-mesh traps perform in a reasonably consistent fashion across estuaries and different conditions, and thus appear to present suitable gear for fisheries independent surveys for portunid crabs. Comparison of the small-mesh traps against other survey gears in different places and times suggest that the traps can catch more crabs, and are more effective at catching smaller crabs when they are present, but also equally or more effective at catching larger size classes. The beam trawl appeared to be effective at capturing a reasonable size range of crabs, however, the number of crabs caught was substantially lower than traps (5 beam trawl replicates takes roughly a similar amount of time as it takes, to bait, deploy and retrieve 5 round traps). Therefore, small-mesh traps present a good alternative survey method to more active methods such as beam trawling, with advantages including potentially greater catch per unit effort of manpower, minimal bycatch, minimal impact on sensitive habitats, and no interaction with other set fishing gear in commercially fished estuaries.

There are several design characteristics of the small-mesh traps that may have contributed to improvements in capture efficacy, including mesh size, trap shape, and the type and number of entrances to the trap. The effect of mesh sizes, trap type and shape have been assessed previously, particularly in the context of escape gaps as a strategy to reduce capture of undersized crabs (Guillory and Prejean 1997; Guillory and Prejean 1998; Bellchambers and de Lestang 2005; Rotherham *et al.* 2013; Broadhurst *et al.* 2017; Broadhurst *et al.* 2019; Broadhurst *et al.* 2020). Previous studies have shown reduced effectiveness of finer mesh traps due to clogging of the mesh with weed (Miller 1980), however, this work mostly investigated traps with two entrances, and these problems were not encountered during our study. Previous work on the congeneric *Portunus pelagicus* also shows that round traps tended to encourage greater searching time around the trap, which enhanced the probability of finding an entrance leading to the bait (Archdale 2012). Leland *et al.* (2013), also found round shaped traps to be more effective in catching Blue Swimmer Crab when compared to rectangular, wire and hoop nets. In addition, funnel-type entrances tend to have higher catch efficiencies than other types of trap entrances (Archdale *et al.* 2006; Archdale *et al.* 2007; Bergshoeff *et al.* 2019), as they are easier to enter (Archdale *et al.* 2006) and may decrease antagonistic interactions around entry funnels that can hinder the ingress of individuals into the trap. Thus, a greater number of funnel-type entrances will aid ingress of crabs into the trap, and the decreased chance of antagonistic interaction while entering the trap is likely to particularly benefit smaller crabs.

Despite the promising results observed for small-mesh traps, any trap survey generally suffers from imprecise knowledge of the areal measure of sampling effort. In contrast, beam trawl surveys have the advantage of known or controlled swept area, such that numbers can be expressed per unit area covered (i.e., crabs ha<sup>-1</sup>). Traps on the other hand, rely on the use of bait to attract animals in the surrounding area to encounter and enter the trap. While soak time for traps can be easily determined and used to standardise catches among deployments (i.e., crabs h<sup>-1</sup>), the spatial extent of the bait plume can vary, and this is difficult to quantify. Bait plume is affected by several abiotic factors including benthic features, tide, wind and rainfall, all of which can contribute variable “sampling effort” (Taylor *et al.* 2013a) and non-circular attraction zones (Winger and Walsh 2011). This is particularly relevant where soak time transcends tidal cycles or weather events. While drogues and/or current meters can be used to provide a comparative measure of current movement during deployment (Taylor *et al.* 2013a), this is only really useful for very short-term trap deployments. Another potential issue is the decline in the strength of the olfactory stimulus throughout the deployment, which means that attraction of crabs may taper off before traps are retrieved. This would be expected to occur at similar rates between traps, so is unlikely to impact relative measures of crab abundance. While common across all trap surveys, these issues are difficult to overcome,

although there is some evidence to suggest that biological factors such as variable movement rates introduce much greater variation than plume size does (Brethes *et al.* 1985).

When used to generate an index of relative abundance, it is important that independent survey data is representative of actual abundance across population densities at the spatial scale of interest (Addison and Bell 1997; Bacheler *et al.* 2013). However, the cumulative impacts of the design and deployment of traps may create biases that impact this relationship (Miller 1980). For example, a decline in catch rate as soak-time and accumulated catch increase (i.e. saturation) is a potential source of bias in trap surveys (Bacheler *et al.* 2013). In the small-mesh traps, the observed increase in the abundance of Blue Swimmer Crab both above and below 60 mm CL, particularly in Wallis Lake (the estuary with the greatest abundance), suggests that saturation of the traps did not occur at the population densities at which crabs were sampled, and the presence of larger crabs in traps did not inhibit small crabs from entering the trap.

The small-mesh trap presented here shows promise for fisheries-independent surveys of portunid crabs, particularly where sampling of smaller recruits is important. While the choice of gear for research surveys is context- and question-specific, these traps represent a useful stand-alone sampling gear for quantifying relative abundance and size structure in crab populations. Furthermore, these traps may also be a good complementary approach to surveys of crab populations using beam trawl surveys. As with any gear, it is important to understand sources of bias that impact their efficacy, and in particular, whether this varies across different sampling conditions, different sampling locations or different size structures in the target population.

# An automated image analysis system for estimating fecundity in portunid crabs

## Background and rationale

Quantifying the effects of environmental variation on reproduction can include monitoring of fecundity, including egg production and egg quality (Lambert 2008; Grazer and Martin 2012). Previous work has demonstrated high variability in brood size for portunid crabs—for example, egg counts in Blue Swimmer Crab have been reported to range between  $10^4$  and  $10^6$  per egg mass (Sukumaran and Neelakantan 1997; de Lestang *et al.* 2003b). Several different methods for enumeration of the entire egg mass have been reported (Dodgshun 1980; Bycroft 1986; Witthames and Walker 1987; Emerson *et al.* 1990; Friedland *et al.* 2005). The early approaches described by Davis (1984) and later by Bycroft (1986) have been developed over the previous 3 decades, and contemporary approaches for estimating fecundity in invertebrates in general have been summarised by Ramirez-Llodra (2002). For vertebrates such as Atlantic Cod, Thorsen and Kjesbu (2001) described the auto-diametric oocyte method to estimate potential fecundity. Klibansky and Juanes (2008) later used a flatbed scanner and a free image analysis software to improve efficiency and precision when enumerating Atlantic Cod eggs. Friedland *et al.* (2005) describe a method to measure and count oocytes from gravimetric gonadal subsamples in Gilson's solution. More recently, for teleosts, Barnes *et al.* (2013) used an ultrasonic cleaning device to separate oocytes from preserved ovarian tissue for enumeration. Increasing the efficiency by which egg masses can be processed and counted, and the associated precision, ultimately means that more individuals can be analysed or larger subsamples can be processed, and the quality of data improved. We built on these existing approaches to develop an automated, high-throughput image capture and analysis approach for estimating fecundity in portunid crabs, employing waterproof flatbed scanner technology—ZooSCAN (Hydroptic, France, Gorsky *et al.* 2010).

## Methods

### Sample collection and processing

Blue Swimmer Crab were collected in Wallis Lake over the months of February, March, and April 2019, and Lake Macquarie (in August 2020). These surveys collected up to twenty randomly selected berried (egg bearing) female Blue Swimmer Crab with stage 1 eggs (Johnson *et al.* 2010) per month using round traps (55 mm or 25 mm mesh). Retained crabs were placed in individual bags, on ice, and transported back to the laboratory, with processing commencing within a few hours.

Initially, whole Blue Swimmer Crab (with eggs mass intact) were measured (Carapace Length [CL], mm) and weighed (g). The entire pleonal flap containing the fresh egg mass from the Blue Swimmer Crab was removed using scissors, weighed and immersed in 400 mL of 1 M KOH for 12 h to dissolve the funiculae that attach the eggs to the setae (Johnson *et al.* 2010). Following the separation process, the pleonal flap was removed and gently shaken off the pleopods using stainless steel forceps to ensure all setae were removed from the separated egg batch and weighed. The separated egg mass was then sieved through a 63  $\mu\text{m}$  sieve, rinsed using distilled water and placed into a Petri dish, and wet weight of the egg mass recorded.

The utility of the ZooSCAN was examined through direct comparisons with manual counts made using a more traditional microscopic approach (referred to as the 'manual microscope approach').

Fresh egg masses were prepared as outlined above, and five ~0.1 g subsamples were extracted from each of 10 individuals. Each subsample was placed into a Petri dish marked with quadrants, and visually counted under a compound microscope (Nikon SMZ745T), using a hand counter, before performing automated counts as described below. Two approaches were employed using the ZooSCAN; one that involved manual counts of scanned images (hereafter ‘manual ZooSCAN approach’) and an automated routine (hereafter ‘automated ZooSCAN approach’).

## ZooSCAN approaches

Following the manual microscope approach, each subsample was diluted in 100 mL of distilled water and poured into the sample receptacle of the scanner. Manual inspection was carried out to ensure eggs were separated and not attached to each other; if eggs were stacked vertically, a bamboo needle was used to manually isolate them. The image capture routine was executed using the propriety ZooSCAN software (v.2.0.1), at a resolution of 2400 dpi (Figure 10).

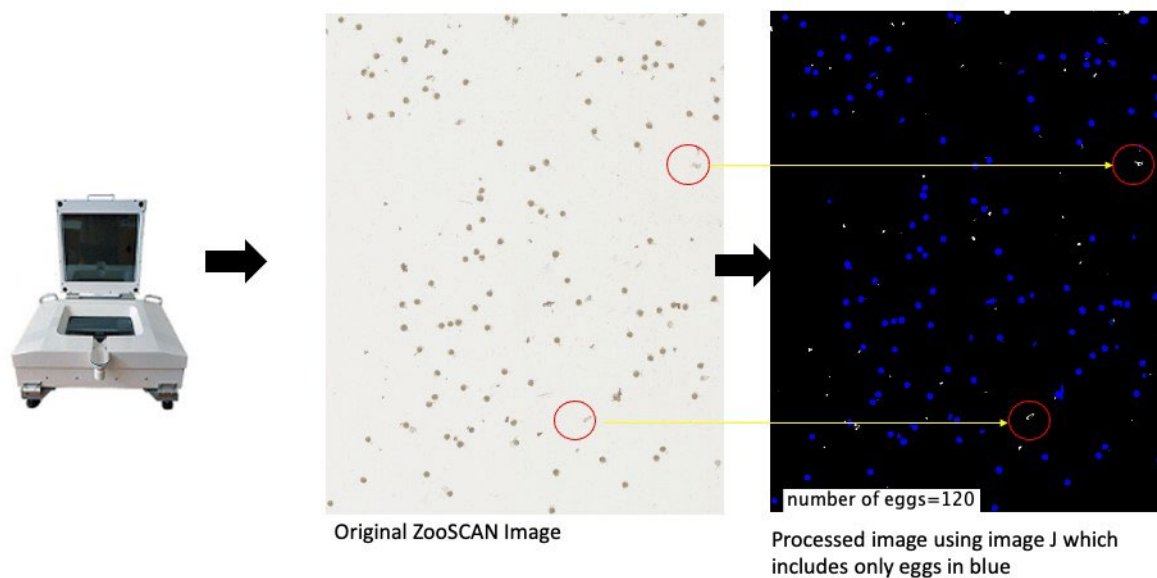


**Figure 10** Schematic of the ZooSCAN (left) processing methodology with the digitised image (middle) and enhanced image (right), processed using a custom macro in ImageJ (total number of eggs is 120).

Counted eggs are highlighted in blue and debris that is automatically excluded from counts is highlighted in yellow within the red circle.

The manual ZooSCAN approach involved performing a manual count on the image, as had been done under the microscope. Following this, automated ZooSCAN approach employed a custom macro that enhanced, filtered, and enumerated eggs in the image (the macro code is provided in Supplementary Information) in ImageJ (v.1.52.a) developed from earlier work (Friedland *et al.* 2005; Klibansky and Juanes 2008; Barnes *et al.* 2013; Schilling *et al.* 2019). Enhancement included converting the image to 8-bit and applying several rules to remove background “noise” (which included floating debris such as setae or lysed eggs, largely determined initially through trial and error). This was followed by filtering the threshold to a black and white image while manually adjusting the threshold between 0 – 255 and converting to a masked binary image (Figure 10). The image was assessed for any clumping of eggs which was separated using the watershed function, which separated the clumping by 1 pixel

(Duan *et al.* 2008). The egg abundance and egg size assessments were performed using the analyse function by setting the circularity (0.8-1). The time taken to perform each of the above workflows was recorded for each sample (nearest second), to compare the efficiency of this approach.

## Data analyses

All statistical analyses were conducted in R v.4.0.2. The new approach was compared with the manual microscope approach, both in terms of the time taken to perform each workflow, and the paired counts of each subsample that were obtained using each approach. The consistency of counts between manual microscope approach and each of manual ZooSCAN and automated ZooSCAN approach was estimated by fitting a linear regression between the two variables, and then conducting a Wald's test to evaluate the null hypothesis of parity (i.e.  $\beta = 1$ ) between the sets of counts.

A simulation model was used to evaluate the relationship between the number of egg masses enumerated and the precision of the resultant estimate of mean eggs-per-gram (eggs  $\text{g}^{-1}$ ), using data from the ~20 egg masses per month collected from Wallis Lake. Mean and variance estimates of eggs  $\text{g}^{-1}$  were used to generate a probability distribution for each month separately to investigate if monthly variations on sample size was present. These distributions were then sampled to generate egg count data through 10 sets of simulations, with each set reflecting scenarios whereby 2, 4, 6, 8, 10, 12, 14, 16, 18 or 20 individuals ( $n$ ) were randomly sampled from the artificial population and the resultant egg count data used to estimate a summary statistic (i.e., mean) for that month. This approach was intended to simulate the effect of sampling and analysing  $n$  individuals from a population at a particular time point (month), to derive an estimate of mean eggs  $\text{g}^{-1}$  for use in fecundity calculations. A log-linear regression was fitted to all simulated data to provide a unifying model that related the number of samples to the probability that the derived estimate was reasonably close (within a threshold of 15%) of the actual population mean.

## Results and Discussion

The automated ZooSCAN approach was able to successfully replicate the egg counts ( $n = 10$ ) derived using the manual microscope approach, with a high throughput workflow. There was some minor variability in the subsample size ( $0.098 \pm 0.000$  g, mean  $\pm$  SE; range 0.089 - 0.106 g) and coupled with differences in egg size meant the counts from these samples ranged from ~50-500 eggs. This gave a good range of variation over which to evaluate the methodology. While there was a relationship between the number of eggs enumerated using the manual microscope approach and the manual ZooSCAN approach ( $R^2 = 0.984$ ,  $\beta = 0.948$ ,  $t = 55.56$ ,  $P \ll 0.001$ , Figure 11), Wald's test showed that the minor difference in the slope ( $\beta = 0.948$ ) from parity ( $\beta = 1$ ) was statistically significant ( $F_{1,49} = 9.022$ ,  $P < 0.004$ ). This was due to the counts from the manual ZooSCAN approach appearing to be slightly lower than the manual microscope approach for samples where eggs were more numerous. There was similarly a relationship between the number of eggs enumerated using manual microscope approach and the automated ZooSCAN approach ( $R^2 = 0.988$ ,  $\beta = 0.981$ ,  $t = 63.84$ ,  $P \ll 0.001$ ), and Wald's test indicated that the relationship between these two variables was not significantly different to parity ( $F_{1,49} = 1.482$ ,  $P < 0.229$ ), meaning the two approaches were effectively yielding the same data (Figure 11).

The advantage of the automated ZooSCAN approach becomes apparent when the time taken to process the workflow is considered. For the manual counting methods, regardless of technique, processing time per subsample increased in proportion to the number of eggs in the subsample.

However, it was more difficult to manually count eggs on the ZooSCAN image than using the microscope, and particularly for a larger number of eggs (evident in a steeper relationship for manual ZooSCAN in Figure 12). The processing time for automated counts of the ZooSCAN image were largely invariant (~30 seconds), regardless of the number of eggs in the subsample. To our knowledge, this is the first application of the ZooSCAN to quantify and measure portunid eggs. The ZooSCAN is most commonly used to process samples of other small biological particles, such as zooplankton (Gorsky *et al.* 2010). The ZooSCAN has however been used to enumerate eggs in teleost fish (Barnes *et al.* 2013) with similar improvements in efficiency.

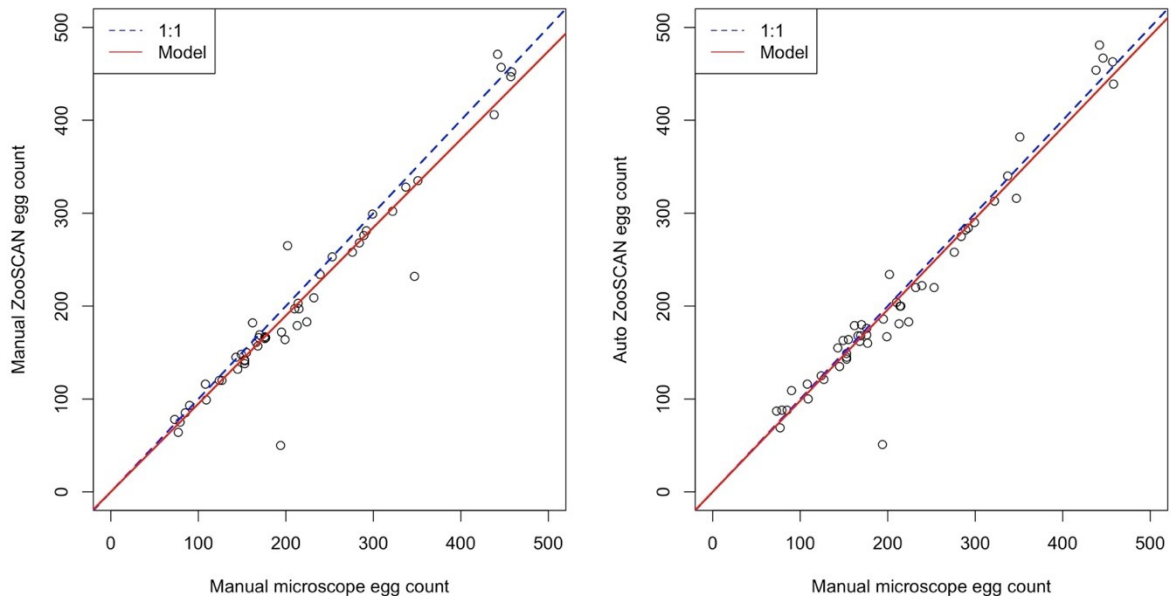


**Figure 11** Linear regression between egg counts derived from the manual microscope approach and the manual ZooSCAN approach (left panel), and automated ZooSCAN approach (right panel). The dashed blue line represents the 1:1 line and the red line represents the linear models described in the text ( $n = 10$ ).

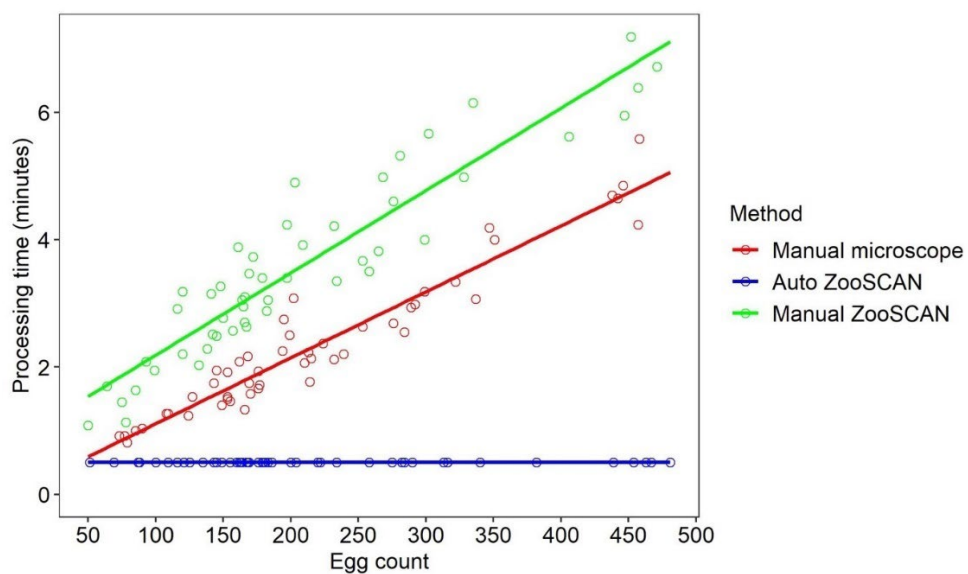


**Figure 12** Processing times for the different egg counting methods examined, including manual microscope approach (red line), manual ZooSCAN approach (green line) and the automated ZooSCAN approach (blue line).

The simulation model for Wallis Lake Blue Swimmer Crab egg masses indicated that only a comparatively small number of individuals would need to be sampled to produce a reasonable estimate of eggs  $g^{-1}$ . The results inform the number of individuals that should be considered in sampling programs to estimate eggs  $g^{-1}$  for each sampling point; given the field-derived data  $\sim 10$  individuals would need to be collected to produce a 90% probability that the estimated mean egg count was within the error threshold, and only  $\sim 6$  individuals would be required for an 80% probability. We note that this is not intended to inform the size-fecundity relationship (i.e., what size range of individuals need to be sampled). We also note that there was some variability in this relationship among months (at least within the three months sampled, Figure 13), which probably reflected temporal changes in the overall variability within the population as the breeding period progressed (e.g. Hamasaki *et al.* 2021).

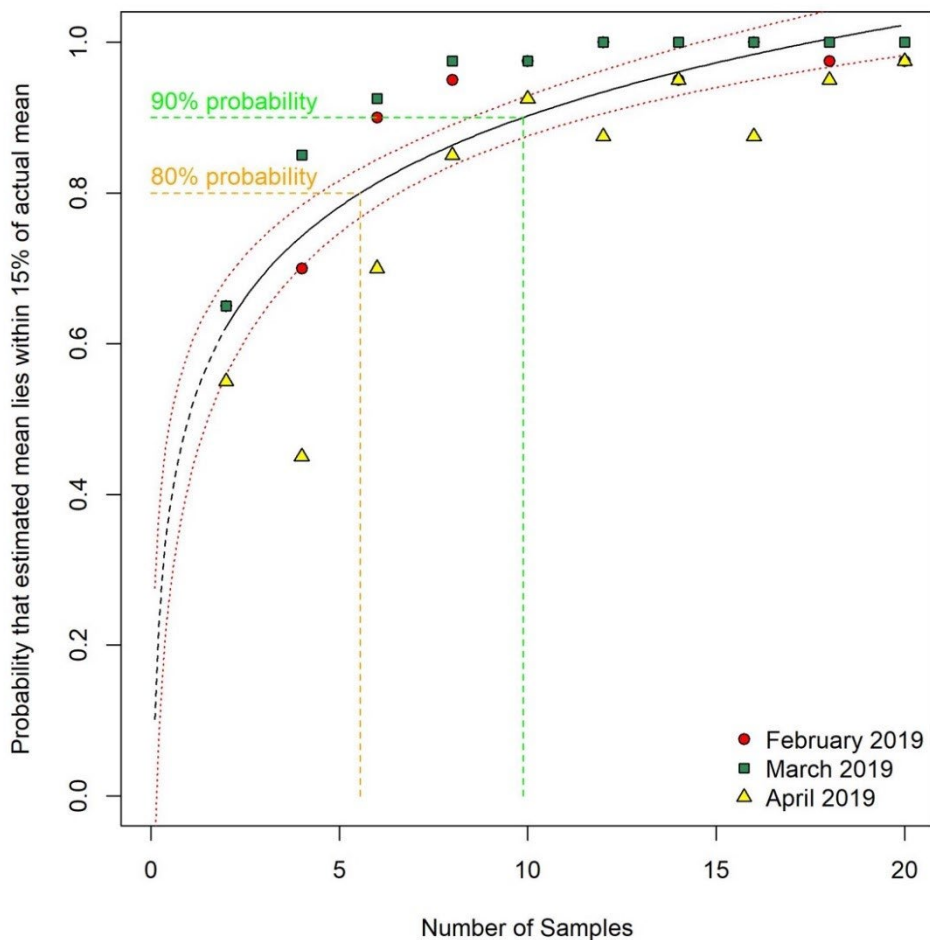


**Figure 13** Fitted model relating sampling effort of Blue Swimmer Crab egg masses with the probability that the estimated mean lies within the error threshold (i.e., the true mean estimated from the data,  $\pm 15\%$ ). The solid black curve indicates the fitted model, and the black dashed line indicates a curve segment that is extrapolated past the range of data simulated (confidence intervals are indicated as dotted red lines). Data points from simulations for each month are as indicated in figure legend (note that some data points overlap). Also indicated is the corresponding number of

samples required to achieve an 80% (orange dashed line) and 90% (green dashed line) probability that egg count mean estimates lie within 15% of the actual mean.

The number of egg masses examined in fecundity studies is highly variable, we suspect due to variations in the resources assigned to sample and analyse the specimens—a review of recent studies reported sample sizes ranging between 1-69 individuals for each month to inform estimates of fecundity for crustaceans (Johnson *et al.* 2010; Ravi and Manisseri 2013; Hamasaki *et al.* 2021). As is to be expected, sampling a greater number of individuals is more likely to approximate the true mean of the population in a particular location. This relationship provides some goal posts which can be used to guide sampling effort when conducting population surveys to inform estimates of fecundity, and while our relationship is probably specific for Blue Swimmer Crab, the approach employed is broadly applicable to other species. This will be advantageous both for optimising resources (in terms of enumerating eggs for as few individuals as necessary but over as broad a time period as possible), and limiting the overall number of egg-bearing females that are removed from the population for enumeration of egg counts. Swiney *et al.* (2010) found that fecundity in the Alaska Red King Crab (*Paralithodes camtschaticus*) varied temporally and spatially and recommend that temporally stratified sampling should be used to capture these variations. In addition, temporal variability in size-specific fecundity has been observed in the Hawaiian spiny lobster (*Panulirus marginatus*), suggesting the importance of routine data collection to support stock assessment (DeMartini *et al.* 2003).

Overall, the novel method we propose here has obvious implications for sampling efficiency of egg-bearing decapods, and simultaneous determination of patterns in egg size. The sample mounting and image capture methodology afforded by the ZooSCAN means that image quality is consistent, image collection is easily standardised, and digitisation means that images can be easily archived for later reference. Using the automated processing macro supports processing times up to 6x faster than manual counting under the microscope, while providing comparable data, with the additional advantage that the macro simultaneously captures information on egg size.

# Fishery independent survey of Blue Swimmer Crab – Description and data summary

## Background and study locations

Following initial pilot work, a long-term fishery independent survey targeting Blue Swimmer Crab was established which ran through the duration of the project. This was implemented to provide an extended time series of crab abundance, size structure, and reproductive data to provide a basis for understanding seasonal and interannual variation in these variables, model potential abiotic drivers, and support the design and development of an ongoing independent survey program for the species. The data from this independent survey is analysed in later sections of the report, but broad patterns in the data are summarised below.

The survey took place within three estuaries on central section of the NSW coast (Figure 1): Wallis Lake (Figure 14), Port Stephens (Figure 15), and Lake Macquarie (Figure 16). These estuaries were selected for the fact that Wallis Lake and Port Stephens generally support abundant Blue Swimmer Crab, which is in turn reflected in these estuaries supporting the largest commercial catches within NSW (Figure 2). Lake Macquarie is a Recreational Fishing Haven (RFH) so no commercial fishing is permitted, but the estuary supports the largest recreational Blue Swimmer Crab fishery in the state (Ochwada-Doyle *et al.* 2014). All three estuaries are geomorphologically distinct.

Wallis Lake is a wave-dominated barrier estuary of waterway area of 99 km<sup>2</sup> draining a catchment of 1,196 km<sup>2</sup>, with a narrow, trained entrance to the sea (Figure 14). The estuary is fed by two main tributaries which enter in the north adjacent to the mouth; the Wallamba River and Khappinghat Creek. The bulk of the waterway area lies in the south of the lake, delineated from the northern section by a network of deltaic islands. The estuary is comparatively shallow (2.3 m average depth) and has extensive seagrass beds (3,480 ha), comprising ~35% of available waterway area.

Port Stephens is an immature tide-dominated estuary with a waterway area of 134 km<sup>2</sup> draining a catchment of 297 km<sup>2</sup>. The estuary has an expansive mouth, is much deeper than Wallis Lake (14.1 m average depth), and is fed by the Karuah River to the west and the Myall River to the north (Figure 15). The estuary also has extensive seagrass beds (1,400 ha, Glasby and West 2018), and falls within the Port Stephens Great Lakes Marine Park (<https://www.dpi.nsw.gov.au/fishing/marine-protected-areas/marine-parks/port-stephens-marine-park>), which includes habitat protection zones and no-take sanctuary zones where fishing is not allowed.

Lake Macquarie is an immature, wave-dominated barrier estuary with a waterway area of 114 km<sup>2</sup> draining a catchment of 604 km<sup>2</sup>. The estuary is connected to the sea by a shallow and narrow channel with a trained entrance (Figure 16), and consequently conditions in the lake are primarily wind-driven (Taylor *et al.* 2017d). The lake has a deep central basin surrounded by a shallow periphery where seagrass is abundant (1,500 ha, Glasby and West 2018). There is minimal freshwater input into the estuary, but two power stations situated on the shores of the lake have a significant influence on the water temperature in the system (Taylor *et al.* 2017e).

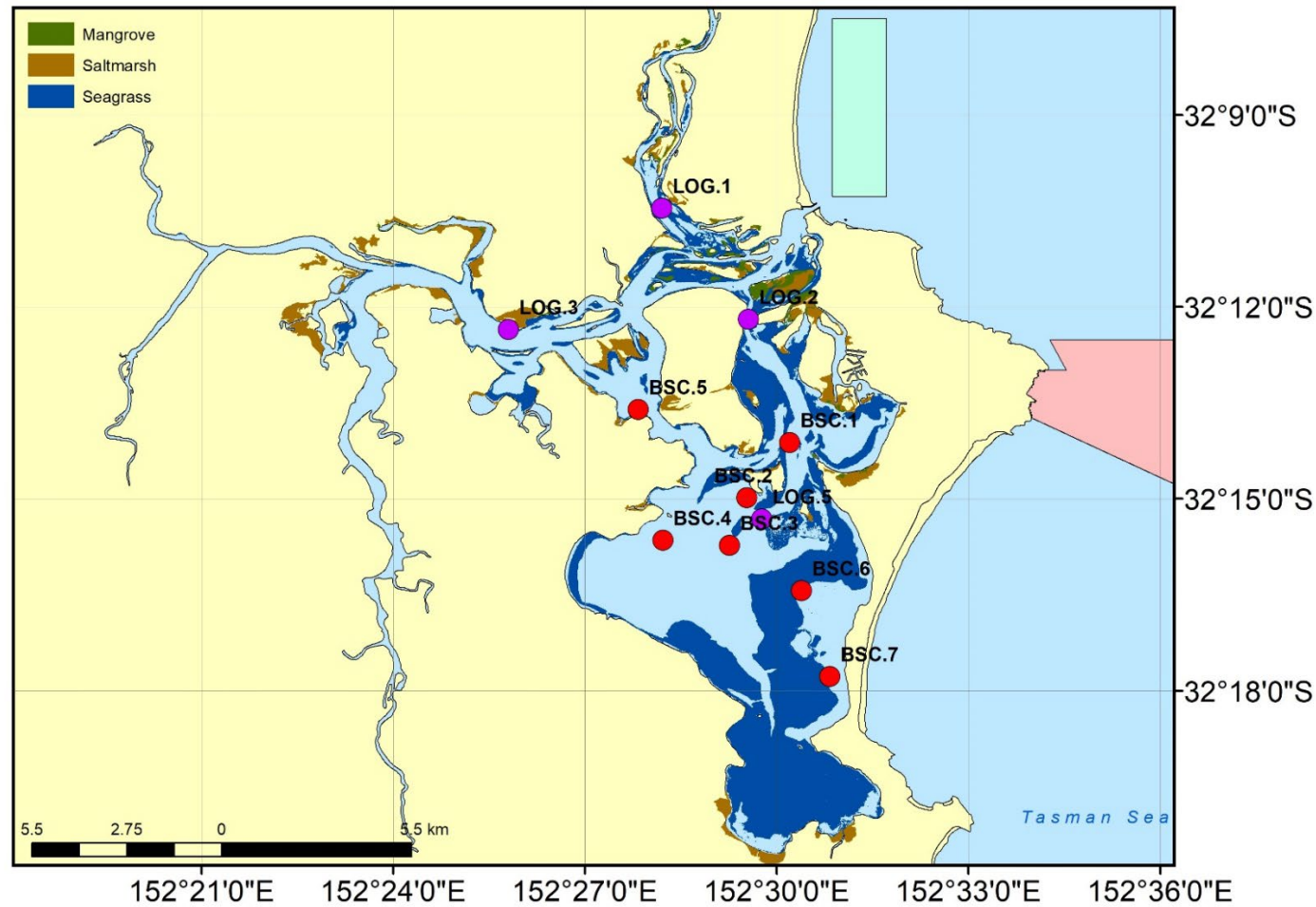


**Figure 14** Detail map of Wallis Lake showing sites targeted during the regular independent survey program (denoted as BSC.*n*), the inshore sub-program (teal polygon), and logger stations (denoted as LOG.*n*) where water quality was continually monitored during the program. Also indicated are emergent aquatic habitat types within the estuary (see legend) and marine park no-take zones (pink polygons).

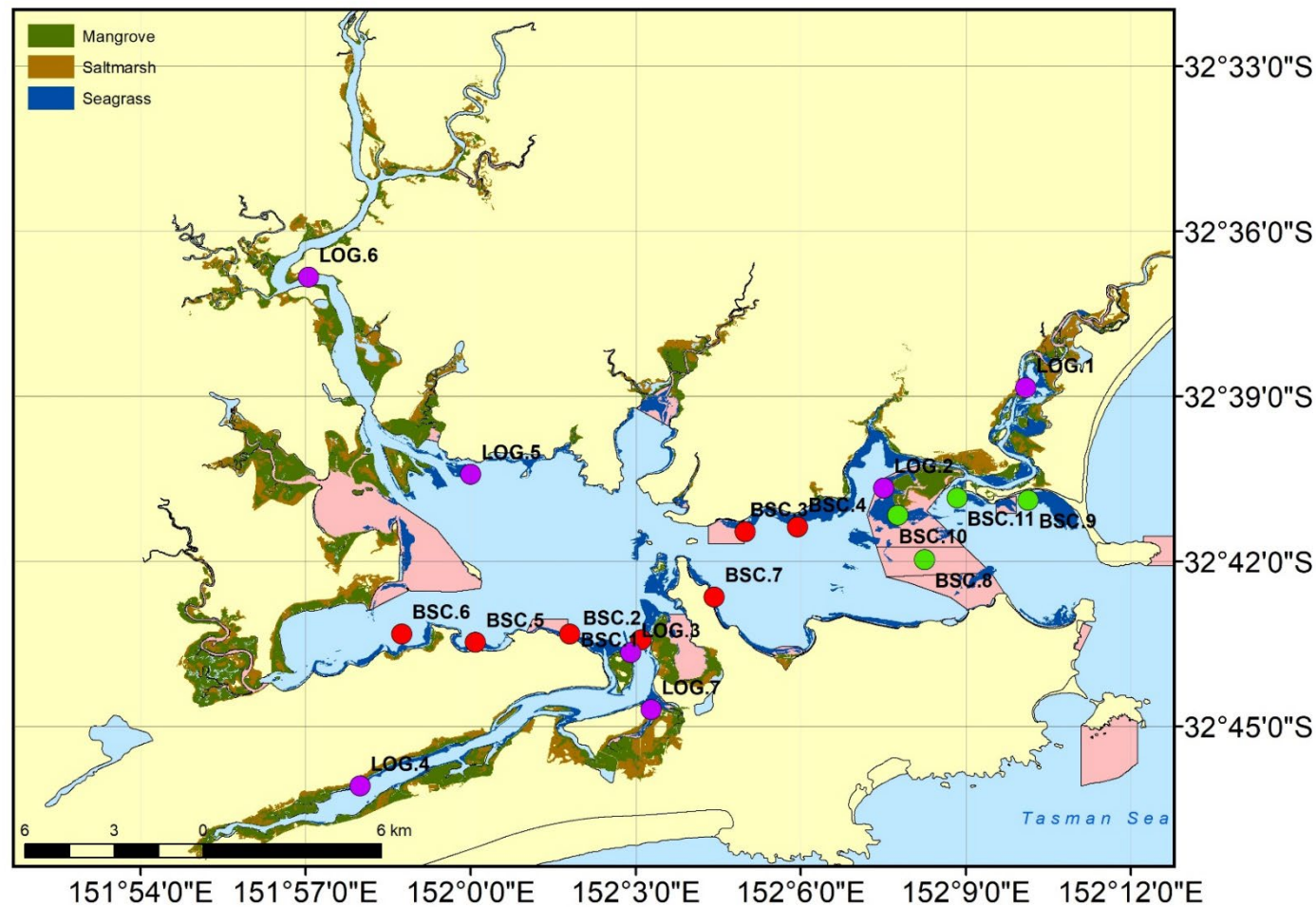


**Figure 15** Detail map of Port Stephens showing sites targeted during the independent survey program (denoted as BSC.n, red circles for regular independent survey, green circles for Port Stephens sub-program), and logger stations (denoted as LOG.n) where water quality was continually monitored during the program. Also indicated are emergent aquatic habitat types within the estuary (see legend) and marine park no-take zones (pink polygons).

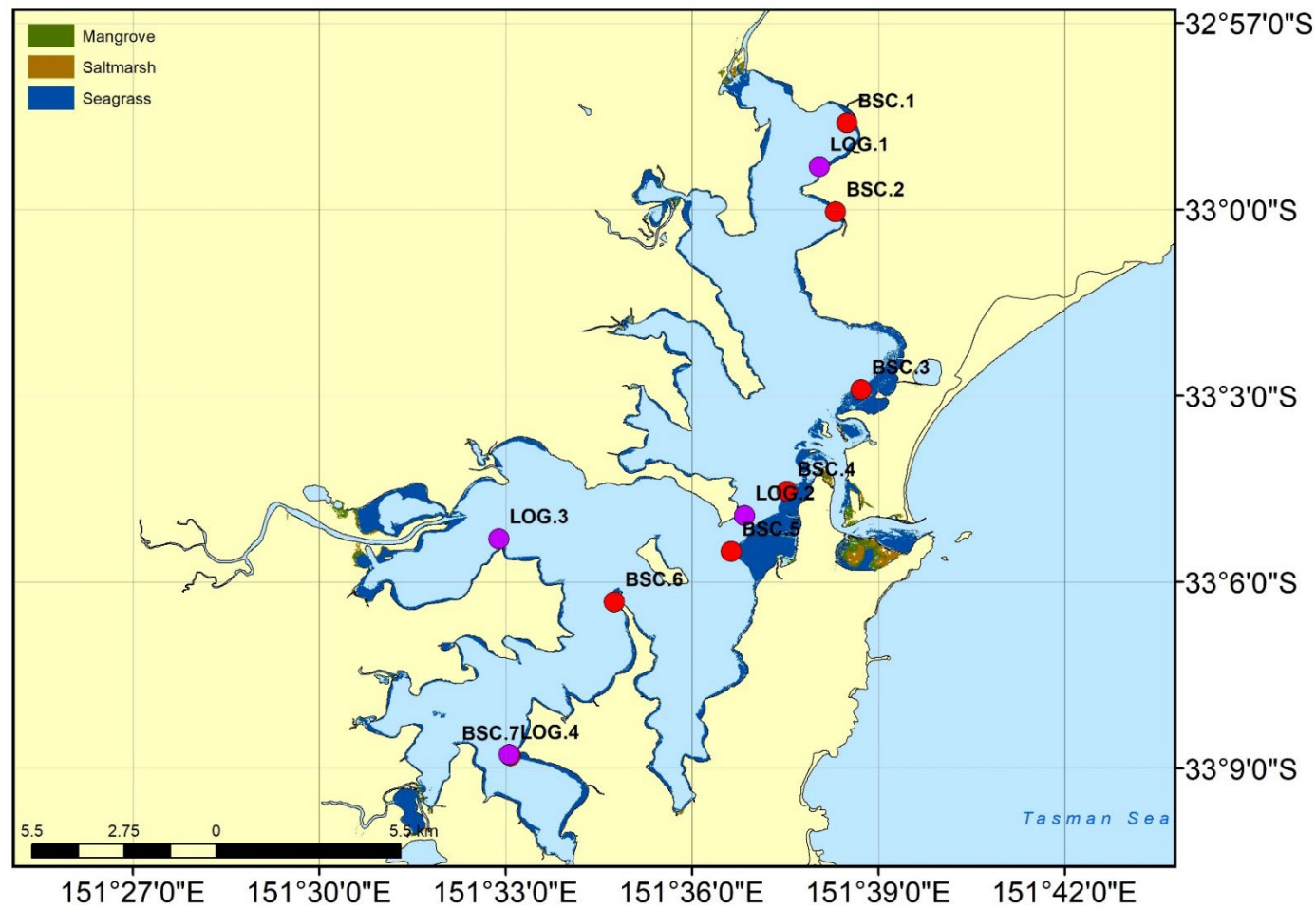


**Figure 16** Detail map of Lake Macquarie showing sites targeted during the independent survey program (denoted as BSC.*n*), and logger stations (denoted as LOG.*n*) where water quality was continually monitored during the program. Also indicated are emergent aquatic habitat types within the estuary (see legend).

## Survey design and approach

The regular independent survey spanned the period from November 2018 – March 2021 (with the Wallis Lake survey extended to June 2021). Seven sites were sampled within each estuary using six small-mesh traps, with the exception of the period prior to May 2019, during which five sites were sampled using five large-mesh and five small-mesh traps. Sampling was conducted monthly within each estuary, with two nights sampled during each month. Sampling involved deploying traps at each site, generally in waters of depth 2 – 4 m adjacent to shallow seagrass habitats, with each trap separated by >50 m. Traps were baited with two thawed Sea Mullet per trap, chopped in half, with the two tails placed inside a 20 x 20 cm bait bag of 1-cm mesh, and the two heads skewered on a metal hook, with the baits secured to the centre of the trap. Traps were cleared and re-baited after 18-24 hours, and redeployed for the second night. GPS waypoints were used to mark the location of each trap, and traps were deployed and retrieved in the same order to ensure similar soak times. Water quality measurements were recorded at each site.

Upon retrieval of gear, bycatch was cleared and crabs were placed into an ice slurry for 30 seconds or less to calm them so that they could be identified and measured (Bellchambers and de Lestang 2005). Crabs were counted, sexed, stage of maturity determined, and the carapace length (CL, the distance between the frontal notch and the posterior carapace margin) was measured using vernier callipers and then released. Crabs were returned to the water at the location of capture following data collection, with the exception of a subsample of up to 20 crabs (including berried females) per estuary per month, which were retained on ice for laboratory analysis following the conclusion of each sampling event.

## Supplementary sampling

In addition to the above sampling design, the regular independent survey was supplemented by three additional sampling sub-programs for Blue Swimmer Crab. The 'inshore sub-program' was designed to provide data on the relative abundance and size structure of crabs that had moved from Wallis Lake to adjacent inshore waters following the cooling of estuarine waters in late Autumn and Winter. Consequently, inshore waters were sampled adjacent to the mouth of Wallis Lake (Figure 14), monthly, between May and September, during each year of the survey, using 20 traps of 130 cm diameter, 30 cm height, and 5.5 cm mesh size. Twenty traps were deployed in a rough line extending from the mouth of the estuary along the sandy habitats to the north (with the sampling region informed through consultation with commercial fishers), on each of two nights per month, with traps baited as outlined above.

The 'Port Stephens sub-program' extended the independent survey in Port Stephens to evaluate relative abundance and size structure of Blue Swimmer Crab within waters adjacent to the mouth of Port Stephens, which were subject to protection from fishing mortality (Figure 15). Thus, the regular independent survey was expanded to include sampling at two additional sites within the Fly Point – Corrie Island Sanctuary Zones near the mouth of the estuary (BSC.8 and BSC.10), alongside two adjacent 'reference' locations (BSC.9 and BSC.11). This work followed the approach outlined for the regular independent survey, with trapping occurring on two consecutive nights per month from October 2019 to April 2020.

The 'latitudinal sub-program' extended the independent survey into two additional estuaries to the south of the main survey estuaries, to capture a broader latitudinal spread of samples (Botany Bay and Lake Illawarra, Figure 1 and Figure 17). Sampling targeted four sites within each of these estuaries, with six replicate large mesh crab traps deployed per site over one night per month

between October 2019 and February 2020 (the data from this subprogram were analysed alongside a subset of four sites closest to the mouth in each of Wallis Lake, Port Stephens and Lake Macquarie). Again, this work followed the approach outlined for the regular independent survey.

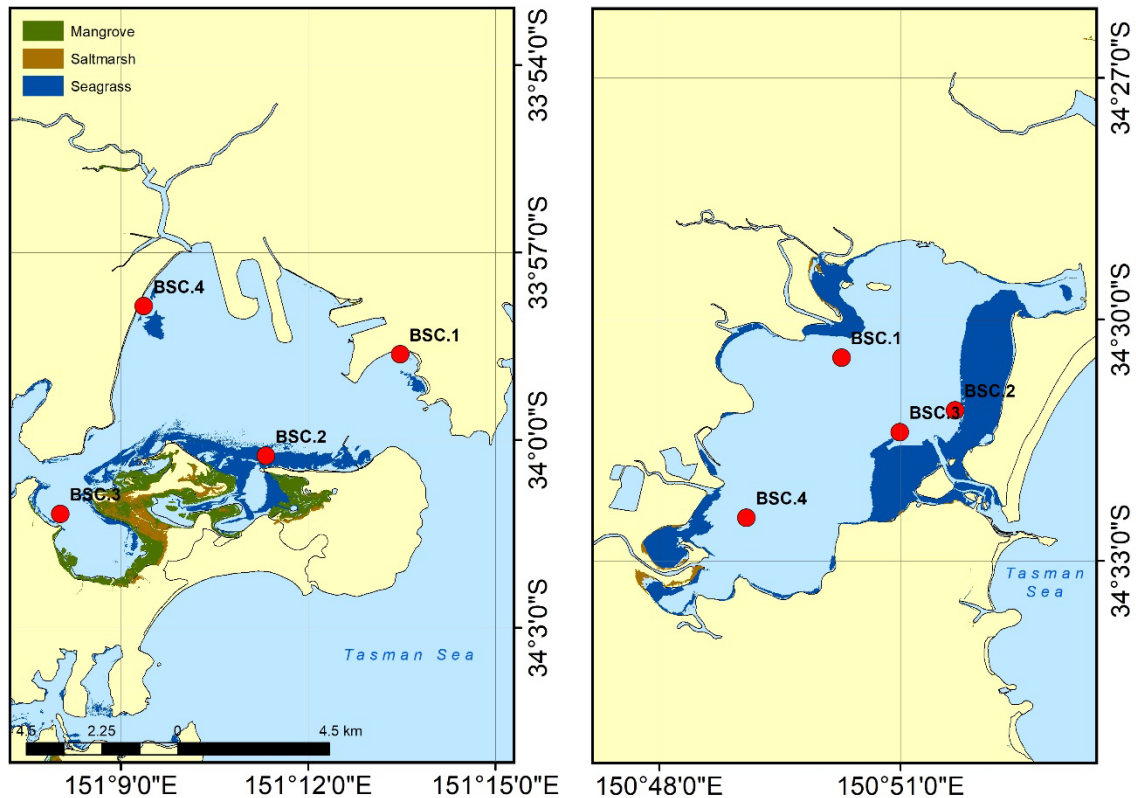


**Figure 17** Detail map of Botany Bay (left panel) and Lake Illawarra (right panel) showing additional sites targeted during the latitudinal sub-program (denoted as BSC.*n*). Also indicated are emergent aquatic habitat types within the estuary (see legend)

## Laboratory processing

In the laboratory, Blue Swimmer Crab were macroscopically examined for sexual maturity and gonad stage. Female crabs were determined to be mature when the oval shaped pleonal flap could be separated from the carapace. In addition, during the puberal moult, the pleonal flap changes shape from triangular to oval while becoming loosely fixed to the carapace (Smith *et al.* 2004; Johnson *et al.* 2010). Crabs were weighed (g), carapace length measured (mm), and the ovaries were staged (Johnson *et al.* 2010; Liu *et al.* 2014). For the latitudinal sub-program, the ovaries and hepatopancreas were then dissected out and weighed (wet weight). Dissection protocols detailed above were similar for the berried female crabs, with additional steps performed to process eggs (as below). Again for the latitudinal sub-program, the pleonal flap and the attached fresh egg mass were removed from each crab and immersed in 400 mL of 1M potassium hydroxide (KOH) solution for 12 hours to dissolve the funiculae that hold the eggs to the setae (Johnson *et al.* 2010). Following separation, eggs were washed and strained thoroughly using a 60 µm sieve, then the total egg mass was weighed (to 0.01 g).

## Water quality monitoring

In addition to the point measurements of water quality collected during the independent survey program, several logger stations were established in the main survey estuaries to provide a continuous time series of temperature and conductivity data to support modelling and interpretation of patterns observed in Blue Swimmer Crab abundance, size structure, and reproduction. These stations are indicated in Figure 14, Figure 15, and Figure 16. Each station was equipped with a Hobo U24-002-C (<https://www.onsetcomp.com/products/data-loggers/u24-002-c>), which was moored above the benthos either on existing infrastructure or independent moorings. Loggers were set to record a temperature and conductivity measurement every 15 minutes, and loggers were downloaded every 1-3 months. There were several instances of logger theft, logger loss, or logger failure, that led to breaks in the time series at various stations during the program.

Estuarine inflow was also recorded during the study period through the permanent flow gauge network maintained by WaterNSW (available at <https://realtimedata.watersnsw.com.au/water.stm>). At the conclusion of the sampling program, daily averaged flow data was downloaded from the online database for flow gauges at Wang Wauk (station 209006, on the Wang-Wauk–Coolongolook River which flows in Wallis Lake), Booral (station 209003, on the Karuah River which flows into Port Stephens), and Cooranbong (station 211008, on Dora Creek which flows into Lake Macquarie).

## Summary of broad trends in water quality, abundance, and size structure

### Water quality and flow throughout study period

Divergent patterns in inflow, conductivity, and temperature were observed among months and estuaries throughout the study period (Figure 18, Figure 19 and Figure 20). During the first year of the project, coastal and inland NSW was experiencing severe drought, and there were no obvious flow pulses until February 2020. This contributed to comparatively stable conductivities at most logger stations during this period. Following February 2020 there were infrequent, but obvious, peaks in flow at various points during the time series, which in turn led to noticeable reductions in conductivity. However, the magnitude of impact of these flow pulses also varied across the estuary. The bulk of variation in temperature followed a long-run seasonal cyclicity, but there was also considerable short-term variation, including reductions in temperature coinciding with flow pulses.

In Wallis Lake, an increasing conductivity trajectory was observed at most stations from the project commencement until February 2020, reflecting the influence of drought conditions on the estuary. A series of minor flow pulses accompanied a larger flow pulse over late summer in 2020. This led to sharp declines in conductivity at logger stations in the north of the lake (Wallamba River and Coolongolook River, Figure 18), which is heavily influenced by tributaries. In contrast, only minor perturbations in conductivity were evident in the main southern waterway area in the south during this period (Green Point, Figure 18). A protracted series of minor and major flow pulses occurred from late December 2020 through to early autumn 2021, which led to considerable variation in conductivity over this period. Conductivity levels approached or reached  $0 \text{ ms cm}^{-1}$  for extended periods at some stations. Similar to the earlier flow pulses, the impact on conductivity was somewhat reduced in the main body of the lake, with a minimum conductivity of around  $20 \text{ ms cm}^{-1}$  (Figure 18). Temperature was also influenced by these flow pulses, but the declines observed were generally  $6^\circ\text{C}$  or less. Seasonal temperature fluctuations appeared to account for the majority of

temperature variability, with the scale of fluctuations lower in the main body of the lake relative to the northern section.

With the exception of the Myall River, conductivity in Port Stephens was comparatively stable for the first ~2.5 years of the study period, with only minor flow events in February and July 2020 (Figure 19). Estuary inflow increased in early 2021, and a major inflow event led to a dramatic decrease in conductivity in at the end of March 2021, coinciding with the conclusion of sampling in the estuary. As for Wallis Lake, temperature mostly reflected seasonal cyclicity, but abrupt declines (4-5°C, over a few days) also coincided with flow events (Figure 19). Temperature was generally warmer for logger locations closer to the ocean in winter, and vice-versa in summer.

Lake Macquarie had considerably lower freshwater inflow than the other two estuaries, and the three large pulses observed failed to have a major influence on conductivity (Figure 20). Consequently, conductivity was comparatively stable throughout the entire study period, with a minor decline occurring at some locations just as sampling concluded in the estuary (Figure 20). Overall, temperature was warmer in Lake Macquarie than Wallis Lake and Port Stephens, and exceeded 25°C for multiple months each year. This was likely due to the influence of power station water releases, which ensured that winter temperatures nominally remained above 15°C, and contributed to warmer temperatures overall in the south of the lake (Figure 20).

For each estuary, a single reference station was selected to derive continuous variables for use in statistical modelling of factors driving abundance. These reference stations included Green Point (Figure 18) for Wallis Lake (LOG.5 in Figure 14), Pindimar (Figure 19) for Port Stephens (LOG.2 in Figure 15), and Wangi Point (Figure 20) in Lake Macquarie (LOG.2 in Figure 16).

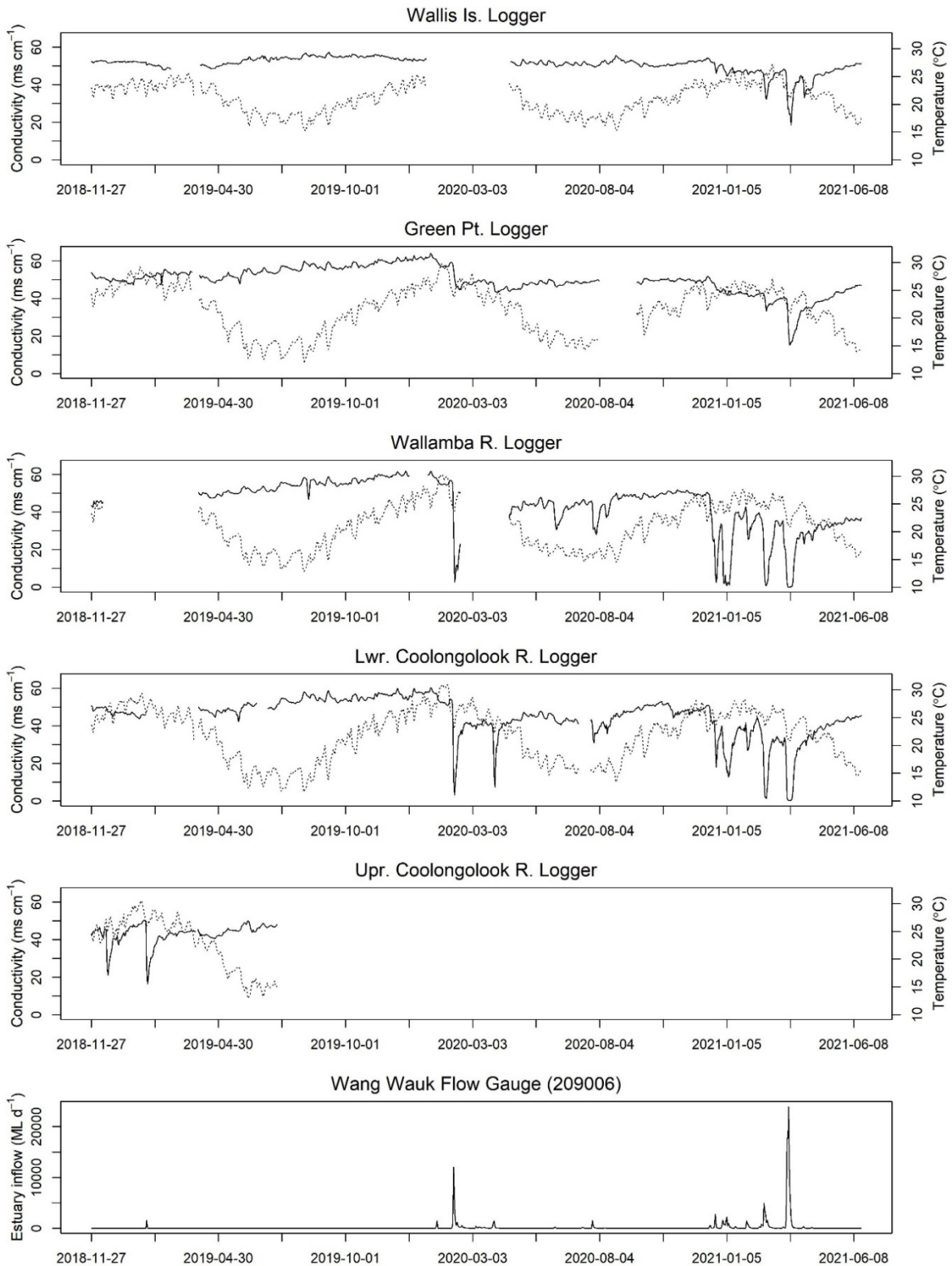


**Figure 18** Trace plot of water quality (conductivity, solid line; temperature, dotted line) and flow data over the study period summarised from loggers deployed within Wallis Lake including Wallis Is. (LOG.2), Green Pt. (LOG.5), Wallamba R. (LOG.1), lower Coolongolook R. (LOG.3), and the Wang Wauk flow gauge on the Coolongolook R. Also presented is data for the upper Coolongolook R. (originally LOG.4), which was discontinued in June 2019. Gaps in the trace indicate logger loss, theft or failure.

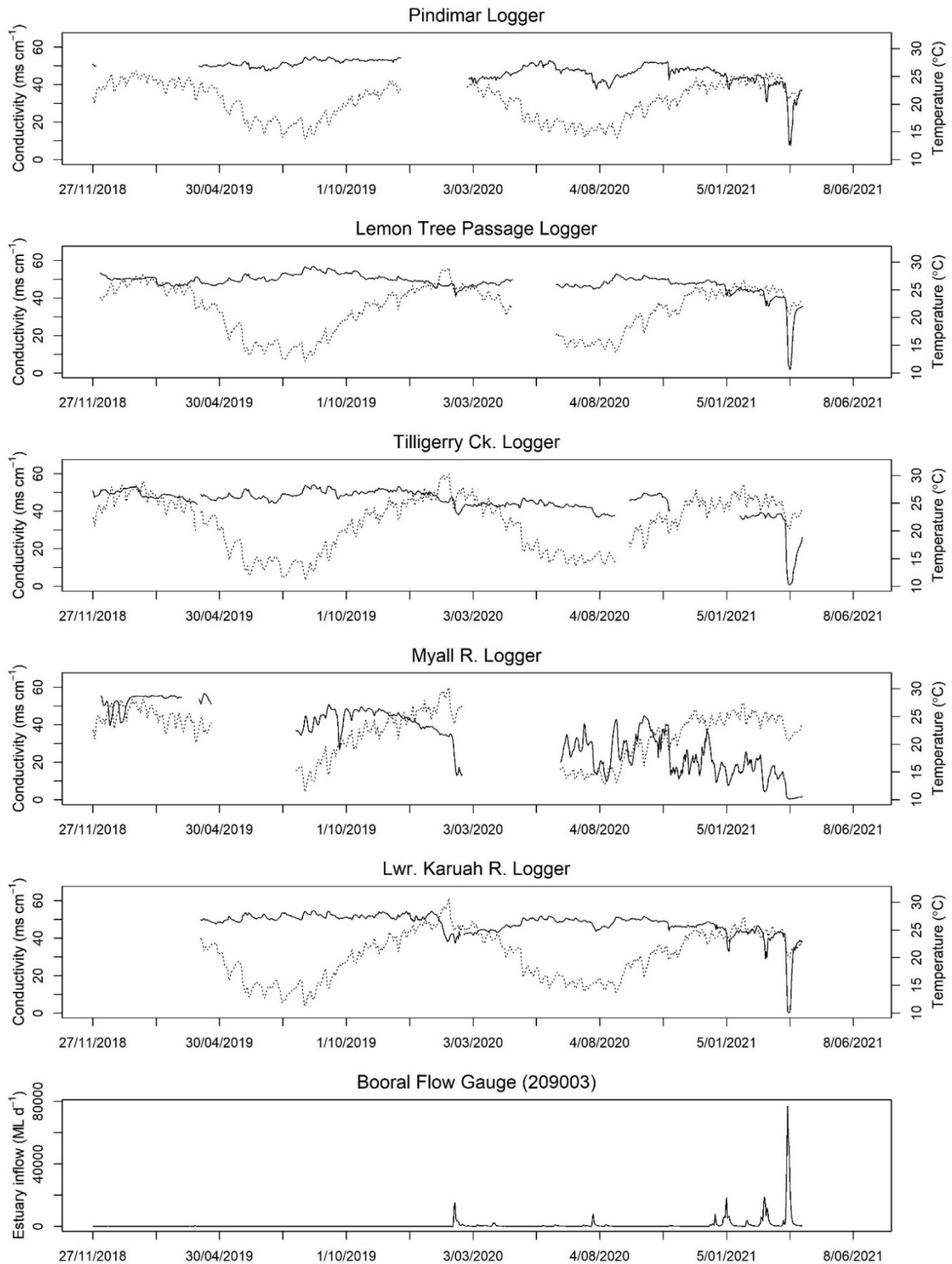


**Figure 19** Trace plot of water quality (conductivity, solid line; temperature, dotted line) and flow data over the study period summarised from loggers deployed within Port Stephens including Pindimar (LOG.2), Lemon Tree Passage (LOG.3), Tilligerry Ck. (LOG.4), Myall R. (LOG.1), lower Karuah R. (LOG.5), and the Booral flow gauge on the Karuah R. Gaps in the trace indicate logger loss, theft or failure.

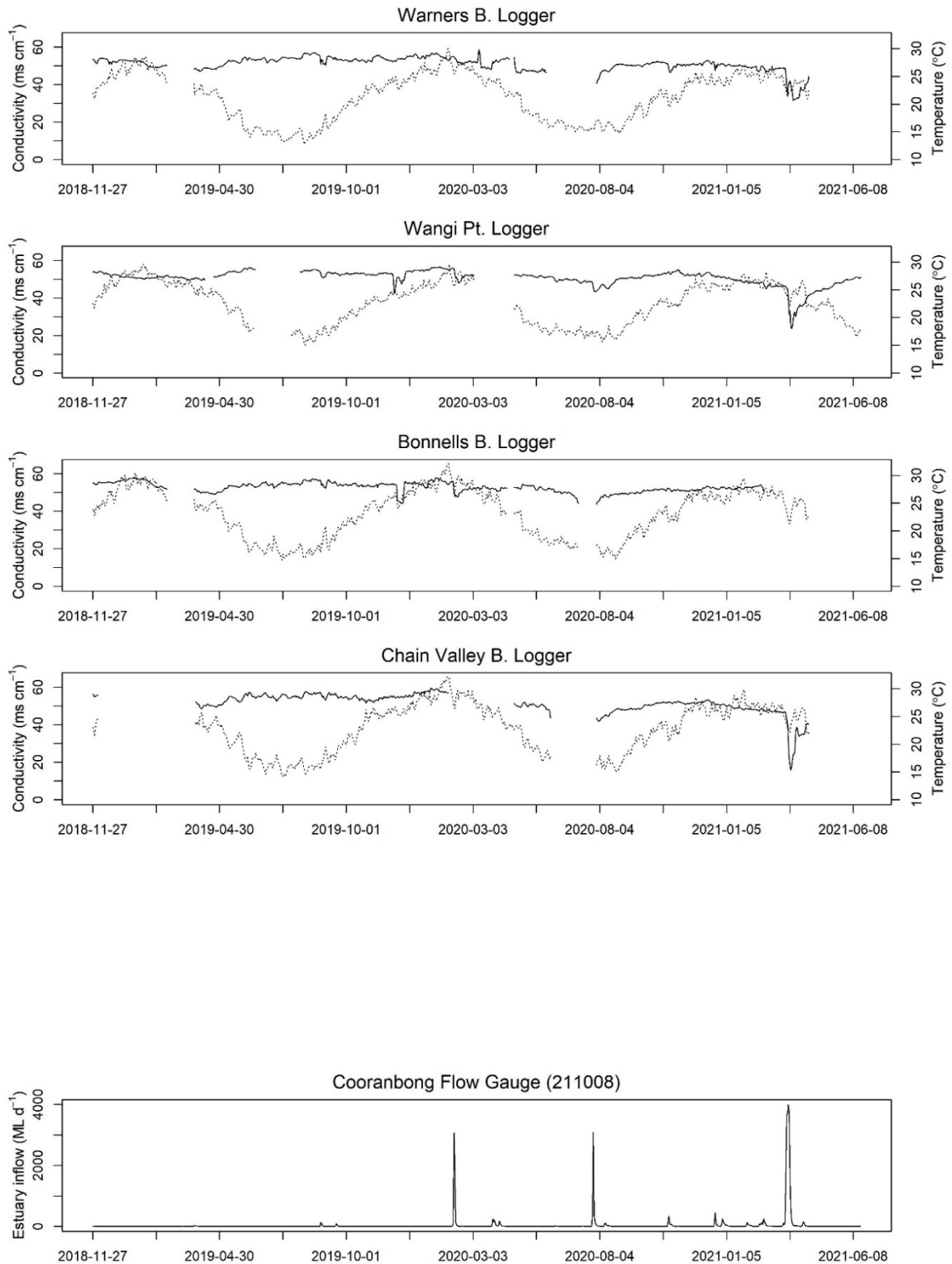


**Figure 20** Trace plot of water quality (conductivity, solid line; temperature, dotted line) and flow data over the study period summarised from loggers deployed within Lake Macquarie including Warners Bay (LOG.1), Wangi Pt. (LOG.2), Bonnells Bay (LOG.3), Chain Valley Bay (LOG.4), and the Coorabong flow gauge on Dora Ck. Gaps in the trace indicate logger loss, theft or failure.

## Broad patterns in abundance and size structure

Overall, 8,271 successful trap deployments were undertaken over the regular independent survey and supplementary sampling program, and 29,728 Blue Swimmer Crab were captured. There was substantial spatial and temporal variability observed within the time series of Blue Swimmer Crab abundance data that was collected through the regular independent survey (Figure 21). The greatest catch rates were observed in Wallis Lake, with a peak catch rate 3x that observed in Port Stephens and 5x that observed in Lake Macquarie (Figure 21). Size-structure data suggested that, for all estuaries, there was usually only a single large cohort moving through the fishery in any one summer-autumn period (Figure 22, Figure 23 and Figure 24), however there were some exceptions to this general observation, which are discussed below.

In Wallis Lake, Blue Swimmer Crab were most abundant at sites 1-4, which were located in and around Wallis Island and the centre section of the lake. Catch rates at the sites further to the south (sites 5-7) were usually lower than the more northern sites, however this relationship tended to reverse during the winter months, with greater catches per trap at sites 6 and 7 than other sites (Figure 21). Overall, there was strong seasonal cyclicity evident in catch rates at all sites, with a well-defined annual peak appearing in mid-late summer (January or February). The peak rapidly declined by the end of autumn, and supported high catch rates for only a single month in 2019 (January), for two months in 2020 (February and March), and three months in 2021 (January through March; Figure 21). The presence of multiple cohorts in late spring and early summer suggests a potential reason for the different durations in catch peaks (Figure 22). During December 2018 there was little evidence for two distinct cohorts in the size structure data, with the exception of a left shoulder on the main peak (Figure 22). However, in November and December 2019 there was a distinct peak of smaller crabs between 20-40 mm CL, in addition to the main peak. Similarly, there was evidence for a second cohort present in November and December 2020, and the December peak was much more pronounced (perhaps indicating a stronger cohort) than previous years (Figure 22). The lack of an obvious peak in size classes greater than the minimum legal size (MLS), and generally lower abundance above this threshold, suggests that the crabs are rapidly removed by fishers as soon as they enter the fishery (Figure 22). This effect appeared to be much more apparent for males in some instances, which may be a combination of the fact that berried females cannot be retained, and males tend to grow faster and to larger sizes during the warmer months, which may lead to some sex-selective fishing mortality during the peak harvest period for the fishery. Larger size classes were however represented within the inshore waters adjacent to Wallis Lake (samples were only collected from May to August), with a peak size between 70- and 80-mm CL (Figure 22). It is important to note when considering these data that the different gear used for inshore sampling may have had a selectivity effect, although the size range of crabs caught in inshore waters ranged from 45 mm to 107 mm CL, which aligns with expected patterns given that crabs tend to remain in the estuarine nursery until they reach a certain size.

In Port Stephens, Blue Swimmer Crab catch rates were greatly reduced relative to Wallis Lake. During the first two years of the program, catch rates remained comparatively stable with only minor seasonal cyclicity observed (Figure 21). In early 2019, greatest catch rates occurred at sites 3-4, in the central-northern section of the estuary, but in summer 2019/20 this had switched to sites 5-7 further up the estuary (Figure 21) with catches dominated by new recruits (Figure 23). There was an early peak in catch rates, in October and November 2020, followed by a clear pulse of new recruits in December and January 2021 (Figure 23). These recruits supported a substantial peak in catch rates during March 2021 (Figure 21), which coincided with a pulse flow and a 15 ms cm<sup>-1</sup> drop in conductivity (described in the previous section). Sampling in the Port Stephens sub-program showed a similar large size mode (~75 mm CL) between Blue Swimmer Crab within the sanctuary zone at the mouth of Port Stephens and other locations in the estuary during October and November 2019, but unlike other sites this larger size mode persisted until February 2020, at which

point it had grown to ~80 mm CL. During this month a second smaller mode (~60 mm CL) was also present in this sanctuary zone, which aligned with modes in the fished areas. This proceeded as the dominant size mode in March and April, with the 80 mm CL size mode progressively decreasing in abundance in the sanctuary zone, presumably as crabs emigrated to sea.

Lake Macquarie catch rates were the lowest sampled during the regular independent survey, but represented a clear reversal of trends observed in other estuaries (Figure 21). Blue Swimmer Crab were present at greatest abundance within winter (June to August) across all years sampled, although there appeared to be secondary peaks that occurred during February and March of 2019 and 2020. During times of peak catch rates, catch rates appeared to be greatest at sites in the north of the lake, but catch rates were comparatively similar across all sites during non-peak periods. The size of Blue Swimmer Crab caught in Lake Macquarie was much larger than other estuaries, with the main size mode well exceeding the MLS during most months (Figure 24). There was limited evidence for well-defined pulses of new recruits in the size structure data, but a major shoulder was present in the size distributions over summer and early autumn, suggesting a smaller size cohort was moving through the population during these periods (Figure 24). Size distributions were usually similar between females and males, with the exception of both the winter (in all years) and summer (in 2020 and 2021) months, when females tended to be larger than males. As noted earlier, water temperatures within the lake were warmer than the other estuaries, particular during the winter, which may have contributed to the bifurcate trends observed. These warmer conditions may have supported much faster growth rates of early juveniles, leading to the general lack of well-defined size modes for smaller crabs (Figure 24).

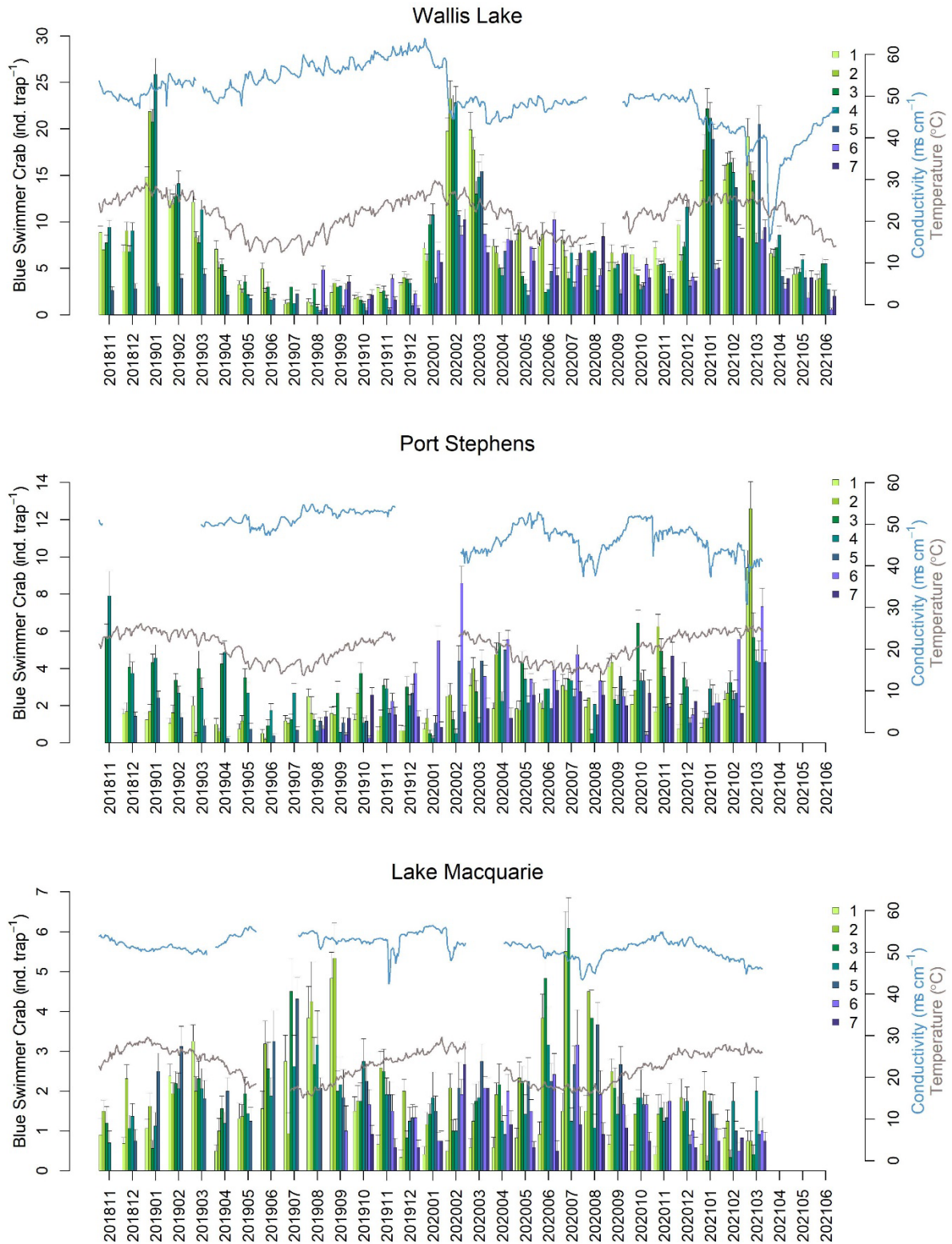


**Figure 21** Composite plot summarising all sampling data for the regular independent survey, presented as mean  $\pm$  standard error (SE), grouped by estuary, site and month. Also overlaid is a conductivity and temperature trace for the reference station within each estuary (colour coded to the secondary y-axis).

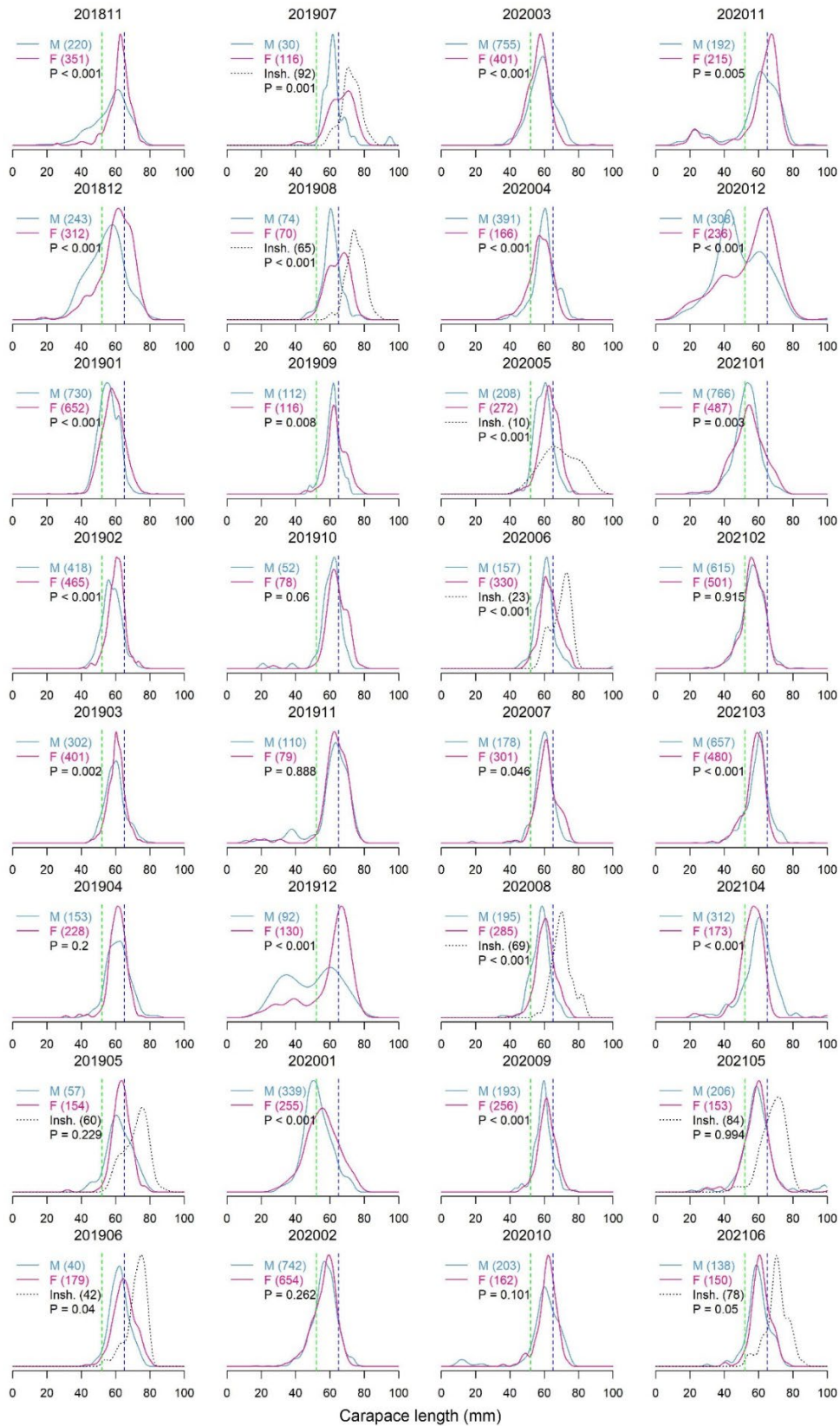


**Figure 22** Monthly sex-specific size structures for samples collected in Wallis Lake, expressed as kernel density estimates (including inshore samples [Insh.], not split by sex). Panel headers indicate sampling period (YYYYMM). Sample sizes are indicated in brackets, and the P-value from a K-S test of differences between male and female size structure is indicated in the legend panel. The green and blue vertical dashed lines indicate female size at maturity, and the MLS respectively.

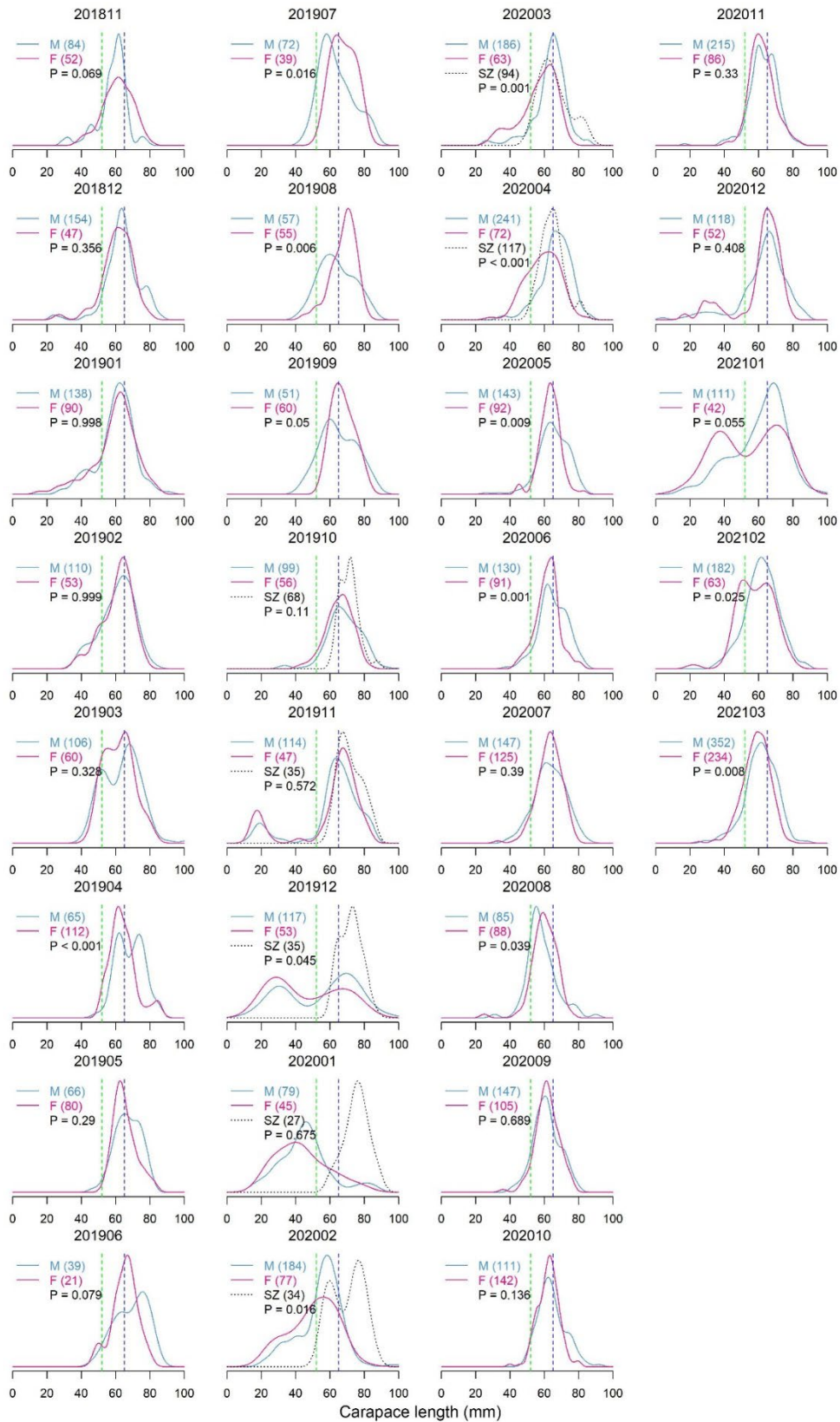


**Figure 23** Monthly sex-specific size structures for samples collected in Port Stephens, expressed as kernel density estimates (including sanctuary zone samples [SZ], not split by sex). Panel headers indicate sampling period (YYYYMM). Sample sizes are indicated in brackets, and the P-value from a K-S test of differences between male and female size structure is indicated in the legend panel. The green and blue vertical dashed lines indicate female size at maturity, and the MLS respectively.

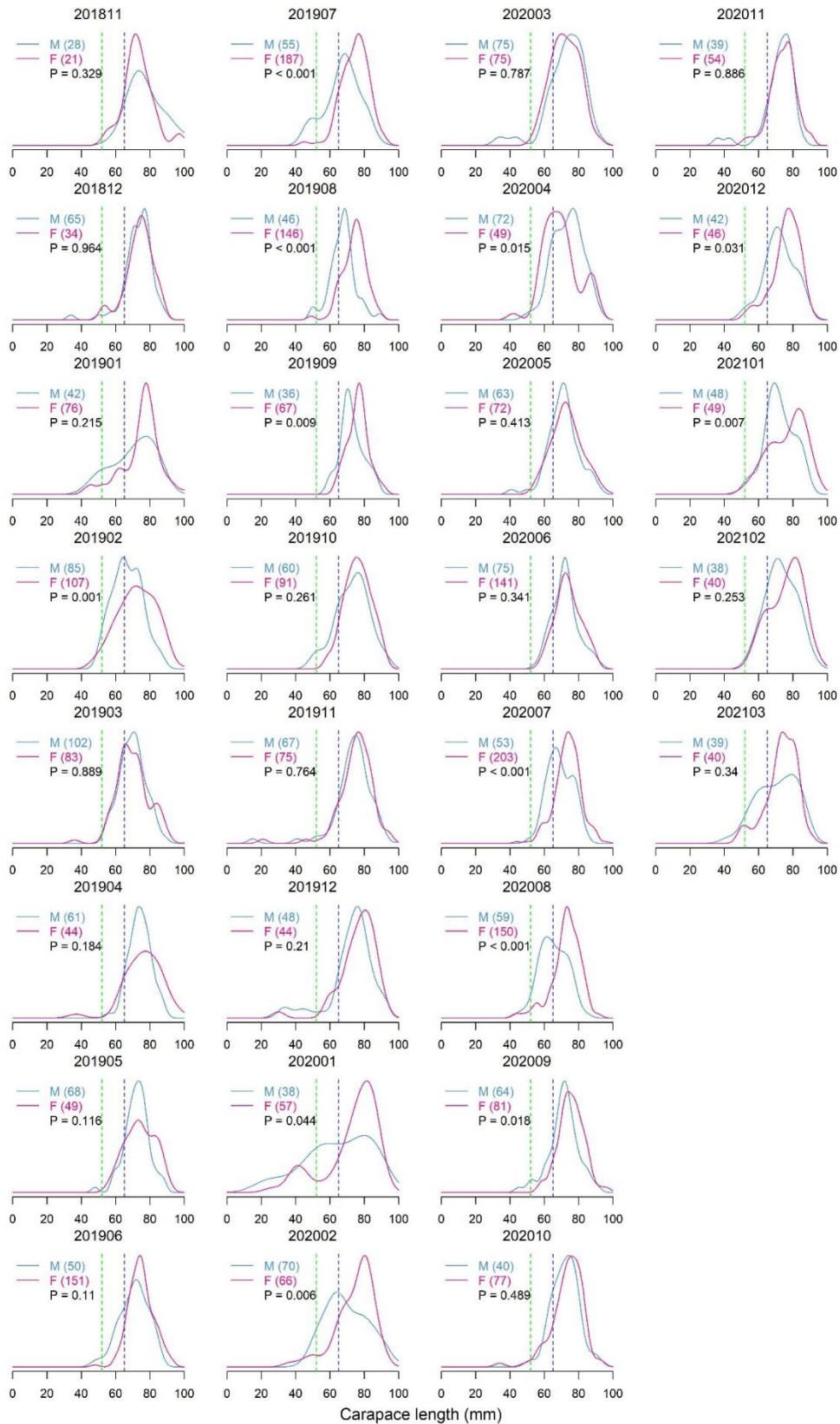


**Figure 24** Monthly sex-specific size structures for samples collected in Lake Macquarie, expressed as kernel density estimates. Panel headers indicate sampling period (YYYYMM). Sample sizes are indicated in brackets, and the P-value from a K-S test of differences between male and female size structure is indicated in the legend panel. The green and blue vertical dashed lines indicate female size at maturity, and the MLS respectively.

# Latitudinal trends in the reproductive biology of female Blue Swimmer Crab in south-eastern Australia

## Background and rationale

A key component of fisheries recruitment is the reproductive output of exploited populations. Gonadal development and egg production are energetically expensive processes, and are known to respond to environmental drivers (Tropea *et al.* 2015; Baliña *et al.* 2018). Gonadal development within a population is often measured using a Gonadosomatic Index (GSI, unit mass of gonad per unit mass of body weight), such that a high GSI indicates reproductive maturity and greater investment into reproduction (Liu *et al.* 2014). The Hepatosomatic Index (HSI, unit mass of hepatopancreas per unit mass of body weight) is a useful measure of relative energy storage, as the hepatopancreas acts as a major store of organic and inorganic reserves in crustaceans (Passano *et al.*, 1960, Magalhães *et al.*, 2012). The Egg Mass Index (EMI, unit mass of eggs per unit mass of body weight) is a measure of relative reproductive output standardised to animal size. This may be used as a proxy for fecundity to evaluate factors affecting variability in reproductive output (Sukumaran and Neelakantan 1997; Hisam *et al.* 2018), where egg count data is not available. The relationships between the GSI, HSI and EMI can inform patterns in female reproductive condition throughout the breeding season. Therefore, quantifying these relationships alongside potential abiotic influences may aid examination of recruitment variability.

As noted in the Introduction, the reproductive development of Blue Swimmer Crab is strongly influenced by water temperature (de Lestang *et al.* 2003b), and this leads to substantial variation in reproductive output (de Lestang *et al.* 2003b; Kumar *et al.* 2003; Johnson *et al.* 2010; Johnston and Yeoh 2021). While Blue Swimmer Crab in tropical waters tend to exhibit reduced seasonality in their reproductive biology (de Lestang *et al.* 2003b), the increased temperature variability in temperate estuaries may drive strong seasonal variation in reproduction (Kumar *et al.* 2003). New South Wales includes the southernmost extent of the main Blue Swimmer Crab range on the eastern Australian coast, where spawning is generally confined to late spring and early summer (Johnston *et al.* 2021a)—previous work in this area has found substantial variation in size-at-maturity and fecundity relative to other populations around Australia. Specifically, crabs had larger batch fecundities than similarly sized individuals in Western Australia, and larger sizes at maturity than females in South Australia (Johnson *et al.* 2010).

Estuaries in south-eastern Australia are warming at an order of magnitude faster than predicted by current global ocean and atmospheric models, with water temperatures increasing at a rate of  $0.2^{\circ}\text{C year}^{-1}$  (Scanes *et al.* 2020a). Continued warming presents a challenge to the health of estuarine ecosystems and the profitability of associated aquaculture and wild fisheries (Madeira *et al.* 2012; FAO 2018). Within estuaries, these changes may cause increased energetic demands and altered development in some species (Parker *et al.* 2013), reduced fecundity and egg viability (Foo and Byrne 2017) and behavioural changes (Madeira *et al.* 2012). Shifting temperature regimes vary according to the estuaries' geomorphology (Scanes *et al.* 2020a), which complicates the prediction of potential reproductive consequences. In this chapter, we considered patterns of reproduction across estuaries covering the main far southern latitudinal range for eastern Australian Blue Swimmer Crab. Specifically, we aimed to: 1) describe the interaction between the GSI (index of gonadal development and reproductive investment) and the HSI (index of energy storage) during gonadal development; 2) characterise EMI trends across south-east Australian Blue Swimmer Crab and; 3) assess the potential

influence of temperature on gonadal development and egg mass production across this extended latitudinal band.

## Methods

### Sampling and analysis

Sampling and processing was conducted as described above for the regular independent survey and the supplementary latitudinal sub-program, from October 2019 to February 2020, which covered the peak spawning period (Johnson *et al.* 2010).

Egg mass index (EMI) was calculated using the total egg mass weight and total body weight, using the formula  $EMI = \frac{Egg\ mass\ weight \cdot 100}{Body\ weight}$  (Sukumaran and Neelakantan 1997; Hisam *et al.* 2018). The GSI and HSI are ratios of organ weight to body weight. In this study, these proportions correlated with the size of the crab, and therefore the comparison of ratios among estuaries could be confounded by the distribution of body size. To remove the influence of total body weight on the relationship between GSI and HSI, linear models were fit to log-organ weight and log-body weight, with the slope of the resulting fit used as the exponent in the formulae as follows:  $Adj.\ GSI = \frac{Ovary\ Weight}{Body\ Weight^{1.292}}$ ; and  $Adj.\ HSI = \frac{Hepatopancreas\ Weight}{Body\ Weight^{0.657}}$ . Linear models were used to assess changes in the relationship between the adjusted GSI and adjusted HSI across the stages of ovarian development in mature females. This relationship was analysed by ovary stage, with stages 2-3 and 4-5 grouped together due to morphological similarities and to account for potential errors in distinguishing these visually similar stages.

Linear models were also used to assess the relationship between crab weight and egg mass weight. Crab weight and egg mass weight followed a logarithmic relationship, so a natural logarithm transformation was used on body weight in the linear model. An analysis of covariance (ANCOVA) was used to test for significant differences in this relationship between estuaries, where the weight of the egg mass was the dependent variable, total body weight was the covariate, and estuary was a fixed factor. A Tukey's post hoc test was used to test for differences across all combinations of estuaries. A two-way ANOVA was used to test for significant differences in the EMI among estuaries and sampling periods and any significant interaction between the two factors, where the EMI was the dependent variable and the estuaries and sampling period were fixed factors. Tukey's post hoc tests were also used to evaluate differences within fixed effects or interactions.

Generalised additive models (GAMs) were used to examine potential non-linear relationships between mean monthly temperature and the adjusted GSIs, adjusted HSIs and total egg mass weights. GAMs are a non-parametric extensions of Generalised Linear Models (GLMs), and can be used to examine complex non-linear relationships between response variables and predictor variables by fitting complex smoothing functions to the data (Hastie and Tibshirani 1990). For each model, a smoothing function ( $s$ ) was fitted to mean monthly temperature and the estuaries were included as parametric coefficients, where the intercept is denoted  $\beta_0$ , as depicted in the formulae below.

$$Adj.\ GSI = \beta_0 + s(\text{Mean Monthly Temperature}) + \text{Estuary}$$

$$Adj.\ HSI = \beta_0 + s(\text{Mean Monthly Temperature}) + \text{Estuary}$$

$$\text{Egg Mass} = \beta_0 + s(\text{Mean Monthly Temperature}) + \text{Estuary}$$

## Results

### Patterns in reproductive development

Overall, 259 mature and 122 berried female crabs were retained for lab analysis. Mature females ranged in size from 51 mm to 93 mm CL, while berried females ranged in size from 57 mm to 89 mm CL. Only female Blue Swimmer Crab in the later stages of ovarian development (4-5) showed a significant negative linear correlation between the adjusted GSI and adjusted HSI ( $F_{1,146} = 7.042$ ,  $P = 0.009$ , Table 2, Figure 25). There was no significant interaction between the GSI and HSI in females with stage 1 ovaries ( $F_{1,45} = 2.767$ ,  $P = 0.103$ , Table 2) or stage 2-3 ovaries ( $F_{1,60} = 0.002$ ,  $P = 0.969$ , Table 2).

**Table 2** Linear regression equations fit for the adjusted gonadosomatic index as a function of adjusted hepatosomatic index during ovarian development in mature females. \* Indicates significant p-value

| Ovary stage | Regression equation | P - value |
|-------------|---------------------|-----------|
| All stages  | $y = 0.25 - 2.79x$  | 0.015*    |
| 1           | $y = 0.19 + 11.71x$ | 0.103     |
| 2-3         | $y = 0.28 + 0.15x$  | 0.969     |
| 4-5         | $y = 0.27 - 4.87x$  | 0.009*    |

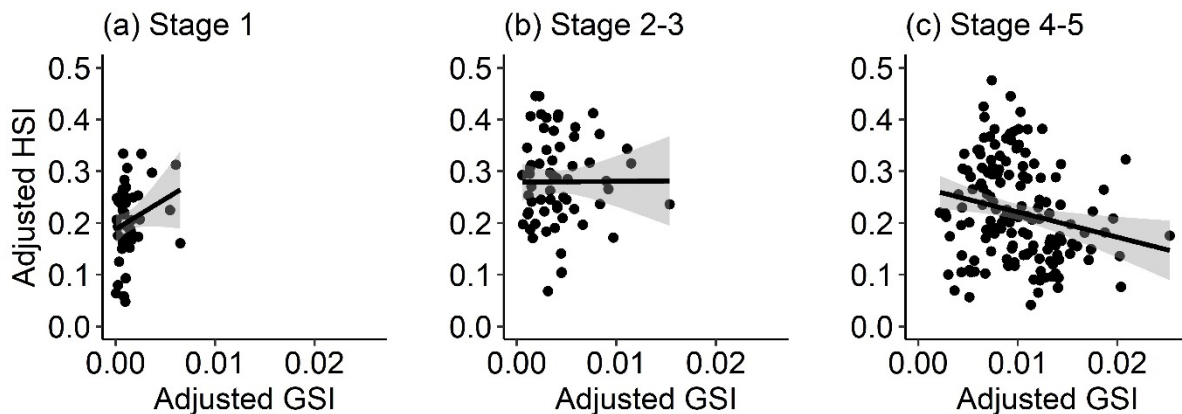


**Figure 25** Linear models illustrating the relationship between the adjusted gonadosomatic index and adjusted hepatosomatic index during ovarian development in mature females (pooled across estuaries) for A) Stage 1 ovaries ( $n = 48$ ), B) Stage 2-3 ovaries ( $n = 62$ ) and C) Stage 4-5 ovaries ( $n = 148$ ). The solid black line represents the linear model, and the grey area represents the confidence interval (95%)

Egg mass weight increased logarithmically with body weight ( $F_{1,111} = 61.430$ ,  $P < 0.001$ , Table 3). There was variability between estuaries (Figure 26), with Blue Swimmer Crab in Lake Macquarie having the smallest coefficient and therefore the smallest increase in egg mass weight relative to body weight (Table 3). Female crabs in Wallis Lake had the largest coefficient and therefore largest increase in egg mass with body weight, however due to a lower intercept than Botany Bay, the Wallis Lake crabs tended to have smaller egg masses than those in Botany Bay (Table 3, Figure 26). The EMI varied significantly among estuaries ( $F_{4,93} = 6.477$ ,  $P < 0.001$ ) and sampling periods ( $F_{4,93} = 6.994$ ,  $P < 0.001$ ), with a significant interaction between the two factors ( $F_{11,93} = 3.575$ ,  $P < 0.001$ , Figure 27). The EMI was as large as 55%, and was significantly larger in Botany Bay than Wallis Lake ( $P = 0.031$ ), Port Stephens ( $P < 0.001$ ) and Lake Macquarie ( $P = 0.001$ , Figure 27). Lake Illawarra had a smaller mean EMI than Botany Bay, however this difference was not statistically significant ( $P = 0.054$ ).

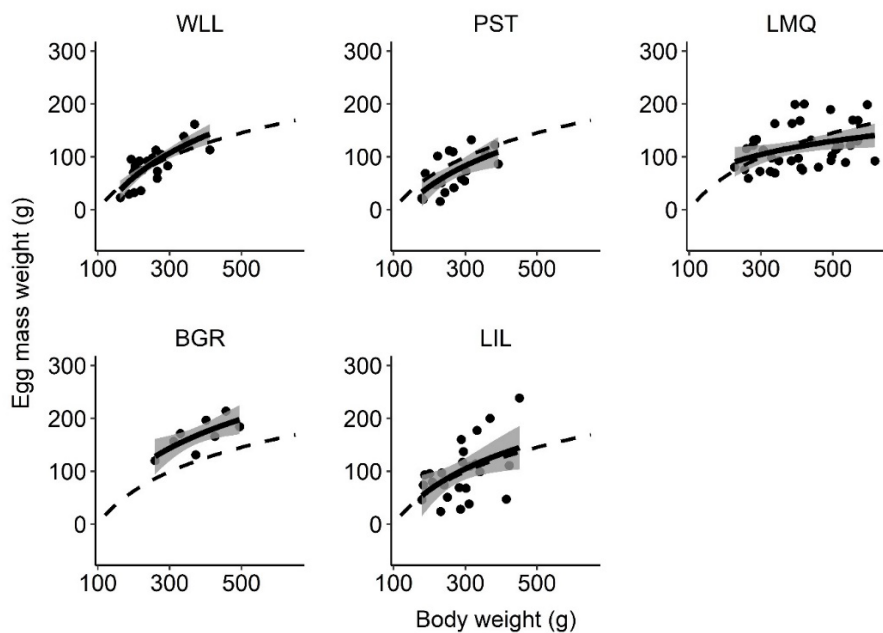


**Figure 26** Non-linear models illustrating the relationship between the total weight of the egg mass (g) and the total body weight (g) of berried crabs in Wallis Lake (WLL,  $n = 25$ ), Port Stephens (PST,  $n = 18$ ), Lake Macquarie (LMQ,  $n = 38$ ), Botany Bay (BGR,  $n = 8$ ) and Lake Illawarra (LIL,  $n = 24$ ). The solid black line represents the non-linear model fit for each estuary and the grey area represents the confidence interval (95%). The dashed black line depicts a model fit for combined estuaries.

## Water temperature as a driver of variability in reproduction

The seasonal warming was evident within all 5 estuaries (Figure 28), reaching a peak in the January and February sampling periods. The two more southern estuaries (Botany Bay and Lake Illawarra) never exceeded the mean monthly water temperatures of the other three more northern estuaries (Figure 28). Generalised Additive Models showed that there was a non-linear relationship between mean monthly temperature and GSI, HSI and EMI (Figure 29). The GAM for adjusted GSI explained 14.5% of the deviance in the data and showed a rapid decline in adjusted GSI above  $\sim 24^{\circ}\text{C}$  ( $n = 229$ , e.d.f = 2.812,  $F = 7.390$ ,  $P < 0.001$ , Figure 29); the GAM for adjusted HSI explained 13.3% of the deviance in the data and appeared to reach a minimum at  $\sim 24^{\circ}\text{C}$  ( $n = 228$ , e.d.f = 3.675,  $F = 6.26$ ,  $P < 0.001$ , Figure 29). The GAM for EMI explained 66% of the deviance in the data, with a maxima occurring at  $\sim 23^{\circ}\text{C}$  ( $n = 80$ , e.d.f = 5.662,  $F = 9.892$ ,  $P < 0.001$ , Figure 29).

**Table 3** Linear regression equations fit for the total weight of the egg mass (g) as a function of the total body weight (g) of the berried crabs by estuary. \* Indicates significant p-value.

| Estuary        | Regression equation          | P - value |
|----------------|------------------------------|-----------|
| All Estuaries  | $y = -402.28 + 87.98 \ln x$  | <0.001*   |
| Wallis Lake    | $y = -539.90 + 113.39 \ln x$ | <0.001*   |
| Port Stephens  | $y = -469.68 + 96.90 \ln x$  | 0.006*    |
| Lake Macquarie | $y = -179.68 + 49.76 \ln x$  | 0.034*    |
| Botany Bay     | $y = -471.62 + 107.82 \ln x$ | 0.039*    |
| Lake Illawarra | $y = -457.14 + 98.45 \ln x$  | 0.018*    |

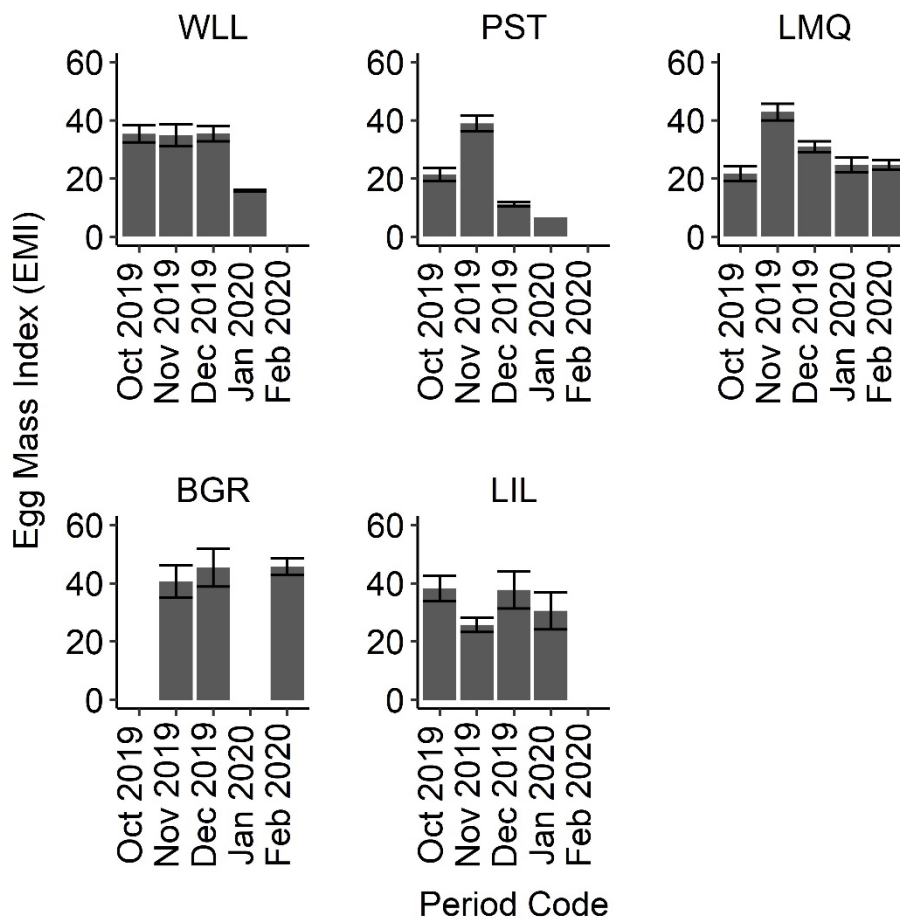


**Figure 27** Bar charts showing egg mass index (EMI) in Wallis Lake (WLL), Port Stephens (PST), Lake Macquarie (LMQ), Botany Bay (BGR) and Lake Illawarra (LIL) for each month with the sampling period (October 2019 – February 2020). The top of grey box indicates the mean, and the error bars indicate the standard error.

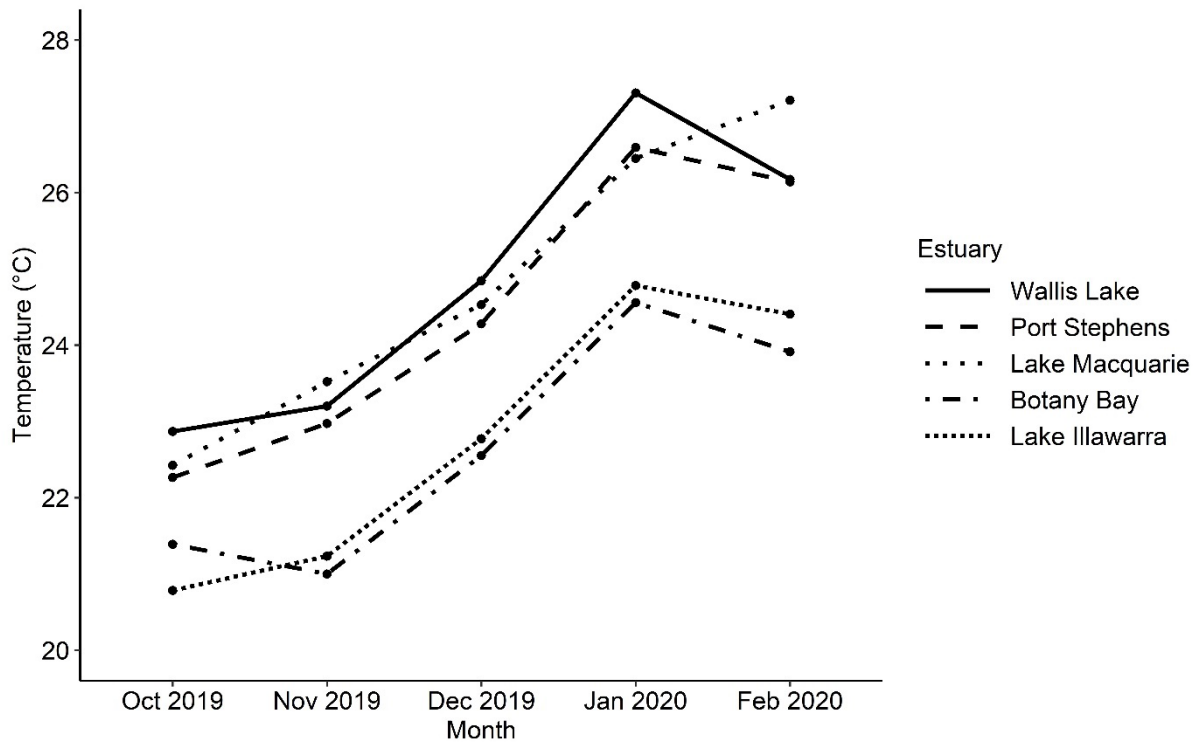


**Figure 28** Mean monthly water temperatures in Wallis Lake, Port Stephens Estuary, Lake Macquarie, Botany Bay and Lake Illawarra between October 2019 and February 2020. The water temperature in these estuaries peaked in the January and February sampling periods, with mean monthly temperatures in Wallis Lake = 27.3°C, Port Stephens = 26.6°C, Lake Macquarie = 27.2°C, Botany Bay = 24.6°C and Lake Illawarra = 24.8°C. The data was gathered using HOBO U24-002-C data loggers deployed at a depth of 1 m throughout the sampling period. Water temperatures in Lake Macquarie are influenced by the release of hot water by the Mannering Park Power Station and Eraring power station, two coal fired power stations situated on the shores of the estuary (Taylor *et al.* 2017e).

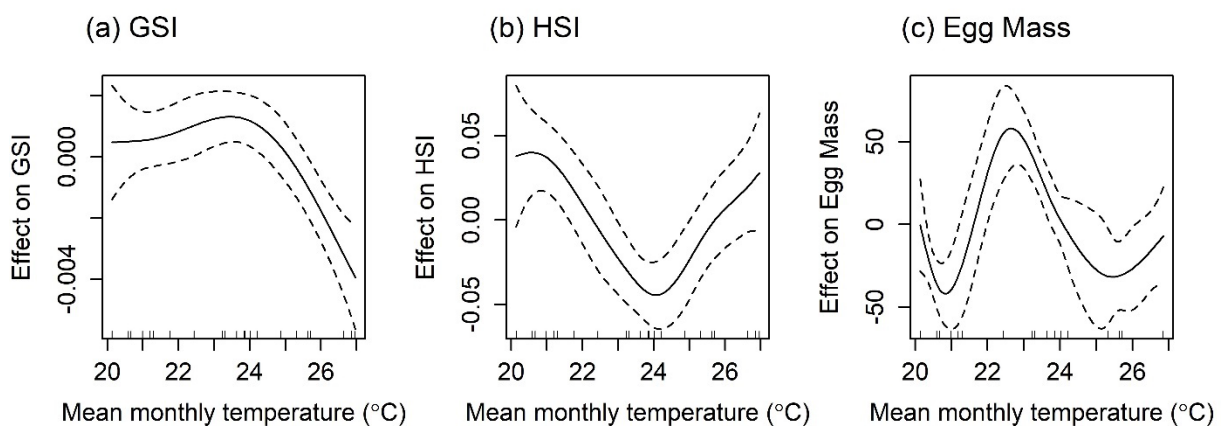


**Figure 29** Thermal performance curves from generalised additive models fit for the A) Gonadosomatic index, B) Hepatosomatic index and C) Total egg mass on mean monthly temperature in each estuary for the month prior to capture. The solid line depicts the fit of the model to the data and the dashed lines represent the confidence interval (95%). The ticks on the x-axis indicate the mean monthly temperatures of each sampling effort.

## Discussion

Our data showed that gonadal development was related to the mobilisation of reserves from the hepatopancreas during the final stages of ovarian development in Blue Swimmer Crab. We found that the weight of the egg mass increased logarithmically with total body weight and was strongly influenced by water temperature. In the cooler waters of Botany Bay, there was a stronger relationship between size and egg mass weight, with larger females producing proportionally larger egg masses. We observed a peak in gonadal development and egg production at  $\sim 24^{\circ}\text{C}$ , with a decline in reproductive development either side of this optimum temperature.

### Relationship between GSI and HSI

The hepatopancreas is the largest store of energy reserves in crustaceans and is crucial in the absorption, storage and metabolism of nutrients for physiological processes (Wang *et al.* 2014). The significant negative relationship between the adjusted GSI and HSI in the final stages of ovarian development reflects the high energy demands of this process (Wang *et al.* 2014). Only in the final stages of ovarian development are the reserves of the hepatopancreas significantly drawn upon, and therefore ovarian development through stages 1 to 3 is presumably directly sustained by foraging. During the final stage of ovarian development, the reproductive output of a female crab is therefore likely to be determined by the quantity of reserves mobilised from the hepatopancreas to the ovaries. Increased stress due to fluctuations in temperature may increase energetic demand from other physiological processes, limiting the resources available for ovarian development and egg production (Tropea *et al.* 2015; Baliña *et al.* 2018). In crustaceans such as *Neocaridina davidi* and *Neocaridina heteropoda* ovarian maturation and spawning were found to be inhibited due to stress at high temperatures ( $33^{\circ}\text{C}$  and  $32^{\circ}\text{C}$ , respectively) because of reduced mobilisation of biochemical reserves to the ovaries (Tropea *et al.* 2015; Baliña *et al.* 2018). Temperature is evidently a key driver of variability in gonadal development and energy expenditure in crustaceans (Tropea *et al.* 2015; Baliña *et al.* 2018), with suboptimal environmental conditions potentially reducing investment into reproduction, as discussed below.

### Relationship between crab size and egg mass weight

Crabs in Botany Bay show a larger increase in egg mass weight per unit of total body weight than crabs in other estuaries. Botany Bay is a drowned river valley, with a deep, wide entrance facilitating oceanic exchange with the Tasman Sea (Kingsford and Suthers 1994), which maintains cooler average temperatures than the other estuaries. In Western Australia, batch fecundity has been shown to increase with latitude from the subtropical estuaries (Shark Bay) towards the temperate estuaries (Geographe Bay) (Johnston and Yeoh 2021). Warmer environments may facilitate the production of smaller and more frequent egg batches (Johnston and Yeoh 2021), a reproductive strategy that may reduce the risk of overall recruitment failure by spawning over a longer timeframe (McEvoy and McEvoy 1992). This may explain why Blue Swimmer Crab in tropical and subtropical environments can achieve rapid batch production and year-round spawning (up to 3 batches per year) (de Lestang *et al.* 2003b), whereas Blue Swimmer Crab in temperate environments are constrained in the production of fewer batches, and a shorter spawning season in which to produce them (up to 3 batches but only in larger individuals, during the period October-January) (Kumar *et al.* 2000).

The egg mass index was as high as 55% in the berried females and was on average 34% in females with 70 – 80 mm CL (equivalent to ~144 – 189 mm carapace width), indicating significant reproductive investment. In contrast, *Portunus pelagicus* in the tropical waters of southern Thailand had a maximum EMI of only 29% (Hisam *et al.* 2018). Another study of *Portunus sanguinolentus* and *P. pelagicus* in the south-west coast of India found that the EMI peaked at an average of 15% in females with 100 – 110 mm carapace width and at an average of 12% in females between 130 – 140 mm carapace width respectively (Sukumaran and Neelakantan 1997). *Portunus pelagicus* in south-eastern India showed similarly low EMIs to these, with a maximum average of ~17% in females with 120 – 129 mm carapace width (Josileen 2013). With a much larger EMI, Blue Swimmer Crab in temperate south-eastern Australia appear to be investing more resources per brood than portunid crabs in other more tropical environments (Sukumaran and Neelakantan 1997; Josileen 2013; Hisam *et al.* 2018). Such a difference in reproductive strategy, likely due to cooler water, would lead to the production of fewer, but larger, egg masses by larger females in temperate environments (de Lestang *et al.* 2003b; Hines *et al.* 2010; Johnston and Yeoh 2021).

## Water temperature as a driver of variability in reproduction

Temperature variability can significantly affect individual reproduction (de Lestang *et al.* 2003b) and contribute to year-on-year variation in recruitment and fisheries productivity (Johnston *et al.* 2011). Gonadal development and egg production is energetically expensive for ectotherms, and the GSI may be used as an index of thermal performance (Payne *et al.* 2016). The total egg mass weight produced by crabs within a single batch peaked during months with a mean temperature between ~23°C – 24°C. Conditions above 24°C approach a critical temperature for Blue Swimmer Crab, at which their reproductive functions begin to slow and lose efficiency, as indicated by the rapid decline in GSI above 24°C (Shelford 1931; Frederich and Pörtner 2000; Jost *et al.* 2012). Concurrently, the adjusted HSI, as an indicator of the energy reserves within the female crab, reached a minimum within the same temperature range, indicating that under these optimal conditions the crabs were drawing more resources from the hepatopancreas to maximise reproductive output.

In their study of climate change within south-east Australian estuaries, Scanes *et al.* (2020a) observed an average warming of 2.16°C over a 12 year period (0.2°C year<sup>-1</sup>). The average summer temperature during this period (2007 – 2018) was 24.8°C in Wallis Lake, 23.5°C in Port Stephens, 25.2°C in Lake Macquarie and 23.3°C in Lake Illawarra; there was no data for Botany Bay from this study (Scanes *et al.* 2020b). The estuaries in this study currently maintain average summer temperatures close to the observed optimal temperature range for Blue Swimmer Crab reproduction, however as the warming trend observed in Scanes *et al.* (2020a) continues, average temperatures in the spawning season may exceed the optimal range and begin to impede reproduction. Incorporating temperature-based reproduction modelling into fisheries assessment may aid in the prediction of variation in fisheries productivity, which can subsequently support adaptation of management arrangements (e.g. de Lestang *et al.* 2010). An extreme heatwave event in Western Australia during 2011 led to major reductions in recruitment within several invertebrate fisheries, including Blue Swimmer Crab, and highlighted the susceptibility of coastal invertebrate stocks to extreme environmental events (Caputi *et al.* 2016; Chandrapavan *et al.* 2019). This event also highlighted the importance of early detection of changes in the temperature-reproduction-recruitment dynamic, to allow for management to protect vulnerable spawning stock (Caputi *et al.* 2016; Chandrapavan *et al.* 2019).

## Potential impacts of tropicalisation

Anthropogenic climate change is driving global ocean warming, with accelerated warming in temperate regions with poleward-flowing western boundary currents (Wu *et al.* 2012; Vergés *et al.* 2014). The accelerated warming and ‘tropicalisation’ of temperate marine environments is particularly rapid in estuaries on the south-east Australian coastline (Scanes *et al.* 2020a). It is still uncertain how tropicalisation may affect the reproduction of Blue Swimmer Crab, and subsequently influence fisheries productivity in south-eastern Australia. The study of latitudinal clines in population size structure, EMI, and batch fecundity may represent a useful proxy for the effect of changing temperatures, and aid prediction of potential climate impacts in the future. In a study examining the effects of climate change on *C. sapidus* in Chesapeake Bay, a temperate estuary in the USA, Hines *et al.* (2010) predicted that warming waters may promote rapid growth and brood production in smaller females, with increased juvenile mortality and a reduced size at maturity. While warming in temperate waters was predicted to potentially increase the reproductive output of this population, it was noted that the complex interactive effects of multiple stressors associated with climate change, alongside exploitation, make it difficult to accurately predict and act on future circumstances (Hines *et al.* 2010). In Western Australia, the reproductive biology in *P. armatus* was found to exhibit high plasticity in response to spatial and temporal variations in temperature (Johnston and Yeoh 2021). For example, size at maturity decreased with latitude (Johnston and Yeoh 2021), but batch fecundity was found to increase with latitude. Considering the findings of our study alongside other recent reports on the effect of temperature on reproduction (e.g. Johnston and Yeoh 2021), tropicalisation of temperate estuaries within south-eastern Australia may lead to a shift toward the production of smaller batches, more frequently throughout a longer spawning season, by females with a larger size at maturity.

## Study limitations and concluding remarks

It is prudent to consider several additional factors that may impact the relationships reported in our study. The use of baited traps has been shown to introduce a bias towards large, sexually mature crabs, potentially causing the overrepresentation of mature females in each size class and an underestimation of the size at maturity of female crabs (Smith *et al.* 2004)—sampling methods such as seine-netting and otter trawling may provide more representative size structures for Blue Swimmer Crab (Smith *et al.* 2004). It is also important to acknowledge that this study was conducted only over a five-month period (October 2019 to February 2020) with no replication across successive years. Year-round sampling over multiple successive years would allow us to better understand the influence of temperature on year-to-year recruitment and fisheries productivity as well as the broader impact of climate change and tropicalisation on Blue Swimmer Crab reproduction. Finally, our study compared only gonad development (ovary weight), energy reserves (hepatopancreas weight) and egg mass weight (as a proxy for egg production) relative to total body mass, whereas fecundity (the number of offspring produced) is also commonly used as a measure of reproductive output. Future studies examining fecundity (i.e., egg production) across similar scales will further strengthen our understanding of the impacts of temperature, climate change, and tropicalisation on Blue Swimmer Crab reproduction.

In conclusion, we found the most fecund females in Botany Bay, the estuary with the largest exposure to the ocean and the lowest summer water temperature. Thermal performance curves showed a peak in individual reproductive output at a mean monthly temperature of  $\sim 24^{\circ}\text{C}$ . Above  $24^{\circ}\text{C}$  the GSI (an index of gonadal development) began to decline. Temperature is a clear driver of spatial and temporal variation in reproduction in female Blue Swimmer Crab. Further investigation that examines similar relationships over broader temporal scales will improve our understanding of how environmental variability and coastal warming influences reproduction, recruitment and

fisheries productivity in south-eastern Australia. Modelling of environment-reproduction-recruitment relationships will also support fisheries management practices, to ensure that harvest levels remain sustainable alongside the influence of environmental change.

# Estuary-specific drivers of Blue Swimmer Crab abundance and distribution

## Background and rationale

As noted in the *Introduction*, previous research on Blue Swimmer Crab indicates that temperature and salinity may have substantial effects on life history, abundance and distribution. This research also highlights the potential for phenological patterns in these variables. However, as also noted earlier, these relationships are largely unknown for Blue Swimmer Crab in south-eastern Australia.

The long-term independent survey was designed to produce a reliable dataset to tease apart these relationships in key estuaries for Blue Swimmer Crab, and provided a time-series of monthly data collected in a standardised fashion, which spanned three growth seasons. *Broad patterns in abundance and size structure* that were observed in each of the three main study estuaries are described earlier. This section outlines statistical analysis of relationships between key variables of temperature, flow, and conductivity, and Blue Swimmer Crab abundance and distribution, during the long-term independent survey, focussing on data from Wallis Lake and Port Stephens. Lake Macquarie was excluded from these analyses, for a number of reasons. Including it is subject to different fishing pressure (with no crab trapping permitted in the estuary), has remarkable differences in geomorphology to the other estuaries, has only minor tributaries relative to an expansive waterway area, and thermal regimes are subject to substantial influence from power station cooling water.

Specifically, this chapter examines spatial and temporal variation of Wallis Lake and Port Stephens Blue Swimmer Crab populations in relation to seasonal and environmental variability, through: 1) Quantifying the putative impact of abiotic drivers on abundance; and 2) Establishing links between putative abiotic drivers and the distribution of Blue Swimmer Crab throughout the estuary.

## Methods

### Sampling and analysis

Sampling and processing was conducted as described above for the regular independent survey, and analysis incorporated temperature and conductivity, and flow data presented in Figure 18 (Wallis Lake) and Figure 19 (Port Stephens). For the analysis presented below, temperature and conductivity data collected at the lower Coolongolook River logger station (LOG.3, Figure 14, Figure 18) and the Lemon Tree Passage logger station (LOG.3, Figure 15, Figure 19) were used for Wallis Lake and Port Stephens, respectively. Flow data was also categorised as 'pulse' and 'no pulse', based on classifying days when the daily flow was in the highest 10% of all daily flows as a 'pulse' event (Taylor *et al.* 2014).

Several graphical and statistical approaches were used for analysis. The temperature and conductivity loggers were missing data for 6% of days (Figure 18 and Figure 19) and data for these days were estimated using linear interpolation between adjacent data points. Prior to analysis all candidate explanatory variables were assessed for collinearity (Pearson  $r > 0.6$ ) using scatter plots matrices and correlation coefficient tests, and none were found to be collinear.

Variations in the abundance of Blue Swimmer Crab in response to varying environmental factors was evaluated using generalised linear mixed models (GLMMs) with a Poisson error distribution (with log link) for each estuary separately, using a full backwards stepwise model selection approach starting with the following equation:

$$\log(Abund_{i,j,k}) \sim \beta_1 * Temp_j + \beta_2 * (Temp_j)^2 + \beta_3 * Cond_j + \beta_4 * (Cond_j)^2 + \beta_5 * Flow_j + Site_i + Date_j$$

$$Site_i \sim Normal(0, \sigma^2_1)$$

$$Date_j \sim Normal(0, \sigma^2_2)$$

$$Offset = \log(Soak_{i,j,k})$$

where  $Abund_{i,j,k}$  represents the abundance of Blue Swimmer Crab at *Site i* on *Date j* in replicate trap *k*.  $\beta$ 's represent the coefficient values of each explanatory variable, where  $Temp_j$  is the mean temperature of the 30 days prior to *Date j*,  $Cond_j$  is the mean conductivity of the 30 days prior to sampling *Date j*, and  $Flow$  is a categorical variable reflecting whether there were any 'pulse' flow events in the 30 days prior to sampling *Date j*. Both linear and quadratic forms of  $Temp$  and  $Cond$  were included in the model as there may be non-linear responses to these variables.  $Site$  and  $Date$  both represented random intercept effects which account for dependencies in sampling design. Soak time ( $Soak$ ) of each trap was used as an offset to control for minor differences in sampling effort.

The spatial analysis in each estuary consisted of creating a distance-to-sea variable, by extracting a value for each trap deployment from a raster proximity map reflecting the distance to the mouth of the estuary. Combining all samples within a month, weighted kernel density estimates were then calculated based upon the distance-to-sea and abundance of male and female Blue Swimmer Crab within each trap. For each month, the median distance-to-sea and interquartile range (the difference between 25% and 75% quartile distances) were extracted as indices of 'position' and 'spread' (respectively) of the Blue Swimmer Crab population within the estuary, and were calculated for male and female distributions separately. Linear models were used to determine the influence of environmental variables on the spatial distribution of Blue Swimmer Crab using a similar model selection process as described above starting with the following full model:

$$MDS_{m,s} \text{ or } IQR_{m,s} \sim \beta_1 * Temp_m + \beta_2 * Cond_m + \beta_3 * Sex_s + \beta_4 * Flow_m + \beta_5 * Sex * Flow_m + Period_m$$

$$Period_m \sim Normal(0, \sigma^2_2)$$

where  $MDS_m$  is the median distance-to-sea in month *m* for sex *s*,  $IQR_m$  is the interquartile range in month *m* for sex *s*.  $\beta$ 's represent the coefficient values of each explanatory variable, where  $Temp_m$  is the mean temperature of the 30 days prior to the first day of sampling during month *m* and  $Cond_m$  is the mean conductivity of the 30 days prior to the first day of sampling during month *m*.  $Sex_s$  is a categorical variable for Male or Female and  $Flow_m$  is a categorical variable reflecting whether there were any 'pulse' flow events in the 30 days prior to the first day of sampling during month *m*.  $Sex_s * Flow_m$  represents an interaction term between the categorical factors of sex and flow allowing each sex to respond differently to flow events.  $Period$  represents a random intercept effect controlling for a dependency in the sampling design, where we have 1 value from each sampling period (month) for each sex. During the model selection process, the variables  $Sex$  and the random intercept effect of  $Period$  were forcibly retained in all models due to the dependency structures within the data.

All models were fit using the 'glmmTMB' package (Brooks *et al.* 2017), residuals and assumptions of the model were checked using the 'DHARMA' package (Hartig 2020). These models were used with a manual backwards selection process to derive the final model, whereby each variable was removed, one at a time and the Akaike information criterion values (AIC) compared between competing models. Models with  $\Delta\text{AIC} < 2$  of the lowest AIC model were considered equivalent (Burnham and Anderson 2002b) and selection only stopped if the reduced model was not equivalent or better than the previous model ( $\Delta\text{AIC} > 2$ ). Model results were visualised by manually creating partial effects prediction plots showing the influence of each variable when all other variables were held at mean levels.

## Results

### Influence of environmental variables on abundance

The best fit model for Wallis Lake Blue Swimmer Crab abundance was the full model without flow, which was equivalent to the full model ( $\Delta\text{AIC} < 2$ ; Table 4) containing temperature (both linear and quadratic) and conductivity (both linear and quadratic). This model explained a large portion of the variance (conditional  $r^2 = 0.619$ , marginal  $r^2 = 0.457$ ). There was strong evidence of nonlinear impacts of both temperature ( $\chi^2_2 = 121.07$ ,  $P < 0.001$ ; Figure 30a) and conductivity ( $\chi^2_2 = 81.34$ ,  $P < 0.001$ ). Abundance responded strongly in a positive manner to temperatures above 20°C (Figure 30a), while abundance declined when conductivity was higher than 40  $\text{ms cm}^{-1}$  (Figure 30c). Adding flow to the model did not significantly improve the model (Table 4).

The final model for Port Stephens Blue Swimmer Crab abundance included temperature (both linear and quadratic terms) and conductivity. This model was equivalent to both the full model and a number of other models but this was the simplest equivalent model (Table 5). The Port Stephens model explained less variance than the Wallis Lake model (conditional  $r^2 = 0.251$ , marginal  $r^2 = 0.110$ ). There was evidence of a nonlinear impact of temperature ( $\chi^2_2 = 8.44$ ,  $P = 0.015$ ) and a strong negative effect of conductivity ( $\chi^2_2 = 24.68$ ,  $P < 0.001$ ). Abundance showed a weak quadratic relationship with temperature with an apparent optimum at approximately 21°C (Figure 30b), while abundance declined with increasing conductivity (Figure 30d).

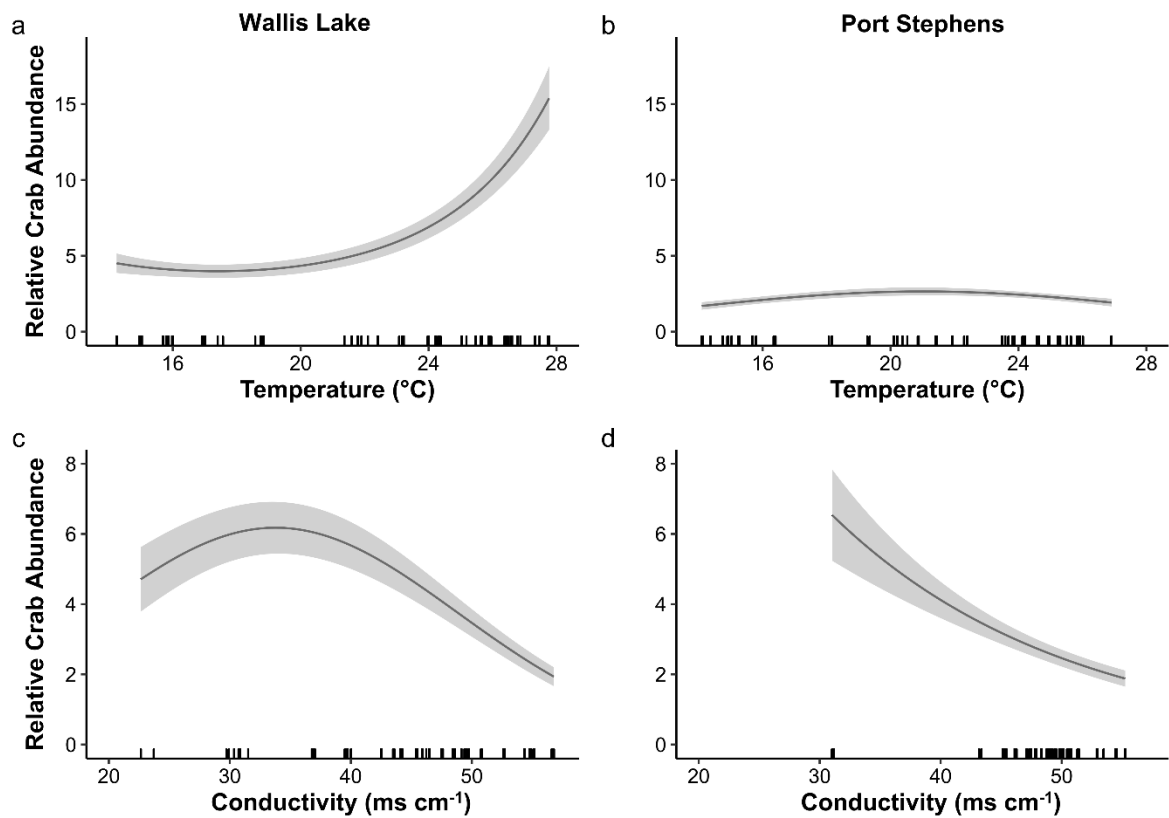


**Figure 30** Modelled relative Blue Swimmer Crab abundance (grey shading is standard error of prediction) in relation to temperature (a, b) and conductivity (c, d), for Wallis Lake (left panels) and Port Stephens (right panels).

**Table 4** Model selection table for Wallis Lake Blue Swimmer Crab abundance constructed with backwards stepwise selection. Linear and quadratic forms of temperature ( $Temp^2$ ) and conductivity ( $Cond^2$ ) were included to test for non-linearity. Models are presented in the order tested, and included random intercept effects for site (1|Site) and date (1|Date).  $\Delta AIC$  shows the difference in AIC values from the best (lowest AIC) model. If two models were equivalent ( $<2 \Delta AIC$ ; shown in bold), the simpler model was retained in the selection process. The best model was M6

| Model   | Comment            | AIC            | $\Delta AIC$ |
|---|--------------------|----------------|--------------|
| <b>M1</b> $Abund \sim Temp + Temp^2 + Cond + Cond^2 + Flow + (1 Site) + (1 Date)$ | Full model         | <b>10573.5</b> | <b>1.2</b>   |
| M2 $Abund \sim Temp + Cond + Cond^2 + Flow + (1 Site) + (1 Date)$                 | M1 + drop $Temp^2$ | 10588.5        | 16.2         |
| M3 $Abund \sim Temp + Temp^2 + Cond + Flow + (1 Site) + (1 Date)$                 | M1 + drop $Cond^2$ | 10591.4        | 19.1         |
| M4 $Abund \sim Cond + Cond^2 + Flow + (1 Site) + (1 Date)$                        | M1 + drop $Temp$   | 10632.7        | 60.4         |
| M5 $Abund \sim Temp + Temp^2 + Flow + (1 Site) + (1 Date)$                        | M1 + drop $Cond$   | 10602.6        | 30.3         |

|           | <b>Model</b>  | <b>Comment</b>              | <b>AIC</b>     | <b>ΔAIC</b> |
|-----------|---|-----------------------------|----------------|-------------|
| <b>M6</b> | <b><i>Abund ~ Temp + Temp<sup>2</sup> + Cond + Cond<sup>2</sup> + (1 Site) + (1 Date)</i></b> | <b>M1 + drop Flow</b>       | <b>10572.3</b> | <b>0</b>    |
| M7        | <i>Abund ~ Temp + Cond + Cond<sup>2</sup> + (1 Site) + (1 Date)</i>                           | M6 + drop Temp <sup>2</sup> | 10586.9        | 14.6        |
| M8        | <i>Abund ~ Temp + Temp<sup>2</sup> + Cond + (1 Site) + (1 Date)</i>                           | M6 + drop Cond <sup>2</sup> | 10589.4        | 17.1        |
| M9        | <i>Abund ~ Cond + Cond<sup>2</sup> + (1 Site) + (1 Date)</i>                                  | M6 + Drop Temp              | 10633.4        | 61.1        |
| M10       | <i>Abund ~ Temp + Temp<sup>2</sup> + (1 Site) + (1 Date)</i>                                  | M6 + Drop Cond              | 10618.8        | 46.5        |

**Table 5** Model selection table for Port Stephens Blue Swimmer Crab abundance constructed with backwards stepwise selection. Linear and quadratic forms of temperature (*Temp<sup>2</sup>*) and conductivity (*Cond<sup>2</sup>*) were included to test for non-linearity. Models are presented in the order tested, and included random intercept effects for site (1|*Site*) and date (1|*Date*). ΔAIC shows the difference in AIC values from the best (lowest AIC) model. If two models were equivalent (<2 ΔAIC; shown in bold), the simpler model was retained in the selection process. The best model was M10

|            | <b>Model</b>   | <b>Comment</b>                    | <b>AIC</b>    | <b>ΔAIC</b> |
|------------|--|-----------------------------------|---------------|-------------|
| <b>M1</b>  | <b><i>Abund ~ Temp + Temp<sup>2</sup> + Cond + Cond<sup>2</sup> + Flow + (1 Site) + (1 Date)</i></b> | <b>Full model</b>                 | <b>7811.2</b> | <b>0.1</b>  |
| M2         | <i>Abund ~ Temp + Cond + Cond<sup>2</sup> + Flow + (1 Site) + (1 Date)</i>                           | M1 + drop Temp <sup>2</sup>       | 7818.2        | 7.1         |
| <b>M3</b>  | <b><i>Abund ~ Temp + Temp<sup>2</sup> + Cond + Flow + (1 Site) + (1 Date)</i></b>                    | <b>M1 + drop Cond<sup>2</sup></b> | <b>7811.1</b> | <b>0</b>    |
| M4         | <i>Abund ~ Cond + Cond<sup>2</sup> + Flow + (1 Site) + (1 Date)</i>                                  | M1 + drop Temp                    | 7817.8        | 6.7         |
| M5         | <i>Abund ~ Temp + Temp<sup>2</sup> + Flow + (1 Site) + (1 Date)</i>                                  | M1 + drop Cond                    | 7828.1        | 17          |
| M6         | <i>Abund ~ Temp + Temp<sup>2</sup> + Cond + Cond<sup>2</sup> + (1 Site) + (1 Date)</i>               | M1 + drop Flow                    | 7813.7        | 2.6         |
| M7         | <i>Abund ~ Temp + Cond + Flow + (1 Site) + (1 Date)</i>  | M3 + drop Temp <sup>2</sup>       | 7817.4        | 6.3         |
| M8         | <i>Abund ~ Cond + Flow + (1 Site) + (1 Date)</i>   | M3 + drop Temp                    | 7816.2        | 5.1         |
| M9         | <i>Abund ~ Temp + Temp<sup>2</sup> + Flow + (1 Site) + (1 Date)</i>                                  | M3 + drop Cond                    | 7828.1        | 17          |
| <b>M10</b> | <b><i>Abund ~ Temp + Temp<sup>2</sup> + Cond + (1 Site) + (1 Date)</i></b>                           | <b>M3 + drop Flow</b>             | <b>7811.8</b> | <b>0.7</b>  |
| M11        | <i>Abund ~ Temp + Cond + (1 Site) + (1 Date)</i>   | M10 + drop Temp <sup>2</sup>      | 7816.9        | 5.8         |
| M12        | <i>Abund ~ Cond + (1 Site) + (1 Date)</i>  | M10 + drop Temp                   | 7815.7        | 4.6         |
| M13        | <i>Abund ~ Temp + Temp<sup>2</sup> + (1 Site) + (1 Date)</i>   | M10 + drop Cond                   | 7829.1        | 18          |

## Influence of environmental variables on location and distribution

Kernel density estimates reflecting trends in the distribution of the Blue Swimmer Crab population along the target estuaries showed variation between estuaries, months and sexes (Figure 31 and Figure 32). In Wallis Lake, the population tended to be concentrated in the area within 14 km of the mouth (Figure 31). Males tended to be better represented (than females) at distances greater than this, and showed a distinctive peak at ~12.5 km during periods 201908, 202012, 202104 and 202105. In contrast, more often than not females appeared to be more heavily concentrated closer to the mouth (Figure 31). In Port Stephens, there was little overall variation in the distribution of the population along the estuary between months and sexes (Figure 32). The key exception to this were distinct peaks in the distribution of females closer to the mouth in periods 201910, 202005, 202010, 202011, and a distinct peak in females further away from the mouth during period 202002 (Figure 32).

The model with the most parsimonious fit for the median distance to sea for Wallis Lake was model containing temperature, conductivity and sex (Table 6; marginal  $r^2 = 0.67$ , conditional  $r^2 = 0.67$ ). There was strong evidence of a negative temperature effect with the median position of the population moving closer to the estuary mouth (ocean) with increasing temperatures ( $\chi^2_1 = 10.674$ ,  $P = 0.001$ ). The model indicated that a 1° C increase in temperature would shift the population  $\approx 61$  m (18.7 m SE) on average closer to the ocean (Figure 33a). There was also strong evidence that as conductivity increased, the median position of the population moved further into the estuary ( $\chi^2_1 = 10.857$ ,  $P = 0.001$ ). For a 1 ms  $\text{cm}^{-1}$  increase in conductivity the median position of the population shifted  $\approx 28$  m (8.5 m SE) on average further into the estuary (Figure 33b). Males were also consistently located slightly further into the estuary compared to females ( $\chi^2_1 = 58.982$ ,  $P < 0.001$ ; Figure 33c). The model selection process for the interquartile spread of the population had problems converging during the model selection process (Table 7), and we therefore retained the full model. There was no evidence of any influence of temperature ( $\chi^2_1 = 0.398$ ,  $P = 0.528$ ), conductivity ( $\chi^2_1 = 0.632$ ,  $P = 0.427$ ), flow ( $\chi^2_1 = 0.001$ ,  $P = 0.980$ ) or sex ( $\chi^2_1 = 0.057$ ,  $P = 0.811$ ) on the spread of the population within Wallis Lake.

For the median distance to sea for Port Stephens analysis, no model showed any significant improvement over the simplest (sex, and period [random] effect) model (Table 8;  $\Delta\text{AIC} < 2$ ). This suggests there are no meaningful effects of temperature, conductivity or flow on the median position of the population. The model itself also showed no evidence of a difference between sexes ( $\chi^2_1 = 1.917$ ,  $P = 0.166$ ). In contrast, the most parsimonious model investigating the spread of the population was the model containing conductivity, sex and the period [random] effect (Table 9). There was no significant effect of conductivity ( $\chi^2_1 = 0.962$ ,  $P = 0.327$ ) but there was a significant effect of Sex ( $\chi^2_1 = 11.626$ ,  $P < 0.001$ ). The male portion of the Blue Swimmer Crab population had a larger interquartile range compared to the female portion (Figure 34).

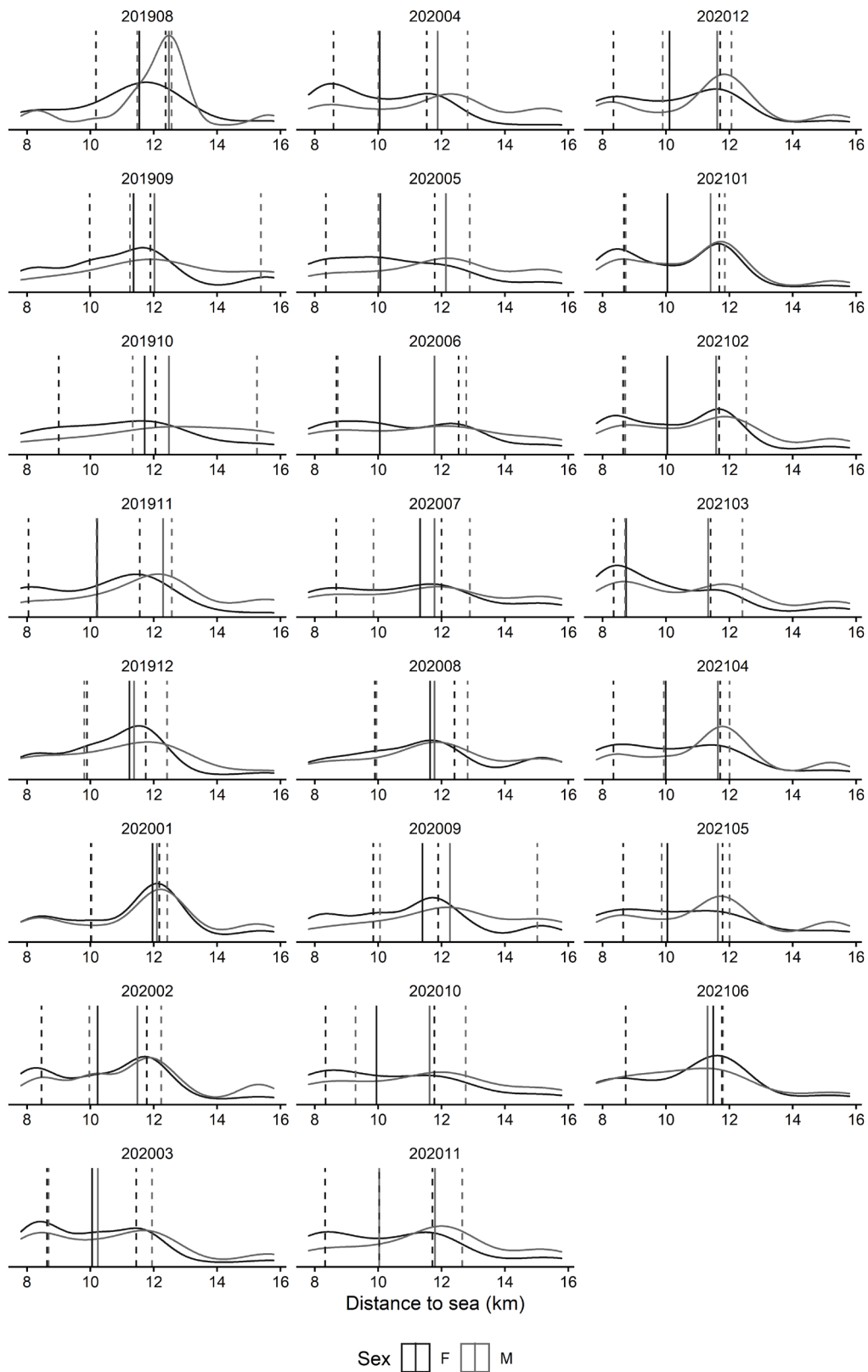


**Figure 31** Monthly sex-specific spatial data for Blue Swimmer Crab samples collected in Wallis Lake, expressed as kernel density estimates. Panel headers indicate sampling period (YYYYMM). The vertical solid lines indicate the median distance-to-sea for female (black) and male (grey) crabs, and the vertical dashed lines indicate the lower and upper bounds for the interquartile range for each sex.

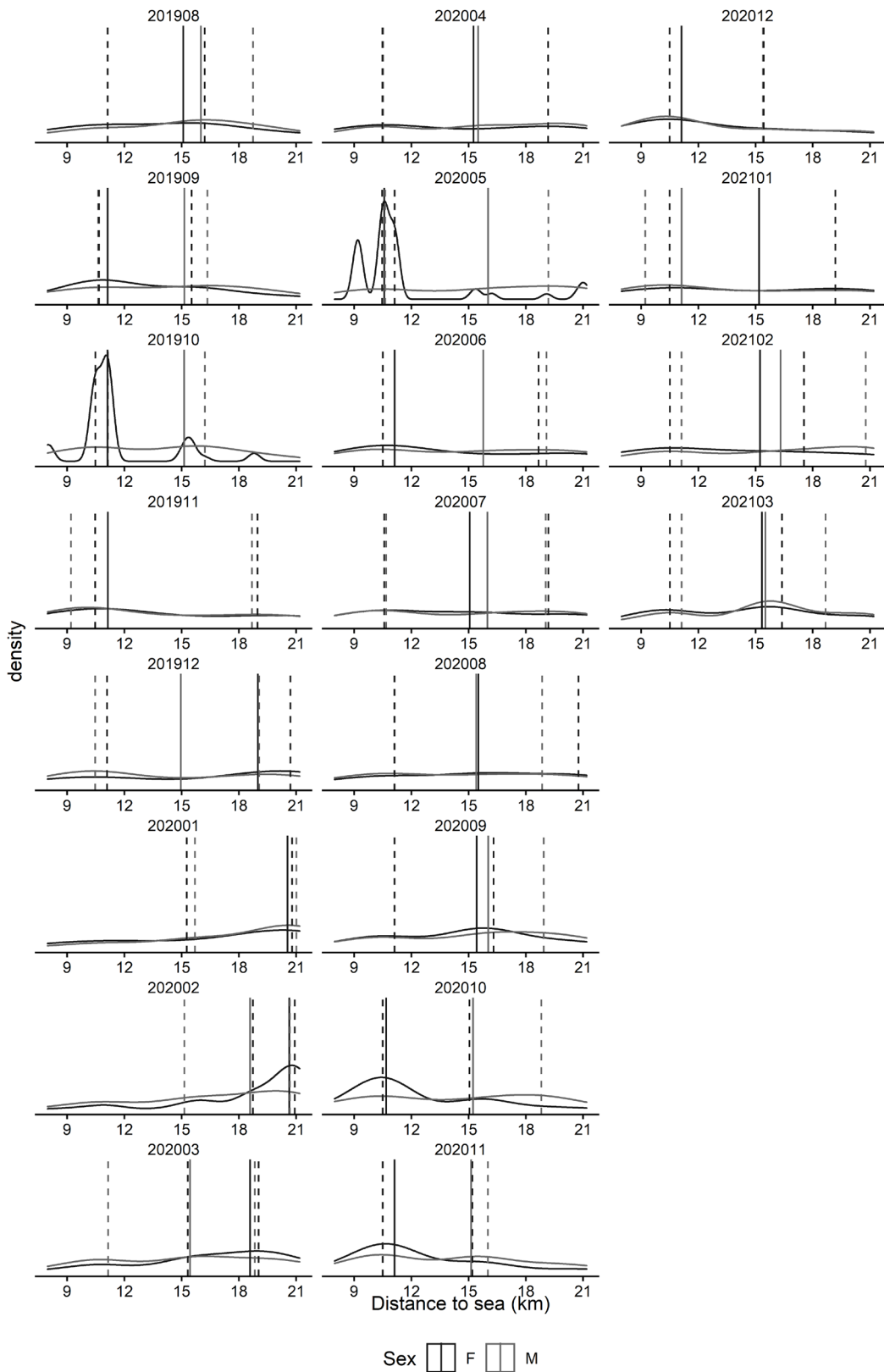


**Figure 32** Monthly sex-specific spatial data for Blue Swimmer Crab samples collected in Port Stephens, expressed as kernel density estimates. Panel headers indicate sampling period (YYYYMM). The vertical solid lines indicate the median distance-to-sea for female (black) and male (grey) crabs, and the vertical dashed lines indicate the lower and upper bounds for the interquartile range for each sex.

**Table 6** Model selection table for Wallis Lake Blue Swimmer Crab distance to sea (*Distance*) constructed with backwards stepwise selection where the least significant (highest P-value) term was removed in each step (‘:’ between two variables indicates an interaction term. Models are presented in the order tested, and included random intercept effects for each sample period (1|Period).  $\Delta$ AIC shows the difference in AIC values from the best (lowest AIC) model. If two models were equivalent (<2  $\Delta$ AIC; shown in bold), the simpler model was retained in the selection process.

|           | <b>Model</b>   | <b>Comment</b>        | <b>AIC</b>   | <b><math>\Delta</math>AIC</b> |
|-----------|--|-----------------------|--------------|-------------------------------|
| M1        | <i>Distance ~ Temp + Cond + Flow + Sex + Flow:Sex + (1 Period)</i> | Full model            | 719.2        | 2.5                           |
| M2        | <i>Distance ~ Temp + Flow + Sex + Flow:Sex + (1 Period)</i>        | Drop Cond             | 720.3        | 3.6                           |
| M3        | <i>Distance ~ Cond + Flow + Sex + Flow:Sex + (1 Period)</i>        | Drop Temp             | 725.7        | 9                             |
| M4        | <i>Distance ~ Temp + Cond + Sex + Flow:Sex + (1 Period)</i>        | Drop Flow             | 719.2        | 2.5                           |
| <b>M5</b> | <b><i>Distance ~ Temp + Cond + Flow + Sex + (1 Period)</i></b>     | <b>Drop Flow:Sex</b>  | <b>718.4</b> | <b>1.7</b>                    |
| M6        | <i>Distance ~ Cond + Flow + Sex + (1 Period)</i>                   | M5 + drop Temp        | 724.8        | 8.1                           |
| <b>M7</b> | <b><i>Distance ~ Temp + Cond + Sex + (1 Period)</i></b>            | <b>M5 + drop Flow</b> | <b>716.7</b> | <b>0</b>                      |
| M8        | <i>Distance ~ Temp + Flow + Sex + (1 Period)</i>                   | M5 + drop Cond        | 719.4        | 2.7                           |
| M9        | <i>Distance ~ Cond + Sex + (1 Period)</i>                          | M7 + drop Temp        | 723.8        | 7.1                           |
| M10       | <i>Distance ~ Temp + Sex + (1 Period)</i>                          | M7 + drop Cond        | 724.0        | 7.3                           |

**Table 7** Model selection table for Wallis Lake Blue Swimmer Crab interquartile spread (*Spread*) constructed with backwards stepwise selection where the least significant (highest P-value) term was removed in each step (‘:’ between two variables indicates an interaction term. Models are presented in the order tested, and included random intercept effects for each sample period (1|Period).  $\Delta$ AIC shows the difference in AIC values from the best (lowest AIC) model. If two models were equivalent (<2  $\Delta$ AIC; shown in bold), the simpler model was retained in the selection process

|           | <b>Model</b>  | <b>Comment</b>       | <b>AIC</b>   | <b><math>\Delta</math>AIC</b> |
|-----------|---|----------------------|--------------|-------------------------------|
| <b>M1</b> | <b><i>Spread ~ Temp + Cond + Flow + Sex + Flow:Sex + (1 Period)</i></b> | <b>Full model</b>    | <b>747.4</b> | <b>1.6</b>                    |
| <b>M2</b> | <b><i>Spread ~ Cond + Flow + Sex + Flow:Sex + (1 Period)</i></b>        | <b>Drop Temp</b>     | <b>745.8</b> | <b>0</b>                      |
| <b>M3</b> | <b><i>Spread ~ Temp + Cond + Sex + Flow:Sex + (1 Period)</i></b>        | <b>Drop Flow</b>     | <b>747.4</b> | <b>1.6</b>                    |
| <b>M4</b> | <b><i>Spread ~ Temp + Cond + Flow + Sex + Flow:Sex + (1 Period)</i></b> | <b>Drop Flow:Sex</b> | <b>747.0</b> | <b>1.2</b>                    |
| <b>M5</b> | <b><i>Spread ~ Temp + Flow + Sex + Flow:Sex + (1 Period)</i></b>        | <b>Drop Cond</b>     | <b>746.0</b> | <b>0.2</b>                    |

|    | <b>Model</b>                                       | <b>Comment</b>            | <b>AIC</b> | <b>ΔAIC</b> |
|----|--|---------------------------|------------|-------------|
| M6 | <i>Spread ~ Cond + Sex + Flow:Sex + (1 Period)</i> | M2 + drop <i>Flow</i>     | *          | NA          |
| M7 | <i>Spread ~ Cond + Flow + Sex + (1 Period)</i>     | M2 + drop <i>Flow:Sex</i> | *          | NA          |
| M8 | <i>Spread ~ Flow + Sex + Flow:Sex + (1 Period)</i> | M2 + drop <i>Cond</i>     | *          | NA          |

\* Convergence error

**Table 8** Model selection table for Port Stephens Blue Swimmer Crab distance to sea (*Distance*) constructed with backwards stepwise selection where the least significant (highest P-value) term was removed in each step (‘:’ between two variables indicates an interaction term. Models are presented in the order tested, and included random intercept effects for each sample period (1|Period). ΔAIC shows the difference in AIC values from the best (lowest AIC) model. If two models were equivalent (<2 ΔAIC; shown in bold), the simpler model was retained in the selection process.

|            | <b>Model</b>   | <b>Comment</b>  | <b>AIC</b>   | <b>ΔAIC</b> |
|------------|--|---|--------------|-------------|
| M1         | <i>Distance ~ Temp + Cond + Flow + Sex + Flow:Sex + (1 Period)</i> | Full model  | 753.4        | 4.7         |
| <b>M2</b>  | <b><i>Distance ~ Temp + Flow + Sex + Flow:Sex + (1 Period)</i></b> | <b>Drop <i>Cond</i></b>                                     | <b>748.7</b> | <b>0</b>    |
| <b>M3</b>  | <b><i>Distance ~ Cond + Flow + Sex + Flow:Sex + (1 Period)</i></b> | <b>Drop <i>Temp</i></b>                                     | <b>748.9</b> | <b>0.2</b>  |
| <b>M4</b>  | <b><i>Distance ~ Temp + Cond + Sex + Flow:Sex + (1 Period)</i></b> | <b>Drop <i>Flow</i></b>                                     | <b>750.4</b> | <b>1.7</b>  |
| M5         | <i>Distance ~ Temp + Cond + Flow + Sex + (1 Period)</i>            | Drop <i>Flow:Sex</i>  | 756.0        | 7.3         |
| M6         | <i>Distance ~ Flow + Sex + Flow:Sex + (1 Period)</i>               | M2 + drop <i>Temp</i>                                       | 754.3        | 5.6         |
| M7         | <i>Distance ~ Temp + Sex + Flow:Sex + (1 Period)</i>               | M2 + drop <i>Flow</i>                                       | *            | NA          |
| M8         | <i>Distance ~ Temp + Flow + Sex + (1 Period)</i>                   | M2 + drop <i>Flow:Sex</i>                                   | 750.9        | 2.2         |
| M9         | <i>Distance ~ Flow + Sex + (1 Period)</i>                          | M8 + drop <i>Temp</i>                                       | 754.5        | 5.8         |
| <b>M10</b> | <b><i>Distance ~ Temp + Sex + (1 Period)</i></b>                   | <b>M8 + drop <i>Flow</i></b>                                | <b>750.6</b> | <b>1.9</b>  |
| <b>M11</b> | <b><i>Distance ~ Sex + (1 Period)</i></b>                          | <b>M10 + drop <i>Temp</i><br/>(Simplest possible model)</b> | <b>750.2</b> | <b>1.5</b>  |

\* Convergence error

**Table 9** Model selection table for Port Stephens Blue Swimmer Crab interquartile spread (*Spread*) constructed with backwards stepwise selection where the least significant (highest P-value) term was removed in each step (‘:’ between two variables indicates an interaction term. Models are presented in the order tested, and included random intercept effects for each sample period (1|Period).  $\Delta$ AIC shows the difference in AIC values from the best (lowest AIC) model. If two models were equivalent (<2  $\Delta$ AIC; shown in bold), the simpler model was retained in the selection process.

|           | <b>Model</b>   | <b>Comment</b>                                     | <b>AIC</b>   | <b><math>\Delta</math>AIC</b> |
|-----------|--|--|--------------|-------------------------------|
| M1        | <i>Spread</i> ~ <i>Temp</i> + <i>Cond</i> + <i>Flow</i> + <i>Sex</i> + <i>Flow:Sex</i> + (1  <i>Period</i> ) | Full model   | 735.6        | 2.8                           |
| <b>M2</b> | <b><i>Spread</i> ~ <i>Cond</i> + <i>Flow</i> + <i>Sex</i> + <i>Flow:Sex</i> + (1 <i>Period</i>)</b>          | <b>Drop Temp</b>                                   | <b>734.3</b> | <b>1.5</b>                    |
| M3        | <i>Spread</i> ~ <i>Temp</i> + <i>Cond</i> + <i>Sex</i> + <i>Flow:Sex</i> + (1  <i>Period</i> )               | Drop <i>Flow</i>                                   | 735.6        | 2.8                           |
| M4        | <i>Spread</i> ~ <i>Temp</i> + <i>Cond</i> + <i>Flow</i> + <i>Sex</i> + <i>Flow:Sex</i> + (1  <i>Period</i> ) | Drop <i>Flow:Sex</i>                               | 736.0        | 3.2                           |
| M5        | <i>Spread</i> ~ <i>Temp</i> + <i>Flow</i> + <i>Sex</i> + <i>Flow:Sex</i> + (1  <i>Period</i> )               | Drop <i>Cond</i>                                   | 756.0        | 23.2                          |
| <b>M6</b> | <b><i>Spread</i> ~ <i>Cond</i> + <i>Sex</i> + <i>Flow:Sex</i> + (1 <i>Period</i>)</b>                        | <b>M2 + <i>Flow</i></b>                            | <b>734.3</b> | <b>1.5</b>                    |
| <b>M7</b> | <b><i>Spread</i> ~ <i>Cond</i> + <i>Flow</i> + <i>Sex</i> + (1 <i>Period</i>)</b>                            | <b>M2 + drop <i>Flow:Sex</i></b>                   | <b>734.7</b> | <b>1.9</b>                    |
| M8        | <i>Spread</i> ~ <i>Flow</i> + <i>Sex</i> + <i>Flow:Sex</i> + (1  <i>Period</i> )                             | M2 + drop <i>Cond</i>                              | *            | NA                            |
| <b>M9</b> | <b><i>Spread</i> ~ <i>Cond</i> + <i>Sex</i> + (1 <i>Period</i>)</b>  | <b>M6 + drop <i>Flow:Sex</i></b>                   | <b>732.8</b> | <b>0</b>                      |
| M10       | <i>Spread</i> ~ <i>Sex</i> + <i>Flow:Sex</i> + (1  <i>Period</i> )   | M6 + drop <i>Cond</i>                              | 739.3        | 6.5                           |
| M11       | <i>Spread</i> ~ <i>Sex</i> + (1  <i>Period</i> )   | M9 + drop <i>Cond</i><br>(simplest possible model) | *            | NA                            |

\*Convergence error

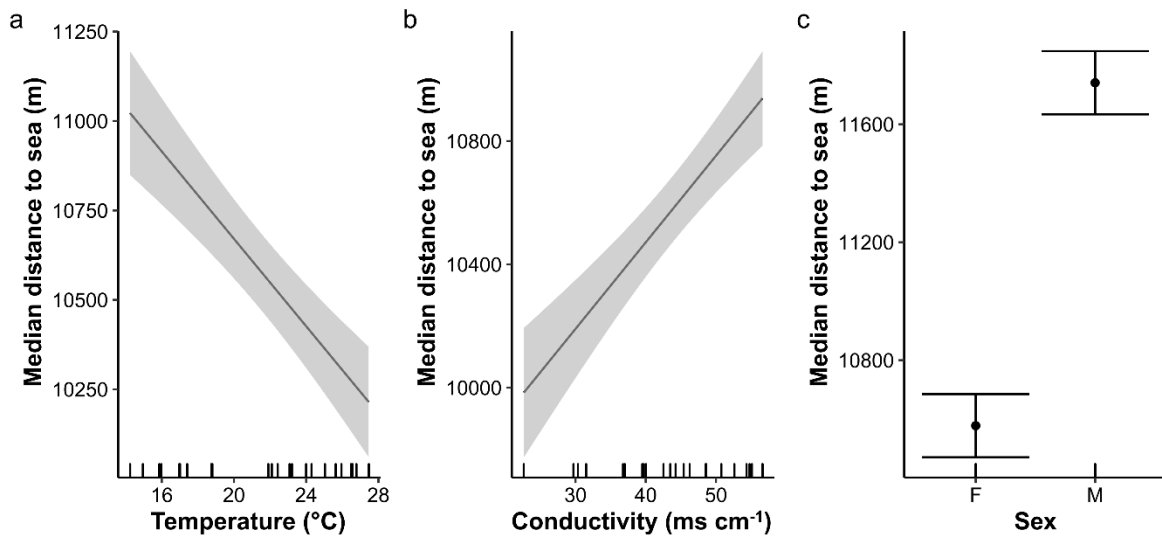


**Figure 33** Modelled Blue Swimmer Crab median distance to sea in Wallis Lake (grey shading and error bars indicate standard error of prediction) in relation to temperature (a), conductivity (b) and sex (c).

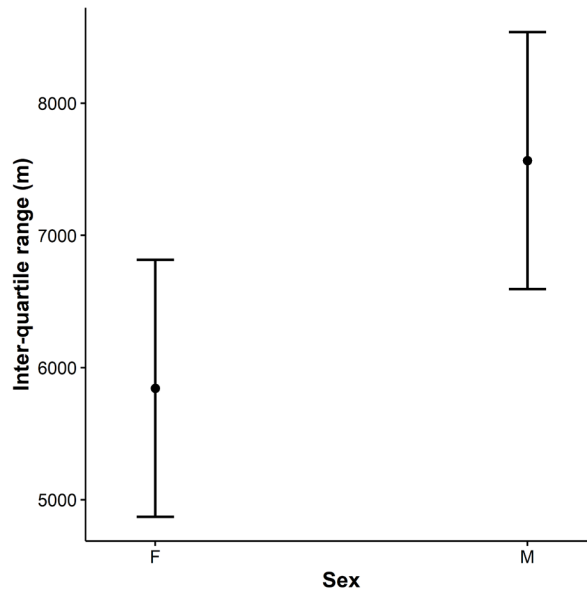


**Figure 34** Modelled Blue Swimmer Crab interquartile range in Port Stephens (error bars show the standard error of the predictions) in relation to sex.

## Discussion

The patterns presented here provide insight in the role of key environmental variables on both the abundance and distribution of Blue Swimmer Crab within the estuary. As established in the *Introduction* (see *Influence of environmental variability on Blue Swimmer Crab*), previous work has highlighted that Blue Swimmer Crab abundance may show a peak at certain temperatures, and that flow can influence the distribution of crabs across the estuary and adjacent inshore areas (Gillson *et al.* 2012). Our analyses showed that both temperature and conductivity (salinity) influenced abundance over the regular independent survey, and these relationships are discussed in the subsections below. The abundance and spatial relationships are also further considered alongside patterns in reproduction, and potential implications for fisheries productivity, in the *General discussion*.

### Influence of temperature on crab abundance and distribution

Temperature was highly influential on the abundance of Blue Swimmer Crab, which aligns with previous work on the species. Patterns in the catch rate data (Figure 21) suggest that this is largely capturing a seasonal effect. This likely arises due to the fact that crabs are ectotherms so metabolic rates and activity are closely tied to environmental temperatures (Halsey *et al.* 2015), and associated feeding and foraging requirements. In Wallis Lake, catch rates elevated considerably during the warmer months of the year (normally January to March), typically representing the main recruitment pulse into the estuary during each year (Figure 21 and Figure 22). Considering that crabs recruit to both the estuary, and the fishery within the same spring/summer period, it is likely that the lower catch rates during cooler months is also reflecting comparatively lower abundance (alongside lower activity), following the cumulative fishing and natural mortality that the estuarine population experiences during late summer and autumn.

There were somewhat contrasting relationships with temperature in Port Stephens, compared with Wallis Lake. There was only a minor influence of temperature on abundance in Port Stephens (although it is important to note that the overall magnitude of abundance was also much lower than Wallis Lake). In contrast to Wallis Lake, there was some evidence for a minor peak in abundance for Port Stephens, at around 22°C. Interestingly, this aligns closely with the findings of Johnston *et al.* (2021b), who found a maxima in catch rates (usually between 20-25°C) in estuaries at higher latitudes, but not at lower latitude. We note that metabolic rate of Blue Swimmer Crab monotonically increased up to the maximum temperature tested (29°C) in the study of Junk *et al.* (2021), indicating that the metabolic thermal optima for the species was at some temperature greater than this level. This suggested that in these environments, metabolic factors are unlikely to be driving this peak, and other factors are likely at play.

Catch rates in Wallis Lake definitely appeared more cyclical across seasons, with greater relative differences between peaks and troughs in abundance, and multiple months of elevated catches during each spring/summer period compared to Port Stephens which usually displayed only a single strong peak during a single month for each spring/summer period (Figure 21). Port Stephens has a large mouth, greater tidal connectivity to the ocean, and a greater depth (reducing the influence of wind and air temperature), than Wallis Lake. These attributes may have contributed to slightly lesser variability in water temperature observed in Port Stephens than Wallis Lake (Figure 18 and Figure 19), which in turn may have contributed to lesser variability in abundance in Port Stephens relative to Wallis Lake.

The population of crabs in Wallis Lake skewed further into the estuary during cooler temperatures (Figure 33). This trend was largely driven by a bias in the catch toward males who are likely to be more gregarious than females during cooler temperatures, and were in general distributed further away from the mouth in Wallis Lake (Figure 31). There were no such relationships evident for Port Stephens, with the only detectable trend in spatial distribution being an elevated interquartile range in males, showing that males were in general distributed further along the estuary than females.

## **Influence of conductivity and flow on crab abundance and distribution**

Although different conductivity ranges were experienced in Wallis Lake and Port Stephens, the curves produced were very similar for the conductivity ranges that overlapped (~30-55 mS cm<sup>-1</sup>, Figure 30). The Wallis Lake curve indicated a peak abundance occurred at around 35 mS cm<sup>-1</sup>, with considerably lower abundance at higher conductivities in both estuaries. There is little published evidence on conductivity/salinity tolerance of late juvenile and adult crabs to aid interpretation of this relationship, however adult crabs are probably more likely to prefer higher salinity conditions (50 mS cm<sup>-1</sup> approximates a salinity of 33 at a temperature of 25°C). One possible reason for the observed decline in abundance at greater salinity may be the migration of crabs further into the estuary, as areas further up the estuary become increasingly marine. This is evident in the median distance-to-sea for Wallis Lake (Figure 33), which increased alongside conductivity—the observed decline in abundance may simply be indicative of the population moving further into the estuary than the areas that were covered by our sampling locations. Conversely, the decline in abundance at lower conductivities is likely indicative of the opposing relationship, with crabs moving closer to sea and into inshore areas.

Freshwater inflow was not identified as an influential parameter under any of the modelled scenarios. This was surprising, given previous research (outlined above) showing that Blue Swimmer Crab may be sensitive to extremely low salinity conditions that occur with strong estuary inflow. However, considering geomorphological features of the sampled estuaries alongside the distributional characteristics of the population reveals some potential reasons behind the lack of

influence of pulse flows. In Wallis Lake, the main tributaries all flow into the north of the estuary, adjacent to the mouth and connection with the sea. This configuration is likely to have a mitigating effect on the influence of the flow on the main body of the lake, which lies to the south (Figure 14). This is certainly evident in the conductivity trace plots for Wallis Island and Green Point (Figure 18), where the large flow pulses had less of an impact than the logger stations in the northern section of the estuary. This implies that the large waterway area in the central and southern sections of the estuary may well provide some refuge from high flow pulses for the estuarine Blue Swimmer Crab populations, such that the majority of the population does not emigrate to inshore areas under high flow scenarios. While these features are not replicated in Port Stephens, the large oceanic influence in the estuary is likely to provide some buffering capacity against high flow pulses (Figure 15). These factors point to a conclusion that, at least for these two estuaries (noting that they represent a considerable proportion of the Blue Swimmer Crab fisheries catch within NSW), large flow pulses may not have as substantial an impact on estuary catches of the species as was previously expected.

# Reproductive cycles of Blue Swimmer Crab in relation to variation in temperature and conductivity

## Background and rationale

Quantitative knowledge of reproductive biology is critical for evaluating the harvest patterns of exploited species. Previous work on reproduction of Blue Swimmer Crab in south-eastern Australia has been limited to a single study which was conducted over an 8-month timeframe (Johnson *et al.* 2010). In addition to the importance of managing the size of animals harvested (i.e., MLS), quantifying patterns of phenology and seasonality of reproductive processes is necessary to holistically define how the stock functions through space and time, and how this relates to harvest patterns and environmental variability.

Previous studies elsewhere (e.g., Johnston and Yeoh 2021), and other information presented in this report for south-eastern Australia (see *Latitudinal trends in the reproductive biology of female Blue Swimmer Crab in south-eastern Australia*) clearly show that temperature has a substantial influence on reproductive output for Blue Swimmer Crab. The temporal and spatial variability in indices of population abundance reported in *Estuary-specific drivers of Blue Swimmer Crab abundance and distribution*, and the environmental drivers of these patterns, may also have some bearing on the reproductive processes of the species. Thus, in addition to re-examination of basal reproductive parameters (e.g., size-at-maturity) using samples collected over a broader spatial and temporal scales (to that reported in Johnson *et al.* 2010), further longitudinal investigation of key reproductive variables will be useful for conceptually defining how the south-eastern Australian stock functions, and informing potential adaptive approaches to manage exploitation patterns in the future.

## Methods

### Sampling and analysis

Sampling and processing is described above for the regular independent survey in *Fishery independent survey of Blue Swimmer Crab – Description and data summary*.

Reproductive data was converted to binary format (immature and mature), and the size-at-maturity (carapace length at which 50% [ $L_{50}$ ] of females were sexually mature [SOM]) was estimated for each estuary by each fishing year (June to July). The SOM was estimated initially using both Frequentist and Bayesian approaches. The Frequentist estimate used a logistic GLM employing non-parametric bootstrap resampling with replacement, from the original data. The Bayesian estimate employed sampling from the posterior distribution of a logistic regression model using a random walk Metropolis algorithm, with 999 iterations for the sampler. All statistical analyses were conducted in R (R Core Team 2022).

## Results

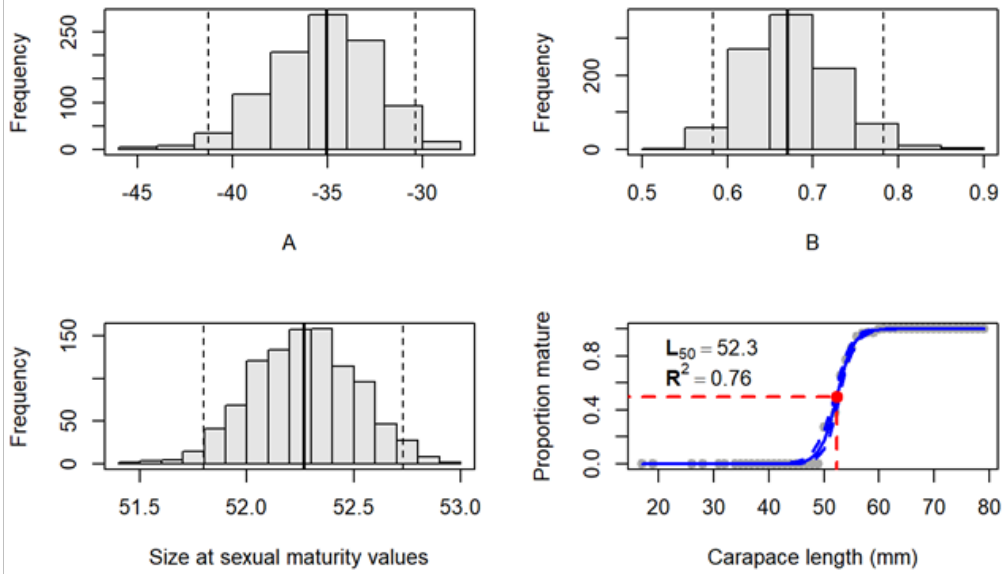
### Size at maturity

Totals of 7,508 (1,207 immature, 6,301 mature), 1,845 (266 immature, 1,579 mature) and 2,145 (49 immature, 2,096 mature) female crabs were sampled from Wallis Lake, Port Stephens and Lake Macquarie, respectively. The number of immature crabs recorded from Lake Macquarie were insufficient to generate reliable estimates of SOM. The smallest mature female crabs sampled from Wallis Lake ranged from 47 mm CL (2020) to 50 mm CL (2018, 2019) and from 46 mm CL (2020) to 50 mm CL (2019) for Port Stephens. The smallest mature crab from Lake Macquarie was 44 mm CL.

Estimates of SOM for Frequentist and Bayesian approaches were similar for years ( $\pm 0.2$  mm) within both estuaries (see Figure 35 for Wallis Lake example). For Wallis Lake, estimates of  $L_{50}$  ranged from 50.9 ( $\pm 0.1$ ) mm (2020) to 52.5 ( $\pm 0.4$ ) mm in 2019 (Figure 36). Similarly, in Port Stephens estimates of  $L_{50}$  ranged from 50.7 ( $\pm 0.6$ ) mm in 2019 to 51.9 ( $\pm 0.4$ ) mm in 2020 (Figure 36).

Seasonally calculated  $L_{50}$  values in Wallis Lake roughly followed general patterns in water temperature between warmer (summer) and cooler (winter) periods (Figure 37). Estimates from winter (51.7  $\pm$  0.8 mm) in 2020 with mean water temperature of 15.7°C were lower than summer (55.7  $\pm$  0.5 mm) with mean water temperature of 24.9°C. However, there also appeared to be some correlation with patterns in conductivity as well, with larger  $L_{50}$  occurring during periods of higher conductivity. The range in estimates of seasonal  $L_{50}$  values (51.28  $\pm$  0.42 mm – 55.74  $\pm$  0.5 mm) was greater than the range of values observed among years (50.9  $\pm$  0.1 – 52.5  $\pm$  0.1 mm).

## Frequentist



## Bayesian

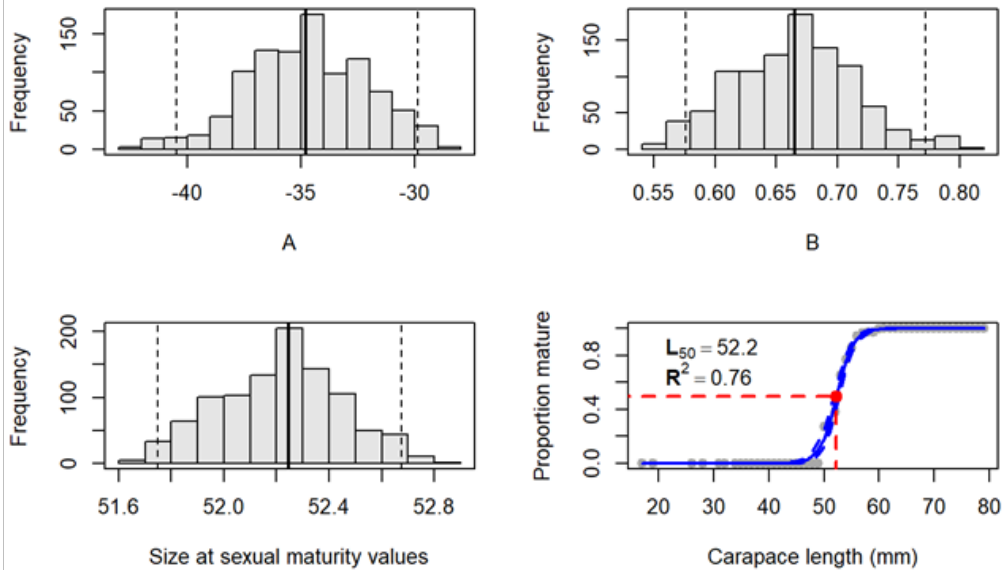


**Figure 35** Comparison of fitted maturity ogives for Blue Swimmer Crab captured from Wallis Lake in 2018 using Frequentist and Bayesian approaches. The top left and right panels present histograms of A, B parameters, the lower left panel is the size at maturity and the lower right is the maturity ogive for size at 50% maturity. Actual data is indicated with light grey dots, dashed blue lines represent 95 % CI, and the intersection of the red lines is the size at which 50% of individuals are mature.

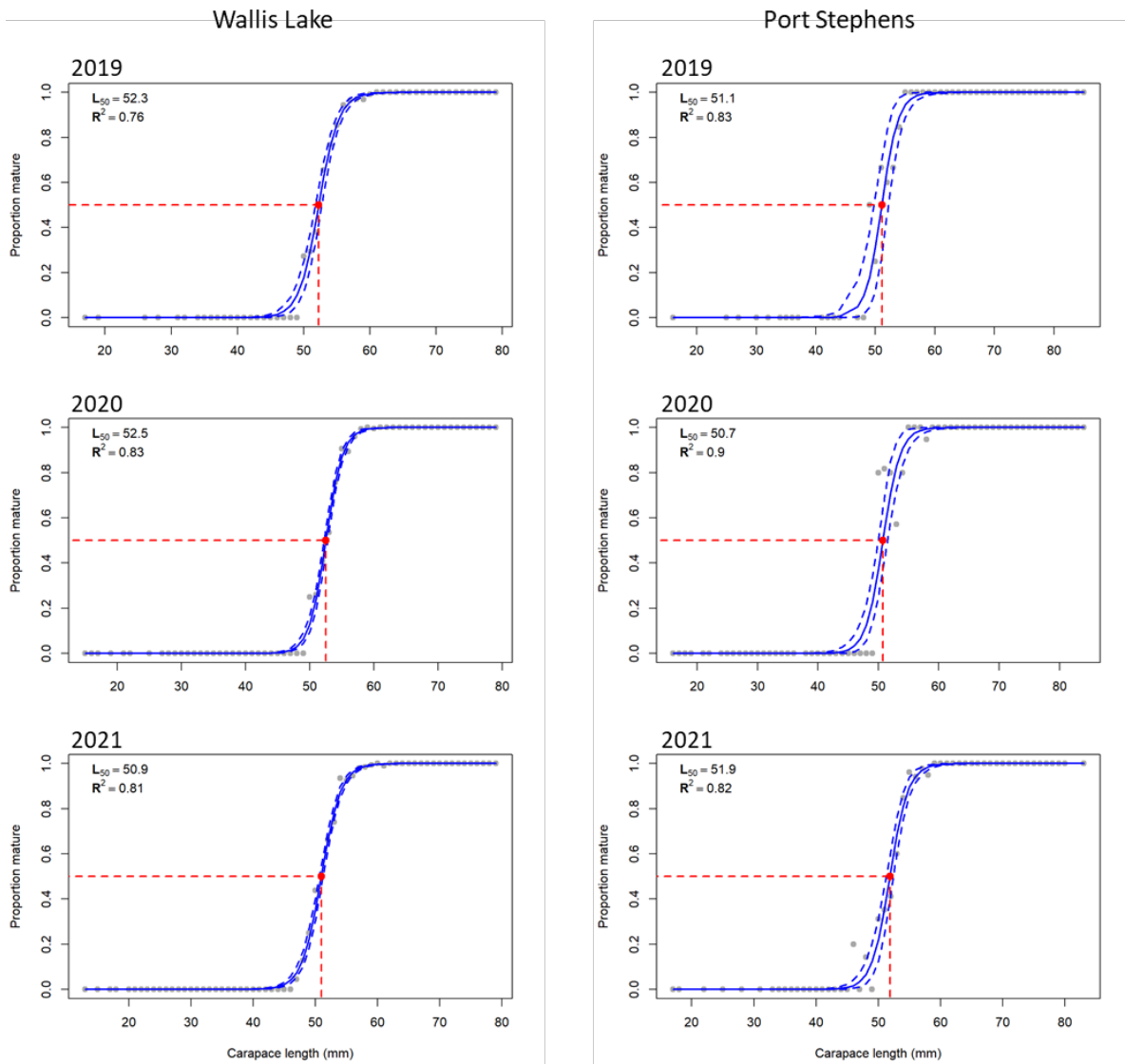


**Figure 36** Spatial and temporal breakdown of size-at-maturity for Blue Swimmer Crab for Wallis Lake and Port Stephens for 2018, 2019 and 2020 fishing seasons, modelled using the Frequentist approach. Actual data is indicated with light grey dots, dashed blue lines represent 95 % CI, and the intersection of the red lines is the size at which 50% of individuals are mature.

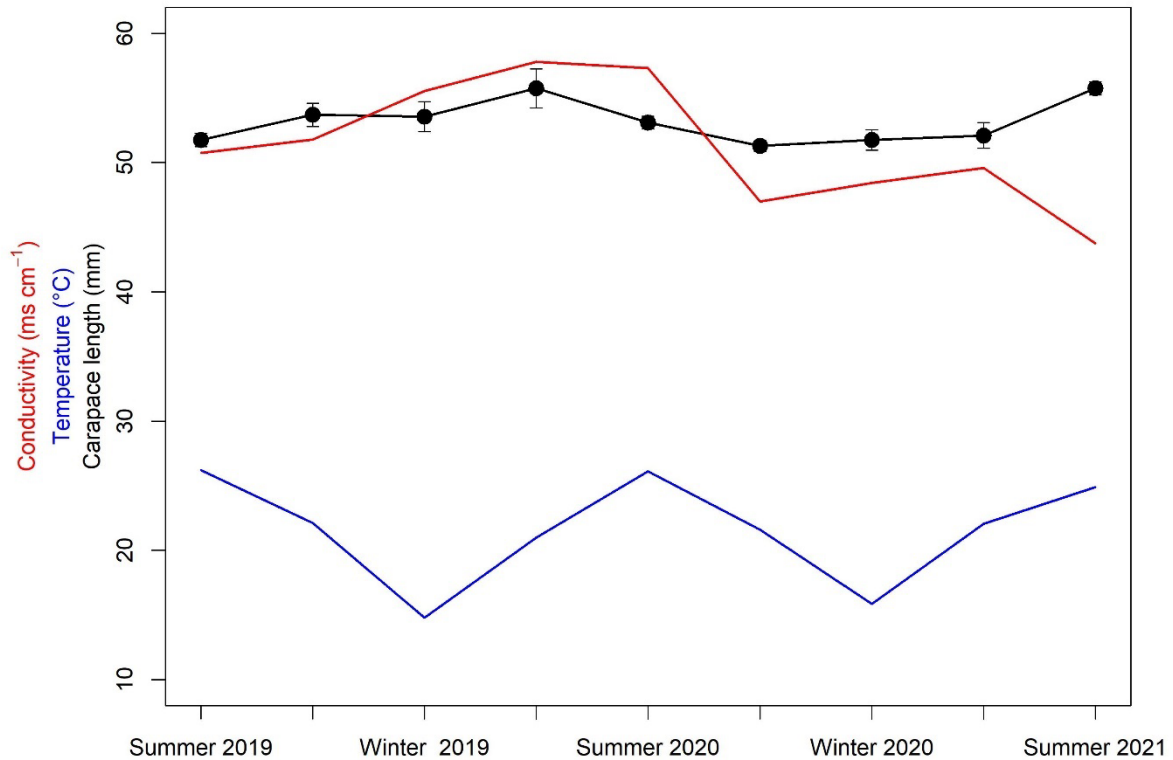


**Figure 37** Seasonally calculated  $L_{50}$  ( $\pm$  95% C.I.) for Blue Swimmer Crab in Wallis Lake plotted alongside seasonally averaged water temperature and conductivity (at the reference station) for the duration of the regular independent survey.

### Size at functional maturity and catches of ovigerous crabs

The proportion of female Blue Swimmer Crab that were found to be functionally mature (i.e., berried) increased with latitude ranging from 7.2% for Wallis Lake, 14.4% for Port Stephens to 19.6% for Lake Macquarie (pooled across years 2018-2021). Across years, despite overall catches of berried crabs ( $n = 451$ ) in Wallis Lake being greater than Port Stephens ( $n = 265$ ) and Lake Macquarie ( $n = 410$ ), the proportions of mature crabs that were berried in Wallis Lake during 2018 (9.4%,  $n = 125$ ), 2019 (3.6%,  $n = 78$ ) and 2020 (8.8%,  $n = 248$ ) were  $\sim$ 50% lower than Port Stephens in 2018 (16.2%,  $n = 46$ ), 2019 (15.6%,  $n = 100$ ), 2020 (13.0%,  $n = 119$ ) and Lake Macquarie in all years (2018; 21.3%  $n = 67$ , 2019; 18.6%,  $n = 180$ , 2020; 20%,  $n = 163$ , Figure 38). However, the smallest berried female crab recorded for Wallis Lake (47 mm) was smaller than both Port Stephens (50 mm) and Lake Macquarie (56 mm). Furthermore, the proportion of mature female crabs <54 mm CL in Wallis Lake that were berried in 2018 (2.4%), 2019 (2.6%) and 2020 (5.6%) were much lower than proportions of 20.0%, 14.1% and 21.4% for crabs in the 55-59 mm size class for 2018, 2019 and 2020, respectively.

The highest proportion of berried females were recorded from September to March in Lake Macquarie (Figure 39), with the proportion of crabs that were berried being generally lowest in the months with the highest catches of mature crabs (June-July). Similarly, in Port Stephens the highest proportion of berried females were recorded from September to February with few berried crabs recorded from June – July (Figure 39). In contrast, with the exception of the short, sharp peaks observed in October 2019 and September 2020, the proportion of the recorded catch of mature Blue Swimmer Crab from Wallis Lake that were berried only varied slightly through time, and remained comparatively low in magnitude (Figure 39).

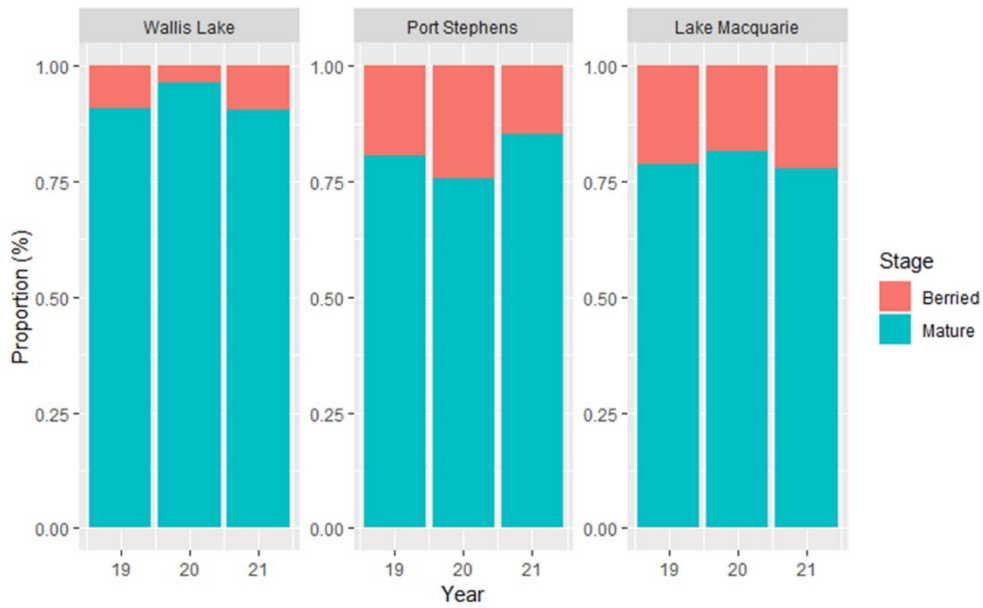


**Figure 38** Proportion of mature female Blue Swimmer Crab recorded as ovigerous from Wallis Lake, Port Stephens, and Lake Macquarie.



**Figure 39** The monthly proportion of mature and berried Blue Swimmer Crab per estuary across three seasons in Wallis Lake, Port Stephens, and Lake Macquarie. Also shown is the total number of mature Blue Swimmer Crab caught during each month (black dot).

The proportion of berried Blue Swimmer Crab caught across 5 (November 2018 to August 2019) or 7 sites (September 2019 to March 2021) in Wallis Lake, Port Stephens, and Lake Macquarie along with the total catch of berried Blue Swimmer Crab (black dot) are shown in Figure 40. In Wallis Lake, sites 1-4 had the greatest proportion of berried Blue Swimmer Crab. Recorded catches of berried crabs during September 2020 in Wallis Lake ( $n = 94$ ) exceeded the total number of berried crabs caught in 2019 ( $n = 78$ ). Excluding the September peak in 2020, catches of berried crabs from Wallis Lake generally followed a similar trend from November to April annually (Figure 6). In Port Stephens, sites 4, 5 and 6 generally had the highest proportion of berried female crabs (counting only months where >5 individuals were caught), and there was a distinct peak in the number of berried crabs caught during October in both 2019 and 2020. In 2020, Port Stephens recorded a small secondary peak in berried crabs during March, however this was not evident in either March 2019 or March 2021; in fact, no berried crabs were captured at all in March 2021. Similarly to Port Stephens, catches of berried females within Lake Macquarie were much greater during Spring than other seasons, and these peaks were generally more protracted than for other estuaries.

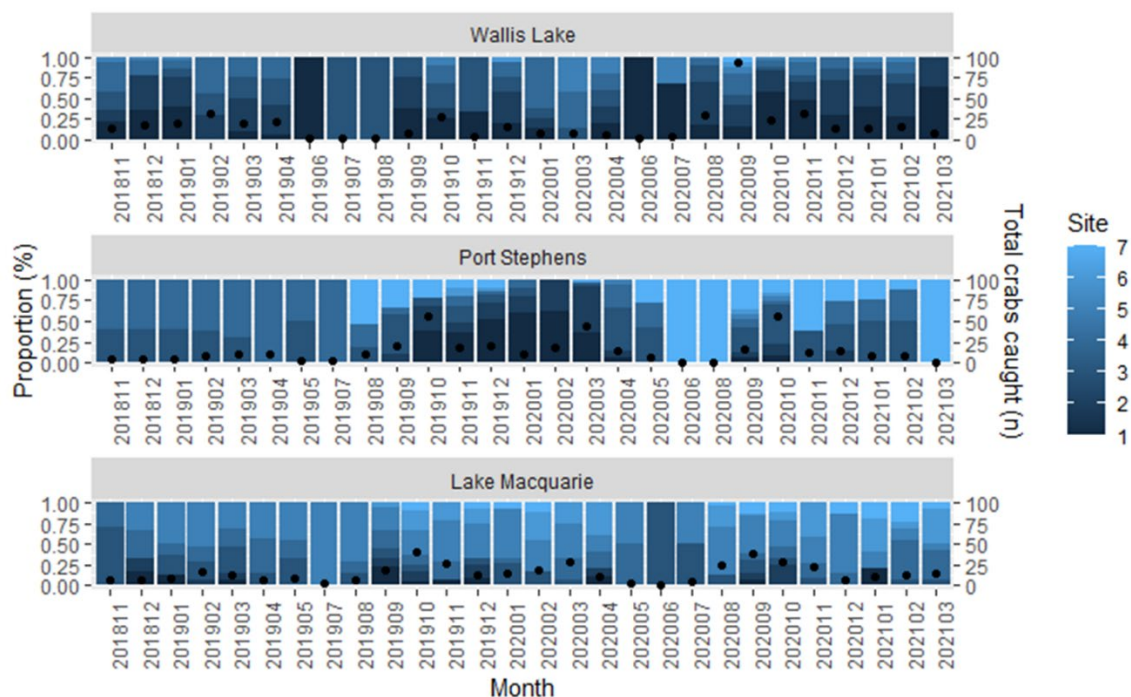


**Figure 40** Proportion of berried Blue Swimmer Crab caught across 5 (November 2018 to August 2019) or 7 sites (September 2019 to March 2021) in Wallis Lake, Port Stephens, and Lake Macquarie and the total number of ovigerous Blue Swimmer Crab caught during each month (black dot).

Size-structure of catches of berried females in Wallis Lake trap survey from 2018-2020 were generally similar with crabs in the 60-64 mm size group most commonly recorded to be berried in all years. When compared to Port Stephens ( $66.1 \pm 0.4$  mm) and Lake Macquarie ( $75.9 \pm 0.4$  mm) the mean size of berried Blue Swimmer Crab from Wallis Lake ( $62.7 \pm 0.2$  mm) were lower (Figure 7). Comparisons between the size structure of berried crabs recorded from the Wallis Lake trap and observer survey (see *Environmental drivers of variation in Giant Mud Crab harvest rates*) in 2018 were similar. However, in 2019, observed catches included a greater number of berried crabs >65 mm (Figure 42).

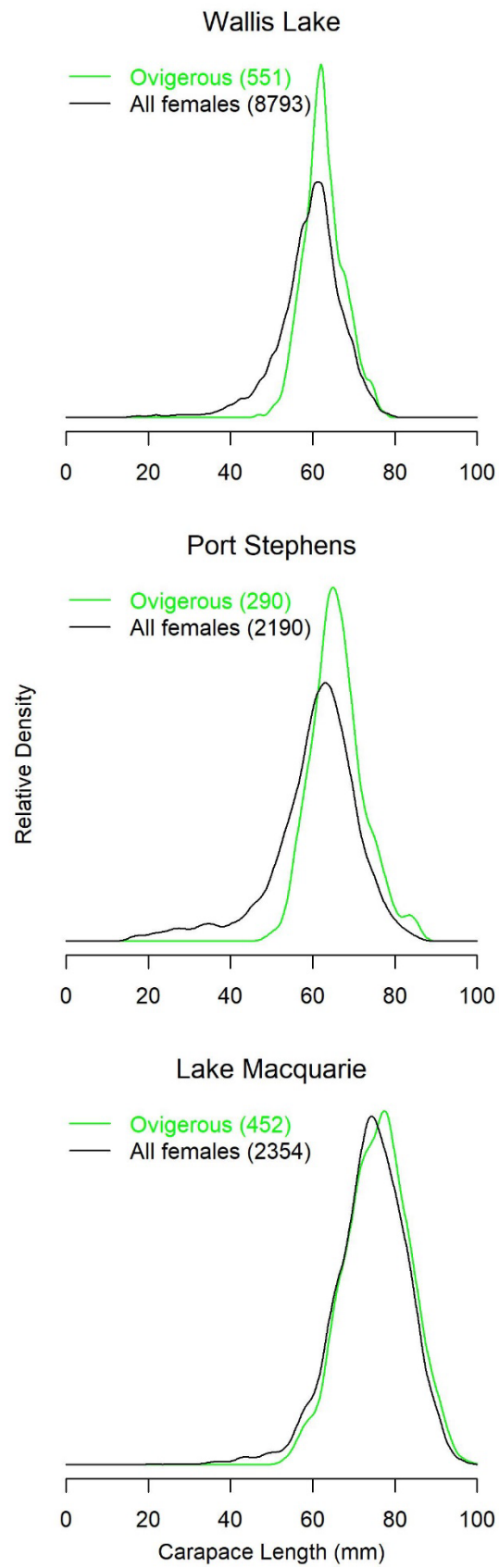


**Figure 41** Size-structure of berried (ovigerous) Blue Swimmer Crab, and all female crabs, from Wallis Lake, Port Stephens and Lake Macquarie (data pooled across years).

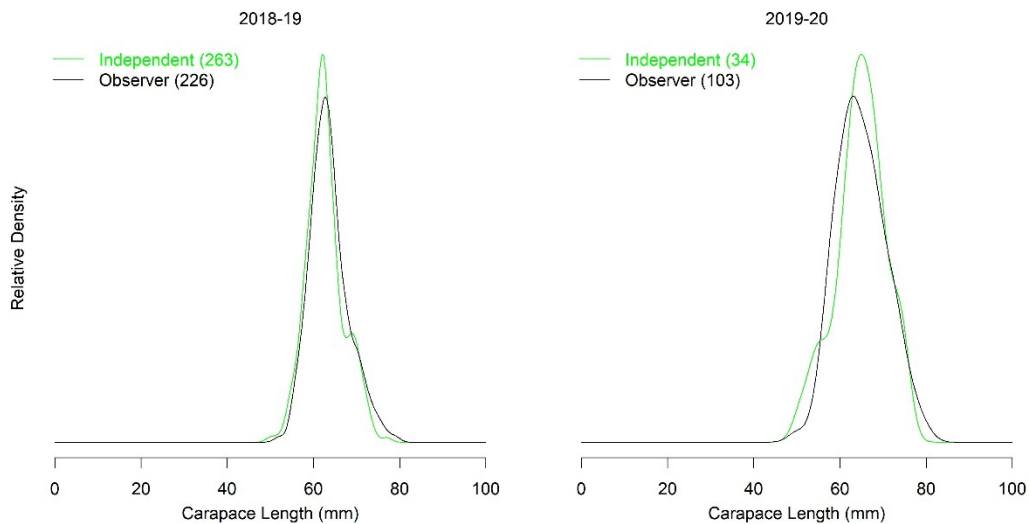


**Figure 42** Size-structure of recorded catches of berried Blue Swimmer Crab during the Wallis Lake regular independent survey and Wallis Lake observer survey for 2018 (November) – 2019 (October) and 2019 (November) – 2020 (March).

### Gonad and ovarian development

Overall, 679, 574, and 653 female Blue Swimmer Crab were retained from Wallis Lake, Port Stephens and Lake Macquarie, respectively, for laboratory analysis. No biological samples were processed in December 2020 (Wallis Lake, Lake Macquarie), February 2021 (Lake Macquarie) and March 2021 (Port Stephens). Female Blue Swimmer Crab representative of all gonad stages were generally present during each month of the sampling period (Figure 43). The proportion of female crabs in Wallis Lake with late-stage ovaries from September to January in 2019 (~53% ) and 2020 (~30%) were greater than 2018 (~15% December to January, Figure 43). The highest proportion of female crabs with late-stage ovaries was recorded during September in Port Stephens (53-55%) and August-September in Lake Macquarie (~50-80%). Female crabs with immature gonads were most frequently recorded from January-April (~20-65%), December-February (~40-60%) and February-May (15-80%) from Wallis Lake, Lake Macquarie and Port Stephens, respectively.

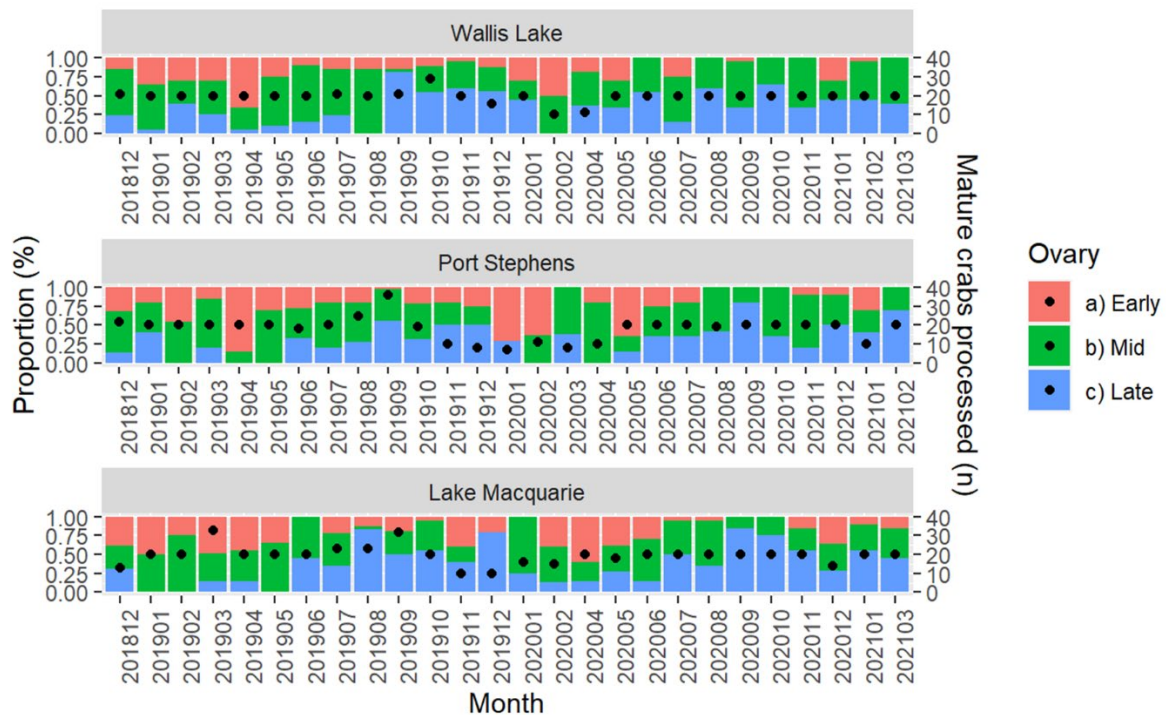


**Figure 43** Categorical representation of ovary stages (expressed as the proportion of examined ovaries) for Blue Swimmer Crab across three estuaries. Also indicated is the total number of crabs that were processed for biological samples (excluding berried females) during each month (black dot).

## Discussion

### Spatial and temporal patterns

The proportion of small female Blue Swimmer Crab caught by trapping in Lake Macquarie was far less than both Port Stephens and Wallis Lake. Catches of female crabs below the previous estimated  $L_{50}$  for Wallis Lake (46 mm CL, Johnson *et al.* 2010) contributed 1.3, 7.0 and 9.8% of total catches (in the regular independent survey) of female Blue Swimmer Crab from Lake Macquarie, Wallis Lake and Port Stephens, respectively (years combined). Previous research has shown that catches of commercially configured traps contain disproportionately greater numbers of large crabs, likely overestimating the proportion of mature female Blue Swimmer Crab in each size-class, and thus risking an underestimate of  $L_{50}$  (Smith *et al.* 2004). However, comparison of small-mesh traps against both commercially configured traps and research beam trawls in Port Stephens and Lake Macquarie showed that the traps were at least as effective at catching smaller Blue Swimmer Crab when present (see *Design and evaluation of a novel research trap for surveying Blue Swimmer Crab populations*). Therefore, despite size composition data being biased towards larger mature individuals (particularly in Lake Macquarie), estimates of  $L_{50}$  are unlikely to be impacted by non-representative sampling. Furthermore, the estimates of  $L_{50}$  for Wallis Lake reported here (50.9 – 52.5 mm CL) exceeded previous estimates that were derived from samples collected using active fishing methods (i.e., beam trawl, prawn seine), that have previously been shown to produce greater  $L_{50}$  estimates than trap catches (Smith *et al.* 2004).

It is interesting to note that the size of the smallest functionally mature female (i.e., berried) crab recorded in Wallis Lake (47 mm) and Port Stephens (50 mm) was just below the lower estimates of

$L_{50}$  from each estuary (i.e., Wallis Lake 50.7 mm, Port Stephens 50.9 mm). This is a substantial contrast to Blue Swimmer Crab in Western Australia, where estimates of functional maturity were ~10–12 mm larger than  $L_{50}$  (in terms of carapace width), with the greatest difference being ~25 mm larger (Johnston and Yeoh 2021).

Although insufficient numbers of immature crabs were recorded within Lake Macquarie to estimate  $L_{50}$ , the smallest functionally mature females (56 – 57 mm CL) exceeded estimates of  $L_{50}$  from Wallis Lake and Port Stephens. Water temperature in Lake Macquarie is artificially warmed by discharge from industrial sources (Taylor *et al.* 2017e). Positive correlations between water temperature, estimates of  $L_{50}$  and functional maturity have previously been reported for populations of Blue Swimmer Crab in Western Australia (Johnston and Yeoh 2021), with the effect of temperature also evident in the seasonal patterns observed in Wallis Lake. The range of variation in estimates of functional maturity from estuaries within our study (47 – 57 mm CL) are similar to the range reported for Western Australian populations (89 mm – 104 mm CW).

In contrast to other studies reporting a low incidence of capture of berried female crabs (Moore *et al.* 2022), catch rates of berried Blue Swimmer Crab from the trap survey, current and previous observer-based survey of Wallis Lake (Johnson *et al.* 2010) and other studies in Australia (Johnston and Yeoh 2021; Nolan *et al.* 2022) suggest that our patterns are likely representative of broader population-level parameters (rather than variability among individuals or influence of gear types, for example). However, despite previous studies estimating the catch of berried females with higher precision than commercial sized crustaceans (Comeau *et al.* 2009), research to understand the relative capture efficiency of traps across different life history stages is important to ensure representativeness of future estimates of spawning potential in Blue Swimmer Crab.

Despite patterns in monthly variation in gonad development being generally consistent among estuaries, the proportion of mature female Blue Swimmer Crab that were berried, and therefore duration of spawning period (>5% of mature females berried) varied between Wallis Lake, Port Stephens and Lake Macquarie with the latter two being generally similar. In Lake Macquarie and Port Stephens, the proportion of mature crabs that were berried was reasonably consistent for 5-6 months (~20-30%). However, in Wallis Lake the proportion of mature female crabs that were berried peaked during the months of October 2019 (37%) and September 2020 (39%) then declined (<10%), despite female Blue Swimmer Crab with late-stage gonads being present every month from September to January (excluding February 2022). The brief observed spawning period in Wallis Lake suggests that female crabs with late-stage gonads could be emigrating from the estuary to spawn in adjacent ocean waters at higher rates than from both Port Stephens and Lake Macquarie. Recorded catches of berried females accounted for ~30% of total mature female crabs encountered during the 'inshore sub-program'. Migration could be driven by environmental influences, with female Blue Swimmer Crab in other locations reported to leave the estuary during winter as a result of increased freshwater flows (Johnston *et al.* 2020), and our own modelling (see *Estuary-specific drivers of Blue Swimmer Crab abundance and distribution*) showing crabs moving toward the sea under lower salinity conditions, and females on average being closer to the sea. Understanding the relative abundance of berried female crabs in adjacent inshore ocean waters outside of the small window sampled by the 'inshore sub-program' (which was based on previously reported commercial catches) is an important future research priority.

## Concluding comments

To avoid recruitment overfishing the MLS of heavily exploited stocks should generally be greater than the onset of sexual maturity. Our findings clearly illustrate the current MLS for Blue Swimmer Crab in NSW (65 mm CL) is greater than estimates of mean size at sexual maturity (for which  $L_{50}$  is a proxy)

and the observed size of functional maturity across the three major estuaries studied. However, the duration of the spawning period, proportion of mature crabs berried, and the size structure of recorded catches of berried females varied between estuaries, with a substantially shorter spawning period in Wallis Lake. These differences, combined with reported variations in reproductive biology of Blue Swimmer Crab in response to environmental drivers (Johnston *et al.* 2021b) highlight the importance of ongoing monitoring of biological parameters to support adaptive management of portunid fisheries in NSW. This is especially important considering that southeast Australia is a global climate warming hotspot (Scanes *et al.* 2020a).

# Long-term drivers of catch variability in Wallis Lake

## Background and rationale

Variable harvests in Portunid fisheries often arise due to environmental influences on catchability, or recruitment of crabs, possibly through impacts on larval or juvenile survival (Loneragan and Bunn 1999; Gillson *et al.* 2012; Johnston *et al.* 2021b). It has also been suggested that long-term cyclical patterns in portunid fisheries may be correlated with climatic indices such as the Pacific Decadal Oscillation (PDO) or Inter Pacific Oscillation (IPO, Meynecke *et al.* 2012b), due to the links between these climate indices and factors such as rainfall. In the face of such variability, it is important to quantify stock-specific relationships with environmental and climatic drivers, so that management can prepare for the future condition of the fishery.

The importance of understanding both the influence of variable environmental conditions, as well as the influence of fishing itself, is evident in the Western Australia Blue Swimmer Crab studies outlined in the *Introduction*. In Cockburn Sound, it was found that cooler than normal temperatures impacted recruitment which, compounded with a change in fishing behaviour, resulting in increased harvest of pre-spawning females during winter which greatly impacted egg production (Johnston *et al.* 2011). In the warmer Shark Bay fishery, abnormally warm sea surface temperatures during the spawning period contributed to poor recruitment (Chandrapavan *et al.* 2019). Both these scenarios led to substantial declines the fisheries catch, which necessitated enacting closures to allow the stocks to recover.

The Blue Swimmer Crab fishery in Wallis Lake experiences substantial fluctuation in catches, which could well be influenced by a combination of the important factors observed for Western Australian studies, and outlined in earlier chapters. In NSW, it has been observed that catches of Blue Swimmer Crab often increase in the ocean adjacent to estuaries following flow events (Gillson *et al.* 2012). This suggests that high rainfall and flow events may promote migrations from estuaries to adjacent inshore areas, which may in turn alter larval dispersal patterns if the movements aligned temporally with the spawning period (and reduce self-recruitment into that estuary). If considerable spawning does occur in inshore areas, it is also possible that estuarine recruitment of coastally spawned larvae may be mediated by onshore winds, as shown for other species off eastern Australia (Schilling *et al.* 2022b). There is some evidence for this seen in Blue Swimmer Crab in Queensland waters, where larvae have been observed to accumulate near the coast and estuaries following periods of onshore wind (Sumpton *et al.* 2003).

While the analyses of the regular independent survey data outlined in *Estuary-specific drivers of Blue Swimmer Crab abundance and distribution* reveal some important relationships with environmental variables, high freshwater inflow to estuaries was not identified as an important factor in any of the models. These patterns thus do not align with the findings for the multi-estuary study of Gillson *et al.* (2012). Given these contrasting patterns, there is merit in further considering the potential effects of flow over time periods greater than the 3-year duration of the independent survey, alongside other factors that may be important and for which data is available. As the NSW Blue Swimmer Crab fishery has recently transitioned to quota management, the influence of fishery-related factors on total catch are particularly important to consider.

This chapter analyses a variety of factors that could influence Blue Swimmer Crab commercial fisheries productivity, through investigation of four hypotheses identified through the research outlined above and existing published knowledge for portunid crab species. Specifically, the four

hypotheses being investigated are: 1) high freshwater flow in one year will negatively impact recruitment as more larvae are spawned in coastal areas increasing dispersal away from the estuary (a dispersal effect); 2) Harvesting of Blue Swimmer Crab during winter will negatively impact the following summer harvest (a spawning stock biomass effect); 3) Environmental and climatic factors including sea surface temperature and onshore wind patterns can influence recruitment success, leading to fluctuations in catch rates the following season (a recruitment effect); and 4) Climatic indices such as the IPO and PDO may correlate with longer term fluctuations in the fishery (a climate effect). We conclude by synthesising the component relationships and evaluating their utility for predicting future productivity for the fishery.

## Data sources, approach and modelling

As this case study is an integrative analysis drawing together information to test specific hypotheses, some contextual detail behind the main hypotheses under consideration is provided below, followed by a description of the data sources used to assess them. As the hypothesis testing includes a wide variety of data sources, many also consisting of <30 datapoints (e.g., annual data) we initially analysed each of the hypotheses separately to maximise the power of the analyses. We then combined the hypotheses for which significant relationships were detected into a single ecologically relevant regression model (detailed below), rather than attempting to perform a traditional model selection which requires consistent amounts of data in each variable.

## Hypotheses

1. Freshwater inflow – As outlined earlier, it was hypothesised that high freshwater flow in one year will negatively impact recruitment as more larvae are spawned in coastal areas increasing dispersal away from the estuary. The mechanism behind this hypothesis is that during periods of high freshwater flow, the Blue Swimmer Crab population will move to the estuary mouths and inshore oceanic habitats (Gillson *et al.* 2012), if the estuary salinity declines too much. Firstly, to determine whether the population does in fact fluctuate between the estuary and ocean environments we used independent survey data (see below) to test for a correlation between the catch-per-unit effort (CPUE; crabs trap<sup>-1</sup>) in Wallis Lake and the CPUE from the inshore samples (collected during the inshore sub-program). We performed this correlation for two sizes classes of Blue Swimmer Crab (50 – 65 mm carapace length [CL] and > 65 mm CL representing sublegal- and legal-sized crabs). Following this we tested whether the catch in the inshore commercial fisheries (see below) was related to flow by correlating the number of ‘large’ offshore catches (> 25 kg) with the occurrence of large flow events with either a one-month lag, or no lag. If increased flow during the spawning season impacted recruitment, then we would expect to see a reduction in CPUE the following catch season. To examine this, we tested for a correlation between flow during three different periods and the difference from the previous year’s summer and the following year’s CPUE. The three periods tested were: July – September, October – December, and January – March (the same year as the following summer). Looking at the difference from previous years CPUE assumes that the CPUE the previous year would represent a proxy for reproductive effort and recruitment, and the deviation from the previous year would be the impact of external factors including environmental variables.

2. Winter harvest – Based on the experience in Western Australia (Johnston *et al.* 2011), it was hypothesised that harvesting of mated, pre-spawning Blue Swimmer Crab during winter may negatively impact the following summer harvest. The mechanism behind this hypothesis is that winter harvesting will reduce the number of spawning females the following season, thereby

reducing the supply of larvae. Using the monthly Wallis Lake commercial catch data (from July 1997), we defined winter harvest as that taken between June and November and used the relative change in CPUE (kg scaled Fisher Day<sup>-1</sup>) from the previous summer to the following summer (January – April) as the response variable. The change in CPUE was used as the overall abundance should be related to the total number of crabs the preceding season. Total winter catch (t) and winter CPUE were highly correlated ( $r = 0.82$ ,  $t_{23} = 6.888$ ,  $P < 0.001$ ) and we therefore limited our comparison to using the total winter catch (similar results are evident if CPUE is used). We tested for a correlation between total winter catch and the change in CPUE during the following summer. To gain more insight into possible mechanisms behind this relationship we used the sex-specific harvest composition from the more recent reporting period (July 2009 onwards) to look at the proportion of each sex taken monthly. We also used the length frequencies from the port monitoring program (see below) to better understand the monthly length structure of each sex within the harvest.

3. Coastal temperature and wind – Environmental factors such as sea surface temperature and the prevalence of onshore winds (see below) can influence recruitment success leading to fluctuations in catch rates the following season for both crabs and other taxa (Chandrapavan et al., 2019; Schilling et al., 2022). To test the idea that the environmental conditions during recruitment can influence the CPUE (kg scaled Fisher Day<sup>-1</sup>) the following season, we tested for a correlation between the change in summer CPUE and both the onshore winds and mean SST during 3 periods (the preceding July – September, the preceding November – December and the January – March of the same summer). These three periods allow us to test for both lagged influences of recruitment and potential changes to CPUE occurring due to changes in catchability (using the January – March period corresponding to the summer CPUE).

4. Climatic indices – The PDO and IPO indices represent large-scale climate modes, and may influence the large multiyear cycles which seem to occur within the Blue Swimmer Crab fishery, following the hypothesis put forward in Meynecke *et al.* (2012b). We therefore used the summer CPUE as the response variable and correlated this with the PDO and IPO from a variety of preceding months. As we are unsure of the exact mechanism behind this relationship, we tested for correlations between the climatic indices in each month from the preceding July to the January at the start of the summer fishing season to account for possible lagged effects. Based upon these initial results we also tested the mean PDO and IPO of some months.

## Data sources

Independent survey data – Data collected during the regular independent survey (see *Fishery independent survey of Blue Swimmer Crab – Description and data summary*) was expressed as catch-per-unit-effort (CPUE) from Wallis Lake and the inshore sampling was calculated as the total number of crabs captured divided by the number of traps deployed in a month.

Commercial fishing data – Since July 1997, commercial fishers in Wallis Lake have been required to report their monthly catch (kg) and effort (number of days fished). Since 2009, reporting has been split by sex with catch (kg) and effort (number of trap lifts) data reported daily. The demersal fish trap sector of the Ocean Trap and Line Fishery and prawn trawl sector of the Ocean Trawl Fishery operate with the same reporting system and we subset the inshore prawn trawl sector data to include only Blue Swimmer Crab catches in the inshore region adjacent to Wallis Lake. A standardised CPUE (kg scaled Fisher Day<sup>-1</sup>) was calculated for each month. Also, since 2017 there has been a 25 kg daily possession limit for Blue Swimmer Crab within inshore areas, which equates to an upper limit on the daily catch that can occur in this habitat. For this reason, ‘large catch’ of Blue

Swimmer Crab was specified where this ceiling was reached, and the number of large catches taken from inshore areas was used as a metric in analysis.

As the key fishing season for Blue Swimmer Crab in Wallis Lake is Summer/Autumn, we calculated a “summer” CPUE index (kg scaled Fisher Day<sup>-1</sup>) including January to April (months comprising >10% of annual catch). To investigate interannual fluctuations in CPUE, we used the first differencing method to calculate a time series of annual changes in summer CPUE. This involved subtracting the previous year’s CPUE from the current year.

Length frequency data – As part of regular fisheries monitoring, representative samples of commercial catches are measured on a monthly basis to calculate sex-specific length frequencies (CL, mm) in the Wallis Lake Fisherman’s Cooperative. To investigate how the size of crabs varies throughout the year, length frequencies were compiled for each month (pooled within each year sampled). To establish if the harvested length frequencies changed after the legal length limit for Blue Swimmer Crab increased in 2017 (from 60 to 65 mm CL), we also investigated the length frequencies prior to this change compared with the pooled length frequencies from all years.

Freshwater flow – Freshwater input into Wallis Lake was sourced from the “Wang Wauk @ Willina” monitoring station, with data accessed through the WaterNSW real time data portal (<http://realtimedata.watersnw.com.au>). This monitoring station measures the daily discharge volume (ML), and discharge data was extracted to match the window of available Blue Swimmer Crab catch data. High flow days were specified as a Boolean parameter, by identifying all days in the top 10% of flow (>279 ML).

Sea surface temperature – The mean monthly sea surface temperature (SST; °C) from the ocean adjacent to Wallis Lake (32.232° S ,152.615° E) was taken from satellite measurements. Due to incomplete coverage in a single sensor, data were extracted as a time-series from the Australian Ocean Data Network portal from two sensors: 1) IMOS - SRS - SST - L3S - Single Sensor - 1 month - day and night time (March 1992 – October 2019) and, 2) IMOS - SRS - SST - L3S - Multi Sensor - 1 month - day and night time (January 2012 – January 2022). The two series were highly correlated ( $r = 0.78$ ,  $P < 0.001$ ) and during the period where the two sensors overlapped a mean of the two was taken.

Onshore winds – Onshore wind data was sourced from the Australian Bureau of Meteorology Atmospheric high-resolution Regional Reanalysis for Australia (BARRA, Su *et al.* 2019). This reanalysis product provides 3 hourly quality controlled atmospheric data including wind speed and direction at an approximate 12 km resolution for 1990 - 2019. Following the procedure in Schilling *et al.* (2022b) we extracted and calculated the onshore winds for the Wallis Lake region at a monthly resolution. A positive value for onshore winds represents a net movement of air from the southeast to the northwest, and indicates wind which would normally generate downwelling and retention of larvae near the coastline (Schilling *et al.* 2022b).

Climatic indices – Monthly climate index data was downloaded from the NOAA website for both the Pacific Decadal Oscillation (<https://www.ncdc.noaa.gov/teleconnections/pdo/>; PDO) and Interdecadal Pacific Oscillation (<https://psl.noaa.gov/data/timeseries/IPOTPI/>; IPO). The National Centre for Environmental Information (NCEI) PDO index is based on NOAA’s extended reconstruction of SSTs (ERSST Version 5). It is constructed by regressing the ERSST anomalies against the Mantua PDO index for their overlap period, to compute a PDO regression map for the North Pacific ERSST anomalies. The ERSST anomalies are then projected onto that map to compute the NCEI index. The NCEI PDO index closely follows the Mantua PDO index and was previously linked to large scale fisheries fluctuations in the Pacific (Mantua and Hare 2002). The IPO is based on the difference between the sea surface temperature anomaly (SSTA) averaged over the central equatorial Pacific

and the average of the SSTA in the Northwest and Southwest Pacific. The index ultimately provides a measure of interdecadal variability in the Pacific and is generally considered more relevant to Australia than the PDO (Power *et al.* 1999).

## **Predictability of fisheries productivity**

To combine the results of the hypothesis testing outlined above in a meaningful way, we combined the significant variables identified within a linear model with the goal of predicting the summer (January – April) CPUE (the period when most of the Blue Swimmer Crab are harvested). The model fit was assessed via simulated residuals (Hartig 2020). As it is not appropriate to test a predictive model upon the data it was built upon, we conducted a leave-one-out cross-validation whereby the model was refit multiple times, each time leaving out a single year before comparing the missing year predicted and observed CPUE.

Following initial testing of predictability, we attempted to create an informative management tool highlighting the trade-offs between winter harvest, previous summer CPUE and total harvest the following financial year (July – June). The financial year data was used as it is the period upon which management and reporting currently occurs for fisheries within NSW (including Wallis Lake). We calculated the mean total harvest over the time series (financial years ending 1998 – 2021) and defined each year as below or above the long-term average (78,710 kg per annum). We then conducted a quadratic discrimination analysis to attempt to classify above and below average financial year harvests based upon the previous summer CPUE (representing the population abundance in the previous season) and amount of harvest taken in the winter leading into the financial year.

## **Results**

### **General observations on Wallis Lake fishery**

Since July 1997, commercial total harvest and CPUE in Wallis Lake have been highly correlated at both the monthly ( $r = 0.89$ ,  $t_{294} = 33.844$ ,  $P < 0.001$ ) and annual scale (July – June;  $r = 0.83$ ,  $t_{22} = 7.074$ ,  $P < 0.001$ ). There was a strong seasonal cycle within the harvest, with most of the catch taken during summer and early autumn (Figure 44)—over 60 % of the total catch was taken between January and April.

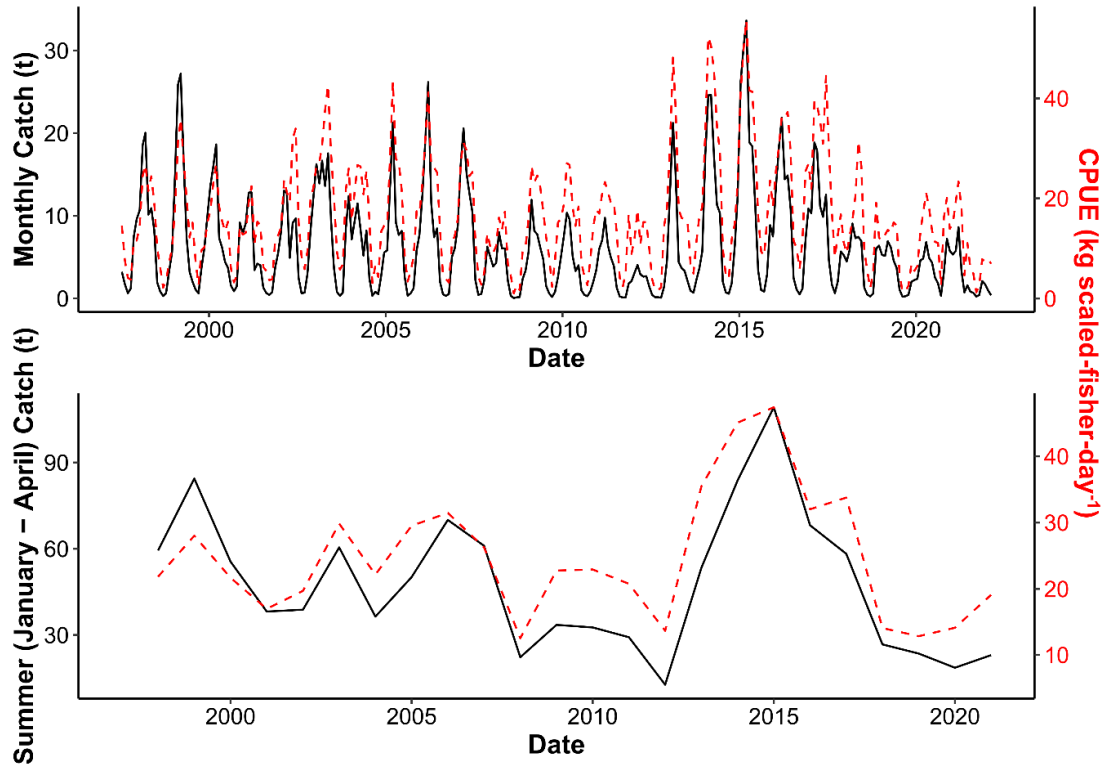


**Figure 44** Time series showing the commercial catch (in black) and catch per unit effort (dashed red; CPUE; kg scaled-fisher-day<sup>-1</sup>) in Wallis Lake from July 1997 – February 2022. The top panel shows monthly catch and CPUE while the bottom panel shows the combined summer (January – April) catch and CPUE. Note the lower plot is truncated to only include 1998 – 2021 which included full summer periods.

### Freshwater flow

For the independent survey data, there was no relationship between CPUE in Wallis Lake and the inshore zone for smaller sub-legal size Blue Swimmer Crab ( $r = 0.103$ ,  $t_7 = 0.273$ ,  $P = 0.793$ , Figure 45). In contrast, there was a moderate negative relationship between CPUE in Wallis Lake and the inshore CPUE for larger legal size (> 65 mm CL) Blue Swimmer Crab ( $r = -0.86$ ,  $t_7 = -4.554$ ,  $P = 0.002$ , Figure 45), suggesting that there is a transition from estuarine to ocean habitats for larger crabs.

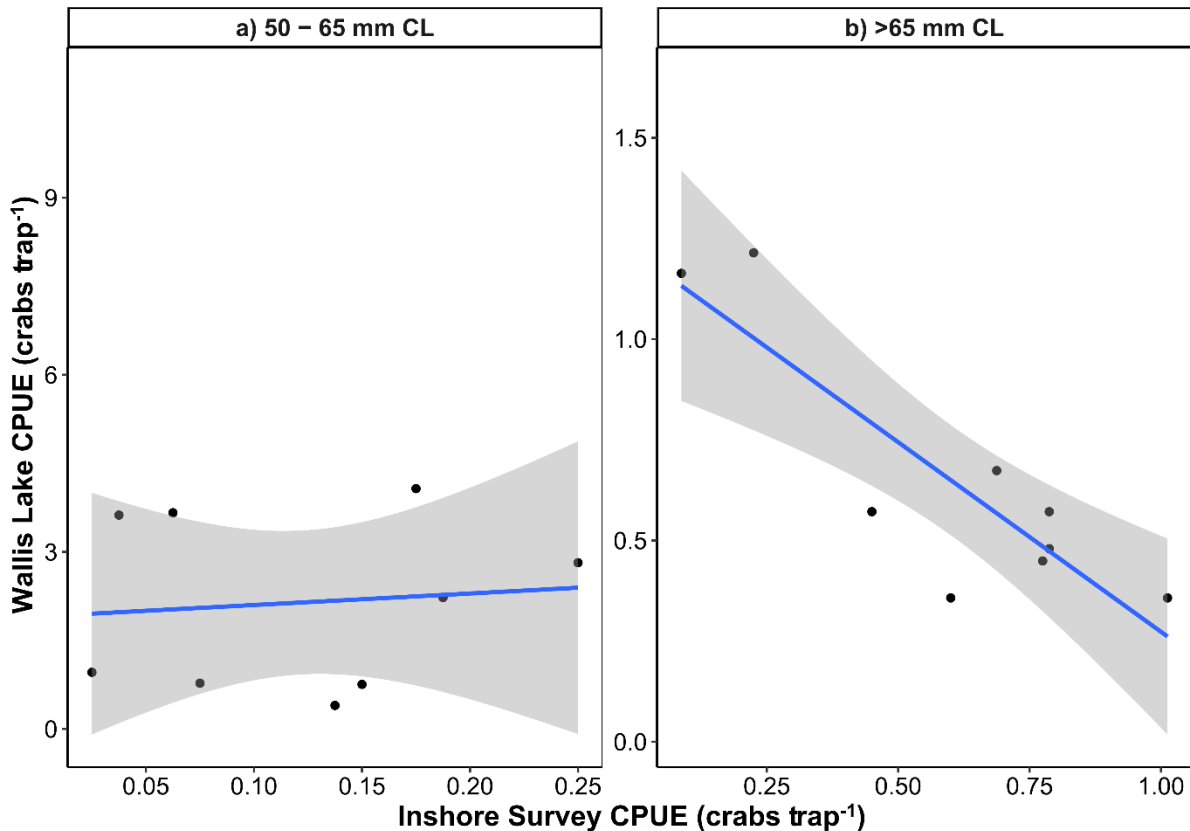


**Figure 45** Relationship between the independent survey catch per unit effort (CPUE; crabs trap<sup>-1</sup>) in Wallis Lake and the adjacent inshore area. The solid blue line shows the linear regression and the grey ribbon shows the 95% confidence interval.

For commercial fisheries data, the number of large catches of Blue Swimmer Crab in the inshore (coastal) catch data showed no relationship to the presence of high flow events in the adjacent estuary at zero ( $r = -0.02$ ,  $t_{136} = -0.334$ ,  $P = 0.739$ ) or one ( $r = 0.02$ ,  $t_{136} = 0.273$ ,  $P = 0.785$ ) month lags. At the annual level there was also no evidence that flow during any of the lagged periods influenced the change in summer commercial CPUE (previous July – September:  $r = -0.19$ ,  $t_{21} = -0.908$ ,  $P = 0.374$ , previous October – December:  $r = 0.03$ ,  $t_{21} = 0.155$ ,  $P = 0.878$ , January – March (not lagged):  $r = 0.23$ ,  $t_{21} = 1.087$ ,  $P = 0.284$ ).

### Winter harvest

A large winter harvest correlated with a summer commercial CPUE lower than the previous year as shown by the moderate negative correlation between the difference from the previous summer commercial CPUE and the size of the winter harvest ( $r = -0.55$ ,  $t_{21} = -3.086$ ,  $P = 0.005$ ; Figure 46).

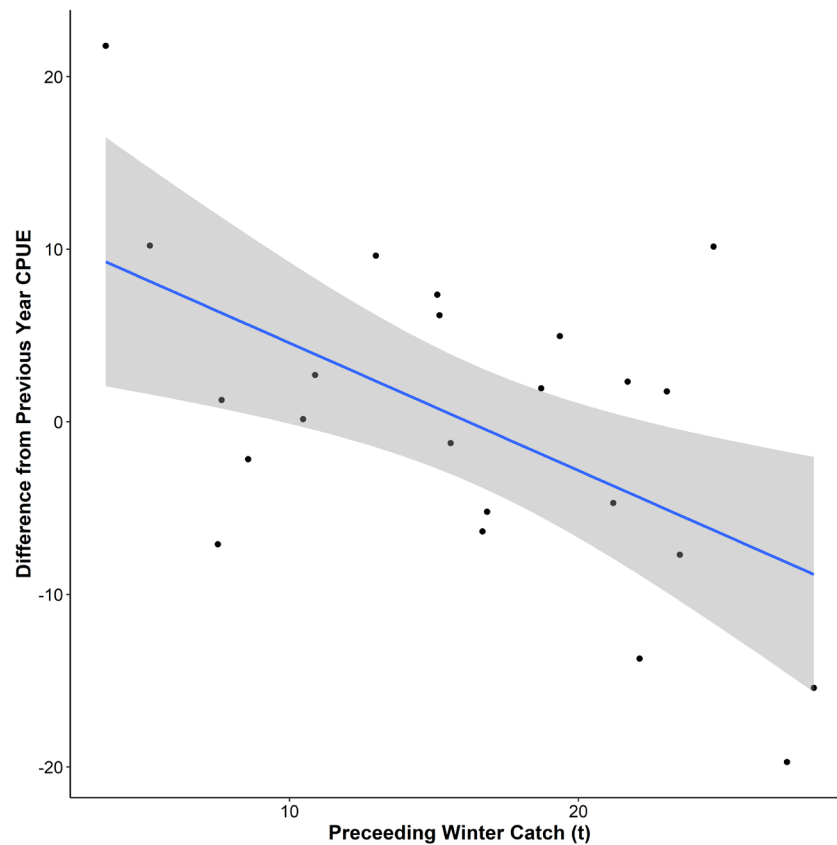


**Figure 46** Relationship between the change in summer (January – April) commercial CPUE (kg scaled fisher-day<sup>-1</sup>; relative to previous summer) and the total catch taken the previous winter (June – November). The solid blue line shows the linear relationship with the grey ribbon showing the 95% confidence interval.

The sex ratio of the commercial catch was highly seasonal. For most of the year, the majority of the harvest was male, but between May and September females accounted for over 50% of the harvest (Figure 47). The female proportions peaked between June and August with ~70% of the catch being female (Figure 47). These proportions were fairly stable over time, but it is evident that around 2013, the magnitude of harvest between April and July increased dramatically (Figure 48). The magnitude of the winter harvest has declined since 2017, corresponding to the overall annual catch decline during the same period (Figure 44).

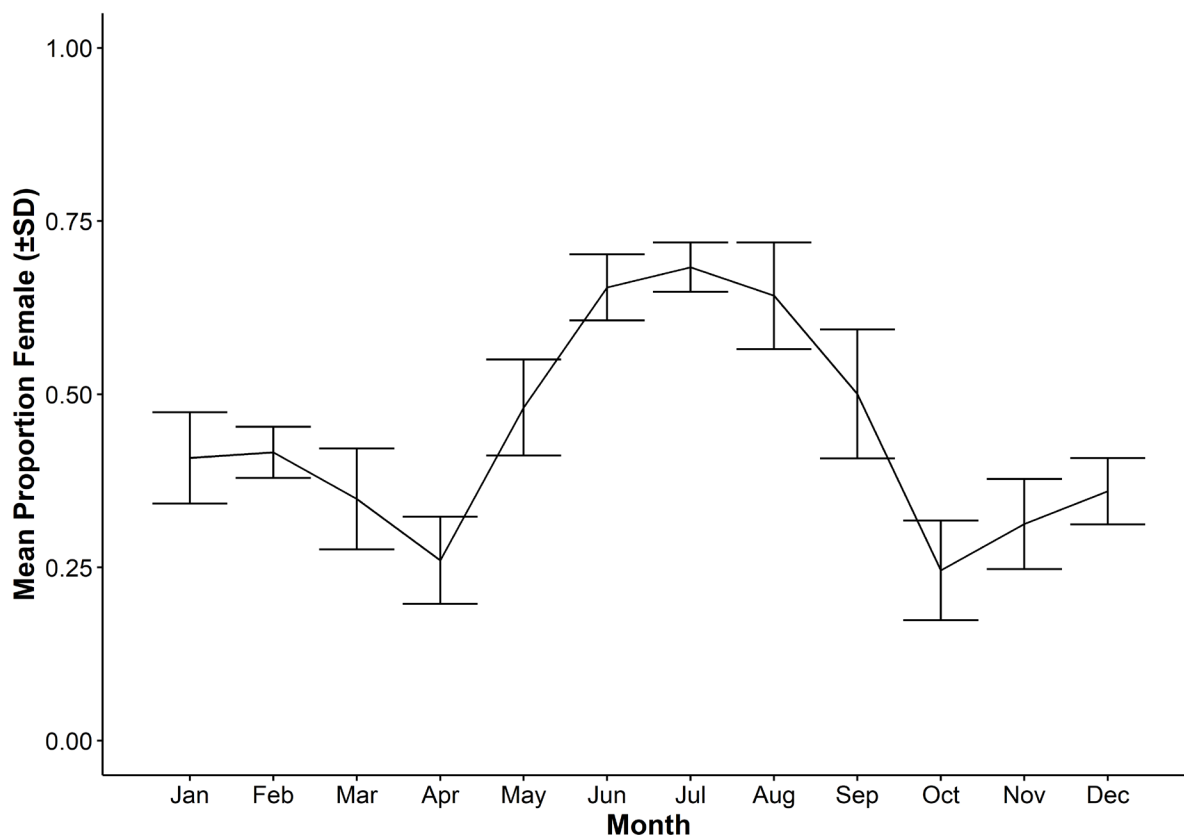


**Figure 47** Proportion of the catch (by weight) which is made up of female Blue Swimmer Crab in the Wallis Lake fishery each month. The mean was calculated using data from July 2009 – June 2020. Error bars show 1 standard deviation around the mean.

While the size structure of harvested male and female Blue Swimmer Crab is similar between October and April, between May and September the harvested females are larger compared to the males (Figure 49). This is particularly evident between June and September where the male harvest is comprised of a narrow size range compared to the broader distribution of size classes evident in the female harvest (Figure 49). No differences were evident using only data before or after the change in size limits.

### Coastal temperature and wind

We found no correlation between the change in summer commercial CPUE and the offshore sea surface temperature during July – September ( $r = -0.05$ ,  $t_{21} = -0.242$ ,  $P = 0.811$ ) or November – December ( $r = 0.03$ ,  $t_{21} = 0.156$ ,  $P = 0.877$ ), suggesting recruitment is not affected by offshore SST. There was weak evidence for a catchability effect with a possible negative correlation between the change in summer commercial CPUE and the offshore SST during January – March of the same year ( $r = -0.36$ ,  $t_{21} = -1.783$ ,  $P = 0.090$ ).

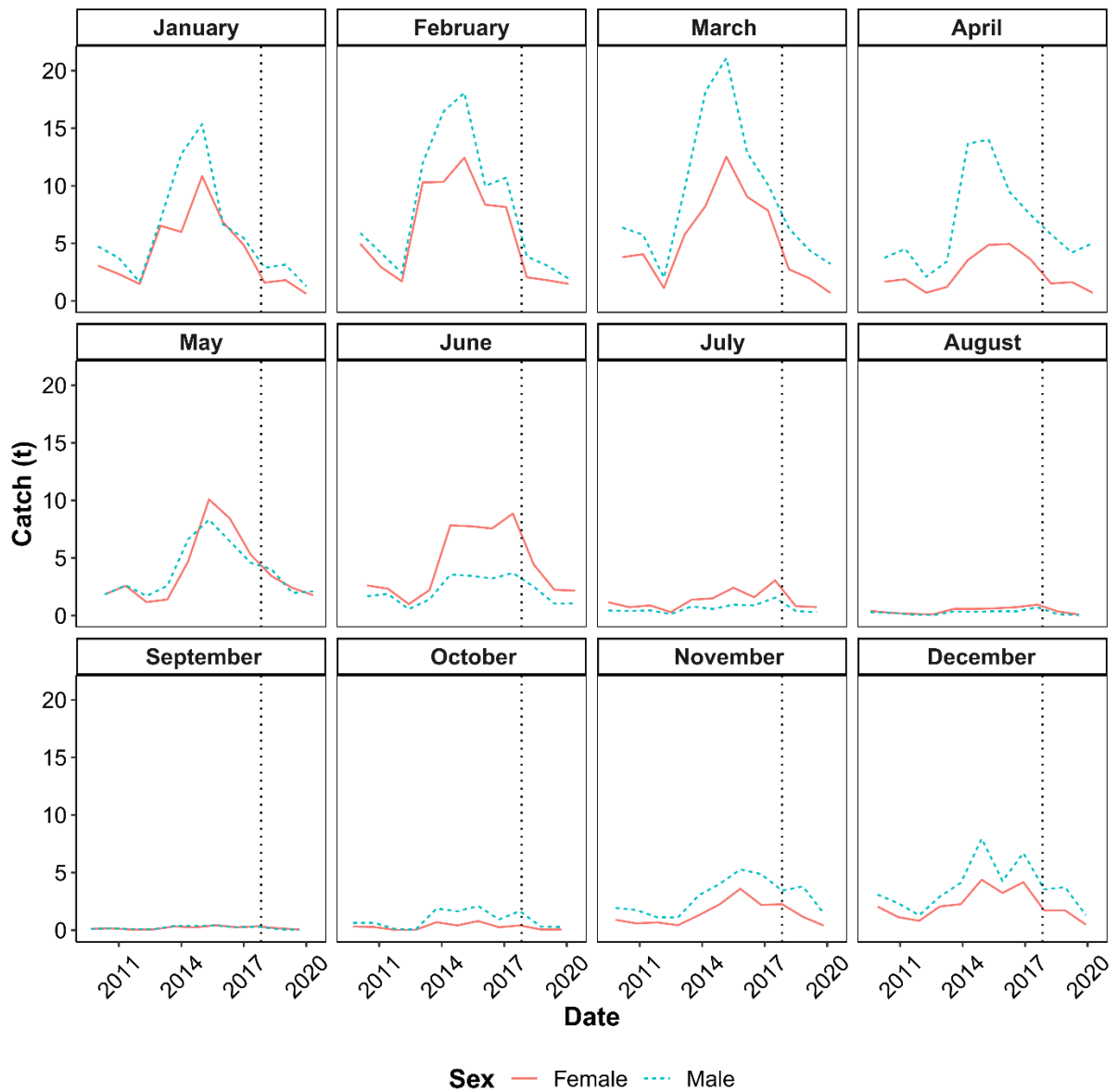


**Figure 48** Time series showing the interannual variations in Blue Swimmer Crab catch by month for each sex (July 2009 – June 2020). For example, the January panel shows the catch of male and female crabs in January each year. The dotted vertical black line shows when the minimum size limit increased from 60 to 65 mm CL

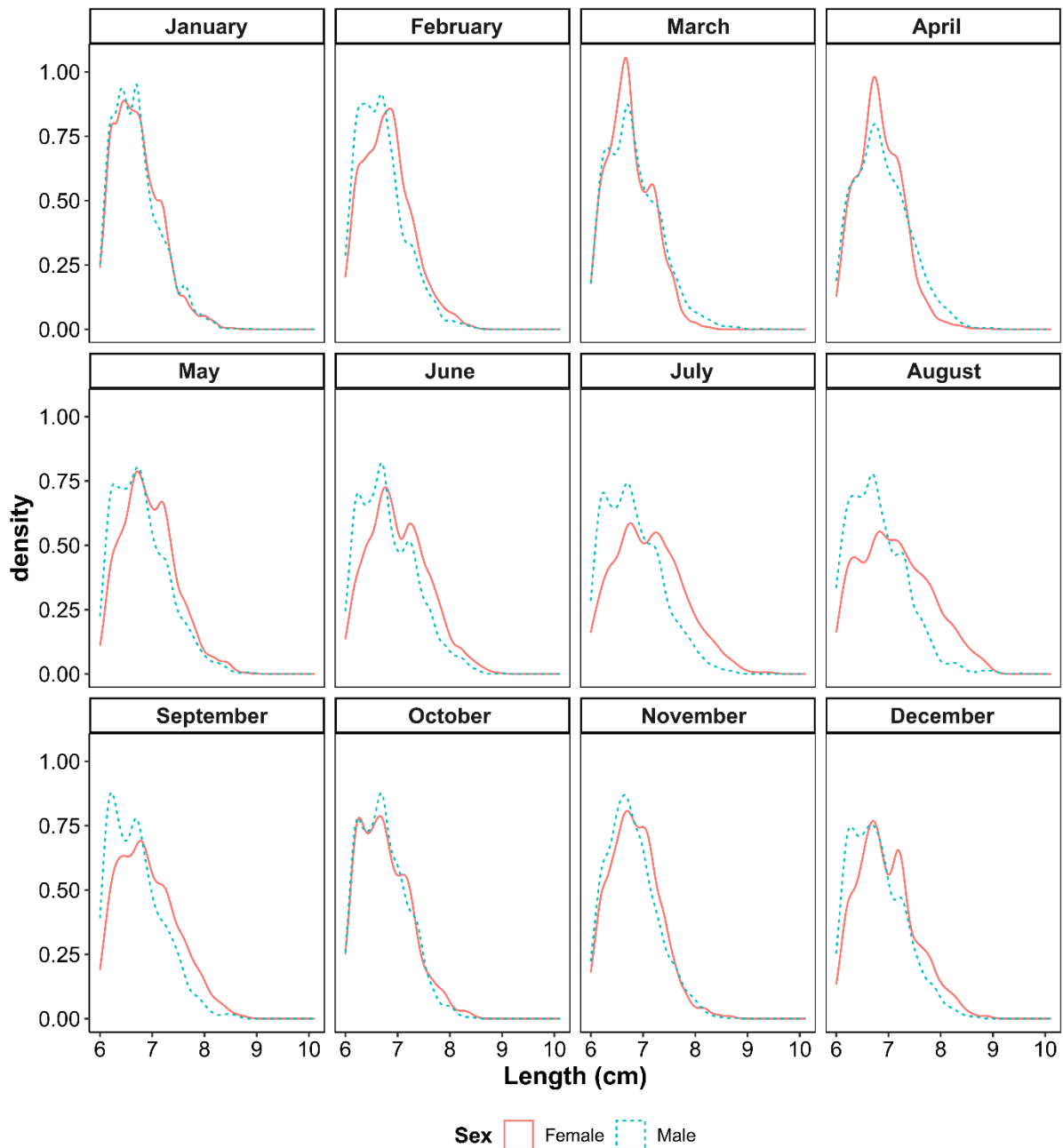


**Figure 49** Size structure of the Blue Swimmer Crab harvest each month, pooled across all years. The solid red line shows the female size structure while the dotted blue line shows the male size structure. Length represents carapace length.

Similar results were found for the analysis of upwelling and downwelling favourable winds and their relationships with the change in summer commercial CPUE. For upwelling favourable winds, no evidence of correlation was found with the change in summer commercial CPUE for the preceding July – September ( $r = 0.18$ ,  $t_{19} = 0.840$ ,  $P = 0.412$ ) or November – December ( $r = -0.30$ ,  $t_{19} = -1.393$ ,  $P = 0.180$ ). There was a weak positive relationship between the change in summer commercial CPUE and the upwelling favourable wind during January – March ( $r = 0.40$ ,  $t_{19} = 1.885$ ,  $P = 0.076$ ). For downwelling favourable winds, no correlations were identified between the change in summer commercial CPUE and any of the periods ( $P > 0.5$ ).

## Climatic indices

For the winter months there were no correlations between the PDO and summer commercial CPUE (July:  $r = 0.08$ , August:  $r = 0.07$ , September:  $r = 0.13$ , October:  $r = 0.28$ ). The correlations became stronger leading into the summer months (November:  $r = 0.42$ , December:  $r = 0.35$ , January:  $r = 0.41$ ). The mean of November, December and January produced the strongest correlation ( $r = 0.42$ ,  $P = 0.043$ ) and we judged this to be the most appropriate correlate as it accounts for multiple months and variability leading into the fishing season (**Figure 50**). While the direction of the trends matched the PDO results, there were no correlations found for any of the lagged months tested with the IPO ( $r < 0.33$ ,  $P > 0.1$ ).

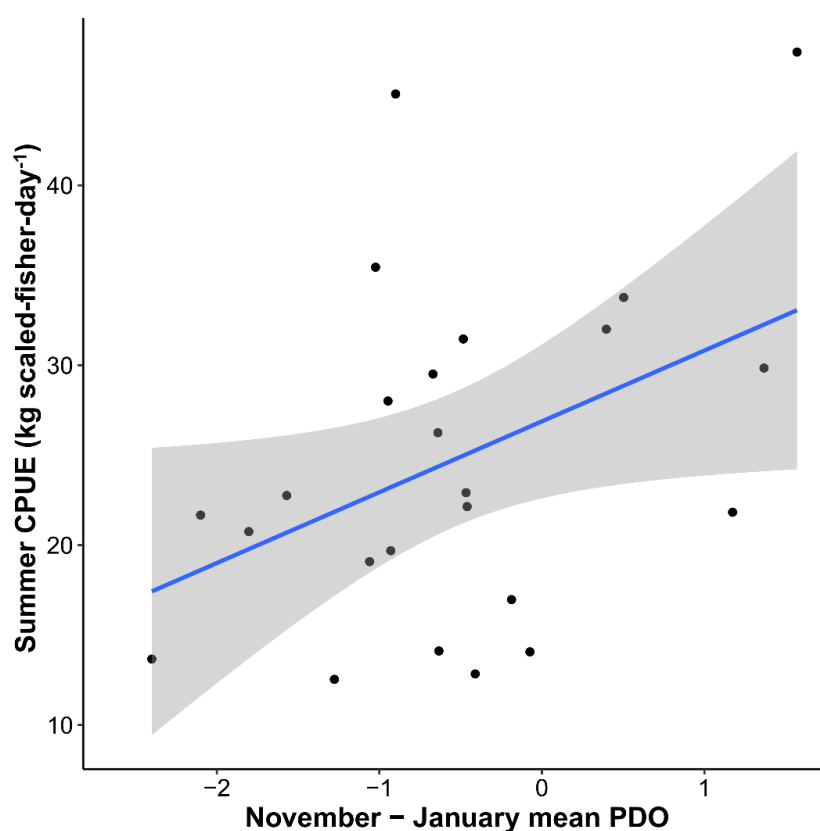


**Figure 50** Relationship between the summer (January – April) commercial CPUE and the mean Pacific Decadal Oscillation Index (PDO; November - January). The solid blue line shows the linear relationship with the grey ribbon showing the 95% confidence interval.

## Predictability

From the key variables identified through hypotheses testing above, we selected the most promising predictors for further modelling, and created a linear model to attempt to predict the summer (January – April) CPUE for Blue Swimmer Crab in Wallis Lake. Predictors included in the model were the previous year's summer CPUE (kg scaled fisher day<sup>-1</sup>), the total catch taken the previous winter (June – November; kg), and the mean PDO index from November – January leading into the fishing season. The final model fitted well (Figure 51) showing strong evidence that all three predictors were important (Table 10), and gave an  $R^2$  value of 0.61 (adjusted  $R^2 = 0.56$ ). Leave-one-out cross-

validation gave a reduced  $R^2$  of 0.44 and a root mean square error of 7.22. The hindcast of predictions using the linear model gave a good reconstruction of previous summer CPUE although the 95% prediction intervals were wide (Figure 52). The equation for the final model is:

$$\begin{aligned}
 CPUE_{Jan\_April}_t &= 27.42 + 6.29 \cdot PDO_{Nov-Jan,t} - 0.001 \cdot Winter\_Catch_{t-1} + 0.74 \\
 &\cdot CPUE_{Jan\_April}_{t-1}
 \end{aligned}$$

where  $CPUE_{Jan\_April}_t$  is the CPUE for January to April in year  $t$ ,  $PDO_{Nov-Jan}$  is the mean PDO for November – January leading into year  $t$ , and  $Winter\_Catch_{t-1}$  is the catch (kg) in June – November in year  $t - 1$ . When the model was run with standardised variables, the standardised effects sizes revealed that while all variables were roughly of equal importance (overlapping effect size and standard errors), the order of importance for the variables was the total catch taken the previous winter (standardised effect size  $\pm$  SE:  $-7.50 \pm 2.07$ ), followed by the previous year’s summer CPUE (standardised effect size  $\pm$  SE:  $7.08 \pm 1.77$ ), then the mean PDO index from November – January leading into the fishing season (standardised effect size  $\pm$  SE:  $6.74 \pm 1.99$ ).

### DHARMA residual diagnostics

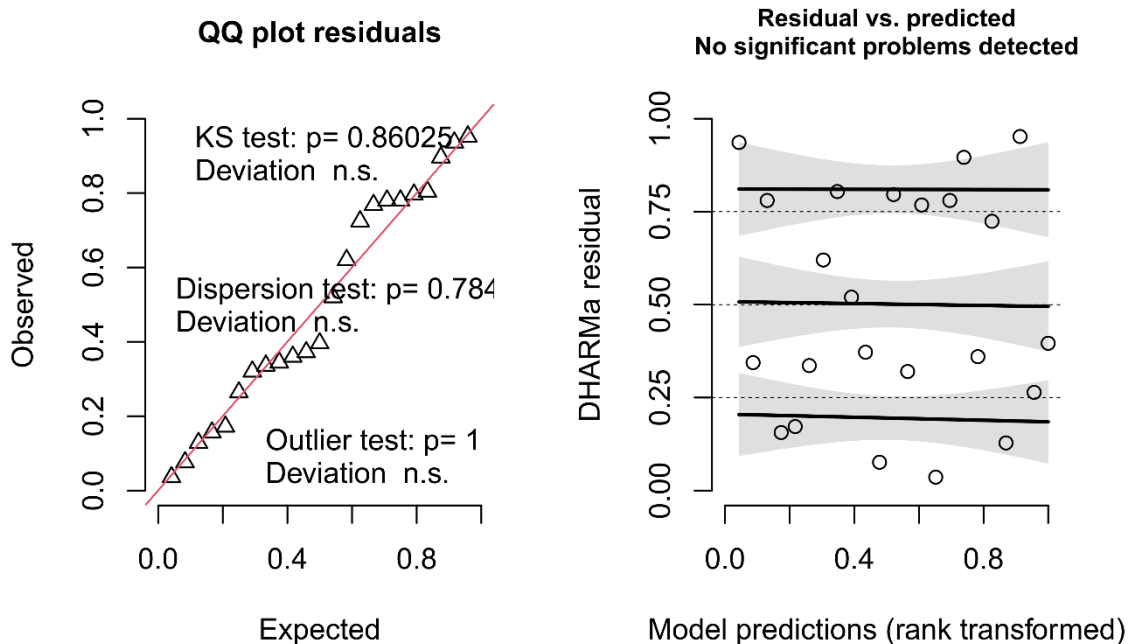


**Figure 51** Simulated residuals for the linear model used to predict summer CPUE. The left panel shows no significant deviations from normality. The right panel shows no deviations in residuals distributions.

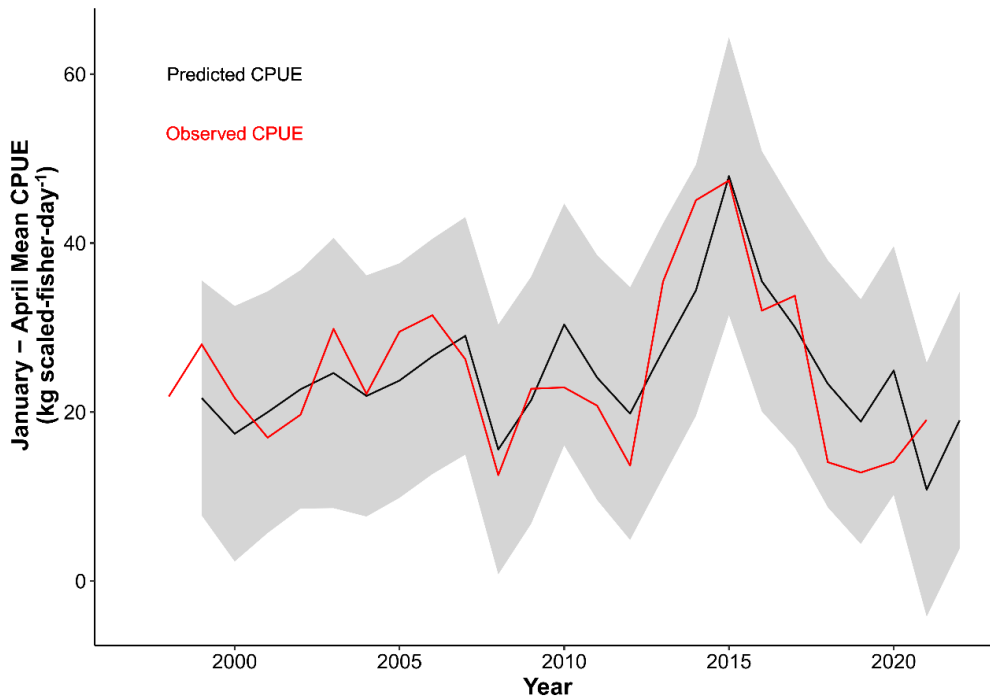


**Figure 52** Hindcast predictions of summer (January – April) CPUE (kg scaled Fisher Day<sup>-1</sup>) for Blue Swimmer Crab in Wallis Lake. The red line shows observed CPUE while the black line shows the predicted CPUE. The grey ribbon shows the 95% prediction interval using the linear model. Note we have predicted CPUE for 2022 but the observations are not yet available to compare.

**Table 10** Results of the linear model predicting summer CPUE.

| Coefficients           | Estimate | Standard Error | t value | P value |
|------------------------|----------|----------------|---------|---------|
| Intercept              | 27.42    | 5.60           | 4.90    | <0.001  |
| November – January PDO | 6.29     | 1.86           | 3.39    | 0.003   |
| Previous Winter Catch  | -0.001   | 0.0003         | -3.62   | 0.002   |
| Previous Summer CPUE   | 0.74     | 0.19           | 4.00    | <0.001  |

Since the aim of the quadratic discrimination analysis was to forecast prior to the fishing season and the PDO mean included the start of the fishing season (note that there are no forecasts of the PDO readily available), the PDO mean was excluded from the quadratic analysis. The quadratic discrimination analysis was successful at using the previous summer CPUE and the winter catch to classify most financial years as above or below average, successfully classifying 20 of 24 years (83.3% accuracy, Figure 53), with 10 of the 11 years matching for the period in which daily reporting data is available (post-2009). The classification analysis showed that when the previous summer harvest was high, the forecast season was likely to be above average but if the winter harvest was too large then there was a risk of a below average financial year harvest. The four years which were incorrectly classified were 1999, 2003, 2004 and 2018 (year ending in July). Of the incorrect predictions, 1999 and 2003 were predicted to be below average years while 2004 and 2018 were predicted to be above average. The years with the highest and lowest harvests were all correctly identified.

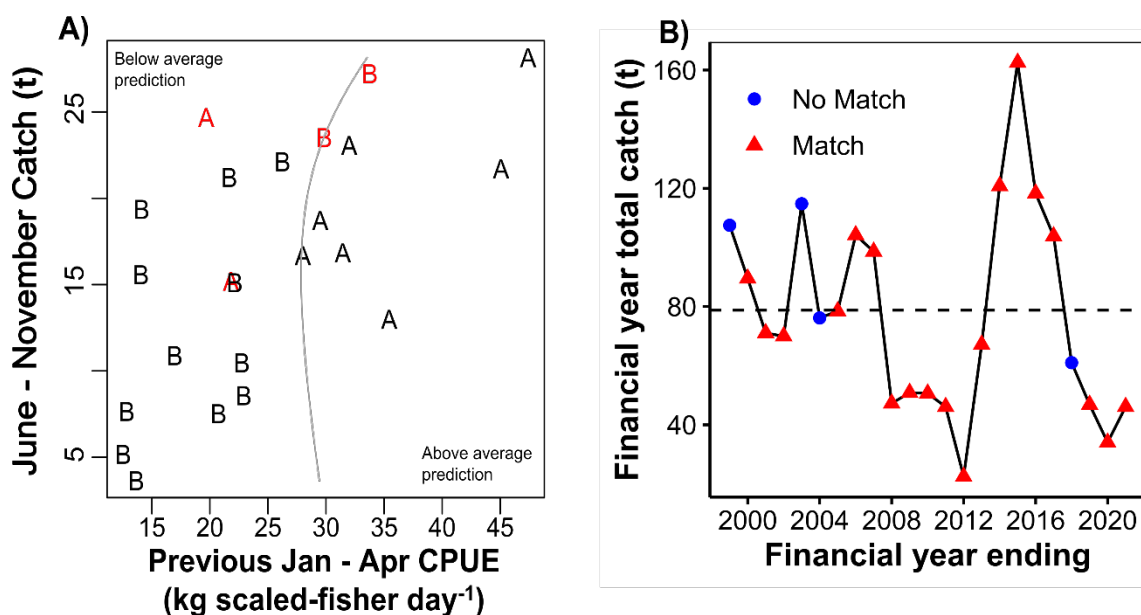


**Figure 53** Visual representation of classification of above- and below-average seasons based upon the quadratic discrimination analysis using winter catch and the previous summer CPUE (kg scaled fisher day<sup>-1</sup>). Panel A shows the outcomes of the discrimination analysis. Letters represent the predicted outcome for the season (A = above average, B = below average) and colour represents whether the prediction was correct (black = correct, red = incorrect). The grey line shows the prediction boundary based upon the two variables. Panel B shows the performance of the predictions over time relative to the observed financial year catch. The dashed line represents the mean total catch.

## Discussion

The high variability in the Wallis Lake Blue Swimmer Crab (*Portunus armatus*) fishery was effectively explained through two factors, one relating to climate, and one to the fishery. We found that fishing activities during winter and the previous year's relative abundance may be the most important contributors to the variability. It is possible that the amount of winter harvest may directly influence the following season due to the disproportionate high impact of winter fishing on mated pre-spawning female crabs. We also identified a strong positive relationship between the pacific decadal oscillation and CPUE, which may be useful for future catch prediction.

## Environmental and climatic influences

While our results showed a negative relationship in catch rates between estuarine and inshore habitats (suggesting that large crabs may be moving between these environments as hypothesised), there was no evidence that this movement was driven by freshwater flow. This again contrasts with the aforementioned research of Gillson *et al.* (2012), and concurs with the conclusions from the analysis of the regular independent survey (see *Estuary-specific drivers of Blue Swimmer Crab abundance and distribution*). As there was no link between the inshore catches and freshwater flow,

it was not surprising that there was no relationship between freshwater flow and recruitment (commercial catch) the following season. While it is possible that inshore spawning could be detrimental to self-recruitment into an estuary, more work is required to understand the spawning cues and the conditions which may influence the location of spawning (e.g., inside or outside the estuary mouth). For Giant Mud Crab in nearby estuaries, acoustic tracking was used to show that migrations are triggered by both cool temperatures, heavy rainfall and coincided with new or full moons (see *Environmental influence on spawning migrations in Giant Mud Crab*). A similar approach could be used with Blue Swimmer Crab to better understand drivers of estuary-ocean exchange.

Despite temperature being a key influence in the Western Australian Blue Swimmer Crab fisheries (Chandrapavan *et al.* 2019; Johnston *et al.* 2021b), we found no evidence that seasonal changes in nearby sea surface temperature correlated with changes in commercial harvest in Wallis Lake. As a key driver of metabolism, particularly in ectotherms, temperature has large physiological impacts on crabs (including both growth and mobility), but the influence of lagged temperature on recruitment often occurs through some impact on spawning females or growth and survival of early life history stages. A local latitudinal gradient in Blue Swimmer Crab reproductive biology (Nolan *et al.* 2022), similar to that observed in western Australia (Johnston and Yeoh 2021) suggests that there may be local adaptation to different temperature regimes and that the temperatures experienced during the current study likely did not negatively impact recruitment. While there is some evidence Blue Swimmer Crab will be resilient to near-future climate change (Champion *et al.* 2020), as marine heatwaves are increasingly common (Oliver *et al.* 2018; Jacox *et al.* 2022) in our study region (Schaeffer and Roughan 2017), it is possible that temperatures could exceed optimal levels. Ideally, it would be better for future work to incorporate temperature that is directly measured in the estuary (Wallis Lake) itself, but at present such extended time series do not exist at a suitable temporal resolution.

While the mechanism by which onshore winds directly influence the movement of Blue Swimmer Crab larvae has been directly observed in Moreton Bay (Sumpton *et al.* 2003), the link from larval transport to catch rates is complex. In the context of Wallis Lake, onshore winds are likely to only be influential if spawning is occurring outside the estuary, and as discussed above it is currently unknown under which conditions spawning does in fact occur in the inshore region. If we could limit the onshore wind analyses to only seasons with suspected inshore spawning there may be a relationship between onshore winds and lagged catch rates, as observed for coastal spawning fish nearby (Schilling *et al.* 2022b). A more suitable proxy for larval supply may be to directly sample larvae or megalopa inside the estuary as has been done for *Portunus* spp. in other coastal regions (Yanagi *et al.* 1995; Bryars and Havenhand 2006).

Relationships between fisheries and the PDO have previously been observed following the original observation that the PDO correlated with decadal scale changes in Pacific Salmon (Mantua and Hare 2002). Unfortunately, due to the decadal scale over which the PDO operates, the exact drivers are uncertain (Power *et al.* 2021) and under novel conditions such as those presented by climate change such indices are becoming less predictable (Li *et al.* 2020). This leads to even less certainty in the mechanisms by which the PDO may influence fisheries productivity (McClatchie 2012). While it has been hypothesised that the PDO could be influential to the northern Australian Giant Mud Crab fisheries due to the link between PDO and freshwater flow (Meynecke *et al.* 2012b), how the PDO influences the Wallis Lake Blue Swimmer Crab fishery is highly uncertain. The lack of a relationship with the more geographically relevant IPO suggests that we should be cautious in the use of the PDO correlation, and further monitoring should be done to understand potential underlying mechanisms for this correlative relationship.

## Effects of winter fishing mortality

The negative relationship between increased winter harvest and a declining summer harvest aligns with previous research in the Western Australian Blue Swimmer Crab fisheries, where it was observed that increased fishing pressure during winter led to increased pressure on mated pre-spawning females (Johnston *et al.* 2011). It is likely that winter fishing has a similar effect in the Wallis Lake fishery, as is being borne out in our analyses. While fishing effort and harvest has traditionally been comparatively low in the winter months (April – November), it has increased since 2013 (before declining after 2017 in line with the overall fishery). While the traditional summer harvest is male biased, the winter harvest in Wallis Lake and both South Australia and Western Australia (Johnston *et al.* 2011) is dominated by females. During winter, harvested females are generally larger than males, also similar to South Australia (Xiao and Kumar 2004) and Western Australia (Johnston *et al.* 2011). This may be caused by the males being preferentially removed over summer (when egg-bearing females cannot be retained). Winter fishing mortality on large female crabs is a source for concern. Firstly, females are likely to have already mated during the warmer growth period, meaning that they are able to spawn when the water warms, and may well already have fertilised eggs in their ovaries. When the size-fecundity relationship is also considered, an even greater amount of fertilised eggs may be being removed from the fishery by the removal of larger females during winter (Johnson *et al.* 2010; Nolan *et al.* 2022). As shown in *Fishery independent survey of Blue Swimmer Crab – Description and data summary*, there is normally a single primary cohort that moves through the Wallis Lake fishery each growth season, that originates from spawning in spring and early summer. Consequently, the harvest of mated pre-spawning females during winter and early spring may adversely impact egg production for the coming season.

## Management implications and conclusion

We tested several hypotheses regarding possible factors driving variability in the Blue Swimmer Crab fishery. We found some evidence that decadal-scale climatic oscillations (i.e., PDO) may be driving long-run variability in productivity, but also found strong evidence that winter fishing mortality significantly impacts catch rates. Two key parameters (previous summer relative abundance and winter harvest) explain a reasonable proportion of the variation in fisheries productivity. While the CPUE from the previous growth season is likely indicative of overall abundance, setting a baseline for number of larvae to be spawned, the harvesting of females during winter and early spring is likely to be having a detrimental impact on the main spawning period of late spring and early summer. These two parameters support the prediction of above- and below-average harvests with reasonable confidence, which can be considered alongside other data sources to inform future assessments of stock status and total allowable catch determinations for the species. However, these relationships also raise the possibility of developing co-management arrangements with stakeholders to reduce winter fishing effort to maximise egg production, support stronger recruitment and catch in the following year, and achieve the best economic and social outcomes from the fishery.

# Oceanic connectivity and particle dispersal for Blue Swimmer Crab and Giant Mud Crab

## Background and rationale

Dispersal of larvae facilitates connectivity among different areas (Cowan and Sponagle 2009), which can maintain spatially extensive metapopulations (Kritzer and Sale 2004). Advection of larvae in ocean currents can create source-sink dynamics within populations (Kritzer and Sale 2004; Figueira and Crowder 2006). While larval production is a significant driver of subsequent recruitment, favorable advection and physicochemical conditions during the larval phase can be just as important (Cowan and Sponagle 2009). Consequently, ocean circulation has a substantial influence on connectivity in marine systems and can be a key driver of variation in fisheries production (Cetina-Heredia *et al.* 2019; Schilling *et al.* 2020; Schilling *et al.* 2022a). Quantifying connectivity is important to inform the assessment and management of exploited populations (Kritzer and Sale 2004; Punt *et al.* 2016; Cadrin 2020).

Quantitative estimates of population connectivity can be obtained by coupling high-resolution oceanographic models with Lagrangian particle tracking to simulate larval dispersal (North *et al.* 2009; Van Sebille *et al.* 2018). These methods have been applied from regional (Roughan *et al.* 2011; Schilling *et al.* 2020) to global scales (Doblin and van Sebille 2016), providing estimates of connectivity for a variety of taxa, such as macroalgae (Coleman *et al.* 2011), sea urchins (Coleman *et al.* 2017), crustaceans (Roughan *et al.* 2005; Everett *et al.* 2017; Cetina-Heredia *et al.* 2019), bivalves (Norrie *et al.* 2020) and fish (Schilling *et al.* 2020). When spawning locations (i.e., 'sources') are known, particles can be tracked forwards-in-time, providing relative estimates of settlement magnitude that can be related to observed settlement and recruitment (Cetina-Heredia *et al.* 2019) or patterns in fisheries productivity (Everett *et al.* 2017; Schilling *et al.* 2020). Conversely, when spawning locations are unknown (or poorly defined), particles can be tracked backwards-in-time from known settlement locations (i.e., 'sinks'), providing estimates of putative spawning locations and recruitment origins (Putman and Naro-Maciel 2013; Torrado *et al.* 2021; Hernández *et al.* 2022).

Both Blue Swimmer Crab and Giant Mud Crab have an oceanic larval phase and an estuarine juvenile–adult phase, off south-eastern Australia (Figure 54). Giant Mud Crab undertake a downstream migration to spawn in oceanic waters, with evidence that mature females continue to migrate northwards once in the ocean (see *Environmental influence on spawning migrations in Giant Mud Crab*). Blue Swimmer Crab are thought to spawn primarily within estuaries, but may also spawn in coastal waters, as outlined in previous sections. For both species, spawning is followed by a dispersive larval phase (Bryars and Havenhand 2006; Nurdiani and Zeng 2007), before settlement in the inshore region (Webley and Connolly 2007) and subsequent recruitment into estuaries (Potter *et al.* 1983; Webley *et al.* 2009).

Genetic evidence suggests there is a high degree of inter-estuarine and inter-jurisdictional connectivity between Queensland and NSW for both species (Chaplin *et al.* 2001; Gopurenko and Hughes 2002). Connectivity between these populations is likely to be facilitated by the East Australian Current (EAC, Figure 54), a southward (poleward) flowing western boundary current (Suthers *et al.* 2011; Oke *et al.* 2019b) that facilitates the dispersal of several exploited species (e.g., fish, prawns and lobsters; Roughan *et al.* 2011; Everett *et al.* 2017; Cetina-Heredia *et al.* 2019; Schilling *et al.* 2020). Given the dominating north-south flow of the EAC, it is possible that the

northern components (i.e., Queensland) of these populations are important sources of larvae for estuaries in NSW, however these dynamics are not well understood.

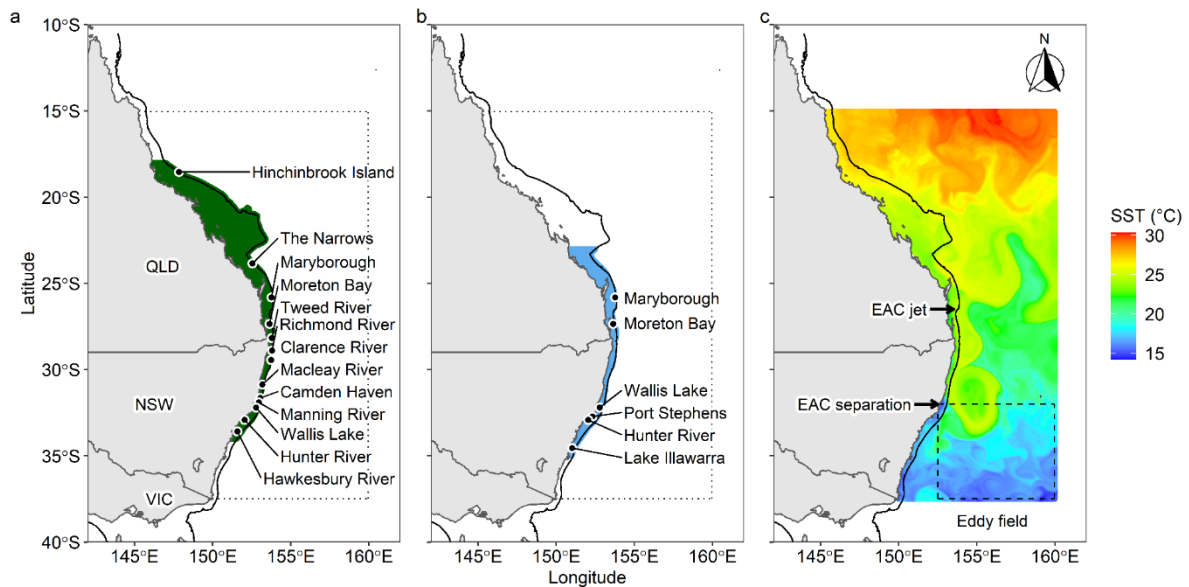


**Figure 54** Map of eastern Australia showing the release locations and range of east coast populations of a) Giant Mud Crab (dark green), b) Blue Swimmer Crab (blue) and c) an example of the structure of the EAC, including sea surface temperature (SST, °C) and the approximate locations of key oceanographic features, including: the EAC jet (~24–28°S); the EAC separation (28–31°S); and, mesoscale eddy field (south of 31°S; dashed box). Features are marked at their centre latitude. The dotted line represents the reduced boundaries of ozROMS that provided the velocity fields used in the simulations (Wijeratne *et al.* 2018) and the solid black line shows the 200 m isobath.

Here, we quantify population connectivity along eastern Australia by simulating dispersal of Giant Mud Crab and Blue Swimmer Crab larvae using output from a high-resolution oceanographic model (Wijeratne *et al.* 2018) within a Lagrangian particle tracking framework (Lange and van Sebille 2017; Van Sebille *et al.* 2018). Since the spawning locations for these species are not well defined, this was achieved by 1) releasing particles from known settlement locations and tracking them backwards-in-time, and 2) comparing patterns in connectivity between different release locations, thereby identifying putative spawning locations and providing estimates of population connectivity.

## Data sources, approach and modelling

### Oceanographic model and regional context

For this study, we used daily output from a 10-year oceanographic simulation (2008–2017) of Australian shelf waters (and adjacent deep ocean), configured in the Regional Oceanographic Modelling System (hereafter ‘ozROMS’) without data-assimilation (Wijeratne *et al.* 2018). The full model extends from 7.4°N–49°S and 92–180°E, but we used a reduced spatial domain for our simulations, covering approximately 2,200 km of coastline (15–37.5°S) encompassing Queensland and NSW waters, and extending ~600 km offshore (160°E; Figure 54). This encompasses the eastern

Australian distribution of both species (Chaplin *et al.* 2001; Gopurenko and Hughes 2002) and the EAC. The EAC exhibits mesoscale variability on seasonal, annual, and decadal timescales (Archer *et al.* 2017; Oke *et al.* 2019a, b; Kerry and Roughan 2020). This area is considered a climate change 'hotspot' (Frusher *et al.* 2014; Hobday and Pecl 2014); showing evidence of warming (Malan *et al.* 2021; Li *et al.* 2022b) and increased poleward penetration (Cetina-Heredia *et al.* 2014; Li *et al.* 2021). Key features of the EAC include: the EAC jet, a region of coherent flow adjacent to the coast (~24–31°S; Oke *et al.* 2019b); the EAC separation, south of the jet where the current strengthens and separates from the coast (~31–33°S; Cetina-Heredia *et al.* 2014). Finally, south of the separation the EAC forms a dynamic mesoscale eddy-field (33–43°S; Everett *et al.* 2012), that feeds the eastern- and southern-extensions towards New Zealand and Tasmania, respectively (Oke *et al.* 2019a; b). It is possible for eddies in this region to entrain and advect larvae offshore (Everett *et al.* 2015), however they may also be returned to the coast via cross-shelf currents (Cetina-Heredia *et al.* 2019; Malan *et al.* 2020; Roughan *et al.* 2022).

ozROMS is eddy-resolving, with a 3–4 km horizontal resolution and 30 vertical *s*-levels. The model employs a vertical stretching scheme that preserves the depth of surface- and bottom-layers to better resolve these currents (Wijeratne *et al.* 2018). ozROMS has open boundaries forced by a daily, 1/12° (~9 km) horizontal resolution output from the data-assimilating global Hybrid Coordinate Ocean Model (HYCOM; Chassignet *et al.* 2007). Atmospheric forcing is obtained from 3 hourly, 0.125° (~14 km) horizontal resolution data from the European Centre for Medium-range Weather Forecasting (ECMWF) Interim archive and tidal forcing is obtained from the Oregon State University TPX07.2 global tidal model (Egbert and Erofeeva 2002). Model bathymetry is derived from the General Bathymetric Chart of the Oceans (GEBCO) 30 arc-second (~0.8 km) gridded bathymetry (Sandwell *et al.* 2002).

While ozROMS has been broadly validated and performs well at reconstructing mesoscale circulation (Wijeratne *et al.* 2018), an important but sometimes overlooked aspect of applying global-scale models in a regional context is validation against local observations that represent regionally important dynamics. To assess the suitability of the model in the EAC and determine our level of confidence in ozROMS we compared model outputs and observations of key EAC metrics that are relevant to larval dispersal, including: sea surface temperature (SST; °C); mean kinetic energy (MKE;  $\text{m}^2 \text{s}^{-2}$ ); eddy kinetic energy (EKE;  $\text{m}^2 \text{s}^{-2}$ ); and, the EAC separation latitude (following Cetina-Heredia *et al.* 2014) which dictates eddy position and hence larval delivery (Cetina-Heredia *et al.* 2019). Readers are referred to Hewitt *et al.* (2022b) and the supplementary material therein for details of the model validation described in Wijeratne *et al.* (2018), accompanied by an independent comparison and discussion of model limitations. In summary, while the model has some limitations it is the most suitable model available for our purposes given the broad spatial domain and high-resolution.

## Particle tracking

Lagrangian particle tracking simulations were conducted using PARCELS v2.2 ('Probably A Really Computationally Efficient Lagrangian Simulator'; Lange and van Sebille 2017; Delandmeter and Van Sebille 2019), using Python v3.6.5 (Van Rossum and Drake 2009). PARCELS is an offline Lagrangian particle tracking framework, designed to efficiently process large quantities of data (Lange and van Sebille 2017; Delandmeter and Van Sebille 2019). Particles were advected using daily average zonal (east-west) and meridional (north-south) velocities ( $\text{m s}^{-1}$ ). Particle positions were interpolated in 5-min time steps, using a fourth order Runge-Kutta scheme, and recorded once daily. A horizontal Brownian walk function of  $8.8 \text{ m}^2 \text{ s}^{-1}$  was applied at each time step, in both zonal and meridional directions (Okubo 1971; Cetina-Heredia *et al.* 2019). This introduces random variation to particle

trajectories, to simulate natural variation caused by sub-grid scale processes (e.g., turbulence, sea breeze; Van Sebille *et al.* 2018). Particle tracking simulations can be sensitive to the number of particles released, particularly in regions where circulation is highly variable (Simons *et al.* 2013; Monroy *et al.* 2017). In the EAC, patterns in larval dispersal and connectivity do not change significantly beyond releases of 455 particles per location (Cetina-Heredia *et al.* 2015), and therefore each release was comprised of  $n = 455$  particles.

Along eastern Australia, some patterns in the fecundity and the spatiotemporal distribution of estuarine spawning have been resolved for Blue Swimmer Crab (Johnson *et al.* 2010; Nolan *et al.* 2022), however there is limited information regarding oceanic spawning for either species. To overcome this, we released passive (i.e., non-swimming) particles from ‘known’ settlement locations and tracked them backwards-in-time to identify putative spawning locations. Here, we define a known settlement location as estuaries that have historically supported notable commercial and/or recreational harvest of either species. This resulted in 7 and 14 release estuaries for Blue Swimmer Crab and Giant Mud Crab, respectively (Figure 54, Table 11). Particles were released adjacent to the mouth of these estuaries over the 100 m isobath in the surface layer. We assume that oceanic spawning takes place at the same time as estuarine spawning, spanning the austral spring–autumn (September–May; Heasman *et al.* 1985; Johnson *et al.* 2010; Nolan *et al.* 2022) and particles were released once daily during this period (282 d) for the duration of ozROMS (10 years; 2008–2017). Since we tracked backwards-in-time, particle releases were offset (in time) so that tracking stopped during the spawning period. We assume that spawning takes place on the continental shelf (i.e., shoreward of the 200 m isobath), and consider a particle trajectory ‘successful’ if it is on the continental shelf at the end of tracking. Any particles that did not meet this criterion, or left the model domain were excluded from our analysis.

**Table 11** Estuaries and embayments included in the study that support notable commercial and recreational harvest of Blue Swimmer Crab and Giant Mud Crab along eastern Australia.

| Estuary          | Latitude (°S) | EAC region <sup>a</sup> | Species <sup>b</sup> | State <sup>c</sup> |
|------------------|---------------|-------------------------|----------------------|--------------------|
| Hinchinbrook     | 18.54         | EAC jet                 | GMC                  | Queensland         |
| The Narrows      | 23.85         | EAC jet                 | GMC                  | Queensland         |
| Hervey Bay       | 25.82         | EAC jet                 | Both                 | Queensland         |
| Moreton Bay      | 27.34         | EAC jet                 | Both                 | Queensland         |
| Tweed River      | 28.17         | EAC separation          | GMC                  | NSW                |
| Richmond River   | 28.89         | EAC separation          | GMC                  | NSW                |
| Clarence River   | 29.43         | EAC separation          | GMC                  | NSW                |
| Macleay River    | 30.86         | EAC separation          | GMC                  | NSW                |
| Camden Haven     | 31.65         | EAC eddy-field          | GMC                  | NSW                |
| Manning River    | 31.90         | EAC eddy-field          | GMC                  | NSW                |
| Wallis Lake      | 32.19         | EAC eddy-field          | Both                 | NSW                |
| Port Stephens    | 32.72         | EAC eddy-field          | Both                 | NSW                |
| Hunter River     | 32.92         | EAC eddy-field          | Both                 | NSW                |
| Hawkesbury River | 33.59         | EAC eddy-field          | Both                 | NSW                |
| Lake Illawarra   | 34.55         | EAC eddy-field          | BSC                  | NSW                |

<sup>a</sup> EAC: East Australian Current; latitudinal limits of these regions based on independent comparison of ozROMS model output with local observations (see *Supplementary Material 1*).

<sup>b</sup> GMC: Giant Mud Crab, BSC: Blue Swimmer Crab

<sup>c</sup> Queensland: Queensland, NSW: New South Wales

Growth during the larval phase in portunid crabs is temperature-dependent, with optimum conditions occurring at ~25–30°C (Bryars and Havenhand 2006; Nurdiani and Zeng 2007). Therefore,

the pelagic larval duration (PLD) was estimated using degree-days (Neuheimer and Taggart 2007; Steele and Neuheimer 2022). Species-specific degree-days were derived from published larval development studies, by multiplying the time taken (in days) to grow from zoea to megalopae by the experimental temperature used in the study (Bryars and Havenhand 2006; Nurdiani and Zeng 2007). To implement this approach, daily temperatures experienced by each particle were sampled from ozROMS, once the cumulative sum of these temperatures equals (or exceeds) the degree-days threshold particle tracking was stopped (Everett *et al.* 2017; Schilling *et al.* 2020). To incorporate natural variability in growth rates, we randomly sampled degree-days for each particle from a normal distribution, with a mean and standard deviation of  $535 \pm 32$  and  $382.5 \pm 50$  degree-days for Giant Mud Crab and Blue Swimmer Crab, respectively (Bryars and Havenhand 2006; Nurdiani and Zeng 2007). In our simulations this means, in a constant water temperature of 22°C, an average Giant Mud Crab or Blue Swimmer Crab particle will have a PLD of ~24 or ~17 d, respectively.

## Summary of model outputs

Model outputs are presented as graphical summaries of the contributions of particles from each direction (i.e., north/south) relative to a given estuary, as well as from each jurisdiction (i.e., Queensland/NSW) and regions of broadly similar mesoscale oceanography along eastern Australia (as simulated by ozROMS). We defined these regions as: the EAC jet (~24–28°S); the EAC separation (28–31°S); and the eddy-field (south of 31°S). In our analysis we included the Great Barrier Reef (north of ~24°S) as part of the EAC jet, however this region is also influenced by the South Equatorial Current, North Queensland Current and the Gulf of Papua Current (Sandery *et al.* 2019). The latitudinal limits of these regions differ somewhat from the literature (e.g., Oke *et al.* 2019b) due to decreased transport in ozROMS (see Hewitt *et al.* 2022b). Finally, since we released an arbitrary number of particles (calculated as the minimum required to represent the variability in the system; Cetina-Heredia *et al.* 2015) these contributions are presented as percentages (%), while for mapping we plot particle density (km<sup>2</sup>) to assist visualization.

## Results

Overall, our simulations resulted in the release of 17,964,765 Giant Mud Crab and 8,983,065 Blue Swimmer Crab particles from known settlement locations, which were then tracked backwards-in-time to putative spawning locations. During our simulations, very few particles left the model domain, with the exception of Giant Mud Crab particles released at Hinchinbrook Island, where it was possible for some to cross the northern boundary. Of the particles that remained within the model domain, 1,631,697 (9.1 %) and 1,482,291 (16.5 %) Giant Mud Crab and Blue Swimmer Crab (respectively) particle trajectories were considered ‘successful’ (i.e., inshore of the 200 m isobath at the end of their PLD). In general, estuaries sourced the majority of particles (51–99 %) from the north, with lower contributions of particles from the south (1–49 %; Table 12). For Blue Swimmer Crab, particles were generally sourced from within 48–319 km (Figure 55) of a settlement estuary. In contrast, Giant Mud Crab particles from a given estuary originated from a broader expanse of coastline 111–406 km (Figure 56).

**Table 12** Mean ( $\pm$  SD) northern/southern percentage particle contribution (%) to estuaries along eastern Australia

| Release estuary  | Latitude ( $^{\circ}$ S) | Particle contribution (%) |             |                |             |
|------------------|--------------------------|---------------------------|-------------|----------------|-------------|
|                  |                          | Blue Swimmer Crab         |             | Giant Mud Crab |             |
|                  |                          | North                     | South       | North          | South       |
| Hinchinbrook     | 18.54                    | -                         | -           | 51 $\pm$ 18    | 49 $\pm$ 18 |
| The Narrows      | 23.85                    | -                         | -           | 99 $\pm$ 1     | 1 $\pm$ 1   |
| Hervey Bay       | 25.82                    | 93 $\pm$ 5                | 7 $\pm$ 5   | 97 $\pm$ 3     | 3 $\pm$ 3   |
| Moreton Bay      | 27.34                    | 93 $\pm$ 5                | 7 $\pm$ 5   | 96 $\pm$ 3     | 4 $\pm$ 3   |
| Tweed River      | 28.17                    | -                         | -           | 95 $\pm$ 5     | 5 $\pm$ 5   |
| Richmond River   | 28.89                    | -                         | -           | 89 $\pm$ 7     | 11 $\pm$ 7  |
| Clarence River   | 29.43                    | -                         | -           | 85 $\pm$ 10    | 15 $\pm$ 10 |
| Macleay River    | 30.86                    | -                         | -           | 78 $\pm$ 15    | 22 $\pm$ 15 |
| Camden Haven     | 31.65                    | -                         | -           | 72 $\pm$ 16    | 28 $\pm$ 16 |
| Manning River    | 31.90                    | -                         | -           | 72 $\pm$ 15    | 28 $\pm$ 15 |
| Wallis Lake      | 32.19                    | 61 $\pm$ 16               | 39 $\pm$ 16 | 68 $\pm$ 15    | 32 $\pm$ 15 |
| Port Stephens    | 32.72                    | 53 $\pm$ 11               | 47 $\pm$ 11 | 58 $\pm$ 15    | 42 $\pm$ 15 |
| Hunter River     | 32.92                    | 56 $\pm$ 12               | 44 $\pm$ 12 | 61 $\pm$ 14    | 39 $\pm$ 14 |
| Hawkesbury River | 33.59                    | 74 $\pm$ 11               | 26 $\pm$ 11 | 77 $\pm$ 14    | 23 $\pm$ 14 |
| Lake Illawarra   | 34.55                    | 85 $\pm$ 9                | 15 $\pm$ 9  | -              | -           |

The distribution of putative spawning latitudes varied depending on the adjacent mesoscale structure of the EAC, and generally exhibited little interannual variability. For particles released from estuaries within the EAC jet or EAC separation, putative spawning latitudes were approximately normally distributed and displaced to the north (Figure 55 and Figure 56). Conversely, for particles released within the eddy-field the distribution became progressively more ‘north-skewed’ the further south a settlement estuary was, and the most likely putative spawning latitudes were at the approximate latitude of release (Figure 55 and Figure 56).

Exchange of particles between estuaries within the eddy-field and putative spawning latitudes to the north of the EAC separation was limited. This pattern was most evident for Blue Swimmer Crab, with only 0.1–27 % of particles released within the eddy-field originating from north of the EAC separation (Table 13), providing little evidence for inter-jurisdictional connectivity in this species (0.2–30 %; Figure 57, Figure 58 and Table 14). A similar pattern was evident for Giant Mud Crab, however connectivity across the EAC separation was higher (6–52 %; Table 13), facilitating much greater inter-jurisdictional connectivity (8–96 %) for this species (Figure 59, Figure 60 and Table 14).

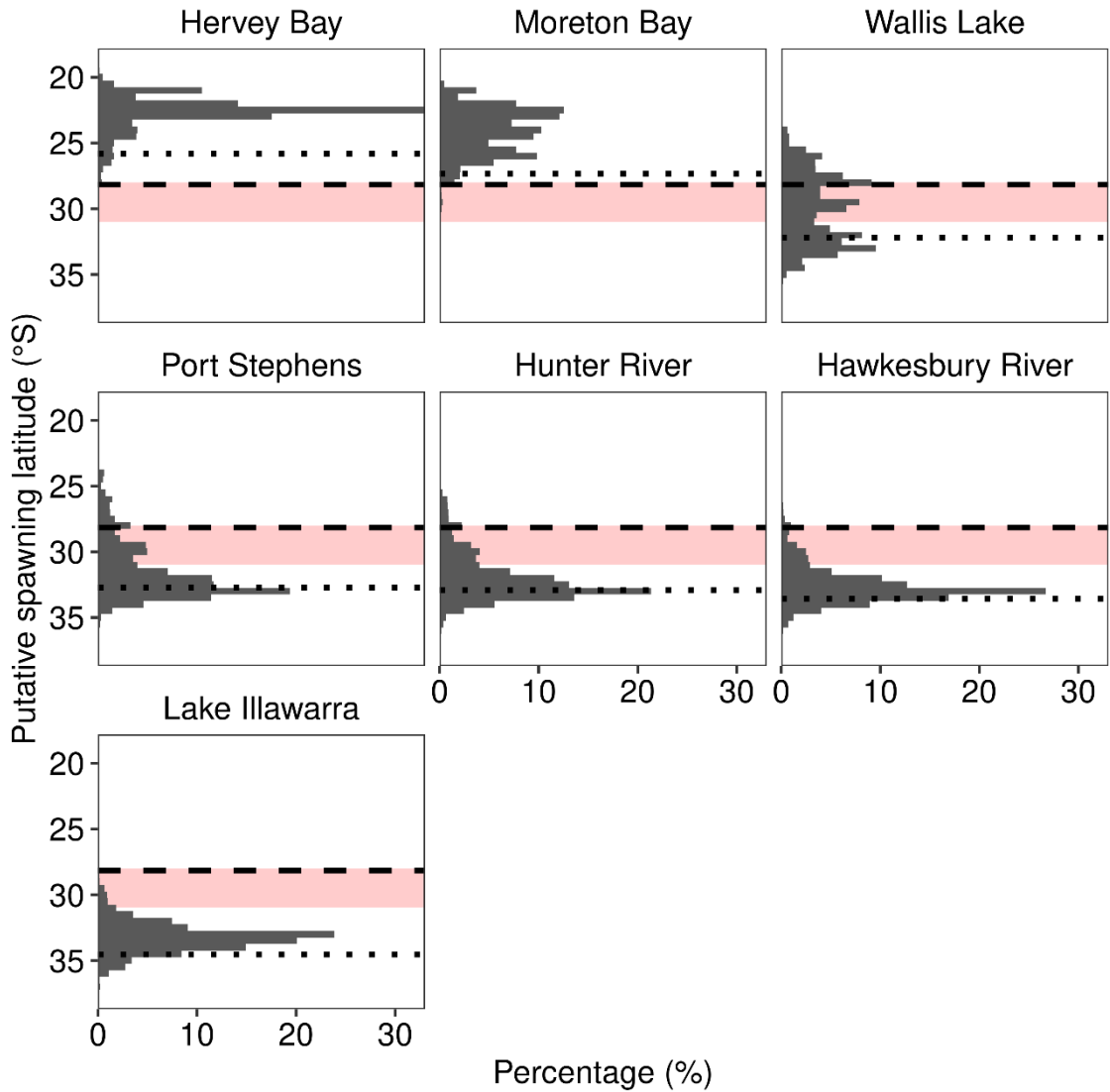


**Figure 55** Percentage contribution (%) of Blue Swimmer Crab particles to settlement at estuaries (indicated by the dotted line) from putative spawning latitudes (in 0.5° latitude bands) along eastern Australia. Note percentages are calculated for each estuary separately and cover the entire simulation period (2008–2017). The dashed line indicates the Queensland/NSW border (~28.2°S), and the area shaded red indicates the approximate location of the EAC separation (28–31°S) as simulated in ozROMS.

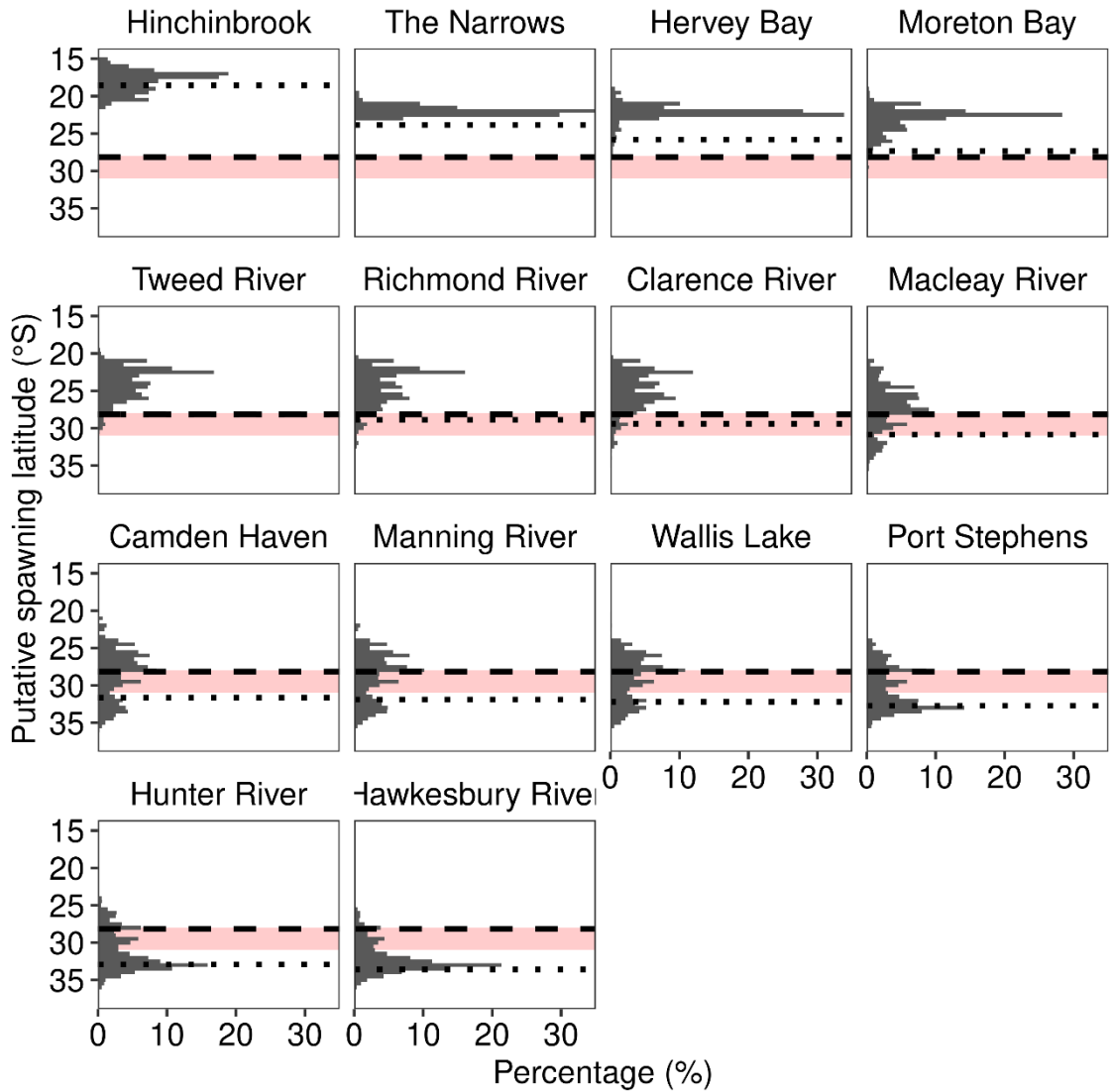


**Figure 56** Percentage contribution (%) of Giant Mud Crab particles to settlement at estuaries (indicated by the dotted line) from putative spawning latitudes (in 0.5° latitude bands) along eastern Australia. Note percentages are calculated for each estuary separately and cover the entire simulation period (2008–2017). The dashed line indicates the Queensland/NSW border (~28.2°S), and the area shaded red indicates the approximate location of the EAC separation (28–31°S) as simulated in ozROMS.

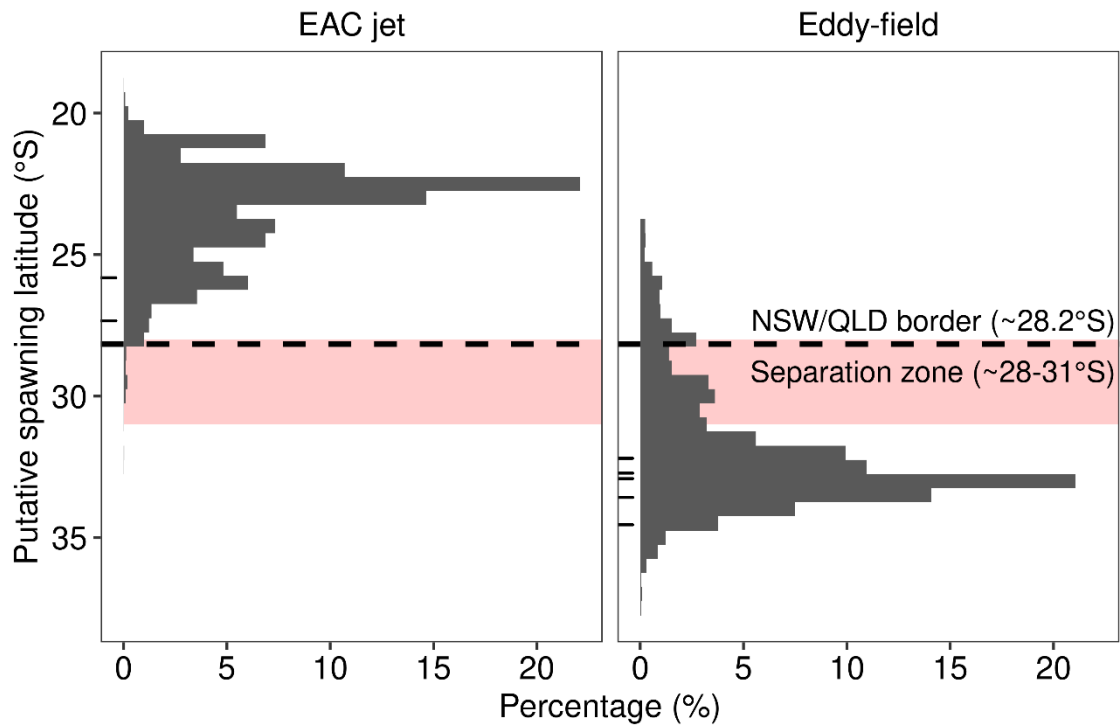


**Figure 57** Percentage contribution (%) of Blue Swimmer Crab particles to settlement at estuaries (indicated by rugs along y-axis) within the EAC jet (north of 28°S) or eddy-field (south of 31°S) from putative spawning latitudes (in 0.5° latitude bins) along eastern Australia. Note percentages are calculated for each region separately over the entire simulation period (2008–2017).

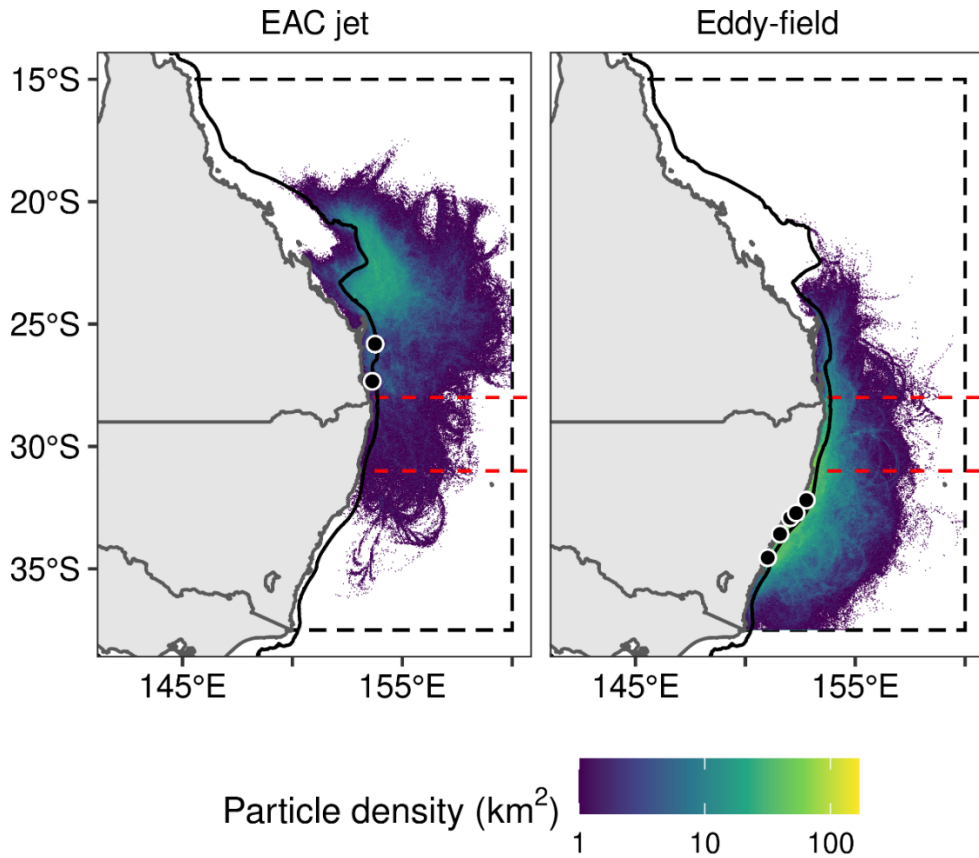


**Figure 58** Geographic distribution of Blue Swimmer Crab particles ( $\text{km}^2$ ) tracked backwards-in-time from estuaries within the EAC jet (north of  $28^\circ\text{S}$ ) or eddy-field (south of  $31^\circ\text{S}$ ) when they reached their degree-days threshold ( $382.5 \pm 50$ ). The dashed red lines represent the approximate EAC separation ( $\sim 28\text{--}31^\circ\text{S}$ ; as simulated in ozROMS) and the dashed black lines represent the reduced model domain used in our simulations. The solid black line represents the 200 m isobath, all particles offshore of this at the end of tracking are excluded from our analysis. Note counts are derived from the entire simulation period (2008–2017) and the  $\log_{10}$ -transformed colour scale.

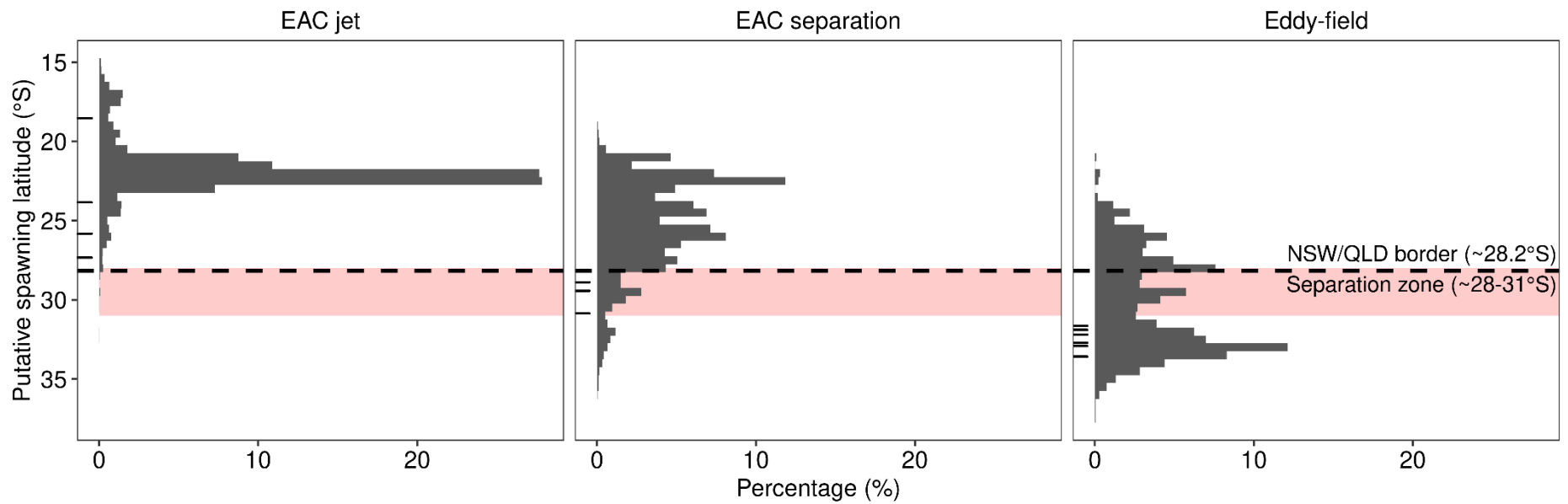


**Figure 59** Percentage contribution (%) of Giant Mud Crab particles to settlement at estuaries (indicated by rugs along y-axis) within the EAC jet (north of 28°S), the EAC separation (~28–31°S) or the eddy-field (south of 31°S) from putative spawning latitudes (in 0.5° latitude bins) along eastern Australia. Note percentages are calculated for each region separately over the entire simulation period (2008–2017).

**Table 13** Mean ( $\pm$  SD) percentage particle contribution (%) to estuaries along eastern Australia from each of the East Australian Current (EAC) regions.

| Release estuary  | Latitude<br>(°S) | EAC region     | Particle contribution (%) |                   |                 |                 |                   |                 |
|------------------|------------------|----------------|---------------------------|-------------------|-----------------|-----------------|-------------------|-----------------|
|                  |                  |                | Blue Swimmer Crab         |                   |                 | Giant Mud Crab  |                   |                 |
|                  |                  |                | EAC jet                   | EAC<br>separation | Eddy-field      | EAC jet         | EAC<br>separation | Eddy-field      |
| Hinchinbrook     | 18.54            | EAC jet        | -                         | -                 | -               | 100.0 $\pm$ 0   | 0.0 $\pm$ 0.0     | 0.0 $\pm$ 0.0   |
| The Narrows      | 23.85            | EAC jet        | -                         | -                 | -               | 100.0 $\pm$ 0   | 0.0 $\pm$ 0.0     | 0.0 $\pm$ 0.0   |
| Hervey Bay       | 25.82            | EAC jet        | 99.7 $\pm$ .07            | 0.3 $\pm$ 0.7     | 0.0 $\pm$ 0.0   | 99.6 $\pm$ 0.7  | 0.4 $\pm$ 0.7     | 0.0 $\pm$ 0.0   |
| Moreton Bay      | 27.34            | EAC jet        | 98.4 $\pm$ 4.0            | 1.5 $\pm$ 3.4     | 0.1 $\pm$ 0.7   | 98.4 $\pm$ 4.2  | 1.4 $\pm$ 3.4     | 0.3 $\pm$ 0.8   |
| Tweed River      | 28.17            | EAC separation | -                         | -                 | -               | 95.0 $\pm$ 6.3  | 4.4 $\pm$ 5.4     | 0.6 $\pm$ 1.1   |
| Richmond River   | 28.89            | EAC separation | -                         | -                 | -               | 91.0 $\pm$ 5.8  | 7.0 $\pm$ 4.8     | 1.9 $\pm$ 1.7   |
| Clarence River   | 29.43            | EAC separation | -                         | -                 | -               | 87.7 $\pm$ 8.0  | 9.2 $\pm$ 6.0     | 3.1 $\pm$ 4.3   |
| Macleay River    | 30.86            | EAC separation | -                         | -                 | -               | 64.4 $\pm$ 17.4 | 22.0 $\pm$ 12.5   | 13.6 $\pm$ 9.3  |
| Camden Haven     | 31.65            | EAC eddy-field | -                         | -                 | -               | 51.5 $\pm$ 20.0 | 23.2 $\pm$ 6.7    | 25.3 $\pm$ 16.1 |
| Manning River    | 31.90            | EAC eddy-field | -                         | -                 | -               | 46.8 $\pm$ 20.1 | 24.8 $\pm$ 5.7    | 28.4 $\pm$ 18.4 |
| Wallis Lake      | 32.19            | EAC eddy-field | 26.6 $\pm$ 13.1           | 31.6 $\pm$ 10.1   | 41.8 $\pm$ 20.3 | 42.6 $\pm$ 16.8 | 27.7 $\pm$ 8.5    | 29.8 $\pm$ 18.5 |
| Port Stephens    | 32.72            | EAC eddy-field | 9.3 $\pm$ 5.0             | 20.6 $\pm$ 10.3   | 70.1 $\pm$ 12.7 | 23.8 $\pm$ 13.2 | 24.8 $\pm$ 10.0   | 51.4 $\pm$ 22.3 |
| Hunter River     | 32.92            | EAC eddy-field | 4.9 $\pm$ 4.0             | 13.3 $\pm$ 16.4   | 78.6 $\pm$ 13.3 | 16.1 $\pm$ 13.4 | 23.1 $\pm$ 10.7   | 60.8 $\pm$ 21.6 |
| Hawkesbury River | 33.59            | EAC eddy-field | 1.3 $\pm$ 1.3             | 10.1 $\pm$ 3.2    | 88.6 $\pm$ 4.0  | 6.1 $\pm$ 5.3   | 18.2 $\pm$ 13.8   | 75.7 $\pm$ 18.3 |
| Lake Illawarra   | 34.55            | EAC eddy-field | 0.1 $\pm$ 0.2             | 3.5 $\pm$ 3.0     | 96.3 $\pm$ 3.0  | -               | -                 | -               |

**Table 14** Mean ( $\pm$  SD) percentage particle contribution (%) to estuaries along eastern Australia from Queensland (Queensland) or New South Wales (NSW).

| Release estuary  | Latitude ( $^{\circ}$ S) | State      | Particle contribution (%) |                 |                 |                 |
|------------------|--------------------------|------------|---------------------------|-----------------|-----------------|-----------------|
|                  |                          |            | Blue Swimmer Crab         |                 | Giant Mud Crab  |                 |
|                  |                          |            | Queensland                | NSW             | Queensland      | NSW             |
| Hinchinbrook     | 18.54                    | Queensland | -                         | -               | 100 $\pm$ 0.0   | 0.0 $\pm$ 0.0   |
| The Narrows      | 23.85                    | Queensland | -                         | -               | 100 $\pm$ 0.0   | 0.0 $\pm$ 0.0   |
| Hervey Bay       | 25.82                    | Queensland | 99.9 $\pm$ 0.3            | 0.1 $\pm$ 0.3   | 99.8 $\pm$ 0.4  | 0.2 $\pm$ 0.4   |
| Moreton Bay      | 27.34                    | Queensland | 98.8 $\pm$ 4.0            | 1.2 $\pm$ 4.0   | 98.7 $\pm$ 4.1  | 1.3 $\pm$ 4.1   |
| Tweed River      | 28.17                    | NSW        | -                         | -               | 95.5 $\pm$ 6.0  | 4.5 $\pm$ 6.0   |
| Richmond River   | 28.89                    | NSW        | -                         | -               | 91.9 $\pm$ 5.6  | 8.1 $\pm$ 5.6   |
| Clarence River   | 29.43                    | NSW        | -                         | -               | 88.7 $\pm$ 7.7  | 11.3 $\pm$ 7.7  |
| Macleay River    | 30.86                    | NSW        | -                         | -               | 67.2 $\pm$ 17.0 | 32.8 $\pm$ 17.0 |
| Camden Haven     | 31.65                    | NSW        | -                         | -               | 54.1 $\pm$ 20.6 | 45.9 $\pm$ 20.6 |
| Manning River    | 31.90                    | NSW        | -                         | -               | 50.2 $\pm$ 21.3 | 49.8 $\pm$ 21.3 |
| Wallis Lake      | 32.19                    | NSW        | 29.7 $\pm$ 15.2           | 70.3 $\pm$ 15.2 | 46.1 $\pm$ 18.2 | 53.9 $\pm$ 18.2 |
| Port Stephens    | 32.72                    | NSW        | 10.5 $\pm$ 5.8            | 89.5 $\pm$ 5.8  | 27.3 $\pm$ 16.8 | 72.7 $\pm$ 16.8 |
| Hunter River     | 32.92                    | NSW        | 5.9 $\pm$ 5.2             | 94.1 $\pm$ 5.2  | 18.9 $\pm$ 17.2 | 81.1 $\pm$ 17.2 |
| Hawkesbury River | 33.59                    | NSW        | 1.7 $\pm$ 1.4             | 98.3 $\pm$ 1.4  | 7.9 $\pm$ 8.3   | 92.1 $\pm$ 8.3  |
| Lake Illawarra   | 34.55                    | NSW        | 0.2 $\pm$ 0.2             | 99.8 $\pm$ 0.2  | -               | -               |

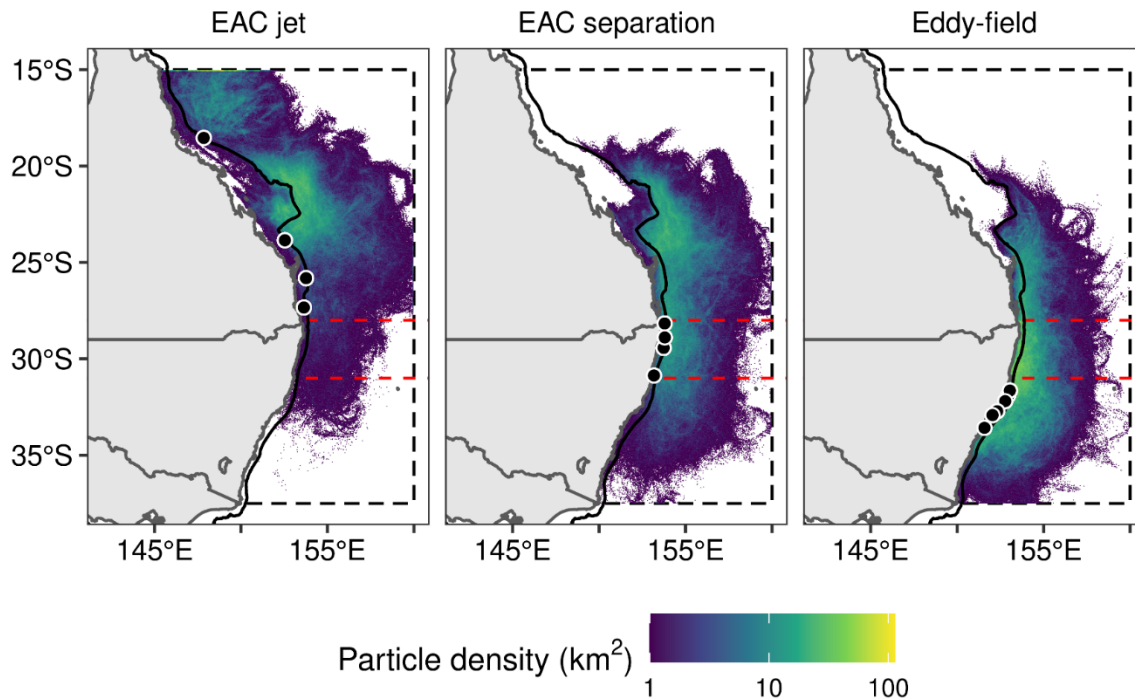


**Figure 60** Geographic distribution of Giant Mud Crab particles ( $\text{km}^2$ ) tracked backwards-in-time from estuaries north of the EAC separation (north of  $28^\circ\text{S}$ ), within the EAC separation ( $\sim 28\text{--}31^\circ\text{S}$ ) or south of the EAC separation (south of  $31^\circ\text{S}$ ) when they reached their degree-days threshold ( $535 \pm 32$ ). The dashed red lines represent the approximate EAC separation (as simulated in ozROMS) and the dashed black lines represent the reduced model domain used in our simulations. The solid black line represents the 200 m isobath, all particles offshore of this are excluded from our analysis. Note counts are derived from the entire simulation period (2008–2017) and the  $\log_{10}$ -transformed colour scale.

## Discussion

The simulations presented above illustrate how the larval dispersal phase facilitates broad-scale connectivity among estuarine crab populations in south-eastern Australia, via the EAC. These patterns are consistent with the genetic structure of populations in the region (Chaplin *et al.* 2001; Gopurenko and Hughes 2002). We demonstrate an overall north-to-south source-sink metapopulation structure (Kritzer and Sale 2004) and show divergent patterns in inter-jurisdictional connectivity between species. Estimates such as these are important for informing the assessment and management of exploited populations (Kritzer and Sale 2004; Punt *et al.* 2016; Cadrin 2020), especially in the context of increasing oceanographic variability under probable climate change scenarios (Cetina-Heredia *et al.* 2015; Coleman *et al.* 2017).

### Patterns in larval dispersal and connectivity

Our simulations demonstrate an overall north-to-south source-sink structure for Blue Swimmer Crab and Giant Mud Crab in eastern Australia, that exhibits a high degree of inter-estuarine connectivity. Broad-scale connectivity is a common feature of exploited estuarine and coastal species inhabiting the EAC, including crustaceans (Everett *et al.* 2017; Cetina-Heredia *et al.* 2019) and fish (Roughan *et*

*al.* 2011; Schilling *et al.* 2020). There appears to be additional structuring in recruitment dynamics dependent on the location of individual estuaries in relation to oceanographic features of the EAC. Estuaries within the EAC jet and EAC separation receive almost all larvae via broad-scale dispersal from the north, consistent with the coherent southward flow in this region (Oke *et al.* 2019b). However, non-trivial contributions from the south are possible for some estuaries towards the south of the EAC separation (e.g., Macleay River, Camden Haven, Manning River, Wallis Lake), indicative of discontinuous flow and eddying in this region (Cetina-Heredia *et al.* 2014; Li *et al.* 2021). While self-recruitment appears to be the primary source of larvae for estuaries further south within the eddy-field, contributions from distant spawning locations are also possible.

Oceanographic discontinuities can limit larval exchange between adjacent regions (Torrado *et al.* 2021), and it appears that the EAC separation may act as a barrier to connectivity for both Blue Swimmer Crab and Giant Mud Crab. There was minimal exchange of particles between the eddy-field region and putative spawning locations to the north of the EAC separation region. We suggest this region could represent a recruitment barrier, with minimal larval exchange between waters north and south. This may be due to increased eddying in this region (Cetina-Heredia *et al.* 2014), leading to the entrainment and advection of larvae offshore (Mullaney *et al.* 2014; Everett *et al.* 2015). However, eddies may also act as nurseries for coastally-spawned larvae of certain species (Garcia *et al.* 2022) and facilitate cross-shelf transport (Malan *et al.* 2020) which may enhance settlement rates for species with longer PLDs (e.g., Eastern Rock Lobster, *Sagmariasus verreauxi* [Milne-Edwards]; Cetina-Heredia *et al.* 2019). This may explain why Giant Mud Crab exhibit some connectivity across the EAC separation region when they have a 30 % longer PLD. For both species, this discontinuity in larval exchange reduces inter-jurisdictional connectivity, almost entirely for Blue Swimmer Crab, and possibly contributing to some degree of demographic isolation of estuaries within southeast Australia (i.e., the eddy-field region) from spawning in Queensland.

The patterns in connectivity resolved here align with the continuous genetic structure of Blue Swimmer Crab and Giant Mud Crab in eastern Australia (Chaplin *et al.* 2001; Gopurenko and Hughes 2002). Genetic homogeneity at this scale can be maintained by the transfer of relatively few individuals (Cowen *et al.* 2007), and it is likely that genetic panmixia is facilitated by a 'stepping-stone' effect (Chaplin *et al.* 2001), whereby recruitment between the southern- and northernmost estuaries occurs over multiple years or generations (Everett *et al.* 2017). Mixing between estuarine populations may be further enhanced by the migratory behaviours of adults. For example, in southeastern Australia, mature female Giant Mud Crab emigrate from estuaries and continue in a northern direction (~30–150 km) to spawn in oceanic waters (Hewitt *et al.* 2022a). This may also introduce a degree of self-recruitment in estuaries that source larvae from the north (e.g., Tweed River). Movements of mature Blue Swimmer Crab outside estuaries is unknown, but northerly migrations are well documented for a range of other estuarine species in eastern Australia (Gray and Barnes 2015; Brodie *et al.* 2018b; Taylor and Johnson 2021), and even species that exhibit limited migratory movements (e.g., Yellowfin Bream, *Acanthopagrus australis* [Günther]) maintain panmictic genetic structure via larval dispersal in the EAC (Roberts and Ayre 2010).

## Implications for management

Our results point to different patterns in inter-jurisdictional connectivity for Blue Swimmer Crab and Giant Mud Crab along eastern Australia. Estuarine populations of Blue Swimmer Crab in Queensland and NSW appear to constitute demographically separate stocks, supporting the current assessment and management at the state level (Johnston *et al.* 2021a). Conversely, Giant Mud Crab maintains a relatively high level of inter-jurisdictional connectivity, predominantly between Queensland and northern NSW (i.e., within the EAC separation) whereas connectivity patterns suggest that estuaries

within the south of the state (i.e., within the eddy-field) may be demographically isolated from the rest of the stock.

In general, estuaries within the EAC separation support higher and more stable catch rates of Giant Mud Crab than those in the south (i.e., within the eddy-field; Meynecke *et al.* 2012b). Some of this variation is likely due to environmental variability (e.g., temperature), which can alter catchability of the species (Williams and Hill 1982; Meynecke *et al.* 2012b). However, the differential patterns in connectivity coupled with the male-only harvest policy implemented in Queensland (Saunders *et al.* 2021) may also play a role. This protection likely provides a degree of stability in spawning biomass, which may support higher levels of recruitment (Cury *et al.* 2014; Kell *et al.* 2016) for estuaries that are well connected to spawning in Queensland waters. Conversely, estuaries in southern NSW that source the majority of their larvae from within NSW, where only ovigerous females are protected, may occasionally become recruitment-limited by a combination of high fishing mortality (i.e., excess removal of mature females; Myers *et al.* 1994) and other factors affecting recruitment (e.g., high larval mortality). However, male-only harvest policies are not guaranteed to ensure adequate recruitment (Hines *et al.* 2003; Carver *et al.* 2005) and the drivers of catch rate variability in NSW require further investigation. Management of Giant Mud Crab in NSW would benefit most from further research into the size-at-maturity to ensure that the current minimum legal size (85 mm carapace length) is providing adequate protection to the reproductively mature component of populations in the state.

In recent decades, mesoscale oceanographic variability has increased across the globe (Martínez-Moreno *et al.* 2021) and climate change is forcing accelerated warming and intensification of western boundary currents (Wu *et al.* 2012). These effects are evident in the EAC, which is considered a climate change ‘hotspot’ (Hobday and Pecl 2014); exhibiting non-uniform and accelerated warming (Malan *et al.* 2021; Li *et al.* 2022b) and increased southern (poleward) penetration (Cetina-Heredia *et al.* 2014; Li *et al.* 2021). Increased warming has the potential to shorten PLD and thereby inhibit connectivity, but increased circulation could counteract this effect. Our results suggest that a southern shift of the EAC separation, induced by increased poleward penetration, (Cetina-Heredia *et al.* 2014; Li *et al.* 2021), may enhance connectivity between some NSW estuaries (e.g., Camden Haven, Manning River, Wallis Lake) and spawning in Queensland. In a simulation of future climate scenarios, Cetina-Heredia *et al.* (2015) showed a 300 km poleward shift in the peak settlement location of Eastern Rock Lobster larvae along eastern Australia. Populations of both Blue Swimmer Crab and Giant Mud Crab already exist further south than modelled here, however they do not generally support notable commercial or recreational harvest. Increased poleward penetration may lead to an increase in abundance in southern NSW and induce a southern extension of each species distribution (Pecl *et al.* 2017; Gervais *et al.* 2021).

## Model limitations and future research

In this section, we focus on the assumptions and limitations as they relate to the biological parameterization of our simulations. A summary and discussion of the underlying oceanographic model used to advect particles, which includes model validation (Wijeratne *et al.* 2018) and an independent comparison with local observations, is contained in Hewitt *et al.* (2022b).

Incorporating larval swimming abilities can improve the accuracy and realism of particle tracking simulations (Leis 2021). Unfortunately, no such information exists for either species, so the larvae were modelled as ‘passive’ particles. Implicit in releasing particles adjacent to the mouth of known settlement estuaries (at the 100 m isobath), is the assumption that settlement is possible from within this range, probably facilitated via a combination of chemoreception and selective tidal-stream transport (Roughan *et al.* 2005; Tilburg *et al.* 2009; Webley *et al.* 2009), providing a crude proxy for

swimming ability at the settlement stage. Furthermore, our simulations were limited to the surface layer, however this is unlikely to alter the patterns in connectivity described here, since portunid larvae are typically concentrated near the surface (Bryars and Havenhand 2004; Tilburg *et al.* 2008) and circulation at the surface is generally representative of the upper 200 m (Everett *et al.* 2017).

In our simulations, we assume spawning is constant both throughout the spawning season (austral spring–autumn; September to May; Heasman *et al.* 1985; Johnson *et al.* 2010; Nolan *et al.* 2022) and interannually. However, both species exhibit clear temporal peaks in reproductive activity (e.g., mating, fecundity) within a spawning season (Heasman *et al.* 1985; Johnson *et al.* 2010; Nolan *et al.* 2022), the timing of which may be seasonal or related to other environmental cues (e.g., heavy rainfall; Hewitt *et al.* 2022a). Furthermore, Blue Swimmer Crab are likely to primarily spawn in estuaries (Johnson *et al.* 2010; Nolan *et al.* 2022), with ocean spawning dominant during wetter years (Potter *et al.* 1983; Gillson *et al.* 2012). Future research would benefit from a more finely resolved model of the spatial (i.e., estuarine vs. oceanic) and temporal dynamics of larval production (e.g., spawning, fecundity) informed through targeted fishery-independent surveys.

# Environmental influence on spawning migrations in Giant Mud Crab

## Background and rationale

The timing and intensity of environmental triggers can alter the timing of spawning (e.g., Rogers and Dougherty 2019; Slesinger *et al.* 2021), which may have significant implications for recruitment and fisheries productivity (Schilling *et al.* 2020). Mismatches between triggers for migration and optimal conditions for egg and larval development can result in poor (or failed) recruitment (e.g., Pankhurst and Munday 2011; Asch *et al.* 2019), and unfavorable advection can arise if spawning occurs at inappropriate locations creating recruitment limitations. Therefore, the timing and magnitude of triggers for spawning migrations can be a substantial cause of recruitment variability. This is particularly so for biphasic species in southeastern Australia, where the East Australian Current and associated mesoscale variability drive variable dispersal this region. Species with an oceanic dispersive phase in this region may experience recruitment limitation in estuarine nurseries if spawning migrations don't align with optimal dispersal currents. Consequently, the drivers of spawning migrations are important to study alongside the dispersive patterns dealt with in *Oceanic connectivity and particle dispersal for Blue Swimmer Crab and Giant Mud Crab*, if the influence of environmental variability on stock biomass is to be fully understood.

As described earlier, Giant Mud Crab in southeastern Australia display highly variable catches (Meynecke *et al.* 2012b), which is thought to occur as a result of both changes in catchability (Hill *et al.* 1982; Williams and Hill 1982), and environmental variability during early life history (Robins *et al.* 2005; Meynecke *et al.* 2012b). The Giant Mud Crab is short-lived and fast-growing, with a biphasic life cycle whereby larvae disperse in ocean currents (Alberts-Hubatsch *et al.* 2016) before settlement in the inshore region as megalopae and subsequent recruitment to estuaries (as crablets; Webley *et al.* 2009), where they inhabit sub- and intertidal habitats (e.g., seagrass, mangroves, mudflats; Hill *et al.* 1982; Hyland *et al.* 1984). Females mature rapidly, mate from mid-spring–early-autumn, and are then thought to undertake a terminal migration to spawn in oceanic waters. This is based on the absence of ovigerous (egg-bearing) females in estuarine waters (Hill *et al.* 1982; Hyland *et al.* 1984) and incidental catches in offshore prawn trawls (Hill 1994). Very little is known about what happens once pre-mated females emigrate, but it is hypothesized that some northward coastal migration occurs, followed by the use of stored spermatophore to fertilise eggs, which are subsequently released into the ocean currents. The timing and triggers of the seaward migration out of estuaries are unresolved (Alberts-Hubatsch *et al.* 2016), but they are likely to be important in determining the timing and location of spawning, and by extension, recruitment.

Acoustic telemetry has been broadly applied to fisheries research (Hussey *et al.* 2015; Taylor *et al.* 2017a), and is a powerful tool for quantifying environmental drivers of marine animal movement (Payne *et al.* 2014), at high-resolution, over broad spatial scales (Brodie *et al.* 2018a). Here, we applied this technique to identify environmental conditions that triggered female Giant Mud Crab spawning migrations within southeastern Australian estuaries. Specifically, this was achieved by 1) tracking the movement of mature females tagged with acoustic tags during the spawning season; and 2) recreating the most likely trajectories of tracked crabs between consecutive detections (Niella *et al.* 2020) within study estuaries, and extracting movement variables (i.e., presence/absence of migration) to model against high-resolution environmental data.

## Methods

### Study systems

This study was conducted in the Clarence River (~29.4°S) and Bellinger-Kalang River system (~30.5°S, hereafter referred to as Kalang River), two estuaries supporting important Giant Mud Crab fisheries on the NSW north coast (Figure 61). Both systems are mature wave-dominated barrier estuaries (Roy *et al.* 2001) and have permanently open entrances with a pronounced salinity gradient from their mouths to the upper reaches. Seasonal recreational fishing for Giant Mud Crab takes place in both estuaries from November–May, with the Kalang River closed to all commercial harvest since 2002. The commercial harvest of Giant Mud Crab in the Clarence River is significant (Meynecke *et al.* 2012b).

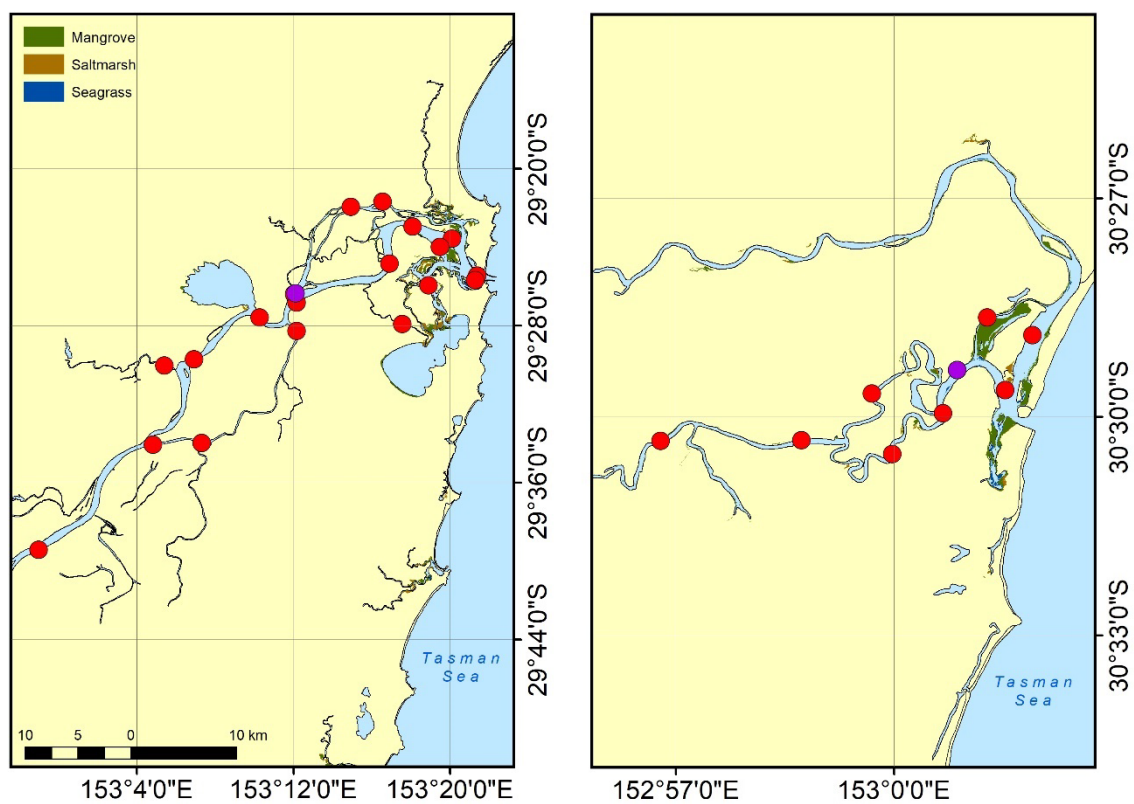


**Figure 61** Map of Clarence River (left panel) and Kalang River (right panel) showing linear array of receivers (red circles) and water quality loggers (purple circles).

### Crab capture and tagging

Giant Mud Crab were tagged during the austral summer–autumn (November–June) in 2018/19 and 2020/21 (Table 15). Crabs were captured using collapsible mesh traps (0.9-m diameter x 0.27-m high), with 55-mm mesh and two (0.25 x 0.05-m) semi-closed funnel entrances. Captured crabs were inspected to identify sex and all males were immediately released. Females were cooled for 10–20 s in an ice/sea-water slurry, and carapace length (CL; nearest mm) and moult-stage were then recorded (Hay *et al.* 2005). The size at maturity for Giant Mud Crab in NSW is unknown, however

Heasman (1980) reports the size at 50 % maturity for female Giant Mud Crab in the nearby Moreton Bay (~27.1°S; Queensland) as 147-mm carapace width (CW). This corresponds to ~100-mm CL on the basis of the following linear relationship:

$$CL = 0.68 \times CW - 1.51$$

derived from morphometric data ( $R^2 = 0.97$ ) collected from 260 female Giant Mud Crab in the nearby Red Rock River (~30.0°S; NSW; P.A. Butcher, unpublished data). Therefore, only crabs that were likely to be mature (i.e., > 100-mm CL), and recently moulted were tagged (i.e., post- or inter-moult; Hay *et al.* 2005), to limit the probability of tag loss during ecdysis. The capture of mature male and female crabs together suggests that these females may have recently mated and would therefore be prepared for a spawning migration. Innovasea V9-2x acoustic tags (24-mm length; 9-mm diameter; wet weight: 2-g; Innovasea, Nova Scotia, Canada; hereafter referred to as 'tags') were affixed to the posterior carapace using instant adhesive (Loctite 406, Henkel Adhesives, Australia) which has shown tag retention of at least 3 months in lab experiments (M.D. Taylor, unpublished data). After tagging, crabs were submerged alongside the research vessel and once normal activity (e.g., attempted swimming) had resumed crabs were released at their capture locations (generally in 2–5 m of water). In general, negative impacts (e.g., stress, limb loss) are low for crabs handled and released in this manner (Butcher *et al.* 2012) and previous tagging studies have not recorded any notable impacts on normal behaviour (e.g., Hill 1978).

**Table 15** Tagging and detection information for female Giant Mud Crab in Clarence River and Kalang River

| Estuary        | Period       | <i>n</i> | Mean CL (mm; ± SD) <sup>a</sup> | Detect <sup>b</sup> | Migrate <sup>b</sup> | Duration (d ± SD) <sup>c</sup> | Migration duration (d ± SD) <sup>d</sup> | Distance (km ± SD) | Max. speed (m s <sup>-1</sup> ) <sup>e</sup> |
|----------------|--------------|----------|---------------------------------|---------------------|----------------------|--------------------------------|--|--------------------|--|
| Clarence River | Feb–May 2019 | 42       | 109.5 (± 6.1)                   | 30 (71 %)           | 21 (50 %)            | 23.6 (16.9)                    | 9.6 (5.6)                                | 25.9 (6.6)         | 1.9  |
|                | Nov–Dec 2020 | 10       | 107.8 (± 4.4)                   | 9 (90 %)            | 5 (50 %)             | 10.7 (7.1)                     | 4.0 (2.4)                                | 26.6 (6.8)         | 1.3  |
| Kalang River   | Feb–Jun 2019 | 18       | 107.5 (± 4.9)                   | 17 (94 %)           | 13 (72 %)            | 12.2 (16.2)                    | 6.5 (8.3)                                | 4.8 (1.3)          | 0.3  |
|                | Jan–Apr 2020 | 19       | 110.6 (± 8.0)                   | 17 (89 %)           | 8 (42 %)             | 12.4 (11.0)                    | 6.6 (8.6)                                | 5.96 (2.2)         | 0.5  |

<sup>a</sup> CL: carapace length.

<sup>b</sup> Number of fish detected (Detect) and migrated (Migrate) from the estuary, with values in brackets denote percentage of all tagged crabs.

<sup>c</sup> Mean tracking duration—values derived only from crabs that migrated (i.e., detected at mouth of estuary).

<sup>d</sup> Mean time (d) between first downstream movement (i.e., onset of migration) and detection at mouth of estuary.

<sup>e</sup> Since our analysis assumes constant movement between detections values represent minimum average speed.

## Tag programming and array design

Tags were programmed to emit a unique signal (69 kHz), at a high-power output (151 dB re 1 µPa at 1 m), at randomly spaced intervals of 90–150 s. Random signal transmission times were employed to minimize potential signal overlap which can block detection and to conserve battery life (estimated 346 d at these settings). Linear arrays of Innovasea VR2W acoustic receivers (69 kHz) were deployed

along all main arms, and downstream of every confluence, of the Clarence River ( $n = 19$ ) and Kalang River ( $n = 9$ ), respectively. Receivers were fixed to existing infrastructure or independent moorings via a weighted float and anchor system. Detection ranges for the receivers in similar estuaries was estimated to be 280–420 m, with a missed detection probability of 0.4–2.7% (e.g., Walsh *et al.* 2012). In both estuaries, these detection ranges intersected with either the shoreline, or overlapped with the range of a neighboring receiver in wider parts of the estuary (except for the receiver furthest from the mouth in the Clarence River; Figure 61), forming a series of ‘gates’, to minimize the chance that a crab could migrate without being detected. In addition, HOBO U24-002-C conductivity/salinity loggers (hereafter referred to as ‘loggers’; Onset Computer Corporation, Massachusetts, USA) were deployed in the Clarence River and Kalang River ( $n = 3$ ), which recorded temperature ( $^{\circ}\text{C}$ ) and conductivity ( $\text{mS cm}^{-1}$ ) at hourly intervals.

## Data collection and storage

Receivers were downloaded every 3–8 months using VUE software (v. 2.6.2; Innovasea, Amirix, Nova Scotia, Canada) and detections were subsequently uploaded to the Integrated Marine Observing System Animal Tracking Facility (IMOS ATF, <https://animaltracking.aodn.org.au>; Taylor *et al.* 2017a). In addition to detections from each array, the IMOS ATF and NSW DPI Shark Management Strategy acoustic array (Spaet *et al.* 2020, b) were interrogated for oceanic (i.e., post-estuarine) detections. Loggers were downloaded using a Universal Optic USB Base Station (and coupler) and HOBOWare Pro (v. 3.7.21; Onset Computer Corporation, Massachusetts, USA). Start- and end-point calibrations were applied to conductivity data, to account for any ‘data drift’, by taking conductivity measurements at the approximate depth of the logger upon download using a Horiba U-52 MultiParameter Water Quality Meter (Instrument Choice, Syntronics Pty Ltd., South Australia). Finally, to quantify potential recaptures and encourage the release of tagged crabs, signage was posted at commonly used boat ramps in each estuary, which included project details and a dedicated recapture hotline.

## Data analysis

All statistical analyses were conducted in R (v. 4.0.2) language for statistical computing (R Core Team 2022), with general data-wrangling carried out using the suite of functions/packages provided by ‘tidyverse’ (Wickham *et al.* 2019). Detection data were preprocessed using the ‘explore’ function in the R package ‘actel’ (Flávio and Baktoft 2021) to evaluate, and remove, potentially spurious detections (e.g., using criteria such as individuals ‘skipping’ receivers, implausible swimming speeds, etc.). Whenever consecutive detections implied movement speeds greater than the maximum recorded for Giant Mud Crab (i.e.,  $> 0.56 \text{ m s}^{-1}$ ; Alberts-Hubatsch 2015), we further inspected detections based on considerations of array design (e.g., proximity of neighboring receivers, detection range) and river flow. Initially, this prompted several warnings of swim speeds  $\gg 0.56 \text{ m s}^{-1}$ . In both estuaries the receivers recording these detections were likely to have overlapping detection ranges, and to be in areas with high flow velocities (e.g., Reinfelds *et al.* 2004). As such, detections from one of each of these pairs of receivers were excluded from further analysis. Subsequent analysis indicated maximum swim speeds of up to  $1.9 \text{ m s}^{-1}$  in the Clarence River (Table 15). While these exceed the maximum recorded movement speed for this species (Alberts-Hubatsch 2015), these detections were retained as some uncertainty remains regarding their true maximum movement speed, particularly when riding high tidal flows in a large estuary. No individuals were flagged as skipping receivers during preprocessing.

Retained detections were used to interpolate locations of crabs using the R package ‘RSP’ (‘Refined Shortest Paths’; Niella *et al.* 2020). RSP uses a least-cost path analysis to interpolate in-water

locations of tagged animals between consecutive detections, at a user-specified spatial interval. This ensures that animal trajectories are realistic in systems with complex geomorphology (e.g., rivers, estuaries; Niella *et al.* 2020). We interpolated continuous trajectories for crabs at 100-m intervals. This relatively short interpolation interval was to ensure that crab trajectories adhered to the winding arms of both rivers. Since we were interested in the triggers of migration, we reduced our data to include only crabs that ‘successfully’ migrated to sea ( $n = 47$ ), indicated by detection at the mouth of the estuary. In the Clarence River, we consider detection at any one of four receivers near the mouth as successful migration (Figure 61), due to high vessel activity and the presence of some seagrass habitats (Taylor *et al.* 2018a) which can decrease detection probability (Swadling *et al.* 2020). Similarly, we considered detections at the mouth of either the Kalang River or Bellinger River as representative of successful migration (Figure 61). Paths were only interpolated between estuarine detections, and therefore did not include any oceanic detections.

We considered the first day where a crab exhibited overall downstream movement to be a standardized measure of the onset of migration. This was determined by comparing the daily distance to the mouth (km) for each crab, with spatial calculations performed using the R package ‘raster’. To model the effects of environmental variation on triggering these movements (i.e., non-migrating/migrating) we used a generalized additive mixed model (GAMM or hierarchical GAM sensu Pedersen *et al.* 2019) using the R package ‘mgcv’ (‘Mixed GAM Computation Vehicle’; Wood 2011). Within this framework, we estimated smooth functional relationships (‘smooths’) between the proportion of crabs beginning migration on a given day and environmental covariates, assuming a binomial error distribution (with a logit link function; Douma and Weedon 2019) via restricted maximum likelihood (REML). We modelled mean daily temperature ( $^{\circ}\text{C}$ ) and conductivity ( $\text{mS cm}^{-1}$ ; which we used as a proxy for freshwater inflow/rainfall), and the difference between these and a 3-d rolling mean (referred to as  $\Delta$ temperature and  $\Delta$ conductivity, respectively), as thin plate regression splines. We also included lunar phase as a candidate variable, measured in radians (rad) where  $0 =$  new moon and  $\pi =$  full moon, calculated using the R package ‘lunar’ as a cyclic cubic spline. These splines are the sum of  $k$  simpler basis functions (i.e., ‘basis dimension’), where the size of  $k$  determines the maximum complexity (i.e., flexibility or ‘wiggleness’) of the smooth. Default basis dimensions ( $k = 10$ ) were used for all smooths, and checked by computing the  $k$ -index for each smooth to ensure sufficient flexibility (see Wood and Fasiolo 2017), which did not indicate any issues. Overfitting was avoided by multiplying the complexity of a smooth by an estimated smoothing penalty ( $\lambda$ ) and subtracting it from the model log-likelihood (Pedersen *et al.* 2019). We implemented variable selection within our modelling framework via the double-penalty approach (Marra and Wood 2011). This approach estimates a second penalty ( $\lambda^*$ ) that applies to flat (i.e., linear) smooths, and can allow their removal from the model if warranted (Marra and Wood 2011). To implement a mixed effects structure, we modelled year of tagging as a random effect using a factor-smooth interaction (Pedersen *et al.* 2019). This allowed us to estimate a ‘global’ smooth and group-level smooths for all environmental covariates, thus permitting intergroup variation in the response (highly analogous to a GLMM with varying slopes; Pedersen *et al.* 2019). Model selection was conducted by applying this overall approach to two additional models that included different lengths for the rolling means of temperature and conductivity (i.e., one day and one week). All models were then compared via Akaike Information Criteria (AIC), where the model with lowest AIC was retained as the ‘true’ model (Burnham and Anderson 2002a). Since these two additional models had  $\Delta\text{AIC} \sim 5$ , and the quantitative results did not differ substantially, they were not considered further. We used ‘gratia’, ‘DHARMA’ (Hartig 2020) and ‘ggplot2’ to visually assess model assumptions, and plot back-transformed (via the inverse-logit function) probabilities of triggering the spawning migration. Finally, we described our results using the language of statistical evidence (rather than ‘significance’, as suggested by Muff *et al.* 2022), and report the results in accordance with the suggestions in Smith (2020).

## Results

In total, 89 crabs were tagged in the Clarence River ( $n = 52$ ) and Kalang River ( $n = 37$ ), across two austral summers (2018/19 and 2020/21) in each estuary, with mean ( $\pm$  SD) CL ranging from 107.4 ( $\pm$  4.9)–110.6 ( $\pm$  8.0) mm (Table 15). Of these crabs, 82 % ( $n = 73$ ) were detected at least once, and 53 % ( $n = 47$ ) were detected at the mouth of the estuary, indicating migration (Table 15). The remaining crabs were either not detected (19 %;  $n = 17$ ) or were only detected over part of the estuary (29 %;  $n = 26$ ; including two reported recaptures). Those that were detected over part of the estuary all exhibited some downstream movement (1–2 km), however we could not determine their fate and these crabs were not included in our analysis. Across estuaries and years, temporal patterns in the spawning migration were similar. Generally, crabs exhibited a protracted resident phase ( $\sim$ 7–14 d), being detected on a receiver near their release location (although some were only detected during migration, likely because they resided away from a receiver), followed by a rapid migration downstream (Figure 62). On average, crabs were tracked for 10.7–23.6 d, however mean migration times (i.e., the time between their first downstream movement and detection at the mouth) were much shorter, ranging from 4.0–9.6 d covering mean distances of 4.8–26.6 km, facilitated by maximum migration speeds of 0.3–1.9 m s<sup>-1</sup> (Table 15).

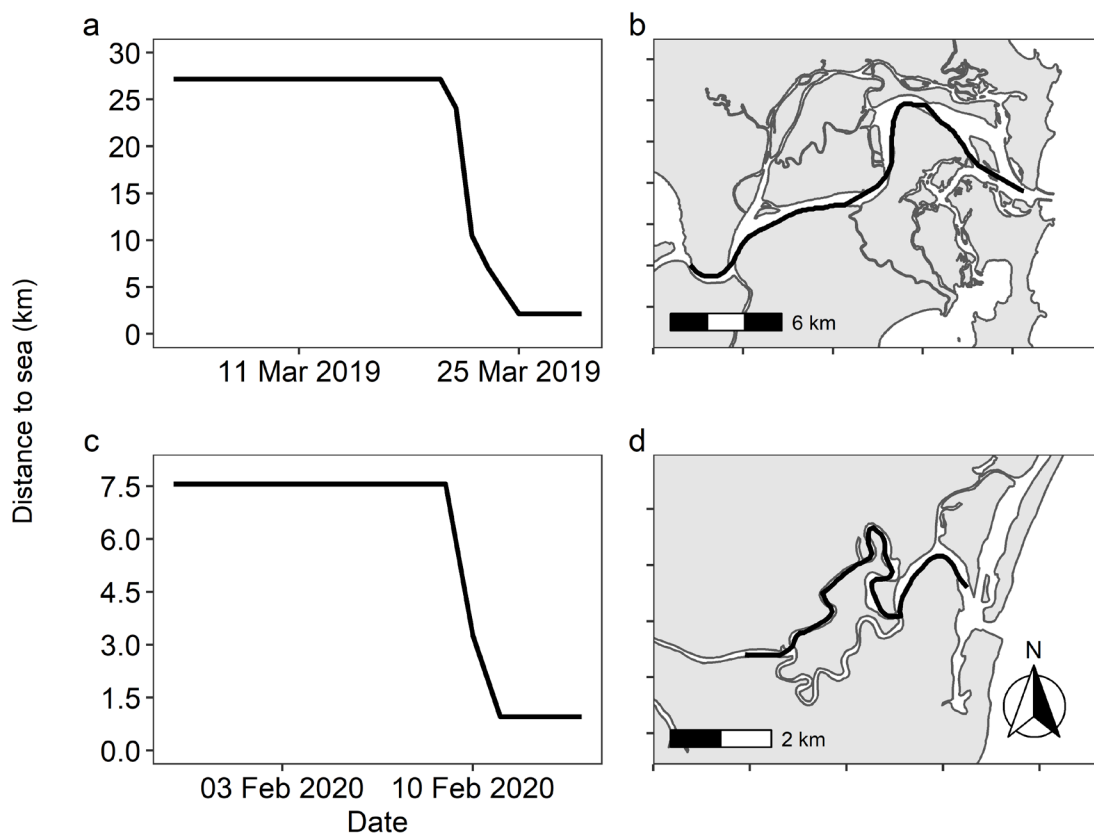


**Figure 62** Example of interpolated female Giant Mud Crab tracks during spawning migration, showing daily distance to sea (km) and path for Clarence River (a and b) and Kalang River (c and d). Note differing x- and y-axis scales in (a) and (c) owing to different estuary lengths and tracking periods.

Visual inspection of the interpolated tracks shows that once a crab began its migration this generally continued rapidly to the mouth of the estuary, which supported our use of the first day moving downstream as a standardized measure of the onset of migration. In both estuaries, a decline in mean daily water temperatures, following the seasonal peak, appeared to precede migration in 2019 (Figure 63), while a strong migratory response to declines in conductivity was evident in 2020 (Figure 63). These observations were supported by the GAMM, which explained 47.1 % of the deviance in the proportion of crabs beginning migration on a given day. Variable selection removed smooths for mean daily conductivity,  $\Delta$ -temperature, and all group-level smooths (estimated degrees of freedom < 1) indicating similar responses across years. We found strong evidence that cooler mean daily temperatures in the summer (i.e., < 22 °C), resulted in the highest probability of triggering migration, which declined with increases in temperature up to ~27 °C (Figure 64; e.d.f. = 1.78,  $\chi^2 = 11.38$ ,  $P < 0.01$ ,  $n = 245$ ). We also found strong evidence that intermediate to large declines in conductivity ( $\Delta$ -conductivity < -10 mS cm<sup>-1</sup>) resulted in very high migration probabilities, but with some uncertainty at the extremes of the covariate range (Figure 64; e.d.f. = 2.23,  $\chi^2 = 19.59$ ,  $P < 0.01$ ,  $n = 245$ ). Finally, we found strong evidence that the lunar phase had a cyclic effect on the probability of triggering the spawning migration, with the highest probabilities coinciding with the new (rad = 0) and full moon (rad =  $\pi$ ; Figure 64; e.d.f. = 5.18,  $\chi^2 = 26.41$ ,  $P < 0.01$ ,  $n = 245$ ).

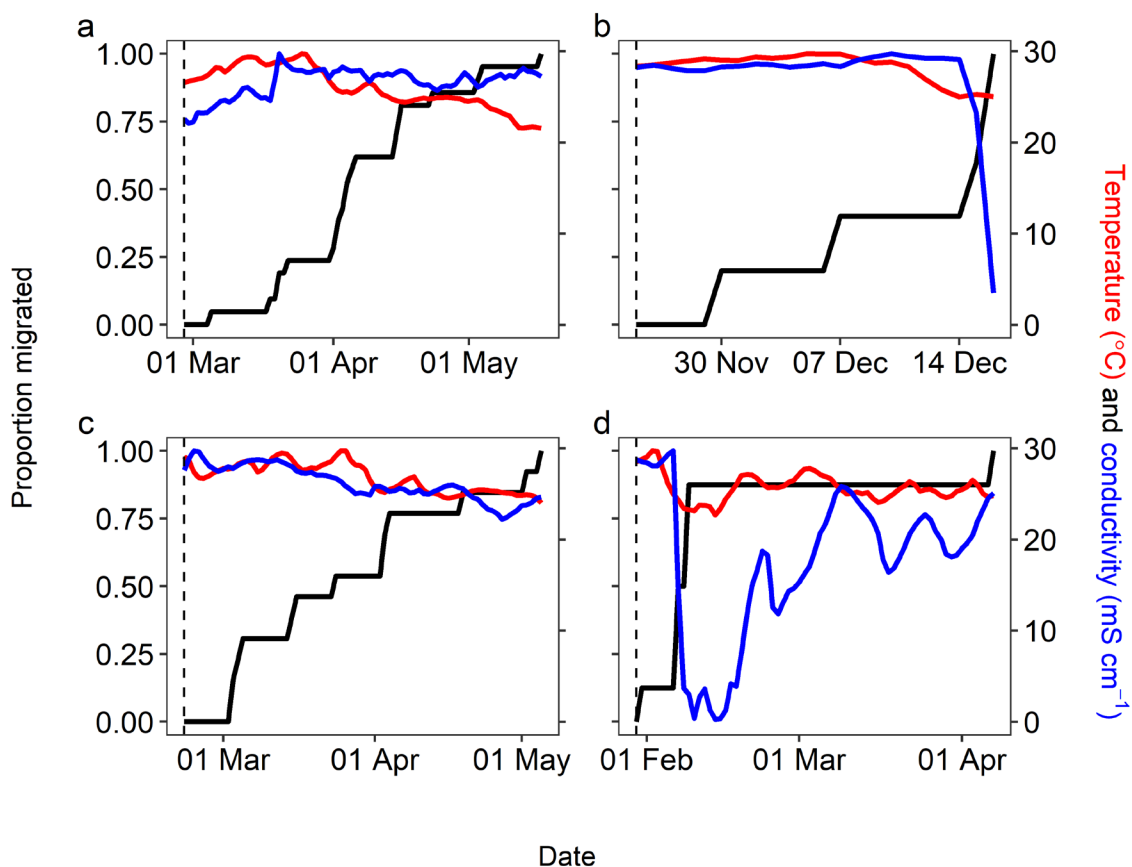


**Figure 63** Cumulative migration curve (solid black line) illustrating proportion of female Giant Mud Crab commencing spawning migration throughout the tracking period for each year (2018/19 and 2020/21) in Clarence River (a and b) and Kalang River (c and d). Red and blue lines indicate mean daily temperature (°C) and conductivity (mS cm<sup>-1</sup>), respectively. Vertical dashed line indicates date of tagging. Note variable scales on x-axis as tagging was undertaken at different times in each estuary/year.

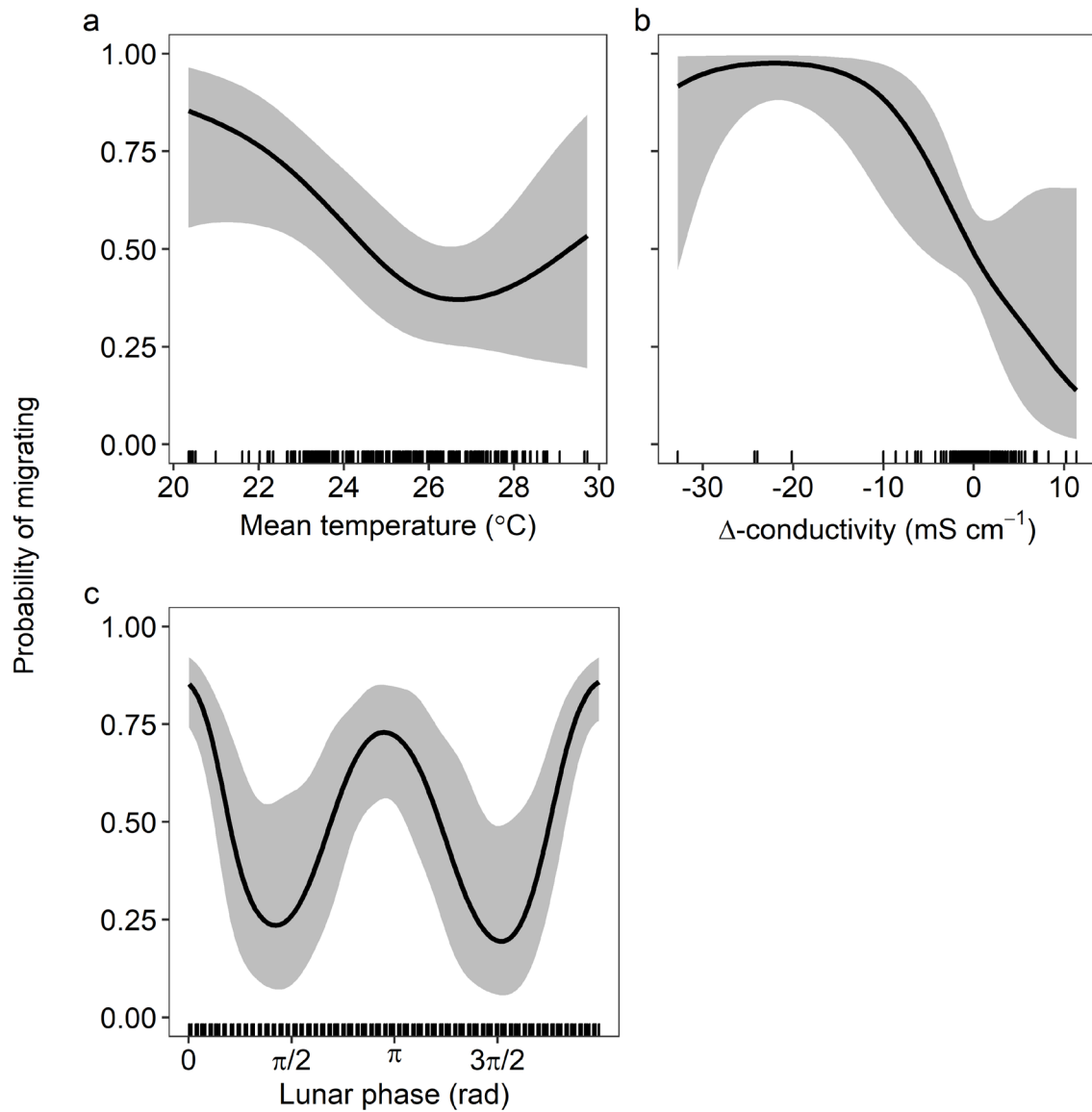


**Figure 64** Smooth estimated probabilities of triggering female Giant Mud Crab spawning migration for mean daily temperature (a; °C),  $\Delta$ -conductivity (b; mS cm<sup>-1</sup>) and lunar phase (c; rad). Shaded area indicates 95 % confidence intervals and rugs along x-axis indicate distribution of covariate values.

Oceanic detections indicated that once crabs had successfully migrated from estuaries, they continued their migration in a northern direction (Table 16, Figure 65). In total, 30 % ( $n = 14$ ) of the crabs that successfully migrated (i.e., were detected at the mouth) recorded oceanic detections, and all of these were to the north of their estuary of origin at distances of 23–69 km over periods ranging from 2–35 d. This suggested minimum average movement speeds between 1–19 km d<sup>-1</sup> once crabs were in the ocean (Table 16). No crabs were detected again within their estuary of tagging (or any other estuary) after being detected at the mouth or in the ocean.

**Table 16** Oceanic detection information for female Giant Mud Crab obtained from IMOS ATF and NSW DPI Shark management strategy acoustic array.

| Crab ID            | Tagging estuary | Receiver latitude | Receiver longitude | Last estuarine detection | First oceanic detection | Last oceanic detection | Duration (d) | Detections | Latitudinal distance (km) <sup>b</sup> | Migration speed (km d <sup>-1</sup> ) <sup>c</sup> |
|--------------------|-----------------|-------------------|--------------------|--------------------------|-------------------------|------------------------|--------------|------------|--|--|
| 12343              | Kalang          | -30.204           | 153.284            | Apr 5 2019               | Apr 10 2019             | Apr 10 2019            | 6            | 6          | 32.93                                  | 5.49   |
| 12350 <sup>a</sup> | River           | -30.212           | 153.207            | Apr 5 2019               | Apr 11 2019             | Apr 11 2019            | 6            | 11         | 32.13                                  | 5.36   |
|                    |                 | -29.878           | 153.435            |                          | Apr 13 2019             | Apr 13 2019            | 2            | 26         | 69.16                                  | 18.52  |
| 12357              |                 | -30.207           | 153.265            | Jun 3 2019               | Jun 5 2019              | Jun 5 2019             | 3            | 2          | 32.60                                  | 10.87  |
| 12359              |                 | -30.213           | 153.190            | Mar 6 2019               | Mar 9 2019              | Mar 9 2019             | 3            | 7          | 31.99                                  | 10.66  |
| 12360              |                 | -30.210           | 153.223            | Apr 21 2019              | Apr 24 2019             | Apr 24 2019            | 3            | 8          | 32.32                                  | 10.77  |
| 12361              |                 | -30.204           | 153.284            | Mar 17 2019              | Mar 23 2019             | Mar 23 2019            | 6            | 7          | 32.93                                  | 5.49   |
| 12362              |                 | -30.212           | 153.207            | Apr 5 2019               | Apr 9 2019              | Apr 9 2019             | 5            | 1          | 32.13                                  | 6.43   |
| 12364              |                 | -30.291           | 153.145            | May 5 2019               | Jun 9 2019              | Jun 23 2019            | 35           | 25         | 23.28                                  | 0.67   |
| 33396              |                 | -30.211           | 153.215            | Feb 13 2020              | Feb 23 2020             | Feb 23 2020            | 10           | 2          | 32.31                                  | 3.23   |
| 33399              |                 | -30.210           | 153.223            | Feb 10 2020              | Mar 8 2020              | Mar 8 2020             | 27           | 3          | 33.42                                  | 1.23   |
| 33400              |                 | -30.204           | 153.284            | Feb 7 2020               | Feb 27 2020             | Feb 27 2020            | 20           | 4          | 33.42                                  | 1.67   |
| 12348              | Clarence        | -28.907           | 153.687            | May 20 2019              | Jun 12 2019             | Jun 13 2019            | 23           | 26         | 57.76                                  | 2.51   |
| 33409              | River           | -28.837           | 153.610            | Dec 12 2020              | Dec 21 2020             | Dec 21 2020            | 10           | 1          | 65.54                                  | 6.55   |
| 33412              |                 | -29.109           | 153.440            | Dec 7 2020               | Jan 9 2021              | Jan 15 2021            | 33           | 4          | 35.36                                  | 1.07   |

<sup>a</sup> Duration, latitudinal distance and migration speed for second detection calculated between consecutive oceanic detections.

<sup>b</sup> North-south distance. Positive values indicate northward movement.

<sup>c</sup> Since our analysis assumes constant movement between detections values represent minimum average speed.

Note: Migration speed and latitudinal distance account only for movements after leaving the estuary

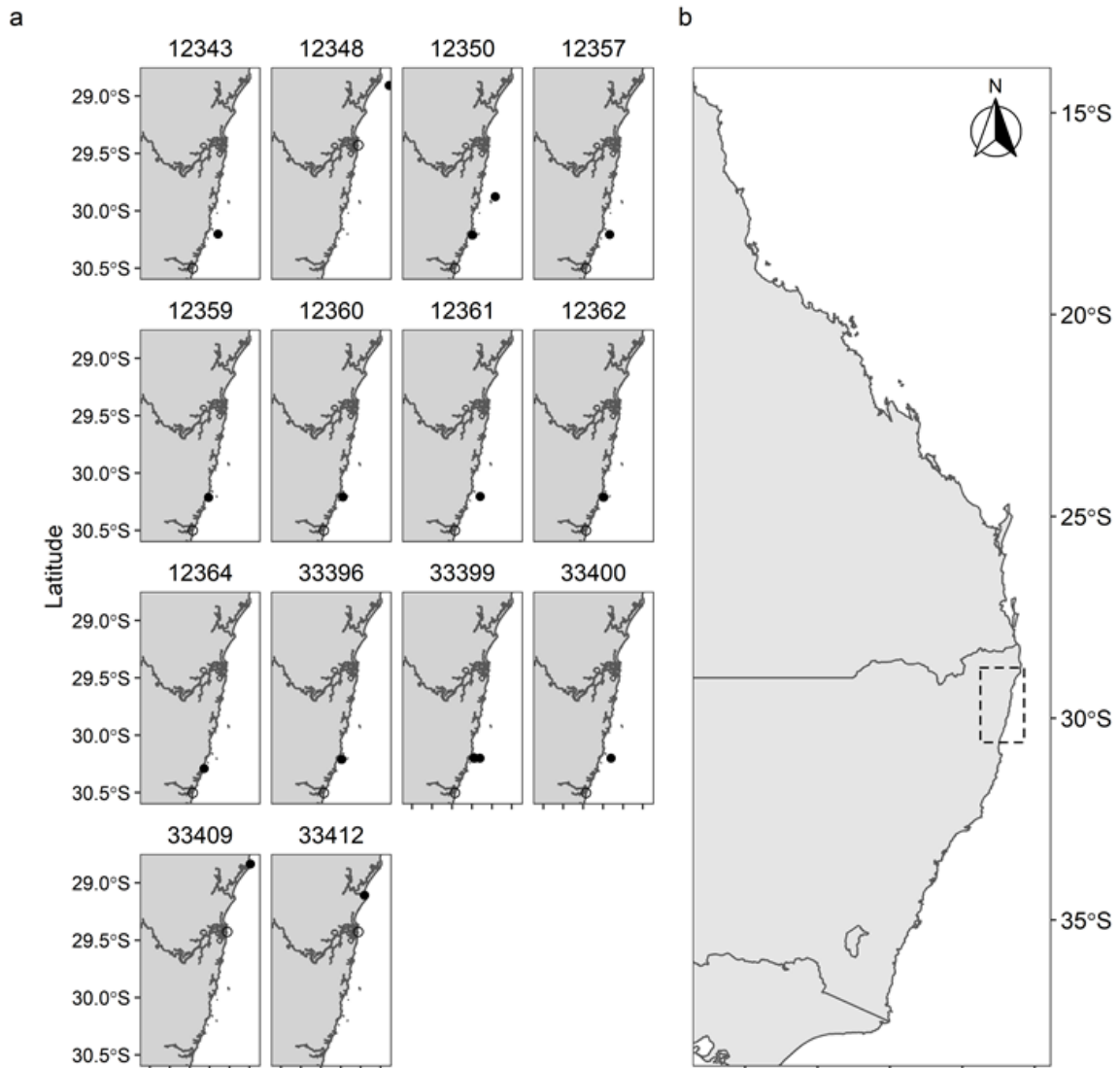


**Figure 65** Maps of oceanic detections of tagged female Giant Mud Crab (a) obtained from IMOS ATF and NSW DPI Shark Management strategy acoustic array and their relative position on the east Australian coast (b). Filled circles (●) indicate the location of receivers and empty circles (○) indicate the mouth of the estuary where the crab was tagged.

## Discussion

Our results provide evidence of environmental triggers for a downstream migration in female Giant Mud Crab within two subtropical southeast Australian estuaries. These patterns suggested that seasonal declines in temperature, and heavy rainfall events which rapidly decrease conductivity, were responsible for triggering the observed downstream migration in mature female crabs. Additionally, high estuarine flow and large tides associated with lunar phases (i.e., new and full moons) facilitated rapid migration downstream. These findings highlight mechanistic linkages between estuarine variability and an important life-history event of a highly valuable exploited species, the effects of which may influence later spawning, dispersal and recruitment processes, and

ultimately impact regional fisheries productivity (Loneragan and Bunn 1999; Robins *et al.* 2005; Meynecke *et al.* 2012b).

## Environmental triggers of the female spawning migration

Tagged female Giant Mud Crab exhibited a strong migratory response at low temperatures ( $< 22\text{ }^{\circ}\text{C}$ ), and when conductivity was rapidly declining. This migration enables spawning in coastal waters (Hill 1994) following seasonal peaks in mating activity during the austral spring–autumn (October–March; Heasman *et al.* 1985). As a predominantly estuarine species, adult Giant Mud Crab are eurythermal (Hill 1980) and euryhaline (Davenport and Wong 1987). However, like many crab species, larval growth and survival is enhanced under oceanic conditions, which include high salinities (25–30) and warm temperatures (26–30  $^{\circ}\text{C}$ ; Hamasaki 2003; Nurdiani and Zeng 2007; Baylon 2010). For Giant Mud Crab, the first larval stage does not survive at temperatures  $< 20\text{ }^{\circ}\text{C}$  or  $> 25\text{--}30\text{ }^{\circ}\text{C}$  (depending on region), or low salinities ( $< 15\text{--}17.5$ ; Hill 1974; Baylon 2010), and these conditions rarely occur inside estuaries for sustained periods. Since female Giant Mud Crab are capable of sperm storage (Brick 1974), it is likely that following mating within estuaries, the females adaptively select oceanic habitats for spawning which maximizes larval growth and survival (Ciannelli *et al.* 2015).

Ovigerous Giant Mud Crab typically suppress feeding (Heasman 1980), suggesting a ‘capital breeding’ strategy, whereby females rely on stored energy reserves during ovarian development (Griffen 2018; Nolan *et al.* 2022). If this is the case, behaviours that are energetically conservative or efficient are likely to be favored. Despite being eurythermal/euryhaline (Hill 1980; Davenport and Wong 1987), crabs are ectotherms, and physicochemical variation can still impose an energetic cost. For example, reductions in temperature can reduce metabolism (Junk *et al.* 2021), while osmoregulation is required at low salinities (Chen and Chia 1996). This may explain why rates of ovarian maturation are highest at warmer (oceanic) temperatures (25–26  $^{\circ}\text{C}$ ; Heasman and Fielder 1983). In closely related species, salinities outside optima can result in smaller oocytes (e.g., Orange Mud Crab, *S. olivacea*; Amin-Safwan *et al.* 2019) or limit ovarian lipid content (e.g., Chinese Mitten Crab, *Eriocheir sinensis*; Long *et al.* 2019), which can have implications for subsequent larval development (Alava *et al.* 2007). Therefore, downstream migration may maximize reproductive output if females avoid suboptimal and variable metabolic conditions in estuaries during ovarian development.

Tagged female Giant Mud Crab exhibited rapid downstream migration, covering distances of up to 40 km in less than a week and with minimum average swimming speeds exceeding previously recorded maximum swimming speeds for the species ( $0.56\text{ m s}^{-1}$ ; Alberts-Hubatsch 2015). This may have been facilitated by selective tidal-stream transport (Gibson *et al.* 2001), a behaviour whereby individuals leverage periods of high flow (e.g., heavy rainfall or tidal flow) to maximize movement (Gibson *et al.* 2001). The use of selective tidal-stream transport could explain the coincidence of migration with the new and full moon – when tides are largest – and estuarine flow (e.g., following rainfall). This is a behaviour common among portunid crabs (e.g., Blue Crab, *Callinectes sapidus*; Carr *et al.* 2004) and has previously been observed in Giant Mud Crab (Alberts-Hubatsch 2015), and may represent a strategy to minimize the energetic costs associated with migration (Gibson *et al.* 2001).

Previous oceanic recaptures of tagged female Giant Mud Crab in southeastern Australia suggest that once they leave estuaries they continue to migrate north, however very few tagged crabs ( $n = 3$ ) have been caught in the ocean in previous studies. Here we present the first evidence that this is a behaviour common across multiple years and estuaries, since all Giant Mud Crab that were detected in oceanic waters exhibited northward movement. In southeastern Australia, a northward spawning migration is common among estuarine-dependent species. For example, Eastern King Prawns (*Penaeus [Melicertus] plebejus*) and Tailor (*Pomatomus saltatrix*) both migrate north to spawn in oceanic waters off northern NSW and Queensland (Montgomery 1990; Brodie *et al.* 2018b; Taylor

and Johnson 2021). This northward migration is probably facilitated by transient, sub-mesoscale currents that flow northward in this region (Schaeffer *et al.* 2017; Kerry *et al.* 2020), however the mechanisms facilitating these oceanic movements should not be overinterpreted given the relatively low number of detections and a paucity of complementary environmental data at the scale necessary to confidently infer mechanisms supporting movement. Despite some studies reporting the occurrence of female Giant Mud Crab with spent ovaries in estuaries (e.g., Heasman *et al.* 1985), we did not detect females within estuaries once they had migrated to sea. This offers some evidence that this is a terminal migration, but these data are insufficient to determine the reproductive mode of the species (i.e., itero- or semelparous), since Giant Mud Crab are capable of multiple spawning after a single mating event (Brick 1974).

## **Potential influence of migration on future recruitment and fisheries catch**

Oceanic spawning can facilitate connectivity among spatially-distinct populations (Cowen and Sponaugle 2009), and lead to metapopulations with source-sink structures that are robust to stochastic environmental variation (Kritzer and Sale 2004). Peaks in mating activity (Heasman *et al.* 1985), and our data, show that conditions that trigger the female Giant Mud Crab spawning migration typically coincide with the period of highest sea surface temperature and southward transport in the EAC (Oke *et al.* 2019b; Kerry and Roughan 2020), which is likely to contribute to the broad genetic connectivity among estuarine populations in the region (Gopurenko and Hughes 2002). Furthermore, the northward migration of female Giant Mud Crab coupled with the predominant southward flow of the EAC (Oke *et al.* 2019b) suggests that a north-to-south source-sink population structure is a possibility. This means that within a given estuary, new recruits may well have originated from the north, and variation in abundance may thus be influenced by spawning stock biomass and environmental conditions outside of the estuary where juvenile crabs settle.

Recruitment variability potentially contributes to fluctuations in Giant Mud Crab abundance (Robins *et al.* 2005; Meynecke *et al.* 2012b). In estuaries south of the Clarence River (~ 29.4°S), 20–70 % of the variation in seasonally-averaged catch-per-unit-effort corresponds with high austral spring (September–November) or summer (December–February) rainfall within the same estuary/catchment two years earlier, but these relationships break down when annual data are considered (Meynecke *et al.* 2012b). Lagged relationships such as these generally suggest some influence of the physicochemical environment on spawning or early life-history processes, but if new recruits are also sourced from other estuaries to the north such relationships may be less clear. Our analyses suggest that there may be a substantial influence of temperature and rainfall on the commencement of spawning activity for female crabs, but if oceanic spawning is followed by southward dispersal of larvae in the EAC then the strength of spawning signals in estuaries to the north of a given estuary may be more important for later recruitment. Further study of larval dispersal is required to identify likely source estuaries, which can be achieved via biophysical particle tracking simulations (e.g., Everett *et al.* 2017; Schilling *et al.* 2020), thereby linking factors that influence spawning processes to spatially segregated fisheries productivity.

## **Technical considerations and caveats**

A central challenge when applying acoustic telemetry to any species is tag loss (Brownscombe *et al.* 2019; Sequeira *et al.* 2019). This is exacerbated when tagging crustaceans, as anything attached to the exoskeleton is shed during ecdysis (Florko *et al.* 2021). We endeavored to control for this by only tagging large, recently moulted females, and this approach was largely successful. Ultimately, the number of crabs that migrated was within the range appropriate for determining behaviours at the

population scale (Sequeira *et al.* 2019). While most tagged crabs migrated, some movements comprised only partial migrations (i.e., did not leave the estuary), which may be due to the crabs not having yet mated. It also raises the question as to whether these individuals may have had an alternate strategy of spawning within the estuary. This is highly unlikely since the capture of ovigerous Giant Mud Crab in estuaries is extremely rare despite extensive trapping, trawling and hauling effort within such systems (Hill *et al.* 1982; Hyland *et al.* 1984; Hill 1994). It is possible that some females overwintered within the estuary before migrating and spawning in the subsequent season (Heasman *et al.* 1985). While the estimated battery life of our tags (346 d) was at the limit of observing this, we did not record any detections of individuals in the year following their tagging, which may suggest a degree of mortality or tag loss.

Our interpolation of crab locations assumed constant movement between detections, but this is unlikely since Giant Mud Crab typically exhibit episodic downstream movement (Alberts-Hubatsch 2015) which may have impacted the accuracy of movement rates derived from the analysis. We overcame this limitation by modeling the onset of migration, rather than basing any inference directly on movement rate data. Detection efficiency in acoustic arrays can be impacted by several factors. These include ambient noise produced by wind or rain, biological noise (Stocks *et al.* 2014; Huveneers *et al.* 2016), and attenuation of acoustic “pings” from animals buried (Grothues *et al.* 2012) or sheltered in complex habitats (e.g., seagrass; Swadling *et al.* 2020). In the present study, the impact of these factors appeared limited as our data preprocessing and quality control did not indicate any irregular movement patterns, such as individuals skipping receivers. Finally, one individual displayed exceptionally high migration speed in the ocean (ID: 12350; Table 16); it is also possible that this crab may have been consumed by a predator during migration (e.g., Romine *et al.* 2014; Rub and Sandford 2020), given that the speed observed was almost double that of any other individual.

## Conclusions and future work

This study provides some mechanistic insight into how seasonal changes in temperature or climatic events (e.g., rainfall) may influence the spawning migration in Giant Mud Crab. These relationships may have implications for larval supply, recruitment and fisheries productivity (Meynecke *et al.* 2012b). While we studied movements in the southern part of the subtropical range, these patterns may reflect drivers in regions further to the north, where the species supports high-value fisheries (although circulation and dispersal patterns may differ). Furthermore, we provide the first evidence of a northward oceanic migration in Giant Mud Crab across multiple years and estuaries, which has previously been reported for a few individuals, and is similar to other species in the region (Ruello 1975; Brodie *et al.* 2018b). In conjunction with the dominating poleward flow of the EAC and the dispersal patterns resolved in *Oceanic connectivity and particle dispersal for Blue Swimmer Crab and Giant Mud Crab*, these observations point to a potential north-to-south source-sink model for populations in this region, however settlement surveys (e.g., de Lestang *et al.* 2015) are required to fully quantify these dynamics. When coupled with other data, these findings provide a foundation for the modelling of future seasonal and interannual variation in exploited stocks, based on present-day environmental variation. Quantifying these relationships is important for guiding management decisions, such as determining total allowable catch or estuarine stocking (Taylor *et al.* 2017c). Such estimates are particularly important in the context of climate change, which is altering the physicochemical regimes in coastal marine environments (Frusher *et al.* 2014; Hobday and Pecl 2014; Scanes *et al.* 2020a).

# Movement, habitat use, and behaviour of free-ranging Giant Mud Crab

## Background and rationale

The measurement of animal movement, behaviour, and associations of behaviour with different habitats, provides important foundational data on habitat-fishery interactions for exploited species. The patterns resolved aid species stock assessment and fishery management, both directly (e.g., identifying important habitats for conservation), and indirectly (e.g., supporting the development and interpretation of quantitative fisheries models). Importantly, quantitative definition of behavioural patterns of exploitable size classes can help ameliorate uncertainty when interpreting fishery-dependent data.

Little is known about habitat associations and associated behaviours for Giant Mud Crab in temperate estuaries. Foraging by Giant Mud Crab is promoted by warmer temperatures (i.e., 25–30°C; Hill 1980; Hill *et al.* 1982), and while diet is associated with productivity within seagrass (Connolly and Waltham 2015; Jänes *et al.* 2022), mangrove (Demopoulos *et al.* 2008) and saltmarsh habitats (Raoult *et al.* 2018; Jänes *et al.* 2022), patterns in physical associations with (or occupation of) these habitats is poorly known. In the semi-diurnal tidal systems of south-eastern Australia, the availability of these habitats is closely linked to the tidal cycle (Hyland *et al.* 1984), and inundation of these habitats occurs only for short, finite windows each day. This may not only create some association between tidal movement and crab movement, but may also lead to nuanced patterns in foraging behaviours in the species, and the association of these behaviours with particular habitats.

As noted in *Environmental influence on spawning migrations in Giant Mud Crab*, acoustic telemetry is a powerful method for quantifying the movement of marine organisms and has been broadly applied in fisheries research. Recent developments in this technology have allowed researchers to track animals at increasingly fine spatial (i.e., metres) and temporal (i.e., minutes) scales (Espinoza *et al.* 2011; Roy *et al.* 2014; Özgül *et al.* 2015). Tags that log auxiliary data, such as accelerometers, have enabled further insight into the behavioural structure of animal movement (Nathan *et al.* 2012; Payne *et al.* 2014). These technological advances have been accompanied by a proliferation of novel statistical approaches to analyze such data (Hooten *et al.* 2017; Patterson *et al.* 2017; Joo *et al.* 2020). Hidden Markov models represent one of the most popular contemporary classes of model for analyzing movement (Langrock *et al.* 2012; McClintock *et al.* 2020) and accelerometry data (Leos-Barajas *et al.* 2017). Conceptually, hidden Markov models decompose observed animal movement or accelerometry data into unobserved (or ‘hidden’) behavioural states, matching our intuitive understanding of animal movement (Langrock *et al.* 2012; Leos-Barajas *et al.* 2017; McClintock *et al.* 2020). A key feature of hidden Markov models is their extension to model the influence of environmental covariates (e.g., temperature) on animal behaviour (Patterson *et al.* 2009).

In this study, we sought to investigate habitat associations, and fine-scale patterns in movement and behaviour, of free-ranging adult Giant Mud Crab, alongside environmental drivers. Specifically, this was achieved by: 1) tracking the movement of adult Giant Mud Crab with acceleration-logging acoustic tags using a hyperbolic positioning system; and 2) modelling the behaviours that underlie observed movement and acceleration, as a function of environmental covariates using a hidden Markov model (Leos-Barajas *et al.* 2017; McClintock *et al.* 2020).

## Methods

### Study site and array design

This study was conducted in Fenninghams Island Creek (32.75°S, 152.05°E, Figure 66), a small tributary to Port Stephens, a mature wave-dominated barrier estuary (Roy *et al.* 2001) situated on the temperate mid-north coast of NSW (Australia, Figure 15). Fenninghams Island Creek is a narrow, relatively shallow creek (0.2 – 2 m depth) that encompasses typical estuarine habitats including unvegetated soft sediments (sub- and intertidal), seagrass (*Zostera* sp.), mangrove (*Avicennia marina*) and saltmarsh (*Sporobolus virginicus*, *Sarcocornia quinqueflora* and *Suaeda australis*; Figure 66). It has a maximum tidal range of approximately 2 m, and mangrove and saltmarsh habitats are inundated twice daily (especially during spring tides). The study area is a ‘Sanctuary Zone’ within the Port Stephens Great Lakes Marine Park, which prohibits fishing or crab-trapping, allowing this study to proceed without the risk of fishing mortality or any effect of baited traps on movement. It is possible that some crabs may migrate in and out of the study area and be exposed to fishing in adjacent areas (Hill 1994). Oyster farming is permitted, and tray cultivation is practiced along both shorelines of the creek (Figure 66)

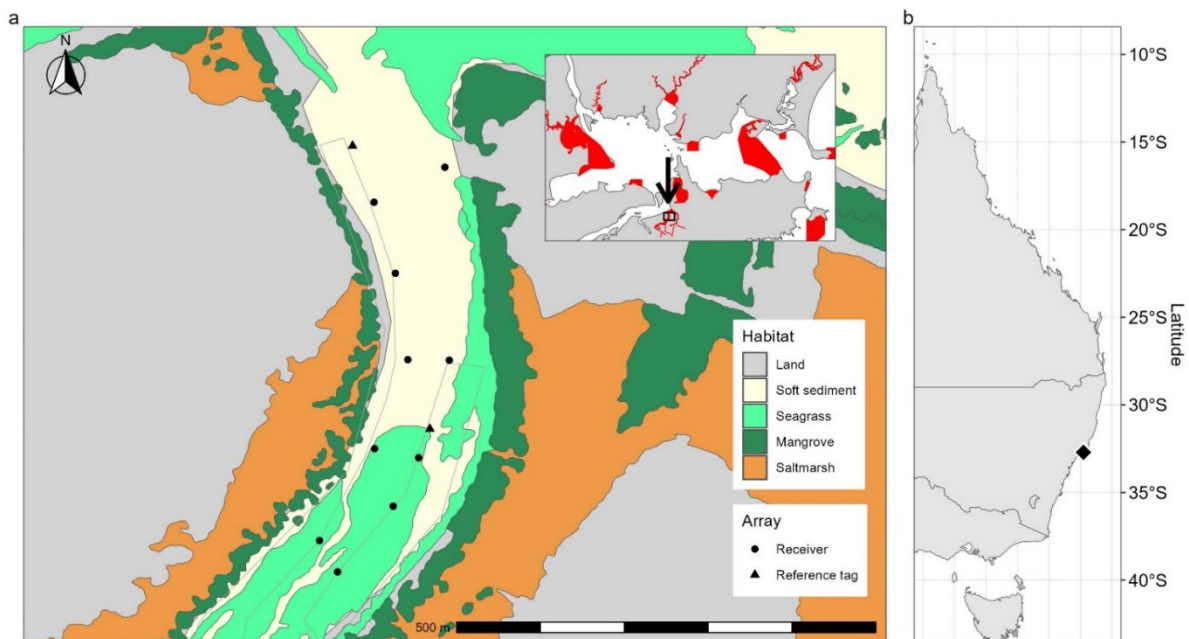


**Figure 66** Map of a) Fenninghams Island Creek showing the locations of receivers (●) and reference tags (▲) within the array, as well as the distribution of seagrass, mangrove and saltmarsh. Oyster farming infrastructure is indicated by the grey outline. The location of Fenninghams Island Creek and within Port Stephens (inset; Sanctuary Zones in red), and b) on the east Australian coast is indicated.

A hyperbolic positioning system (hereafter referred to as the ‘array’), employing 10 Innovasea VR2W receivers and co-located synchronisation (or ‘sync’) tags (Innovasea, Nova Scotia, Canada) was established along approximately 500 m of Fenninghams Island Creek (Figure 66). Range testing of similar arrays in comparable systems (e.g., Walsh *et al.* 2012; Taylor *et al.* 2017e) informed a receiver spacing of 100–200 m. Each receiver and sync tag were chained to existing infrastructure (e.g., oyster trays, jetty), or independent moorings consisting of a float and anchor attached by chain, approximately 0.3–0.4 m from the bottom. To monitor positional error throughout the study, two

fixed-position reference tags (V9-2x-BLU-3), with identical programming as tags deployed on crabs (see *Tag programming* below), except with a longer random transmission interval (240–360 s), were deployed within and immediately adjacent to the array (Figure 66). Since the position of these tags were known, the distance between the estimated position (see *Hyperbolic positioning*) and their actual position provides an indication of the performance of the array throughout the study. The reference tag adjacent to the array stopped transmitting after one day, and was missing at the conclusion of the study, so only detections from the reference tag within the array were used in subsequent analysis. Water temperature (°C) and conductivity was monitored throughout the duration of the study using a HOBO U24-002-C conductivity/salinity logger (Onset Computer Corporation, Massachusetts, USA).

Receivers were retrieved and downloaded using VUE software (v. 2.6.2; Innovasea, Amirix, Nova Scotia, Canada) after the estimated battery life of the last tag deployed had passed (~7 months). Detection data was subsequently uploaded to the Integrated Marine Observing System Animal Tracking Facility (IMOS ATF; <https://animaltracking.aodn.org.au>; Taylor *et al.* 2017a) which was also interrogated for any additional tag detections outside of our array.

## Crab capture and tagging

Giant Mud Crab were captured during the late austral summer (February 2020) using round collapsible mesh traps (i.e., pots; 0.9 m diameter x 0.27 m high, Figure 4), with 55 mm mesh and two semi-closed funnel entrances (0.25 x 0.05 m). Traps were deployed for approximately 24 h periods along 750 m of Fenninghams Island Creek (within and just upstream of the array). Captured crabs were cooled for 10–20 s in an ice/sea-water slurry and subsequently measured (to the nearest mm) for carapace length (CL; distance between the frontal notch and posterior carapace margin), sexed and moult-staged (following Hay *et al.* 2005). Only adult crabs (> 100 mm CL) that were likely to have recently moulted (i.e., post- or inter-moult; Hay *et al.* 2005) were tagged, to limit the probability of tag loss during ecdysis (Florko *et al.* 2021). Innovasea V9A-2H accelerometer tags (hereafter ‘tags’; length: 43 mm, wet weight: 3.3 g; Innovasea, Nova Scotia, Canada) were affixed to the posterior carapace using instant adhesive (Loctite 406, Henkel Adhesives, Australia) which has shown tag retention of at least 3 months. After tagging, crabs were gently submerged alongside the research vessel and once normal activity (e.g., attempted swimming) had resumed crabs were released within the bounds of the array. In general, negative impacts (e.g., stress, limb loss) are low for crabs handled and released in this manner (Butcher *et al.* 2012). During tagging, two previously tagged crabs were recaptured that had lost their tags, evidenced by adhesive present on the carapace. These crabs were re-tagged and data from the initial tags was excluded from our analysis (identified as continuous transmission from a single point), resulting in movement data from 18 crabs.

## Tag programming

Tags were programmed to emit a unique signal (69 kHz) with high power output (151 dB re 1  $\mu$ Pa at 1 m) at random intervals between 150–210 s (180 s nominal). High power output was chosen in an attempt to overcome potential signal attenuation owing to burial of crabs (Hill 1978; 1980; Grothues *et al.* 2012) and the presence of seagrass within the study site (Swadling *et al.* 2020). Random signal transmission times were employed to minimize potential signal overlap (i.e., code-collision) which can block detection. Tags were equipped with an accelerometer programmed to record tri-axial acceleration data, which represents a general index of activity, analogous to overall dynamic body acceleration (ODBA; Wilson *et al.* 2006; Qasem *et al.* 2012). Measurements are transmitted as a root mean square (RMS) acceleration vector with a range 0–3.4  $m s^{-2}$  (Taylor *et al.* 2013b). Since Giant

Mud Crab are expected to be predominantly sessile (Hill 1976; 1978; 1980), acceleration data was recorded at 5 Hz (i.e., 5 samples  $s^{-1}$ ) over a 20 s window to capture ‘bursts’ of acceleration (H. Pedersen, *pers. comm.*). See Taylor *et al.* (2013b) for a discussion of accelerometer programming. Battery life was estimated 196 d at these settings.

## Hyperbolic positioning

Positions of tagged crabs were estimated by Innovasea using proprietary hyperbolic positioning algorithms. This approach estimates the position of tagged animals based on the time-difference-of-arrival (TDOA or multilateration) of detections at 3 or more receivers within an array. Assuming no measurement error, detection on a pair of receivers defines a hyperbola on which a tag may have been during signal transmission. Detection on a third receiver defines a second hyperbola, and the intersection of the two is the position of the tag. Using this approach, the time of a detection is converted to distance based on signal propagation speed. Signal propagation speed was estimated via the Coppens equation (Coppens 1981) using measured water temperature ( $^{\circ}C$ ) and salinity and an assumed depth of 1.8 m, assuming ideal signal propagation. Innovasea receiver clocks can drift by up to  $4 s d^{-1}$  (dependent on water temperature) leading to differences in time among receiver clocks (i.e., clock skew). To account for this, detections from sync tags were used to calculate the skew between receiver clocks and synchronize detection times.

Overall, detections from our fixed-position reference tag indicated that location error within the array was low and positively skewed for the duration of the study, with a mean error of  $2.77 \pm 9.24$  m (SD) and median of 1.26 m (interquartile range = 0.78 m), and 93 % of positions were within 5 m of their actual (known) location. In general, these results indicate that measurement error was low for the duration of the study.

## Data processing

Recently, tagging effects (e.g., elevated activity) have been observed for other crab species (e.g., Snow Crab, *Chionoecetes opilio*) leading researchers to discard the first day of tracking (Cote *et al.* 2019; 2020). However, we found no evidence of such effects, nor have previous tagging studies on the species (e.g., Hill 1978). Furthermore, catch-and-release does not typically induce high levels of stress in the species (Butcher *et al.* 2012). As such, we did not discard any data to preserve our sample size.

In general, hidden Markov models are formulated in discrete-time (McClintock *et al.* 2014; but see Glennie *et al.* 2023), meaning they require temporally regular observations. Many factors can contribute to temporally irregular observations in our study, including temporary emigration from the array, burial (Grothues *et al.* 2012) and random transmission intervals in our tags. To accommodate this, we predicted temporally regular locations at 5, 10 and 15-minute intervals by modelling crab movement as a continuous-time correlated random walk using the R package ‘crawl’ (Johnson and London 2018). We refer readers to Johnson *et al.* (2008) for a full mathematical description of this model. Before predicting temporally regular locations, detections were split into ‘tracks’ where the interval between detections were greater than 4 times the interpolation interval (i.e., 20, 40 and 60-min). This was to ensure we did not introduce unreasonable uncertainty or bias our data by consecutively predicting locations within these longer temporal gaps, which would result in straight and constant movement (Gurarie *et al.* 2016). Furthermore, tracks with less than 100 detections were excluded, as those with few observations can give rise to issues with numerical stability (i.e., non-convergence), and typically reveal less about behavioural state dynamics (Bacheler

*et al.* 2019). Locations were estimated using a state-space framework, allowing incorporation of measurement error in location estimates (Johnson *et al.* 2008). This was achieved by transforming the error (in metres) along the longitudinal and latitudinal axes, derived from the fixed-position reference tag, into a covariance matrix and approximating it with a bivariate Gaussian distribution during model fitting (Johnson *et al.* 2008). Locations were estimated via maximum likelihood, and thus require initial estimates of parameter values. To ensure adequate exploration of the likelihood surface and convergence (to a global maxima) we used 50 random perturbations of the initial parameter values and retained output from the model with the highest log-likelihood (McClintock and Michelot 2018).

Since we predicted locations less frequently (i.e., every 15 min) than the random transmission interval of our tags (i.e., every 46 min) it was possible that there were some intervals where no acceleration data was recorded (~5 % of all locations) as no detection was recorded but a location was predicted (Table 17). Relatively few missing values is typically not an issue when fitting hidden Markov models (Langrock *et al.* 2012), and the missing observations did not contribute to the likelihood during model fitting

**Table 17** Biological and detection information for tagged Giant Mud Crab

| ID   | Sex | CL (mm) <sup>a</sup> | Detections | Predicted locations <sup>b</sup> | Tracks | Missing acceleration values |
|------|-----|----------------------|------------|----------------------------------|--------|-----------------------------|
| 7789 | M   | 125                  | 930        | 399                              | 6      | 49                          |
| 7791 | M   | 119                  | 867        | 362                              | 4      | 27                          |
| 7792 | F   | 124                  | 135        | 53                               | 1      | 5                           |
| 7793 | M   | 124                  | 21, 275    | 6406                             | 17     | 148                         |
| 7795 | F   | 124                  | 1382       | 549                              | 4      | 47                          |
| 7796 | M   | 125                  | 355        | 149                              | 2      | 13                          |
| 7797 | M   | 129                  | 121        | 44                               | 1      | 0                           |
| 7798 | M   | 119                  | 532        | 234                              | 4      | 23                          |
| 7802 | M   | 131                  | 404        | 179                              | 1      | 19                          |
| 7804 | M   | 135                  | 867        | 320                              | 3      | 18                          |
| 7805 | M   | 129                  | 338        | 125                              | 2      | 13                          |
| 7807 | F   | 127                  | 1, 630     | 649                              | 12     | 42                          |
| 7808 | M   | 130                  | 5, 724     | 1927                             | 18     | 119                         |

<sup>a</sup> CL: carapace length.

<sup>b</sup> Locations predicted at temporally regular (15-min) intervals.

## Behavioural state classification

Behaviour of tagged crabs was modelled using a hidden Markov model via maximum likelihood using the R package ‘momentuHMM’ (McClintock and Michelot 2018). Hidden Markov models are stochastic time-series models with two components: an observable (possibly multivariate) state-dependent process, and an unobservable (‘hidden’) state-process (Leos-Barajas *et al.* 2017; McClintock *et al.* 2020). The state-dependent process consists of observed animal detections or metrics derived from them (e.g., step length, turning angle), while the state-process is a series of  $N$ -states, that are taken to represent the underlying behavioural modes of the animal (Leos-Barajas *et al.* 2017; McClintock *et al.* 2020). Two assumptions govern this model structure: (1) observations that comprise the state-dependent process are assumed to be conditionally independent, with the observation at time  $t$  conditional on the state at time  $t$ , and independent of all other states and observations; and (2) the state-process is a Markov chain, which means the probability of being in a

given state at time  $t$  is completely determined by the state active at time  $t - 1$ . Transitions between states are governed by an  $N \times N$  transition probability matrix, the entries in which denote the probability of switching states between time  $t$  and  $t + 1$  (McClintock and Michelot 2018), with entries on the main diagonal representing the probability of remaining in the same state (i.e., state-dwell probabilities; Langrock *et al.* 2012). Hidden Markov models thereby link observed animal movement to unobserved (or 'hidden') underlying behavioural modes and provide a description of how they change through time (Langrock *et al.* 2012; Leos-Barajas *et al.* 2017; McClintock *et al.* 2020).

In our case, observations that comprise the state-dependent processes included step length ( $m$ ; i.e., distance moved) and mean acceleration ( $m\ s^{-2}$ ) between time  $t$  and  $t + 1$  and turning angle (radians) between detections at  $t - 1$ ,  $t$  and  $t + 1$ , where 0 radians corresponds to straight-line movement and  $\pm \pi$  radians indicates course reversal. Step lengths and mean acceleration values were modelled using a zero-inflated gamma distribution (which is defined for non-negative real numbers, i.e.,  $\geq 0$ ), to account for instances where no movement occurred (i.e., step length = 0 m or acceleration = 0  $m\ s^{-2}$ ; McClintock and Michelot 2018). Turning angles were modelled using a wrapped Cauchy distribution, which is a probability distribution that results from 'wrapping' the Cauchy distribution around the unit circle, with a concentration parameter ranging between 0 and 1 that measures how concentrated turning angles are around the mean (between  $-\pi$  and  $\pi$ ; McClintock and Michelot 2018). For each state, the mean ( $\pm$  standard deviation, SD) step length and acceleration was estimated using a log-link function, while turning angle mean was fixed at 0 radians (i.e., straight-line movement) and concentration was estimated using the logit-link function (McClintock and Michelot 2018). Initial parameter estimates were obtained using the same approach as with predicting temporally regular locations (see *Data processing*), whereby the fitting procedure was run 50 times with randomly selected initial values and output from the model with the highest log-likelihood was retained (Michelot *et al.* 2016; McClintock and Michelot 2018). A prior for the log-density of the working scale parameter distributions ( $N[0, 100]$ ) was specified to avoid estimates near the boundary.

A central challenge when fitting hidden Markov models is deciding on the number of states ( $N$ ) to estimate, which must be specified *a priori*, since traditional model selection techniques (e.g., minimizing information criteria) tend to select models that include more states than are biologically meaningful/interpretable (Li and Bolker 2017; Pohle *et al.* 2017). This is because state estimation is data-driven, meaning the estimated states may not correspond to a biologically meaningful behaviour, rather they provide proxies for them and require *post-hoc* interpretation (Leos-Barajas *et al.* 2017; McClintock *et al.* 2020). In this context, adding more states may simply be capturing random noise in the data rather than uncovering additional behavioural states. Pohle *et al.* (2017) argue that the number of states should be chosen pragmatically, based on statistical and biological intuition. As a predominantly sessile species (Hill 1978), we expect Giant Mud Crab to exhibit 2 discrete behaviours, namely: inactivity/resting and foraging (Hill 1978; 1980; 1982; Hyland *et al.* 1984; Alberts-Hubatsch *et al.* 2016); we therefore limited our analysis to a two-state hidden Markov model (i.e.,  $N = 2$ ).

## Behavioural state dynamics

Individual-level variation in behaviour is common among free-ranging animals, due to true differences (e.g., animal 'personality'; Hertel *et al.* 2020) or as an artefact of variable deployment lengths between individuals (DeRuiter *et al.* 2017; McClintock 2021). This can be accommodated by including discrete-valued random effects (e.g., sex, individual) in a mixed hidden Markov model (McKellar *et al.* 2015; Towner *et al.* 2016; DeRuiter *et al.* 2017; Isojunno *et al.* 2017). To do so,  $K$  mixtures ( $K \in [1, \dots, 4]$ ) were included in a 'null' model (i.e., without any environmental covariates), with crab ID as a discrete-valued random effect. Under this formulation, each  $K$  represents a distinct

transition probability matrix allowing for up to 4 behavioural types among individuals (DeRuiter *et al.* 2017; McClintock and Michelot 2018). For  $K = 1$ , behavioural dynamics are assumed to be the same for all individuals (i.e., no random effects; McClintock 2021), while for  $K > 1$  the behavioural dynamics of a given individual are governed by one of  $K$  transition probability matrices (McKellar *et al.* 2015; DeRuiter *et al.* 2017). Following Isojunno *et al.* (2017), these models were compared using Akaike information criteria (AIC) to select the optimal value for  $K$ , where the lowest value is indicative of the best fitting model (Burnham and Anderson 2002a).

The selected random-effects structure was then used to model the influence of environmental covariates on behavioural transitions. Typically, entries within the transition probability matrix are assumed to be constant, however we relaxed this assumption and estimated the effect of a suite of time-varying environmental covariates on these probabilities (i.e., we assume the Markov chain is non-homogenous; McKellar *et al.* 2015). This was achieved using a multinomial logit-link function which ensures all transition probabilities are between 0 and 1, and the rows of the transition probability matrix sum to 1 (Michelot *et al.* 2016). State transition probabilities were modelled as a function of water temperature ( $^{\circ}\text{C}$ ); an interaction term between tide height (m above Port Stephens Height Datum [PSHD]), and the difference in tide height over 15-min intervals (hereafter  $\Delta$ -tide height); habitat type; and a cyclic effect of time (hour) of day. Cyclic effects were estimated via two periodic functions,  $\cos(\frac{2\pi t}{24})$  and  $\sin(\frac{2\pi t}{24})$ , where  $t$  is the time (hour) of day (0–24) and 24 is the assumed daily periodicity of the function (Towner *et al.* 2016; Bachelier *et al.* 2019).  $\Delta$ -tide height includes information about both the direction of the tide (positive/negative values = flood/ebb tide) and the strength of tidal currents, where greater absolute values imply stronger tidal currents. Tide data was obtained from a nearby tide gauge ( $\sim 4$  km away;  $32.72^{\circ}\text{S}$ ,  $152.02^{\circ}\text{E}$ ) maintained by Manly Hydraulics Laboratory (NSW DPIE 2021). Habitat data was obtained from NSW Department of Primary Industries Fisheries Spatial Data Portal (<https://www.dpi.nsw.gov.au/about-us/research-development/spatial-data-portal>). This dataset includes information on the distribution of common estuarine habitats, including: seagrass, mangroves and saltmarsh (Creese *et al.* 2009), with a spatial resolution of approximately  $\pm 2$  m. To account for edge effects around seagrass meadows (Smith *et al.* 2008; 2011) a buffer of 1.26 m was applied (matching the median error in our array; see *Hyperbolic positioning*). All possible combinations of covariates were fit (including ‘null’ models with no covariates), however the tidal covariates were only included together. These models were compared using AIC, where the model with the lowest value was selected as the true model (Burnham and Anderson 2002a). Stationary state probabilities were derived from the transition probability matrix and can be interpreted as the probability of exhibiting a given state for some fixed value of a covariate (i.e., when the system is in equilibrium). Finally, behavioural states at each location were estimated using the Viterbi algorithm, which derives the most likely sequence of states given the observations and fitted model (McClintock *et al.* 2020). Model fit was assessed by computing pseudo-residuals, which fulfil the role of normal-theory regression residuals for hidden Markov models (Zucchini *et al.* 2017).

## Results

### Model selection and diagnostics

For all interpolation intervals (5-, 10- and 15-min), we found no evidence of individual-level variation in crab behaviour (i.e.,  $K = 1$  mixture had the lowest AIC). Therefore, we modelled the influence of environmental covariates on crab behavioural dynamics using a ‘standard’ hidden Markov model (i.e., without random effects). Our model selection indicated that models with no covariates for data interpolated at 5- and 10-min intervals were optimal, while for 15-min intervals the model including an interaction between tide height and  $\Delta$ -tide height was selected.

Model pseudo-residuals indicated that data interpolated at 15-min intervals provided the best fit relative to the 5- and 10-min data. On this basis, we report only results from the model fit to data interpolated at 15-min intervals. There was evidence of a diel cycle in behaviour not captured by this model, indicated by cyclic residual autocorrelation for both step length and acceleration with a ~12 h period. However, the model that included a cyclic effect of time of day did not improve this. Ultimately, model fit was deemed adequate since hidden Markov models do not need to produce perfectly independent pseudo-residuals (Leos-Barajas *et al.* 2017; Zucchini *et al.* 2017) and small violations of this are generally of little concern when estimating behavioural state dynamics is the main goal of analysis (DeRuiter *et al.* 2017) as is the case here.

The selected model was fit to 75 tracks from 13 individuals, ranging in size from 119–135 mm CL (Table 17). The length of tracks ranged from ~8 h–20 d, with an average of  $1.5 \pm 3.2$  d. We found no evidence of tagging effects and only 9 of these 75 tracks included detections from a crab on the same day as tagging (further limiting any possible influence of tagging effects in our analysis). One female crab (ID = 7792) was detected in the coastal ocean (via the IMOS ATF) approximately 150 km north at the Port Macquarie offshore artificial reef (~31.42°S) 27 days after the last detection in our array.

## Crab behavioural states

Our analysis identified behavioural states with considerable overlap in terms of their step length and turning angle concentration, however there was clear separation in terms of acceleration (Figure 67). State 1 is likely to represent foraging (hereafter ‘foraging state’) since crabs spent little time in this state (21 %) and exhibited greater, but highly variable, step

lengths (mean  $\pm$  SD =  $13.98 \pm 18.10$  m  $15 \text{ min}^{-1}$ ) and acceleration ( $0.59 \pm 0.63$  m  $\text{s}^{-2}$   $15 \text{ min}^{-1}$ ), coupled with moderately concentrated turning angles (concentration = 0.51; Figure 67; Table 18), indicative of a combination of straight-line movement and direction changes. In the foraging state crabs also had the lowest probability of no movement (Table 18). However, they exhibited a higher probability of exhibiting no acceleration which is likely due to the relatively high variability in acceleration while in this state (Table 18). State 2 is likely to correspond to periods of inactivity (hereafter ‘inactive’ state), since crab spent the majority of the time in this state (79 %) and exhibited much shorter step lengths (mean  $\pm$  SD =  $0.75 \pm 0.93$  m  $15 \text{ min}^{-1}$ ), low acceleration ( $0.04 \pm 0.01$  m  $\text{s}^{-2}$   $15 \text{ min}^{-1}$ ), and relatively highly concentrated turning angles (concentration = 0.70), indicative of infrequent changes in direction (Figure 67; Table 18). Note, the zero-inflated gamma distribution is defined only for non-negative real numbers (i.e.,  $\geq 0$ ), and standard deviations greater than the mean for step length and acceleration (which were modelled using this distribution) reflect highly positively skewed distributions (Figure 67) and do not imply negative values for either of these processes. An example track, with the most likely sequence of states is depicted in Figure 68.

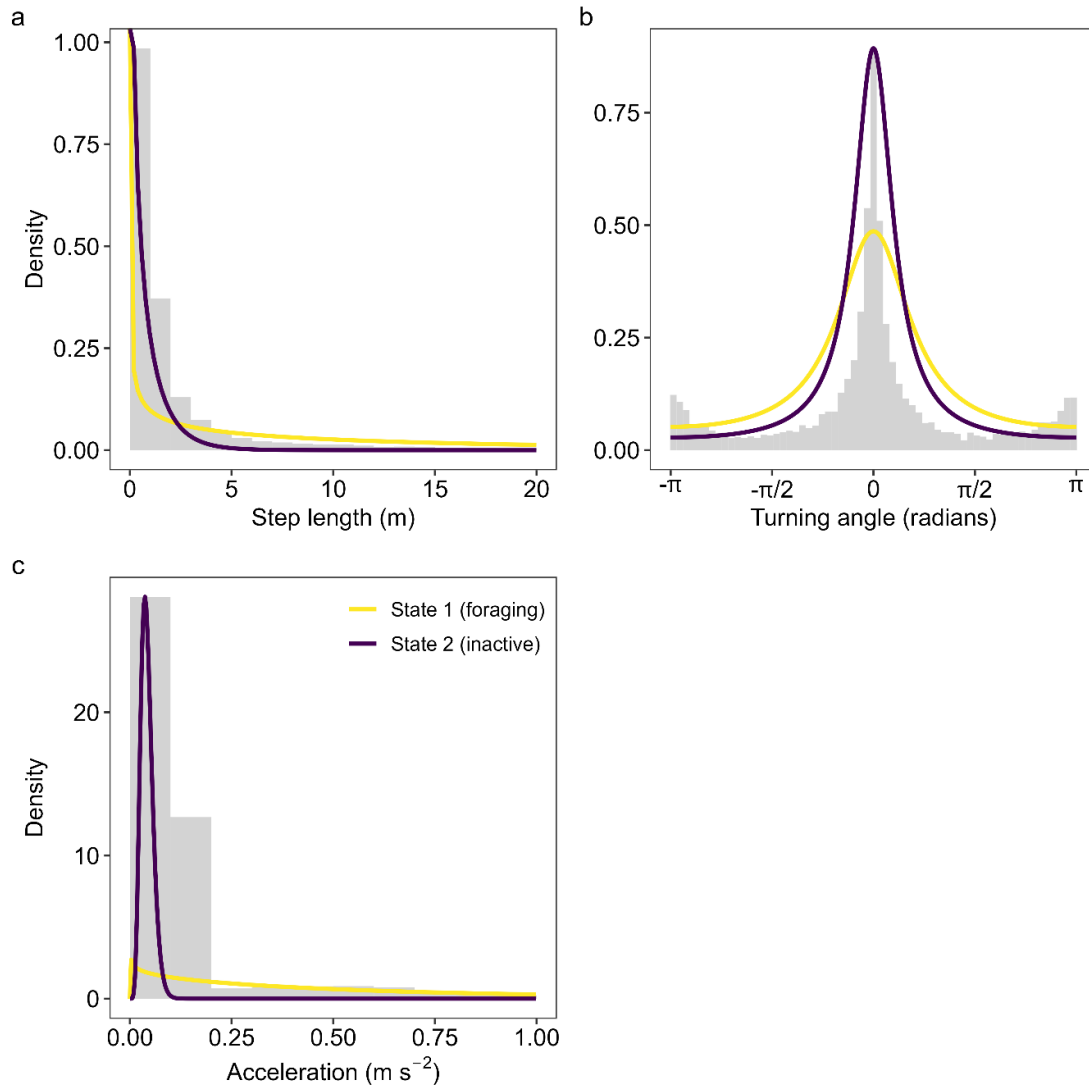


**Figure 67** State-dependent probability distributions (lines) and histograms of observations (grey bars) for a) step length (m), b) turning angle (radians) and c) acceleration ( $\text{m s}^{-2}$ ). Note x-axis on a) and c) has been truncated to aid visualization and excludes the upper  $\sim 3\%$  of observations.

**Table 18** State-dependent parameter estimates for tagged Giant Mud Crab

| State | Step length (m)   |             | Turning angle | Acceleration ( $\text{m s}^{-2}$ ) |       |
|-------|-------------------|-------------|---------------|------------------------------------|-------|
|       | Mean $\pm$ SD     | Pr(0)       | Concentration | Mean $\pm$ SD                      | Pr(0) |
| 1     | 13.98 $\pm$ 18.10 | $\ll 0.001$ | 0.51          | 0.59 $\pm$ 0.63                    | 0.006 |
| 2     | 0.75 $\pm$ 0.93   | 0.014       | 0.70          | 0.04 $\pm$ 0.02                    | 0.002 |

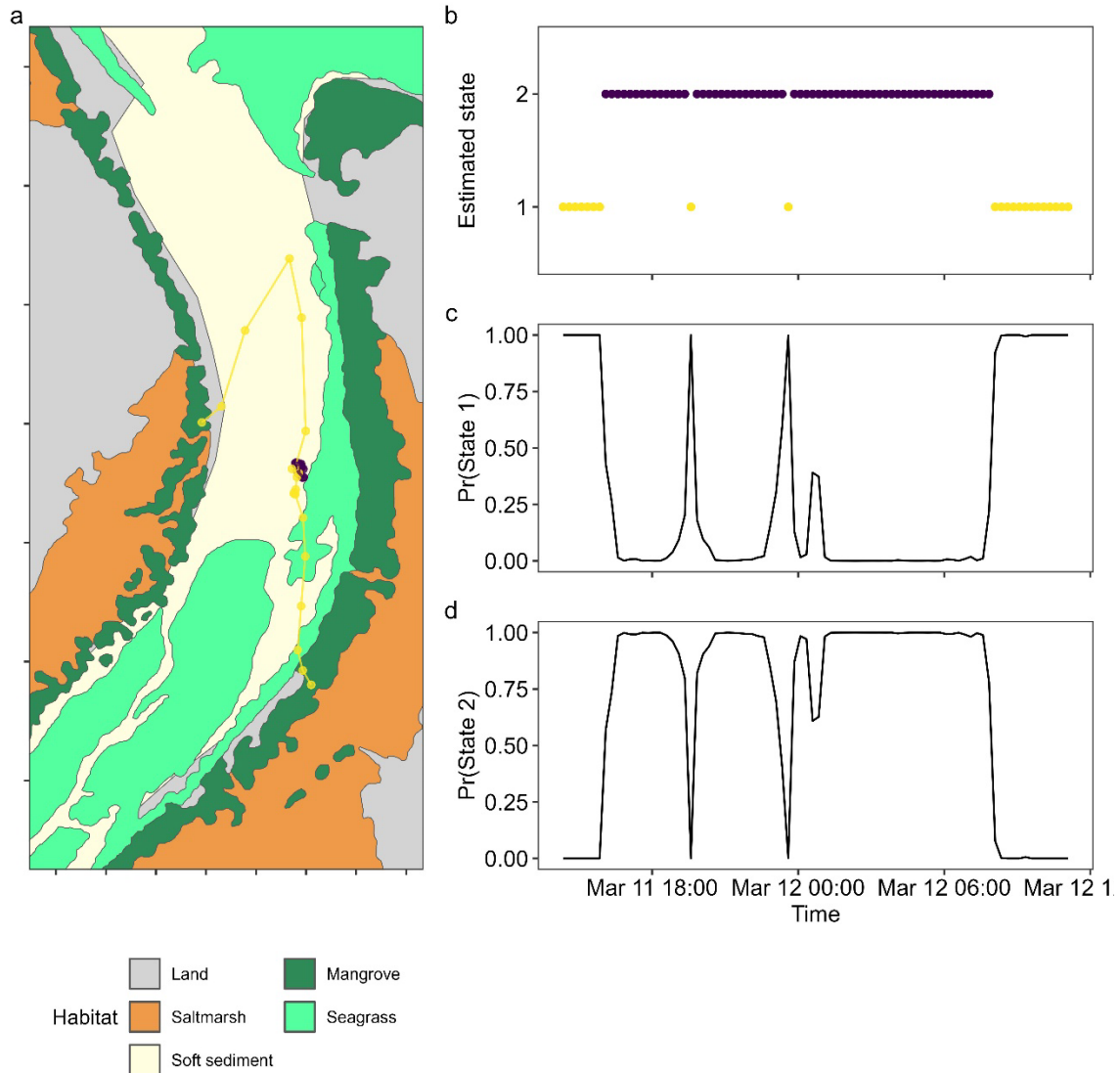


**Figure 68** a) Example track from a tagged female Giant Mud Crab (ID: 7795) and b) the time-series of Viterbi-decoded behavioural states and the corresponding probabilities of c) State 1 (foraging; yellow) and d) State 2 (inactive; purple).

### Behavioural state dynamics

States were highly persistent through time, indicated by very high state-dwell probabilities (i.e., diagonal entries in Table 19). Based on our model selection, water temperature ( $^{\circ}\text{C}$ ), time (hour) of day and habitat type were removed from our model, implying these covariates explain little about crab behavioural dynamics. The interaction between tide height (m) and  $\Delta$ -tide height ( $\text{m } 15\text{-min}^{-1}$ ) suggested that crabs were most likely to be foraging during the low ( $< 0.5$  m) incoming tide (Figure 69), and more likely to be inactive at high tide as the tide recedes (Figure 69). Overall, crabs were always more likely to be inactive than foraging (Figure 70), but they were approximately twice as likely to be foraging at low tide than at high (Figure 70). Conversely, crabs were approximately 1.25 times more likely to be inactive at high tide relative to low (Figure 70). The probability of foraging was higher during an incoming tide than an outgoing tide (Figure 70), while the opposite is true for the inactive state which becomes more likely as the tide recedes (Figure 70).

**Table 19** State transition probabilities of tagged Giant Mud Crab. Diagonal entries indicate the probability of staying in the same state (i.e., state-dwell probabilities).

| Current state | Next state |      |
|---------------|------------|------|
|               | 1          | 2    |
| 1             | 0.91       | 0.09 |
| 2             | 0.04       | 0.96 |

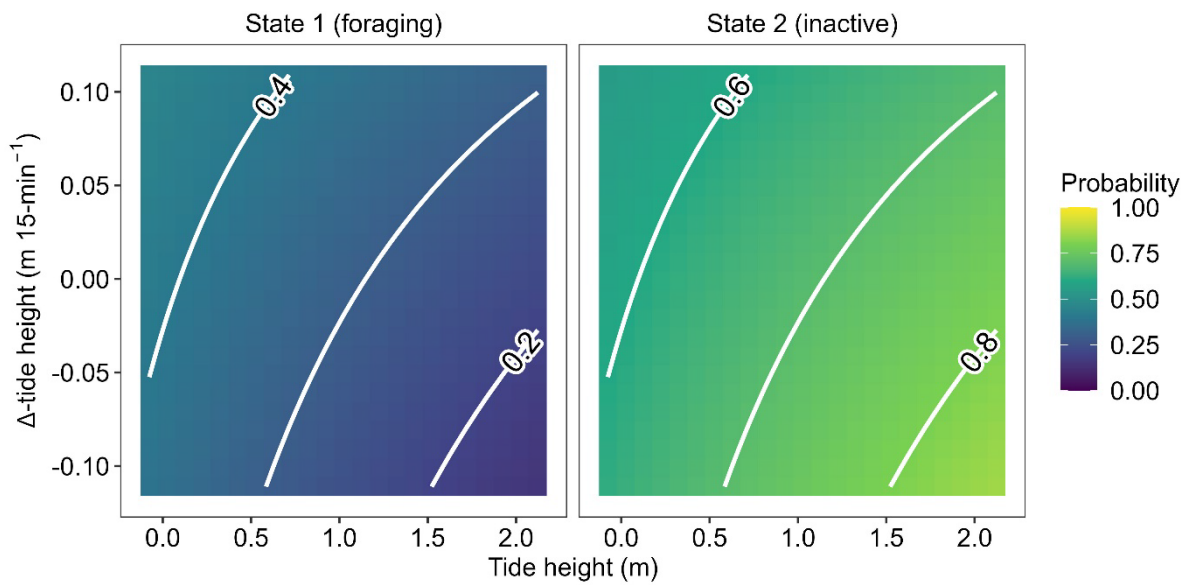


**Figure 69** Stationary state probabilities as function of the interaction between tide height (m) and  $\Delta$ -tide height (m 15-min<sup>-1</sup>) in tagged Giant Mud Crab.

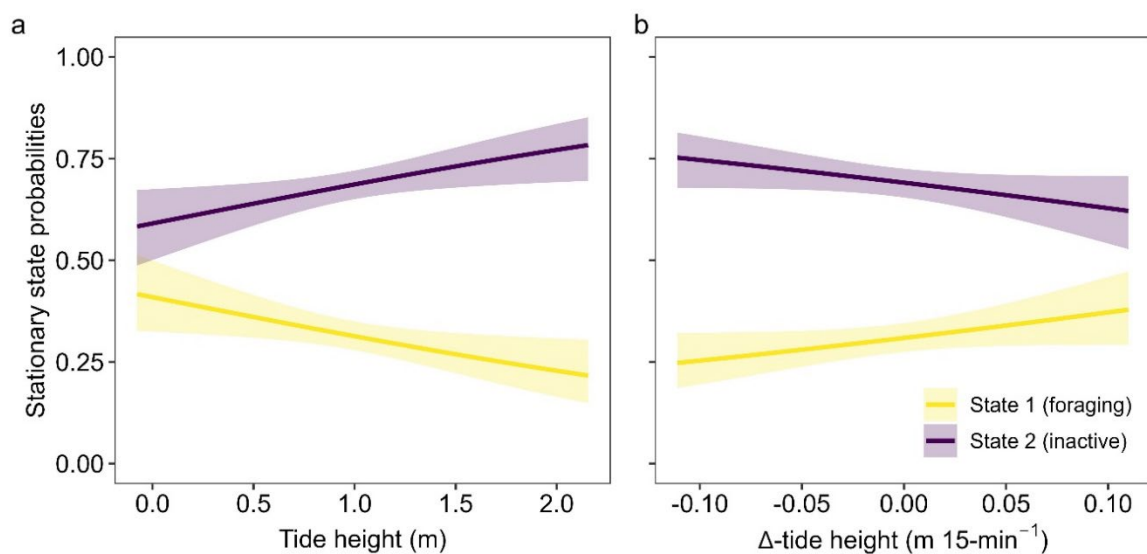


**Figure 70** Stationary state probabilities ( $\pm$  95 % CI) as a function of a) tide height (m) and b)  $\Delta$ -tide height (m 15-min<sup>-1</sup>).

## Discussion

Our study is the first to track the activity of Giant Mud Crab at high spatial and temporal resolution, using accelerometer-equipped acoustic tags, alongside similarly high temporal resolution environmental data (but see Hill 1978 that tracked crabs but did not record any environmental data). Modelling data with a hidden Markov model allowed the integration of observations and provided insight into the fine-scale drivers of behaviour for the species. Our analysis suggested that the tidal cycle has an important role in driving foraging and may represent a strategy to minimize predation risk, alongside optimizing the energetic efficiency of foraging. Quantifying movement and behaviour of mobile exploited species is important for developing effective fisheries management (Cooke *et al.* 2016; Taylor *et al.* 2017a), and our results contribute to the evidence base that underpins management actions for this species.

### Fine-scale movement and behaviour of Giant Mud Crab

Direct observation of aquatic animal behaviour is challenging, especially in turbid estuarine waters. The main advantage of hidden Markov models is the classification of observed animal movement and acceleration data into 'states' that may correspond to biologically meaningful behaviours (Langrock *et al.* 2012; Leos-Barajas *et al.* 2017; McClintock *et al.* 2020). In our analysis, Giant Mud Crab were inactive for a majority of the time (79 %), which is consistent with their status as a predominantly sessile species (Hill 1976; 1978; 1980). Adult Giant Mud Crab are opportunistic scavengers (Webley 2008), and foraging is facilitated via a combination of olfaction (Wall *et al.* 2009) and contact chemoreception (Hill 1979b). Crabs generally exhibit an initial 'searching' response towards olfactory cues (Wall *et al.* 2009) to find the approximate location of the food (Alberts-Hubatsch *et al.* 2016), followed by further tactile investigation using the dactyls of the walking legs to find the exact location of the prey/food item (Hill 1979b). This description of foraging is well explained by the foraging state in our model, which includes a combination of long and short movements with higher overall activity (i.e., acceleration), and variability in terms of directional persistence.

For aquatic species that inhabit shallow-water habitats, the semidiurnal (i.e., twice daily) tidal cycle imposes a regular change in the prevailing conditions (Gibson 2003). We found that Giant Mud Crab are most likely to forage when the tide is low (< 0.5 m) and incoming, while they are most likely to be inactive on an outgoing, high tide. This likely reflects exploration of shallow or intertidal foraging habitat (e.g., mangroves, mudflats; Hill *et al.* 1982; Demopoulos *et al.* 2008) as the tide is rising and they become inundated. Larger predators (e.g., *Carcharhinus leucas*, Bull Shark) are unlikely to be able to access these habitats when water levels are shallower, thereby lowering predation risk – a strategy employed by other estuarine species (e.g., *Acanthopagrus australis*, Yellowfin Bream; Taylor *et al.* 2013b). Similarly, the high probability of inactivity during high tide probably reflects a predator avoidance strategy, since Giant Mud Crab typically bury in the mud during periods of inactivity (Hill 1978; 1980). This description of foraging behaviour closely matches observations of the distribution of Giant Mud Crab in an intertidal region in a nearby estuary (Moreton Bay, Queensland; Hill *et al.* 1982). Additionally, foraging during strong incoming tides may also be indicative of the use of selective tidal-stream transport (Gibson *et al.* 2001), a behaviour exhibited by the species elsewhere (Alberts-Hubatsch 2015; Patterson *et al.* 2023). If crabs use incoming tides to facilitate movement this would decrease the energetic cost of foraging, thereby minimizing the energetic trade-off of searching for prey (Kramer and Weary 1991).

In general, warmer temperatures promote foraging in Giant Mud Crab (Hill 1980). This is probably due to increased metabolism (Junk *et al.* 2021), which may increase their motivation to feed and energetic requirements (Stoner 2004; Green *et al.* 2014). However, our analysis suggests that water temperature is not an important driver of fine-scale movement and behaviour of Giant Mud Crab. It

is likely that the results presented in Hill (1980) represent the seasonal influence of temperature (since they included a period of acclimation) on Giant Mud Crab behaviour, while our analysis is aimed at a much finer temporal resolution (e.g., observations every 15-min over several days) over which the variation of estuarine water temperature is comparatively low. Similarly, we did not find any evidence of nocturnal foraging, which is thought to represent a visual-predator avoidance strategy and has previously been reported for the species (Hill 1976; 1978). However, in highly turbid waters visual predation is somewhat reduced and overall predation pressure is likely to be much more diffuse. This may explain the lack of diel rhythm in Giant Mud Crab behaviour in the present study, and elsewhere (e.g., Robertson 1989).

Our analysis suggests that habitat type has little influence on crab behavioural dynamics, reflecting their status as opportunistic scavengers (Hill 1976; 1979b; Webley 2008). This is further supported by several stable isotope studies that saltmarsh grass (i.e., *Sporobolus virginicus*; Raoult *et al.* 2018; Jänes *et al.* 2022), seagrass (Connolly and Waltham 2015) and mangroves (Demopoulos *et al.* 2008) all contribute to Giant Mud Crab nutrition. Ultimately, stable isotopes provide an indication as to which habitats form the base of an animal's diet, and it is likely that crabs tagged in the present study are carnivorous; feeding on benthic macroinvertebrates (e.g., gastropods, crustaceans and molluscs; Hill 1976) that are primary consumers across these habitats.

## Implications for fisheries management

Quantifying drivers of animal movement is important for effective fisheries assessment, and management that relies on it (Cooke *et al.* 2016; Taylor *et al.* 2017a). For example, catch-per-unit-effort data is assumed to represent an index of relative abundance, and forms the basis of most contemporary stock assessments. However, use of catch-per-unit-effort as an index of abundance assumes that catchability of target individuals is constant (Maunder and Punt 2004; Maunder *et al.* 2006), and it is important to consider how environmental variation (e.g., low temperatures) influences foraging and responding to baited traps (Stoner 2004), when standardizing and interpreting catch rates (Maunder *et al.* 2006). Our results suggest that the tidal cycle is closely related to patterns in foraging, which could influence catchability, making it an important covariate to consider for catch rate standardisation, as is the case for the closely related Blue Swimmer Crab (*Portunus armatus*; Johnston *et al.* 2021b). However, many crab fishers deploy traps for several days at a time, making it difficult to fully capture the influence of semidiurnal tides (since there are multiple cycles during deployment) and proxies for tide magnitude may need to be considered (e.g., maximum difference between high and low tide). While our analysis suggests water temperature does not affect fine-scale behaviours, many studies have shown a strong temperature effect on Giant Mud Crab catch rates (Williams and Hill 1982; Meynecke *et al.* 2012b) and it is likely that this is still an important covariate to include in catch rate standardisation.

Several fisheries management strategies require information about the partitioning of time and behaviours among habitats. For example, stocking of hatchery-reared individuals requires that release locations support the suite of habitats required to support routine behaviours (e.g., foraging). Our analysis suggests that Giant Mud Crab may be highly adaptable in this regard, since they did not exhibit a clear preference for foraging in a particular habitat. However, overall productivity of the system must also be considered (e.g., Smith *et al.* 2019; Junk *et al.* 2021), and specific habitats (e.g., seagrass) may confer other benefits (e.g., enhanced survival of juveniles) that are not considered in our analysis (Hayes *et al.* 2022).

## Technical considerations and caveats

Tag loss is an important concern in acoustic tagging studies (Brownscombe *et al.* 2019; Sequeira *et al.* 2019), especially when externally tagging crustaceans, as the exoskeleton will be shed during ecdysis (Florko *et al.* 2021). In our study, this was avoided by only tagging large, recently moulted individuals and our approach was largely successful, resulting in only two tag loss incidents. These were likely a consequence of re-entering a trap rather than ecdysis, as glue was present on the carapace of these individuals and they were still in ‘hard-shell’ condition (Hay *et al.* 2005) when recaptured. Ultimately, the number of tagged crabs was within the range appropriate for making behavioural inferences at a population scale (Sequeira *et al.* 2019).

The importance of accounting for individual-level variation in behaviour is increasingly being recognized in animal tracking studies (Hertel *et al.* 2020). This variation can be due to true differences (i.e., animal ‘personality’; Hertel *et al.* 2020), variable deployment lengths and different (unmeasured) environmental contexts encountered by tagged individuals (DeRuiter *et al.* 2017). In our analysis, we found no evidence of individual-level variation in fine-scale behavioural dynamics of Giant Mud Crab. This may be because we only tagged large, adult crabs (119–135 mm CL) that had recently moulted. It is possible to modify this approach to account for sex-specific differences in behaviour (e.g., Towner *et al.* 2016), however this approach typically requires larger sample sizes to be reliable (McClintock 2021) and previous studies have not detected any differences in fine-scale behaviour between sexes (Hill 1980). Conversely, at greater temporal scales (e.g., seasonal) differences in movement have been observed. For example, mature female Giant Mud Crab typically migrate to oceanic waters to spawn (Hill 1994; Alberts-Hubatsch 2015; Hewitt *et al.* 2022a), facilitating the broad-scale dispersal of larvae (Hewitt *et al.* 2022b) which may explain the detection of a tagged female ~150 km north of our array in the coastal ocean. While males are typically thought to remain within estuaries, there have been a few examples of broad-scale migrations reported (Patterson *et al.* 2023).

Measurement error within our array was generally low (median = 1.26 m) and consistent with inherent GPS error (2-3 m), which was used to define the ‘known’ positions of receivers and reference tags. Additionally, some error may have been due to the presence of structurally complex habitats such as seagrass, mangroves and oyster farming infrastructure, which can lead to issues with signal attenuation (Swadling *et al.* 2020), refraction, or reflection (sometimes referred to as ‘multipath’; Vergeynst *et al.* 2020). Measurement error can increase the overlap between state-dependent distributions (e.g., similar step lengths) which may lead to difficulty differentiating states (Jonsen 2016). The inclusion of acceleration – which is not subject to any location measurement error – buffers against this in our analysis, and acceleration within the foraging state was markedly different from the inactive state. State classification can be further aided by fitting hidden Markov models in a semi-supervised context via the incorporation of ‘known’ (or labelled) states, which are typically derived from laboratory observations (Leos-Barajas *et al.* 2017). However, movements in a laboratory setting may not be representative of free-ranging animals (Leos-Barajas *et al.* 2017; Morgan *et al.* 2022) and incorporation of labelled data can be practically and computationally challenging (V. Leos-Barajas, *pers. comm.*).

Finally, acoustic tags must be submerged to record detections, and while it is possible for Giant Mud Crab to spend prolonged periods out of the water, this is uncommon for adults in the size range tagged (Hill *et al.* 1982) giving us confidence that this did not exert undue influence on the results presented here.

## Conclusions

Our description of Giant Mud Crab behavioural dynamics are in close agreement with observations of Giant Mud Crab behaviour (Hill 1976; 1979b; 1980; Wall *et al.* 2009) and qualitatively similar to a previous active-tracking study (that did not record/report any environmental data; Hill 1978). Furthermore, these results provide a mechanistic explanation of the observed distribution of the species across sub-intertidal habitats (Hill *et al.* 1982). We demonstrate the importance of the tidal cycle in driving foraging of Giant Mud Crab, likely as a strategy to minimize predation and maximize energetic efficiency, similar to other estuarine species (Taylor *et al.* 2013b). Determining such relationships adds to the evidence base supporting fisheries management (Cooke *et al.* 2016; Taylor *et al.* 2017a) and the patterns resolve aid the standardisation and interpretation of catch-per-unit-effort data.

# Environmental drivers of variation in Giant Mud Crab harvest rates

## Background and rationale

Catch rate standardisation is used in stock assessment to model time series of stock biomass (Punt *et al.* 2000; Maunder and Punt 2004; Maunder *et al.* 2006). Standardising commercial catch and effort data to account for changed fishing practices, increased fishing power, and impacts of management reform is the primary method used to minimise bias due to the confounding of apparent abundance patterns with such factors. This can also include partitioning out variance that may be associated with other influential factors, such as environmental variation (e.g., temperature, rainfall; Loneragan and Bunn 1999; Johnston *et al.* 2021b). Such information is rarely captured in standard logbook reporting, and this reporting also often occurs at coarse spatial and temporal resolution (e.g., Marriott *et al.* 2014). Model-based standardisations can incorporate time-varying catchability in simple CPUE-based stock assessments, rather than making an assumption of constant catchability where changes in CPUE may be attributed to changes in abundance, but in reality may be due to variations in catchability. To achieve this, however, the influence of multiple factors need to be quantified, including the effect of local environmental conditions, nuances of gear (e.g., size and shape of traps, presence of escape gaps), and unreported measures of effort (e.g., 'soak [immersion] time' of traps, or 'searching time' for trawl or haul shots).

Fisheries observer programs represent a useful 'middle-ground' between fishery-independent surveys and compulsory logbook reporting for collecting data on exploited stocks. These programs involve a scientific observer accompanying commercial operators during normal fishing operations, to record biological and operational information, and validate logbook records. Such programs allow scientists to collect quality-controlled biological and operational information, that is not captured within standard logbook reporting, at high spatial and temporal resolution without incurring the cost of fishery-independent sampling. This not only validates self-reported logbook data, but also supports the exploration of other factors that may impact catchability that are not normally captured in fishing logbooks, such that they can be included in catch rate standardisations.

In fisheries that employ passive gear types (e.g., baited traps), the catchability of target individuals is closely linked to their movement patterns (e.g., foraging, migration), which can be influenced by environmental variation. For example, mature female Giant Mud Crab migrate to ocean waters to spawn in response to declines in temperature and high flow events (e.g., rainfall; Hewitt *et al.* 2022a). Moreover, females of the species typically suppress feeding in the lead up to spawning (Heasman 1980) which may decrease their probability of being caught. Conversely, warmer temperatures promote foraging (Hill 1980; Hyland *et al.* 1984) and generally enhance catch rates (Williams and Hill 1982). In addition, estuarine flow (i.e., rainfall), the lunar cycle and wind/tidal mixing can influence movement in portunid crabs, which may also have implications for catchability (Loneragan and Bunn 1999; Spencer *et al.* 2019; Johnston *et al.* 2021b; Hewitt *et al.* 2022a).

Here, we present analysis of data collected from an extensive fishery-wide observer program, to examine putative factors impacting Giant Mud Crab catch rates—specifically, we examine the influence of soak time and key environmental variables. The relationships are considered in the context of species biology, and utility in broader modelling of portunid crab abundance.

## Methods

### Fishery observer program

Sampling was undertaken by scientific observers accompanying commercial fishers during normal operations from the beginning of the austral spring (September) in 2018 until the end of the austral winter (August) in 2020. The six estuaries that were monitored were distributed along approximately 500 km of the southeast Australian coast, spanning subtropical–temperate latitudes. These estuaries account for ~80 % of commercial harvest of Giant Mud Crab in NSW and include Tweed River (28.17°S), Richmond River (28.88°S), Clarence River (29.43°S), Macleay River (30.87°S), Wallis Lake (32.17°S) and Port Stephens (32.71°S); Figure 1, Table 20). These estuaries are all classified as wave-dominated, barrier estuaries with permanently open (trained) entrances, except for Port Stephens which is a tide-dominated, drowned river valley with a permanently open (untrained) entrance (Table 20). The estuaries vary widely in terms of waterway (17.9–129.8 km<sup>2</sup>) and catchment area (1,000–22,400 km<sup>2</sup>), and support typical vegetated estuarine habitats including seagrass, mangrove and saltmarsh (Table 20).

Planned observer coverage was stratified using recently reported patterns in effort through a theoretical two-factor matrix which allocated the number of available observed fishing days among months, according to a weighting that reflected the patterns in reported average fishing effort (for the period 2014/15–2016/17). For observed fisher-days, observers recorded operational data including gear specifications (trap shape, number of entrances/escape gaps), bait type, soak time (d), location, as well as catch data including number, size (CL) and sex of all Giant Mud Crab caught (legal and sub-legal; see Barnes *et al.* 2022 for full description of data collection).

### Environmental data

The term ‘environmental data’ refers the data as it was supplied by the relevant agencies, distinct from ‘environmental covariate’ which refers to the data as it was summarized and included in modelling (see *Data processing and analysis* below). Environmental data obtained for this study included water temperature (°C), river flow (m<sup>3</sup> s<sup>-1</sup>), wind speed (km h<sup>-1</sup>) and lunar phase (radians). Water temperature (°C) was obtained from WaterNSW monitoring stations (<https://realtimedata.watarnsw.com.au/>; reported as daily means), or *in-situ* HOBO U24-002-C conductivity/salinity loggers (hereafter ‘*in-situ* loggers’; HOBO Data Loggers Australia, OneTemp Pty Ltd, Australia; recorded at 15-minute intervals) maintained by the project team. No temperature data was available for the Tweed River, and values from the nearby Richmond River (~80 km south) were substituted based on similarity between these systems (Scanes *et al.* 2020a). River flow (m<sup>3</sup> s<sup>-1</sup>) was also obtained from a public archive of data collected at WaterNSW monitoring stations (reported as daily means; <https://realtimedata.watarnsw.com.au/>). Wind speed (km h<sup>-1</sup>) was obtained from Bureau of Meteorology (BOM) weather monitoring stations (reported as daily means; <http://www.bom.gov.au/climate/data/>). Lunar phase (radians) was calculated using the R package ‘lunar’, where 0 and 2π = new moon and π = full moon. For each trap, environmental data was obtained from the nearest monitoring station (as the crow flies), with spatial calculations conducted using the R package ‘sf’ (Pebesma 2018).

**Table 20** Characteristics of study estuaries adapted from Roy *et al.* (2001), with areal coverage of mangrove, seagrass and saltmarsh for each study estuary also included (as reported in Creese *et al.* 2009)

| Estuary        | Latitude (°S) | Estuary type                        | Entrance        | Water area (km <sup>2</sup> ) | Catchment area (km <sup>2</sup> ) | Mangrove area (km <sup>2</sup> ) | Seagrass area (km <sup>2</sup> ) | Saltmarsh area (km <sup>2</sup> ) |
|----------------|---------------|-------------------------------------|-----------------|-------------------------------|-----------------------------------|----------------------------------|----------------------------------|-----------------------------------|
| Tweed River    | 28.17         | Wave-dominated barrier estuary      | Open, trained   | 17.9                          | 1 000                             | 4.0                              | 0.8                              | 0.8                               |
| Richmond River | 28.88         | Wave-dominated barrier estuary      | Open, trained   | 19.1                          | 6 850                             | 6.0                              | 0.3                              | 0.6                               |
| Clarence River | 29.43         | Wave-dominated barrier estuary      | Open, trained   | 89.2                          | 22 400                            | 7.7                              | 0.8                              | 2.9                               |
| Macleay River  | 30.87         | Wave-dominated barrier estuary      | Open, trained   | 18.2                          | 11 385                            | 5.7                              | 1.0                              | 4.2                               |
| Wallis Lake    | 32.17         | Wave-dominated barrier estuary      | Open, trained   | 85.6                          | 1 420                             | 1.5                              | 31.9                             | 5.9                               |
| Port Stephens  | 32.71         | Tide-dominated drowned river valley | Open, untrained | 129.8                         | 7 150                             | 24.1                             | 14.5                             | 14.4                              |

**Table 21** Number of observer trips (*n*), traps deployed (*n*) and total soak time (d; from left to right) in each estuary per month throughout the observer program (2018–2020).

| Month | Estuary               |                       |             |                       |                       |             |                       |                       |             |                       |                       |             |                       |                       |             |                       |                       |             |
|-------|-----------------------|-----------------------|-------------|-----------------------|-----------------------|-------------|-----------------------|-----------------------|-------------|-----------------------|-----------------------|-------------|-----------------------|-----------------------|-------------|-----------------------|-----------------------|-------------|
|       | Tweed River           |                       |             | Richmond River        |                       |             | Clarence River        |                       |             | Macleay River         |                       |             | Wallis Lake           |                       |             | Port Stephens         |                       |             |
|       | Trips<br>( <i>n</i> ) | Traps<br>( <i>n</i> ) | Soak<br>(d) | Trips<br>( <i>n</i> ) | Traps<br>( <i>n</i> ) | Soak<br>(d) | Trips<br>( <i>n</i> ) | Traps<br>( <i>n</i> ) | Soak<br>(d) | Trips<br>( <i>n</i> ) | Traps<br>( <i>n</i> ) | Soak<br>(d) | Trips<br>( <i>n</i> ) | Traps<br>( <i>n</i> ) | Soak<br>(d) | Trips<br>( <i>n</i> ) | Traps<br>( <i>n</i> ) | Soak<br>(d) |
| Jan   | 8                     | 122                   | 195         | 6                     | 122                   | 122         |                       |                       |             | 8                     | 251                   | 286         | 10                    | 308                   | 599         | 4                     | 114                   | 114         |
| Feb   | 6                     | 81                    | 139         | 9                     | 171                   | 171         |                       |                       |             | 7                     | 189                   | 213         | 5                     | 106                   | 184         | 3                     | 77                    | 140         |
| Mar   | 6                     | 84                    | 135         | 12                    | 236                   | 279         | 1                     | 9                     | 27          | 12                    | 305                   | 406         | 1                     | 26                    | 26          | 8                     | 219                   | 251         |
| Apr   | 2                     | 33                    | 49          | 3                     | 59                    | 59          | 1                     | 4                     | 4           | 10                    | 235                   | 321         | 3                     | 47                    | 123         | 3                     | 26                    | 58          |
| May   | 2                     | 35                    | 53          | 2                     | 38                    | 38          |                       |                       |             | 3                     | 87                    | 194         |                       |                       |             |                       |                       |             |
| Jun   |                       |                       |             | 4                     | 85                    | 234         |                       |                       |             | 4                     | 100                   | 260         |                       |                       |             |                       |                       |             |
| Jul   |                       |                       |             |                       |                       |             |                       |                       |             | 3                     | 119                   | 398         |                       |                       |             |                       |                       |             |
| Aug   |                       |                       |             | 4                     | 79                    | 219         |                       |                       |             | 4                     | 56                    | 232         |                       |                       |             |                       |                       |             |
| Sep   |                       |                       |             |                       |                       |             |                       |                       |             | 5                     | 73                    | 226         |                       |                       |             |                       |                       |             |
| Oct   | 3                     | 33                    | 33          | 3                     | 60                    | 270         | 2                     | 10                    | 10          | 6                     | 157                   | 679         | 2                     | 74                    | 205         | 1                     | 44                    | 132         |
| Nov   | 2                     | 38                    | 38          | 1                     | 20                    | 20          |                       |                       |             | 4                     | 68                    | 88          |                       |                       |             |                       |                       |             |
| Dec   | 8                     | 82                    | 135         | 2                     | 42                    | 42          | 1                     | 20                    | 80          | 11                    | 282                   | 424         | 9                     | 234                   | 465         | 1                     | 4                     | 28          |
| Total | 37                    | 508                   | 777         | 46                    | 912                   | 1,454       | 5                     | 43                    | 121         | 77                    | 1,922                 | 3,727       | 30                    | 795                   | 1,602       | 20                    | 484                   | 723         |

## Data processing and analysis

All data processing and statistical analyses were conducted in R (v. 4.0.2) language for statistical computing (R Core Team 2022). Traps with a soak time > 10 days ( $n = 22$ ) were removed from the analysis as these are unlikely to occur during normal operations (i.e., assumed outliers). In addition, we removed trap lifts where river flow exceeded  $1,000 \text{ m}^3 \text{ s}^{-1}$  as this led to unreasonable uncertainty in initial model fitting attempts—there were very few observations beyond this value ( $n = 180$ , ~3 % of all trap lifts). Within the constraints of normal fishing operations, it was not possible for observers to weigh each individual crab, so weight was estimated using an empirical carapace length (CL) weight ( $W$ ) relationship ( $W = a \times \text{CL}^b$ ). The parameters  $a$  ( $0.754 \pm 0.043$ ) and  $b$  ( $2.901 \pm 0.0422$ ) were estimated ( $R^2 = 0.83$ ) from measurements of 992 individuals from across NSW.

To model the effects of environmental covariates on catches of Giant Mud Crab, we used a generalized additive mixed model (GAMM or hierarchical GAM; Pedersen *et al.* 2019) using the R package 'mgcv' ('Mixed GAM Computational Vehicle'; Wood 2011; Wood and Fasiolo 2017). Within this framework, we estimated smooth functional relationships between catch of legal-sized (> 85 mm CL) crabs, in terms of abundance (crabs trap<sup>-1</sup>) and biomass (kg trap<sup>-1</sup>), and soak time (d), mean temperature (°C) during the trap immersion period, mean river flow ( $\text{m}^3 \text{ s}^{-1}$ ) in the 7-days prior to trap deployment (to capture lagged effects), mean wind speed ( $\text{km h}^{-1}$ ) during the soak and the lunar phase (radians) when the trap was set. Models were fit via restricted maximum likelihood (REML) assuming a negative binomial error distribution (with a log-link function) for relative abundance and a Tweedie error distribution (with a log-link function; Foster and Bravington 2013) for relative biomass. All environmental covariates were modelled using thin plate regression splines (Wood 2003), except for lunar phase which was modelled as a cyclic cubic spline. Each spline is the sum of  $k$  simpler basis functions, where the value of  $k$  determines the maximum complexity (i.e., flexibility or 'wiggleness') of the smoother. Within this framework, overfitting is avoided by multiplying the complexity of a smooth by an estimated smoothing penalty (denoted by  $\lambda$ ) and subtracting it from the model log-likelihood (Pedersen *et al.* 2019). However, the resulting smooth is completely data-driven and may not be biologically/ecologically sensible (i.e., excessive wiggleness without a reasonable mechanistic interpretation), so as an additional step to avoid overfitting we restricted  $k = 5$ . Variable selection was automated within our model fitting framework by estimating a second penalty ( $\lambda^*$ ) that applies to linear smooths, thereby allowing their removal from the model if warranted (i.e., estimated degrees of freedom [EDF]  $\sim 0$ ; Marra and Wood 2011).

For each covariate, we specified an interaction with estuary (*sensu* Rose *et al.* 2012), as such our model incorporates a separate smoother for each estuary into a single model across estuaries (Rose *et al.* 2012). In addition, we implemented a mixed-effects structure by specifying random intercepts for estuary, fisher ID, trap shape, number of entrances and number of escape gaps, to account for differences in skill and strategy (i.e., searching) amongst commercial operators and efficacy of the gears employed (Butcher *et al.* 2012; Broadhurst *et al.* 2014; Barnes *et al.* 2022). The R packages 'gratia' and 'ggplot2' were used to visually assess model assumptions and produce figures.

## Results

The observer dataset used in this analysis included 215 observer-days, which equated to 4,664 trap deployments for a total soak time of 8,404 days (Table 21). In total, 6,022 crabs were harvested with an estimated combined weight of 3,605 kg. Observer days mostly occurred during spring–autumn months (i.e., October–May), and varied widely between estuaries, ranging from 5–77 observer-days

for total soak times of 121–3,727 days (Table 21; note that Table 21 includes only observer days that were included in the analysis).

Model checking did not indicate any issues with model assumptions (Supplementary Figures X–Y). On an estuary-by-estuary basis, results from the relative abundance model and relative biomass model were broadly similar (Table 22), explaining 33.8 % and 31.8 % of the deviance in crab catches, respectively. In both models, soak time was removed as a covariate in all estuaries (i.e.,  $EDF \sim 0$ ), except for Richmond River (Table 22), however the effect here was minor (Figure 73). In the estuaries from Macleay River northward, there was an increase in crab catches at warmer temperatures (Figure 74) while in the southern estuaries (i.e., Wallis Lake, Port Stephens) temperature was removed as a covariate (Table 22). We note that the comparatively small number of few observer trips at the Clarence River resulted in a sparse distribution across observed temperatures (Figure 74), which may explain the highly variable (and probably unrealistic) estimated response (Figure 74). In the Richmond River, Clarence River and Macleay River, flow had a positive, approximately lineal effect on crab catches, although in the Macleay River (where the curve was better conditioned by higher flow events) there was some evidence that the increase in the effect diminished under higher flow scenarios (Figure 75). In Macleay River and Port Stephens, crab catch generally increased with wind speed, while it was removed as a covariate in all other estuaries (Table 22; Figure 76). Finally, there was a moderate cyclic relationship between lunar phase and crab catch in all estuaries, except for abundance in the Clarence River. The new moon (i.e., lunar phase = 0 or  $2\pi$  radians) generally resulted in the highest crab catches (Table 22; Figure 77), but in Port Stephens there was also a positive effect of the full moon (i.e., lunar phase =  $\pi$  radians; Figure 77) but only crab biomass (not abundance).

## Discussion

Analysis of patterns in commercially harvested abundance and biomass in an extensive fishery-wide observer program showed that a number of environmental covariates influence the catch of Giant Mud Crab. Primarily, our results showed that crab traps are likely to quickly become saturated (possibly within < 24 h), warmer temperatures increase catches of the species, but river flow, wind speed and the lunar cycle also influence Giant Mud Crab catch rates. These findings support the development of catch rate standardisation and stock assessment, as well as highlight the link between estuarine variability and fisheries productivity which will support broader scale modelling of abundance variability.

### Drivers of variation in Giant Mud Crab catch

Our analyses indicated that across the scale typical of trap deployments by commercial fishers in NSW, trap soak time did not affect catches of Giant Mud Crab. While we cannot explicitly identify the cause of this from our data, ‘trap saturation’ may have contributed to this outcome. Trap saturation is known to occur within the first 6–12 hours post deployment for Giant Mud Crab (Robertson 1989), as commercial traps are highly selective for large adults (especially when equipped with escape gaps; Butcher *et al.* 2012; Broadhurst *et al.* 2014; Barnes *et al.* 2022), which can be aggressive towards other crabs (Williams and Hill 1982; Huntingford *et al.* 1995; Butcher *et al.* 2012). The rapid accumulation of large crabs in the trap may discourage additional crabs from entering the trap, leading to ‘saturation’ occurring over short periods. Unfortunately, no soak times less than 24 hours were recorded in our study, so this effect could not be further examined within the current data set.

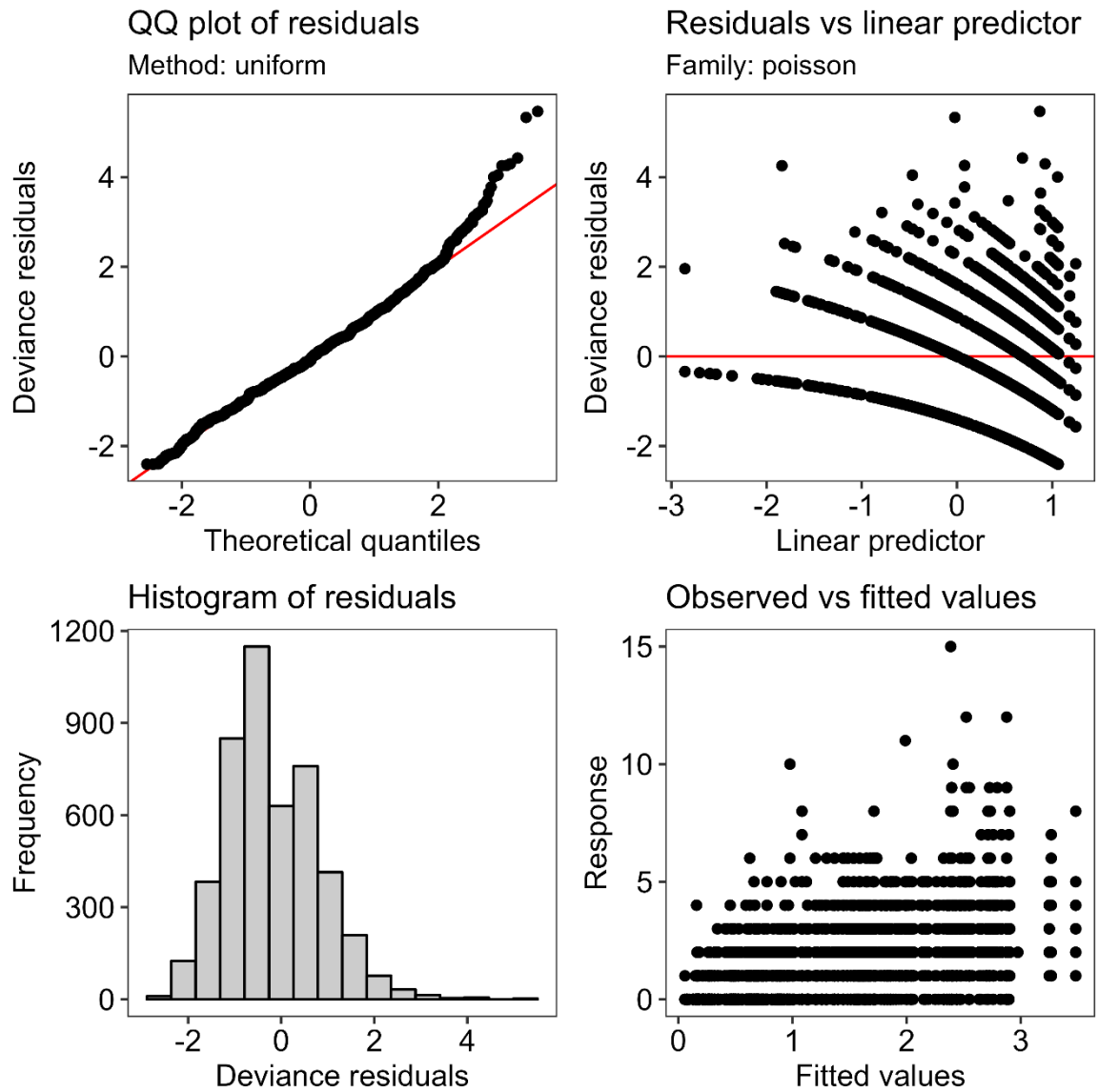


**Figure 71** Model diagnostics plots for the abundance model, including residual QQ-plot (top left), residuals vs. linear predictor (top right), histogram of residuals (bottom left) and observed vs. fitted values (bottom right).

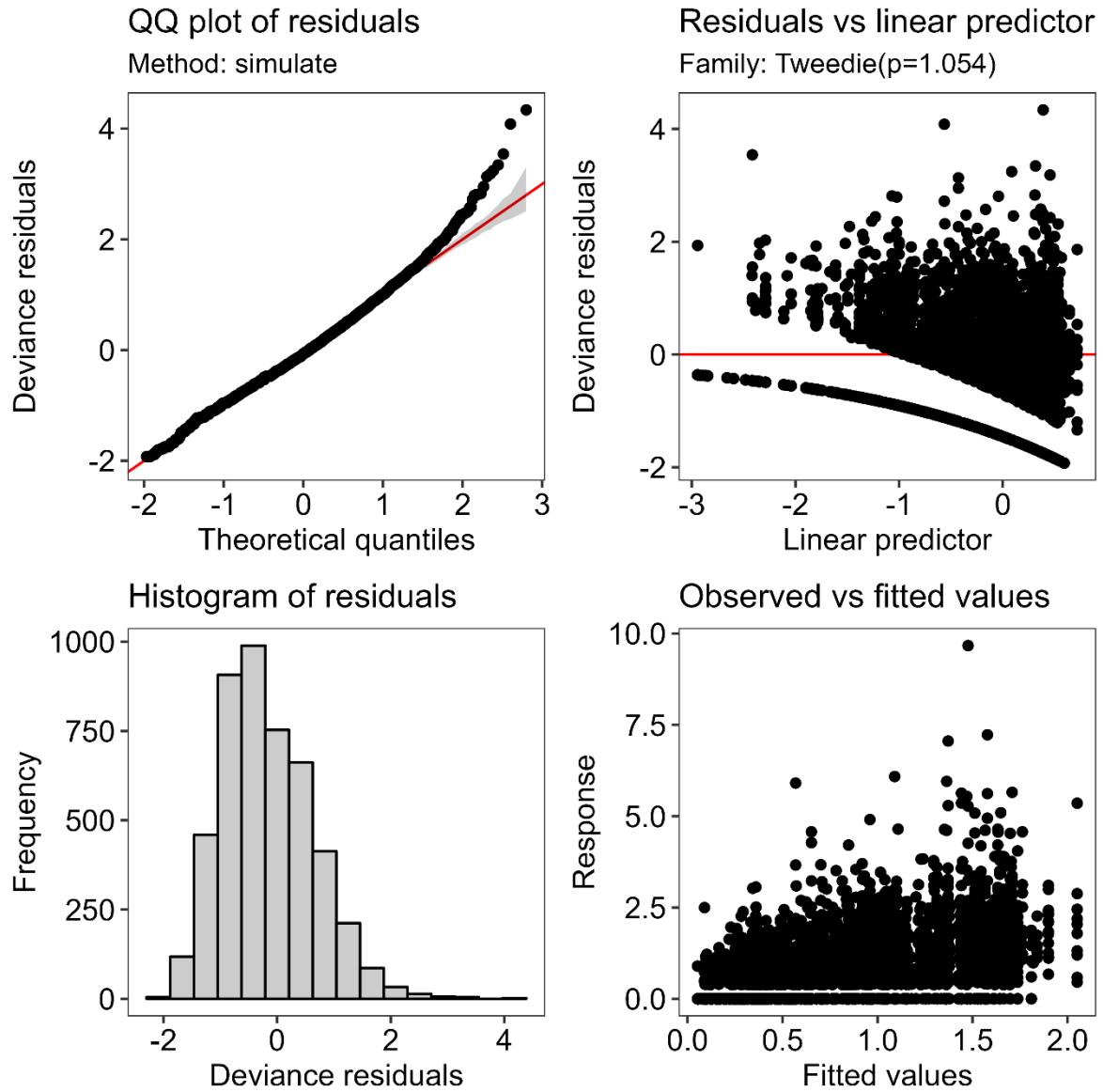


**Figure 72** Model diagnostics plots for the biomass model, including residual QQ-plot (top left), residuals vs. linear predictor (top right), histogram of residuals (bottom left) and observed vs. fitted values (bottom right).

**Table 22** Summary of estuary-specific model smoothers for abundance (crabs trap<sup>-1</sup>) and biomass (kg trap<sup>-1</sup>) of Giant Mud Crab in southeast Australian estuaries. Bold values indicate statistical significance.

| <u>Abundance model</u>                 |             |              |             |                |              |             |                |              |             |               |               |             |             |          |          |               |              |             |  |
|--|-------------|--------------|-------------|----------------|--------------|-------------|----------------|--------------|-------------|---------------|---------------|-------------|-------------|----------|----------|---------------|--------------|-------------|--|
|  | Tweed River |              |             | Richmond River |              |             | Clarence River |              |             | Macleay River |               |             | Wallis Lake |          |          | Port Stephens |              |             |  |
| Covariate                              | EDF         | $\chi^2$     | <i>P</i>    | EDF            | $\chi^2$     | <i>P</i>    | EDF            | $\chi^2$     | <i>P</i>    | EDF           | $\chi^2$      | <i>P</i>    | EDF         | $\chi^2$ | <i>P</i> | EDF           | $\chi^2$     | <i>P</i>    |  |
| Soak (days)                            | 0.00        | 0.00         | 0.52        | <b>1.79</b>    | <b>17.30</b> | <b>0.00</b> | 0.00           | 0.00         | 0.49        | 0.00          | 0.00          | 0.81        | 0.00        | 0.00     | 0.52     | 0.00          | 0.00         | 0.68        |  |
| Temperature (°C)                       | <b>0.98</b> | <b>68.56</b> | <b>0.00</b> | <b>3.59</b>    | <b>63.36</b> | <b>0.00</b> | <b>1.85</b>    | <b>19.77</b> | <b>0.04</b> | <b>3.82</b>   | <b>535.27</b> | <b>0.00</b> | 0.53        | 1.61     | 0.15     | 0.00          | 0.00         | 0.36        |  |
| Flow (m <sup>3</sup> s <sup>-1</sup> ) | 0.00        | 0.00         | 0.92        | <b>0.89</b>    | <b>8.34</b>  | <b>0.00</b> | <b>0.73</b>    | <b>2.89</b>  | <b>0.03</b> | <b>2.86</b>   | <b>410.32</b> | <b>0.00</b> | 0.00        | 0.00     | 0.39     | 0.00          | 0.00         | 0.91        |  |
| Wind speed (km h <sup>-1</sup> )       | 0.00        | 0.00         | 0.54        | 0.00           | 0.00         | 0.38        | 0.00           | 0.00         | 0.99        | <b>2.49</b>   | <b>106.86</b> | <b>0.00</b> | 0.00        | 0.00     | 0.32     | <b>1.32</b>   | <b>30.31</b> | <b>0.00</b> |  |
| Lunar phase (radians)                  | <b>2.49</b> | <b>74.53</b> | <b>0.01</b> | <b>2.52</b>    | <b>29.87</b> | <b>0.00</b> | 0.00           | 0.00         | 0.15        | <b>2.20</b>   | <b>115.1</b>  | <b>0.00</b> | 1.27        | 8.13     | 0.19     | 0.00          | 0.00         | 0.41        |  |
| <u>Biomass model</u>                   |             |              |             |                |              |             |                |              |             |               |               |             |             |          |          |               |              |             |  |
| Soak (days)                            | 0.00        | 0.00         | 0.40        | <b>1.92</b>    | <b>9.61</b>  | <b>0.00</b> | 0.00           | 0.00         | 0.17        | 0.00          | 0.00          | 0.52        | 0.05        | 0.03     | 0.31     | 0.00          | 0.00         | 0.52        |  |
| Temperature (°C)                       | <b>0.98</b> | <b>15.04</b> | <b>0.00</b> | <b>3.78</b>    | <b>20.12</b> | <b>0.00</b> | <b>1.79</b>    | <b>4.49</b>  | <b>0.00</b> | <b>3.80</b>   | <b>101.05</b> | <b>0.00</b> | 0.00        | 0.00     | 0.37     | 0.00          | 0.00         | 0.71        |  |
| Flow (m <sup>3</sup> s <sup>-1</sup> ) | 0.00        | 0.00         | 0.89        | <b>0.94</b>    | <b>4.14</b>  | <b>0.00</b> | 0.00           | 0.00         | 0.09        | <b>2.95</b>   | <b>86.85</b>  | <b>0.00</b> | 0.00        | 0.00     | 0.42     | 0.00          | 0.00         | 0.41        |  |
| Wind speed (km h <sup>-1</sup> )       | 0.24        | 0.15         | 0.25        | 0.00           | 0.00         | 0.79        | 0.00           | 0.00         | 0.57        | <b>2.49</b>   | <b>24.14</b>  | <b>0.00</b> | 0.00        | 0.00     | 0.43     | <b>0.88</b>   | <b>2.45</b>  | <b>0.00</b> |  |
| Lunar phase (radians)                  | <b>2.45</b> | <b>18.52</b> | <b>0.00</b> | <b>2.52</b>    | <b>10.72</b> | <b>0.00</b> | <b>0.93</b>    | <b>1.25</b>  | <b>0.02</b> | <b>2.24</b>   | <b>39.92</b>  | <b>0.00</b> | 0.57        | 0.46     | 0.32     | <b>2.65</b>   | <b>8.08</b>  | <b>0.04</b> |  |

EDF: estimated degrees of freedom.

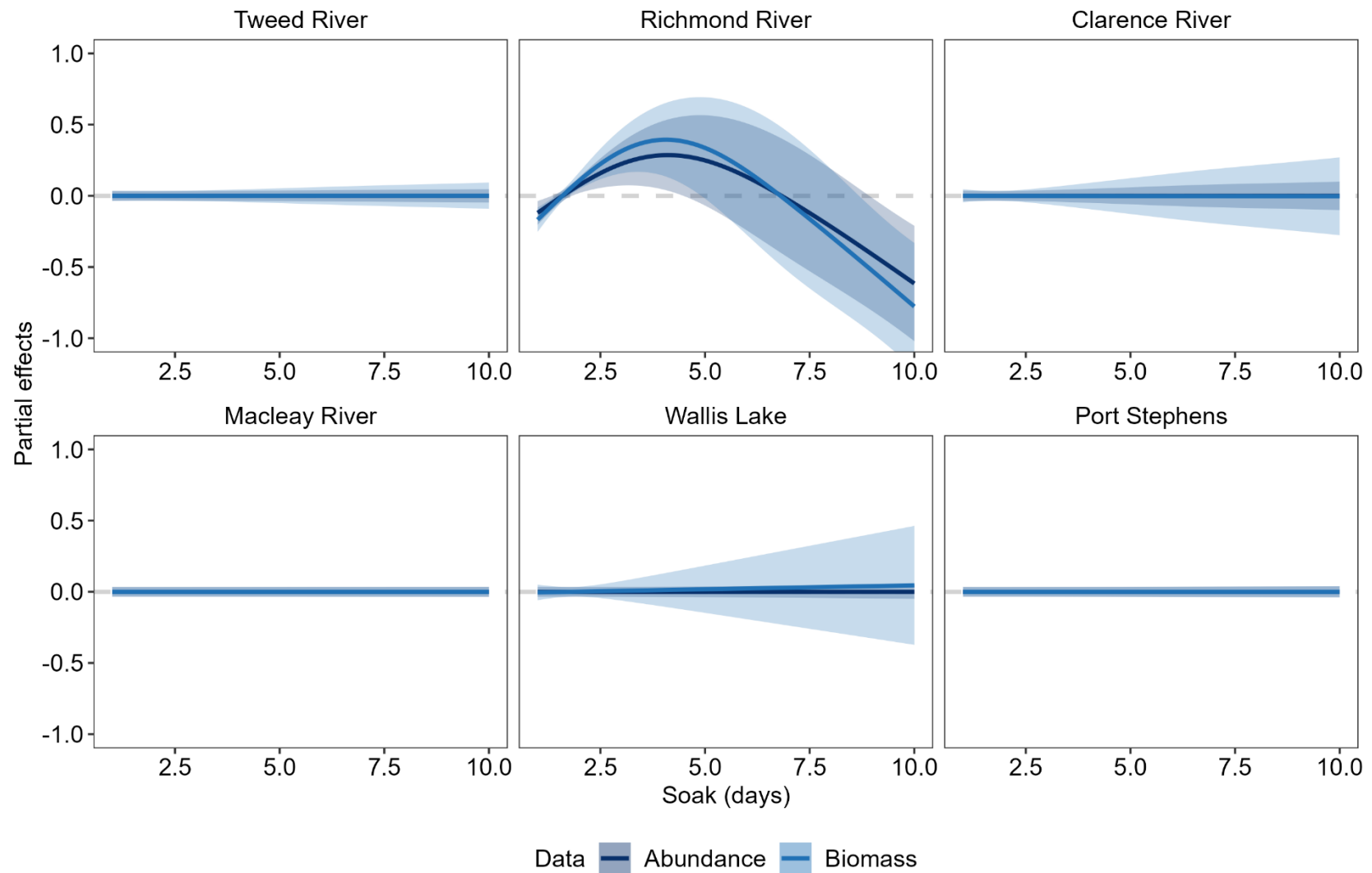


**Figure 73** Estimated partial effects ( $\pm 95\%$  CI) of soak time (days) on abundance (crabs trap<sup>-1</sup>; dark blue) and biomass (kg trap<sup>-1</sup>; light blue) of Giant Mud Crab in southeast Australian estuaries. Rugs indicate the distribution of observations.

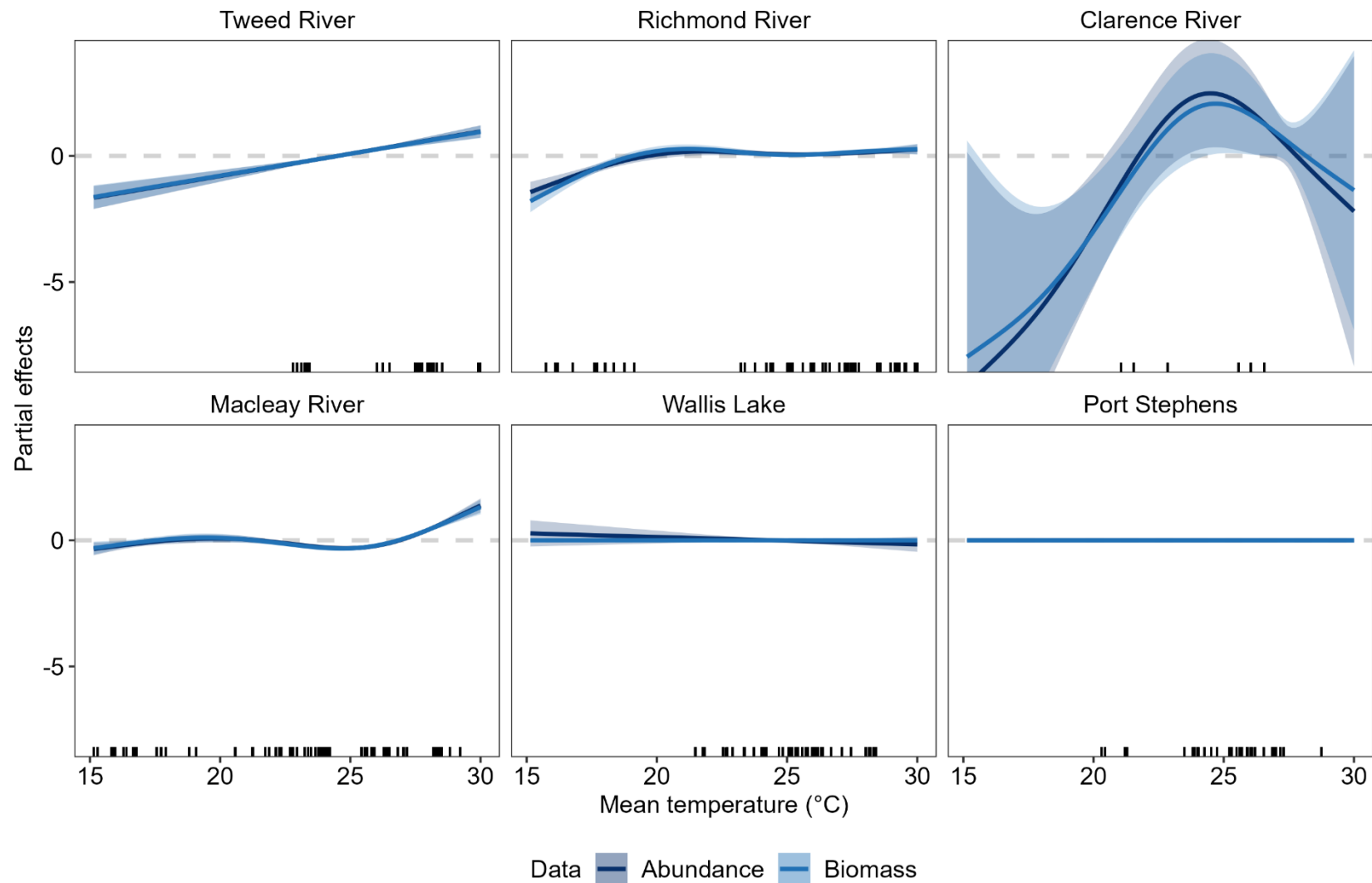


**Figure 74** Estimated partial effects ( $\pm 95\%$  CI) of mean temperature ( $^{\circ}\text{C}$ ) during trap deployment on abundance (crabs  $\text{trap}^{-1}$ ; dark blue) and biomass ( $\text{kg trap}^{-1}$ ; light blue) of Giant Mud Crab in southeast Australian estuaries. Rugs indicate the distribution of observations.

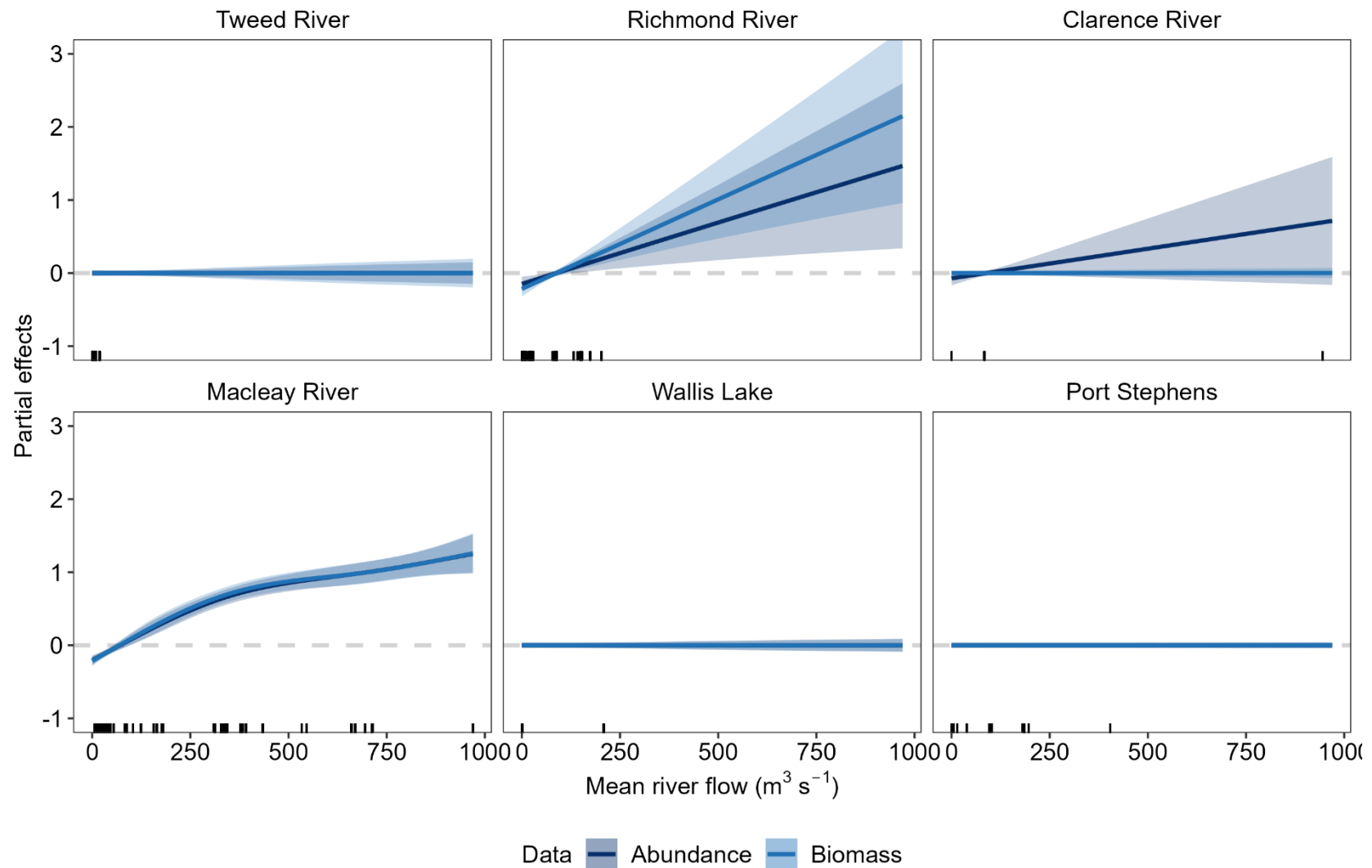


**Figure 75** Estimated partial effects ( $\pm 95\%$  CI) of mean river flow ( $\text{m}^3 \text{s}^{-1}$ ) in the 7 days prior to trap deployment on abundance (crabs  $\text{trap}^{-1}$ ; dark blue) and biomass ( $\text{kg trap}^{-1}$ ; light blue) of Giant Mud Crab in southeast Australian estuaries. Rugs indicate the distribution of observations

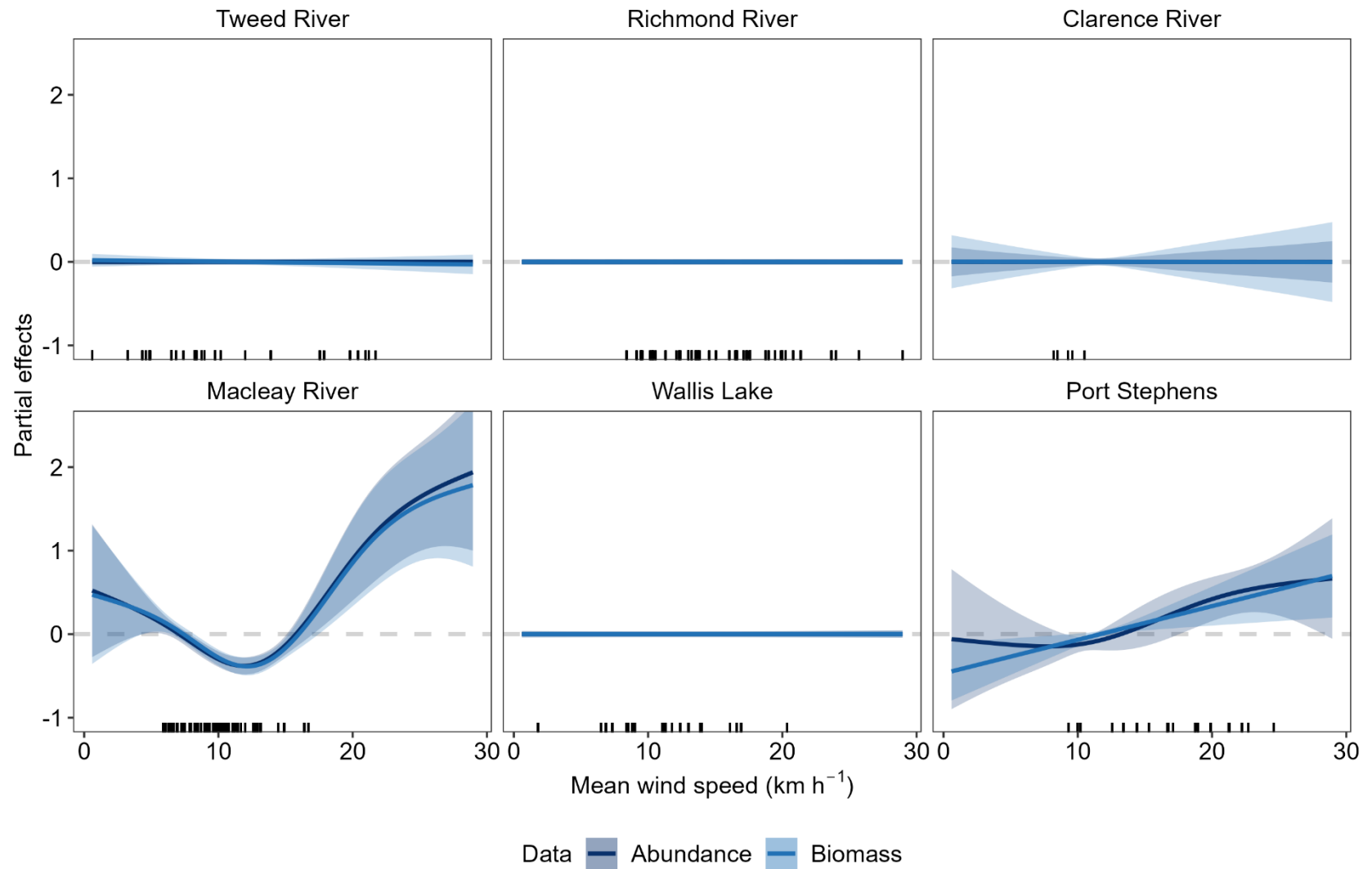


**Figure 76** Estimated partial effects ( $\pm$  95 % CI) of mean wind speed (km h<sup>-1</sup>) during trap deployment on abundance (crabs trap<sup>-1</sup>; dark blue) and biomass (kg trap<sup>-1</sup>; light blue) of Giant Mud Crab in southeast Australian estuaries. Rugs indicate the distribution of observations.

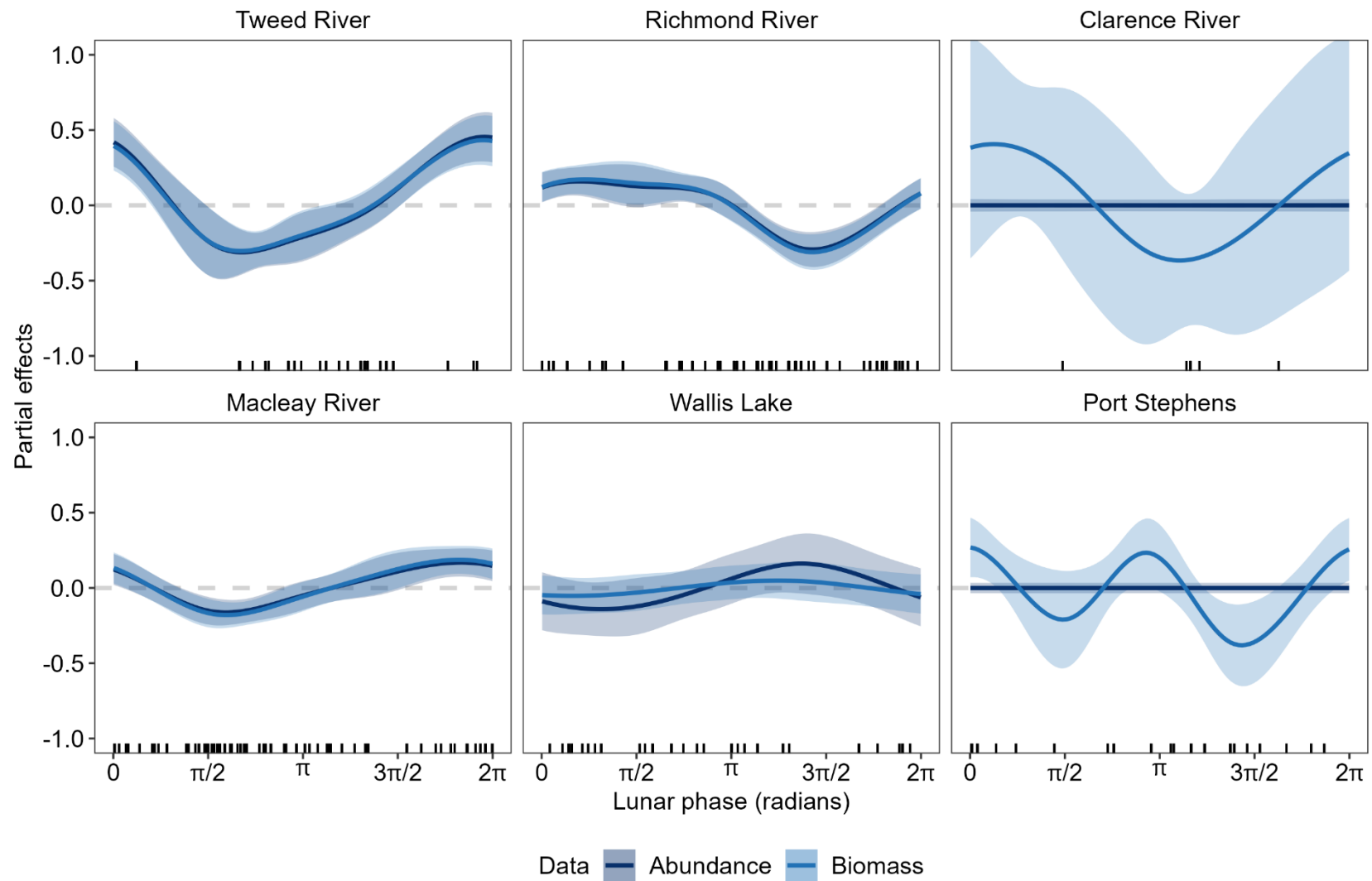


**Figure 77** Estimated partial effects ( $\pm 95\%$  CI) of lunar phase (radians) at trap deployment on abundance (crabs trap<sup>-1</sup>; dark blue) and biomass (kg trap<sup>-1</sup>; light blue) of Giant Mud Crab in southeast Australian estuaries. Note: 0 and  $2\pi$  radians = new moon;  $\pi$  = full moon. Rugs indicate the distribution of observations.

Overall, water temperature was the most influential environmental covariate in our analysis. The most likely mechanism explaining the influence of warmer waters is that crabs are ectothermic and increases in temperature elevate their metabolism (Junk *et al.* 2021). This subsequently increases their propensity to forage (Hill 1980) and feed (Stoner 2004; Green *et al.* 2014), thereby increasing their catchability. This is a common observation for Giant Mud Crab (e.g., Williams and Hill 1982; Meynecke *et al.* 2012a), other portunid crabs (e.g., Blue Swimmer Crab, *Portunus armatus*; Johnston *et al.* 2021b) and decapod crustaceans more broadly (e.g., Southern Rock Lobster, *Jasus edwardsii*; Ziegler *et al.* 2003). The reason behind the limited effect of temperature in the southern estuaries is uncertain, however may be due to catch rates within these estuaries being more closely linked to abundance (or 'availability') of crabs. This explanation makes sense given that these estuaries are close to the poleward boundary of the species distribution, and bottlenecks in the recruitment of coastally spawned larvae to these estuaries may arise from variability in the East Australian Current (Hewitt *et al.* 2022b).

Increases in estuary inflow generally improve the productivity of estuarine fisheries (Gillson 2011). For Giant Mud Crab, several studies have shown that inflow enhances motility, and also has an aggregative effect, which in turn enhances catch rates (Hill *et al.* 1982; Loneragan and Bunn 1999; Meynecke *et al.* 2012b). While our results are generally in agreement with this, they were not evident in all estuaries. Considering the geomorphological information in Table 20, the effect of flow appears to occur mainly in estuaries that have a smaller ratio between catchment area and waterway area. This feature would generally exacerbate the influence of rainfall on estuarine processes, and is likely to be responsible for the effects observed. We also wish to point out that the Macleay River experienced the broadest distribution of flows during the study period, so the response observed in this estuary may be more indicative of the response expected across a broader range of flows. In contrast, there was no effect of flow in Wallis Lake and Port Stephens. These estuaries are large embayments (rather than lineal estuaries), with larger waterway area per unit catchment, which likely results in a diminished influence of high flows. When considering the effect of flow, it is also important to consider potential changes in fisher behaviour, whereby commercial operators who have multiple endorsements may switch to targeting other species (e.g., School Prawn, *Metapenaeus macleayi*; Glaister 1978) which aggregate under high flow conditions (Gillson 2011).

There was some evidence that increased wind speed was associated with enhanced catches of Giant Mud Crab; however, the response differed between estuaries. A similar effect has been observed for Blue Swimmer Crab (Johnston *et al.* 2021b). While the exact mechanisms for this are unclear, the effect could arise through some combination of decreased visual predation risk (Lunt and Smee 2014), and increased mixing which may enhance transmission of bait plumes, or elevate bottom temperatures where crabs typically reside (Drinkwater *et al.* 2006). Furthermore, the estuary-specific patterns may be influenced by geomorphological nuances of individual estuaries, such as the presence and location of winding and branching arms, and where fishers concentrate their fishing effort within these systems and relative to these features.

Finally, our results suggest that catchability of Giant Mud Crab increases around the new moon. The comparatively low illumination during the new moon (relative to the full moon) may offer lower visual predation risk for crabs (Wassenberg and Hill 1994), however this part of the lunar cycle also brings larger tides and greater overall tidal amplitude. This may contribute to more preferential foraging conditions, greater inundation of intertidal habitats (see *Movement, habitat use, and behaviour of free-ranging Giant Mud Crab*), and as well as supporting increased movement rates through selective tidal-stream transport (Gibson *et al.* 2001). The deviating pattern within Port Stephens suggests that 'larger' Giant Mud Crab may be more catchable during both the new and full moon (since there was no overall effect on abundance, but biomass exhibited a clear cyclic pattern). The exact cause of this pattern is unclear, although this estuary has considerably more intertidal

habitat (Table 20), which may be producing some interaction with tidal conditions that is not present in the other estuaries.

## Implications for management and assessment

Our results show that environmental processes can influence catchability across a hierarchy of spatial and temporal scales, which needs to be considered when interpreting estimates of stock size and fishing mortality rates from stock assessment. Inconsistent effects of temperature, the most influential environmental covariate on catch rates across estuaries in the northern and central sections of NSW indicates that the spatial scale for data aggregation may influence the standardisation of catch rates. Although the NSW stock of Giant Mud Crab is currently assessed and total fishing mortality controlled through a state-wide TAC, commercial fishers are generally authorised to harvest the species in one of seven spatial regions of the fishery, with total effort (i.e., trap numbers) allocated at a regional level based on shareholdings of individual fishing businesses. Considering the varying impact of temperature with increasing latitude, if commercial catch rates are used as the primary biological performance indicator within a harvest strategy it should be integrated as an average of multiple catch rate time series calculated at the estuary or regional level, to adequately capture spatial variability.

In NSW, extended soak times are likely a strategy employed by fishers to reduce input costs associated with fishing. The lack of any effect of soak time on catch rate, suggests that the current measure of effort in commercial logbook reporting (number of traps) is probably adequate. However, if fishers are regularly clearing or re-baiting their traps, extended deployments carry a risk that effort may be under-reported, since a single trap cleared many times may still be reported as a single trap deployment. This creates a risk of hyperstability in catch rates (Erisman *et al.*, 2011), but also highlights the need for clear messaging of reporting requirements to ensure fishery-dependent data (i.e., logbook reporting) is reflective of true effort.

## Technical considerations and caveats

Observer-based data provides a quality-controlled alternative to commercial logbook reporting that enables the collection of additional data on operational aspects of a fishery. Additionally, high-resolution information about the spatial distribution of trap catches enables the incorporation of locally relevant environmental data, provided such data exist. However, incorporating environmental data at the correct temporal scale remain a challenge when modelling this data. This is relatively straightforward for gear that is set overnight, but for multi-day soak times, summarizing environmental data over this timeframe may dampen some variation that influences catchability.

Our modelling approach estimates 'global' and estuary-level effects of each covariate, allowing some 'information sharing' (see Rose *et al.* 2012) between estuaries. However, we remind readers that caution should still be used when interpreting estimates outside the observed range of a covariate (e.g., temperatures below 20°C in the Tweed River; Figure 74). Moreover, estuaries where few observations are available also need to be treated with caution. For example, while the estimated effect of temperature in the Clarence River is in agreement with other estuaries and studies (Williams and Hill, 1982), the magnitude of the effect is likely unrealistic (note effects are plotted on the log scale; Figure 74).

## **Conclusions**

Many of the factors that impact indices of stock abundance are well known; however, the impact of changes in environmental and oceanographic conditions, operational aspects of the fishery, combined with the influence of management and economic decisions are less clear, and this may inhibit interpretation of commercial catch rates as indices of stock abundance. Our study investigated processes known or expected to impact catchability of Giant Mud Crab, and the patterns resolved will improve the application of catch rate time series in stock assessment and modelling of species abundance patterns more broadly. Observer surveys and collection of detailed effort and operational data for commercial fishing operations are a useful means of reducing uncertainty in indices of stock abundance.

# Testing broad-scale environment-catch relationships for Giant Mud Crab

## Background and rationale

The previous chapters dealing with Giant Mud Crab, principally *Oceanic connectivity and particle dispersal for Blue Swimmer Crab and Giant Mud Crab* and *Environmental influence on spawning migrations in Giant Mud Crab*, provide new information on critical processes in the reproduction and dispersal components of the Giant Mud Crab lifecycle. These studies reveal two key pieces of information: 1) what environmental conditions promote spawning migrations; and, 2) which spawning latitudes reflect the most likely sources for new recruits to commercially fished estuaries.

The broader rationale underpinning these two studies was to identify whether broader source-sink relationships could provide a basis for indicators of future stock performance in the context of fisheries catch within individual commercially fished estuaries. Specifically, Meynecke *et al.* (2012b) sought to model commercial catch rates against a set of lagged and unlagged climatic variables in common commercially fished estuaries along eastern Australia. The models may have been hindered by the fact that critical 'lagged processes' (i.e., processes that influence spawning and recruitment) were not playing out within the estuary where the crabs later recruited as juveniles, and subsequently recruited to the fishery, and also that the lag duration (24 months) was too great. Furthermore, since a mix of lagged and unlagged parameters were included in the models of Meynecke *et al.* (2012b), they could not be used for predicting future catch.

By examining the questions above, it was hoped that defining source-sink dynamics would provide a means to establish a linkage through space and time by which commercial catch could be related to historic environmental conditions. The intention of this chapter was to undertake some preliminary modelling that explored these relationships in the context of catch prediction, with the intention of developing a predictive tool in much the same fashion as that put forward for Blue Swimmer Crab in *Long-term drivers of catch variability in Wallis Lake*. Thus, we use a conceptual understanding of environmental factors that are likely to be important in Giant Mud Crab recruitment as a basis to explore the utility of a range of lagged variables, including some derived from earlier chapters and others from contemporary publications (i.e., PDO, and onshore winds, Schilling *et al.* 2022b; Schilling *et al.* 2023), for heuristic prediction of stock performance for Giant Mud Crab.

## Data sources, approach and modelling

The integrative analysis presented here develops a preliminary framework that synthesises various data sources to establish whether above- or below-average catch years can be predicted prior to the commencement of a fishing season. For this reason, we focused on mechanisms for which data would be available before the fishing season commences. In effect, this limited us to exploring lagged relationships, or mechanisms related primarily to settlement and recruitment processes. The various components/relationships that were explored are outlined below.

## Larval supply

As shown in previous chapters, Giant Mud Crab spawn in oceanic waters, typically to the north of the estuary where they originated, with spawning triggered by seasonal declines in temperature, or

rainfall events and estuary inflow. Following spawning, larvae typically drift south in the East Australian Current before settling in the inshore region and moving into estuaries. This forms the basis for a source-sink relationship where estuaries will generally source larvae from reproductive activity to the north. Theoretically, larval supply has a significant influence on recruitment success (Cury *et al.* 2014), and so it is possible that spawning stock biomass to the north of a given estuary is an important predictor of future fisheries harvest, especially since Queensland (QLD, in the north) implement a male-only harvest policy.

## Larval settlement and recruitment

As shown in previous chapters, the mesoscale oceanography of the East Australian Current (EAC) is likely to influence connectivity between spawning and recruitment of Giant Mud Crab in eastern Australia. Specifically, the EAC separation appears to mediate connectivity between spawning and recruitment to the north/south of this region. Furthermore, the EAC separation latitude typically provides information about the 'mode' that the EAC is flowing—more southerly separation typically indicates a strong, coherent jet, while more northerly separation (i.e.,  $> -33^\circ$ ) indicates either an eddying mode or an eddy-dipole mode (Roughan *et al.* 2022). These latter two generally result in greater eddying and cross-shelf transport (Roughan *et al.* 2022; Malan *et al.* 2023) and higher chlorophyll concentrations (Malan *et al.* 2023). Such conditions may be beneficial for Giant Mud Crab larvae, as eddies can act as nurseries for coastally spawned larvae (Garcia *et al.* 2022) and cross-shelf transport may enhance inshore larval settlement rates (Cetina-Heredia *et al.* 2019).

Recruitment of Giant Mud Crab may also be influenced by coastal winds, which have been shown to influence the catch of coastally spawned species off eastern Australia. In south-eastern Australia, larval retention is generally promoted by southeasterly (SE) winds (Schilling *et al.* 2022b), which promote onshore transport (alongside downwelling, Middleton *et al.* 1996) that in turn enhances larval retention near the coast (Schilling *et al.* 2022b). Finally, as larvae settle in the inshore region, it is likely that they then recruit to estuaries as megalopa, which is thought to be facilitated by chemoreception of estuarine habitats (e.g., smelling seagrass, Webley *et al.* 2009) or detecting a salinity gradient. In either case, river flow may represent a useful proxy for these mechanisms, as higher river flow would enhance both of these signals. However, river flow beyond an (unknown) upper threshold may also negatively impact recruitment, as survival of early life history stages is diminished at low salinities (Nurdiani and Zeng 2007) and larval or megalopa motility may not be sufficient to overcome currents that accompany high river flow.

## Climate drivers

As discussed earlier, there is some evidence to suggest that large-scale climate drivers can influence the productivity of fisheries. For example, the El Niño Southern Oscillation (ENSO) has been shown to influence Giant Mud Crab harvest (Meynecke *et al.* 2012b). Meynecke *et al.* (2012b) also suggested that other climate drivers such as the Pacific Decadal Oscillation (PDO) and the Interdecadal Pacific Oscillation (IPO) may also have implications for fisheries productivity. The most likely mechanism by which this index relates to capture of Giant Mud Crab is through rainfall (and hence river flow), and sea surface temperature (SST), variability that aligns with these indices. Although, the precise links remain unclear, we include these drivers as an 'exploratory' exercise.

## Data sources

Catch data (NSW estuaries) – Daily catch (kg) records were extracted from commercial logbook reporting over the period 2008/09–2018/19. Reporting changed from monthly to daily in the 2008/09 fishing season, which had some impacts on the quality of reported data (primarily through aggregative reporting, such as reporting a whole month of catch on a single day). For this reason, we excluded 2008/09 from our analysis, however, some remaining records were in excess of 200 kg, which were also deemed likely to be erroneous and were excluded by applying a decision rule where any catch records greater than the 75<sup>th</sup> percentile for a particular estuary were excluded (Figure 78, Table 23).

**Table 23** Catch (kg d<sup>-1</sup>) thresholds for estuaries included in modelling, reflecting the 75<sup>th</sup> percentile of daily catches in each estuary. Records that reported values greater than this were not used in modelling.

| Estuary        | Catch 'cutoff' (kg) |
|----------------|---------------------|
| Tweed River    | 54.2                |
| Richmond River | 46.2                |
| Clarence River | 98.1                |
| Nambucca River | 32.5                |
| Macleay River  | 101.6               |
| Camden Haven   | 59.4                |
| Wallis Lake    | 90.9                |
| Port Stephens  | 44.0                |

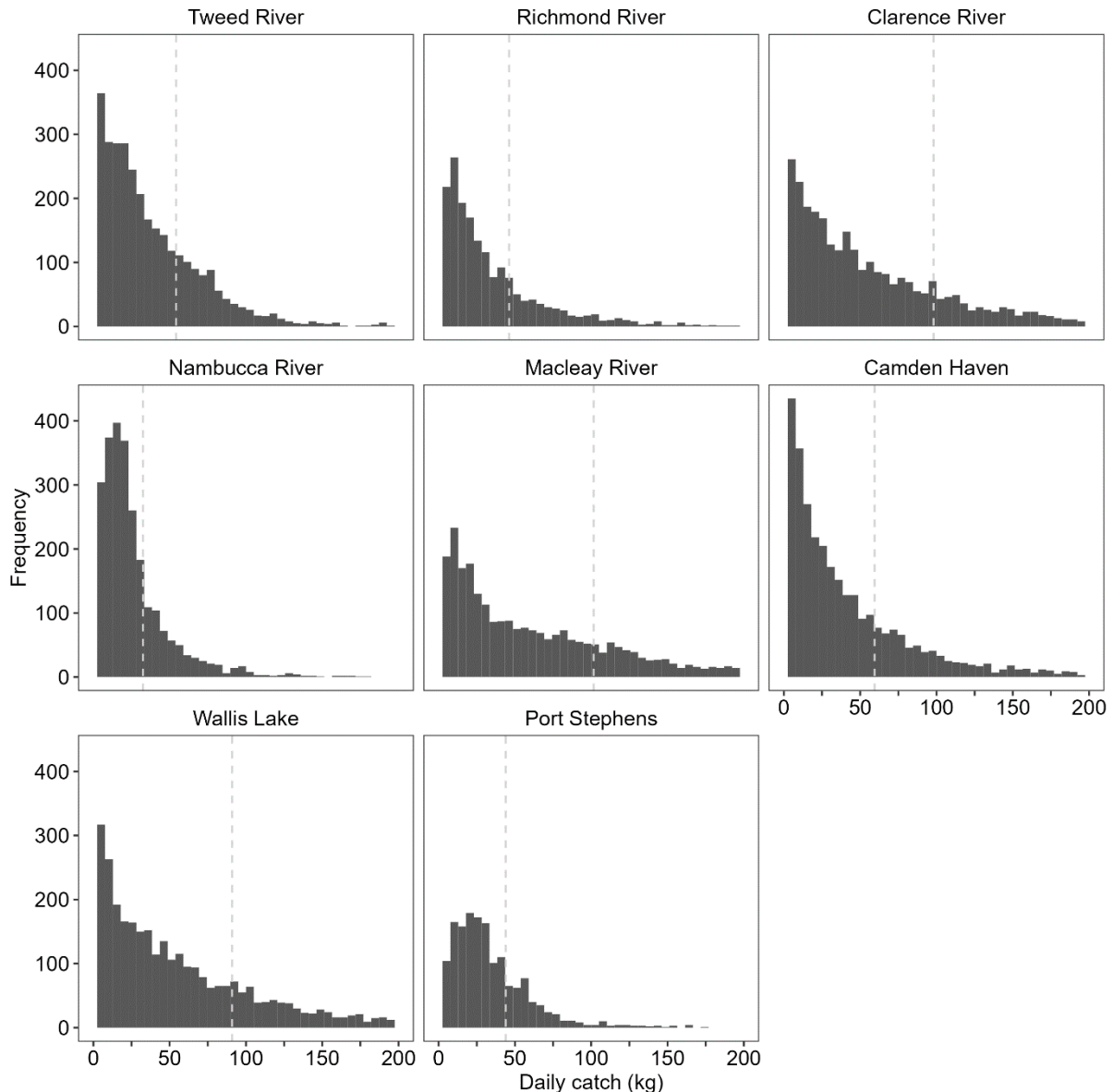


**Figure 78** Distribution of daily catch (kg) in each estuary. Dashed grey lines indicate the 75<sup>th</sup> percentile, catch records greater than this are assumed erroneous and are excluded from modelling (see Table 23). Note x-axes were truncated to show the majority of the data (3% of data exceeds 200 kg).

Index of spawning stock (as a proxy for larval supply) – For each estuary, we defined the spatial scale over which larval supply likely originated, based on larval dispersal simulations presented in *Oceanic connectivity and particle dispersal for Blue Swimmer Crab and Giant Mud Crab*. Within these ‘source areas’ we then used austral spring–summer (September–February) catch as a proxy for spawning stock biomass (SSB). For catch reported in NSW, data was available by sex, and only female catch was included. However, in Queensland (QLD), a male-only harvest policy is implemented which meant that catch corresponds to the male biomass only. To deal with this in our analysis, we made the simplifying assumption that the sex ratio was 1:1. Aggregating to the seasonal (i.e., spring–summer) level carries the implicit assumption that an even sex ratio persists throughout the season, however it may well vary throughout this period (Meynecke and Richards 2013). To aid interpretability and avoid confusion with ‘true’ SSB, we rescaled this variable between 0–1 for each estuary.

River flow – Discharge volume (ML) was used as a proxy for river flow in estuaries within which the catch occurred. Ideally, we had hoped to also examine the influence of flow from potential source estuaries/regions, however suitable data from putative source areas in Queensland could not be obtained in time, so this part of the analysis was set aside for future exploration. Discharge volume was obtained from monitoring stations maintained by WaterNSW via their online data portal (<https://realtimedata.waternsw.com.au>). For each estuary, discharge volume was taken from the monitoring station closest to the estuary mouth and was summed over the austral spring–summer to give a total for each fishing year.

Coastal winds – Coastal wind data were extracted from the Bureau of Meteorology Atmospheric Regional Reanalysis for Australia (BARRA; Su *et al.* 2019). This product provides 3-hourly wind speed/direction at ~12 km resolution from 1990–2019. From this product, we extracted wind speed and direction from the grid cell closest to the mouth of each estuary and calculated net displacement according to Schilling *et al.* (2022b). Positive values indicate winds that are likely to promote downwelling (SE) and contribute to retention of larvae near the coast, while negative values indicate winds that are likely to cause upwelling (NE) and advection of larvae away from the coast (Schilling *et al.* 2022b).

Regional oceanography – As an index of the EAC separation latitude (°), we used a timeseries of monthly mean sea surface height (SSH) contours published in Li *et al.* (2022a). This timeseries delineates the Pacific subtropical gyre by the 0.9 m SSH contour, and is extracted from daily satellite observations from the *Archiving, Validation and Interpretation of Oceanographic* (AVISO) data collection (CNES 2015). This dataset has a  $0.25^\circ \times 0.25^\circ$  horizontal resolution. For further details regarding the derivation of this metric see Li *et al.* (2022a).

Climate indices – Climate indices were obtained from the National Oceanic and Atmospheric Administration (NOAA) National Centre for Environmental Information (NCEI) and included: the Tripole Index for the IPO, which is the difference between sea surface temperature anomaly (SSTA) over the equatorial Pacific and the north- and south-west Pacific (Henley *et al.* 2015); the NCEI PDO Index. The PDO index is calculated by generating a PDO regression map (regressing SSTA in the north Pacific against the Mantua PDO Index (Mantua 1999) for the duration of their overlapping period to) and projecting SSTA from the NOAA NCEI extended reconstruction of sea surface temperature (ERSST v. 5; Huang *et al.* 2017) onto this map. The Southern Oscillation Index (SOI) was also used, which is measured as the difference in sea level pressure (SLP) between Tahiti and Darwin. All indices were reported daily and summarized as the average during the austral spring–summer.

## Modeling approach

Random forests were used to model the influence of putative predictor variables on Giant Mud Crab catch for commercially fished estuaries in NSW. Random forests are an ensemble machine learning algorithm, that can handle high-dimensional data with complex interactions and non-linear responses (Biau and Scornet 2016) making them highly suitable for ecological questions that require classification (Cutler *et al.* 2007) or regression (Prasad *et al.* 2006) analyses. Originally devised in Breiman (2001), random forests operate based on a ‘divide and conquer’ principle, where fractions of the data are sampled, a predictor tree is ‘grown’ on each small piece using a randomized subset of predictor variables, and then predictions of all trees are aggregated (Biau and Scornet 2016).

Random forests were trained on daily catch (kg) data over the period 2009/10–2018/19. We split our data in a random fashion into 75 % training data, with the remaining 25 % reserved as test data used to evaluate model predictions using ‘unseen’ data. In an effort to develop a heuristic management tool, we compared predicted and observed daily catch with the long-term average catch for each

estuary. In this context, we considered a fishing season ‘good’ or ‘bad’ if it was above or below this average, respectively. Model predictions were considered ‘correct’ if they were classified the same way as observations. Predictors included in the model included our index of larval supply, rescaled river discharge, net wind displacement, mean EAC separation latitude, the Tripole Index for the IPO, the NCEI PDO Index and SOI, as predictor variables. In addition, month and estuary were included as ‘nuisance’ variables, since these are expected to explain a high degree of the variation in crab catch. When fitting these models, the algorithm proceeds by sampling fractions of the data based on decision rules applied to a randomized subset of predictor variables ( $mtry$ ) which must be specified *a priori*. Each split occurs at a ‘node’, and splitting stops when the sample size in a node falls below some threshold ( $n_{min}$ ), which must also be specified *a priori*.

Model predictions can be sensitive to the settings of  $mtry$  and  $n_{min}$ , collectively referred to as hyperparameters, or so-called ‘tuning’ parameters since they cannot be learned from the data. Setting these hyperparameters is an exercise in balancing the trade-off between over- and underfitting, while minimizing the predictive error of the model. In the present study, optimal settings for these hyperparameters were found by conducting a grid search over the combinations of  $mtry \in [1, \dots, 9]$  and  $n_{min} \in [1, 2, 5, 10, 20, 100]$  and assessing the predictive error via 10-fold cross validation. Predictive error was measured using root mean square error (RMSE) and mean absolute error (MAE). We note that RMSE penalizes larger errors more heavily than MAE but also report the latter due to its clear interpretability.

## Results and discussion

### Modelling outcomes

The data processing rules outlined above resulted in the removal of  $n = 5,323$  reported catch records over the period 2009/10–2018/19, leaving a total of  $n = 15,922$  for model fitting which was split into 75 % training ( $n = 11,941$ ) and 25 % test data ( $n = 3,981$ ). Hyperparameter tuning resulted in similar settings regardless of which measure of error was used (RMSE or MAE). RMSE was minimized when 7 variables were used for splitting and the minimum sample size in leaf nodes was 50 (RMSE = 16.22 kg; Figure 79a). MAE was minimized when 6 variables were used for splitting and the minimum sample size in leaf nodes was 20 (MAE = 12.15 kg; Figure 79b). Overall, both measures of predictive error appeared to stabilize for  $mtry > 4$ , with little variation between values of  $n_{min}$  (Figure 79). We preferentially used the settings that minimized RMSE, since this measure penalizes larger errors more heavily, however models fit under both settings yielded similar results and we continue to report MAE due to the clear interpretability of this metric.

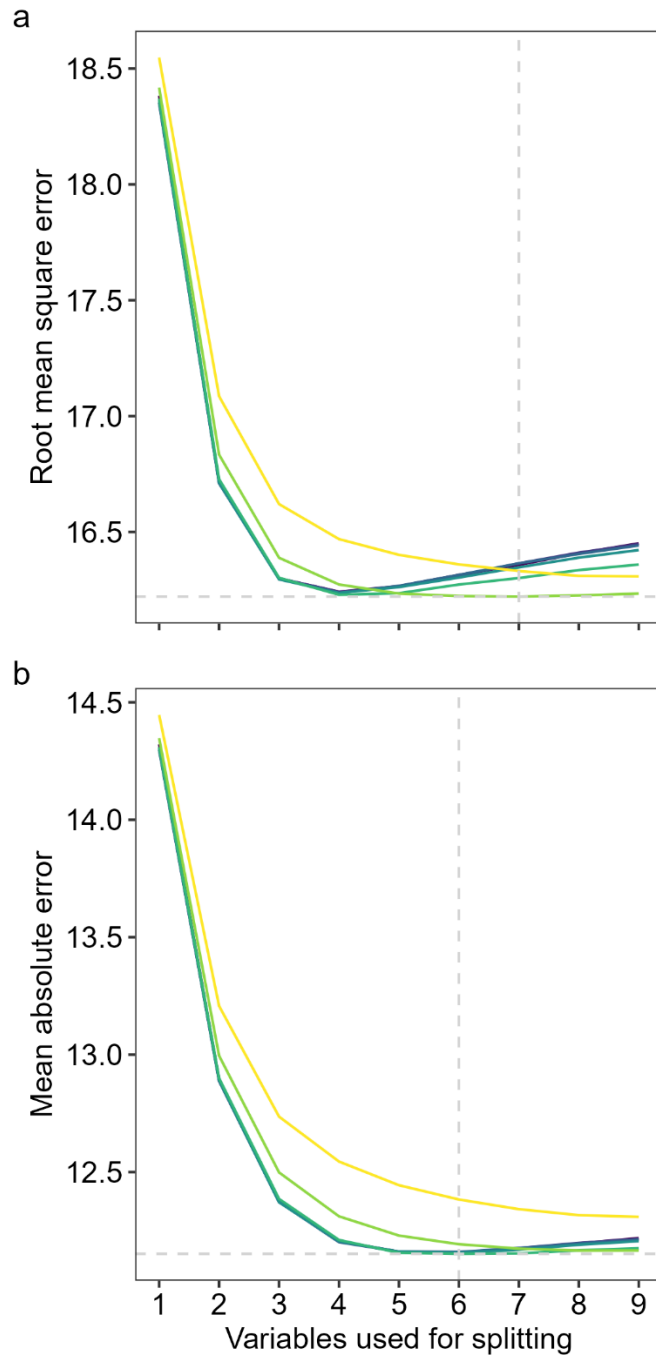


**Figure 79** a) Root mean square error (RMSE) and b) mean absolute error (MAE) of model predictions obtained via 10-fold cross-validation on our training data for varying numbers of variables used for node splitting ( $mtry \in [1, 9]$ ) and minimum sample size of leaf nodes ( $n_{min} \in [1, 2, 5, 10, 20, 50, 100]$ ). Each colour represents a different value for  $n_{min}$ .

When used to predict daily catch (kg) on our test data, predictions were positively correlated ( $r = 0.67$ ) and the model explained a moderate amount of the variation in the data ( $R^2 = 0.45$ ). Moreover, predictive error was comparable to that obtained during cross-validation on the training data (RMSE = 16.06 kg; MAE = 11.99 kg). On an estuary-by-estuary basis, model predictive error varied from 6.62–22.06 kg and 5.35–17.69 kg, for RMSE and MAE, respectively (Table 24). Correlation between

predicted and observed catch (kg) was moderate and positive for all estuaries ( $r \in [0.41, 0.65]$ ; Table 24, Figure 80). When used as a heuristic management tool, to predict ‘good’ or ‘bad’ catch years (defined as above or below the 2009/10–2018/19 average for an estuary), our model performed well, with predictions matching observations 86 % of the time (Figure 81).

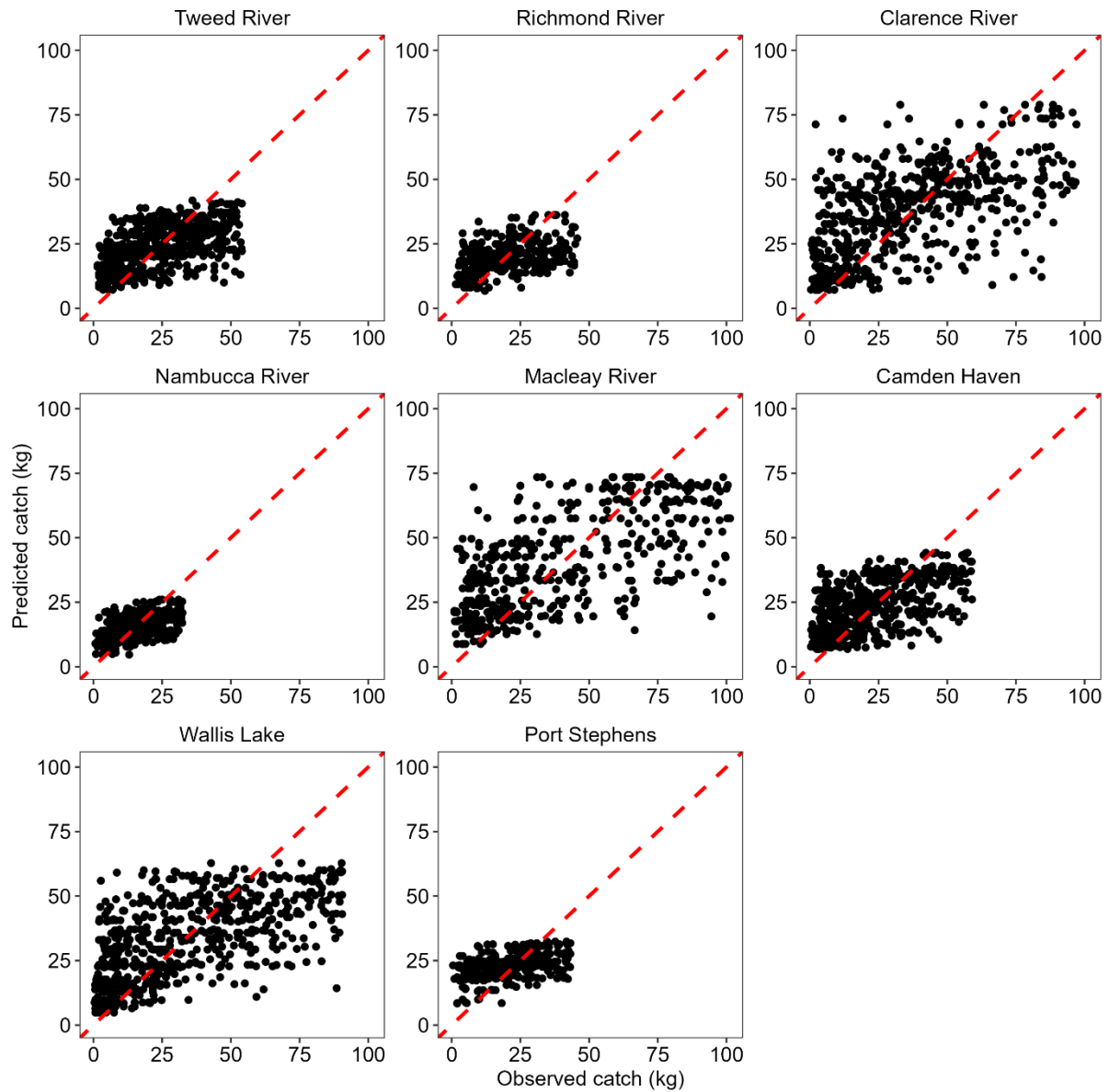


**Figure 80** Observations versus predictions of daily catch (kg) from the test data. Points along the red line indicate perfect prediction.

**Table 24** Prediction error and correlation between observed and predicted daily catch (kg) from the test data set.

| Estuary        | RMSE  | MAE   | Correlation coefficient ( <i>r</i> ) | Coefficient of determination ( <i>R</i> <sup>2</sup> ) |
|----------------|-------|-------|--------------------------------------|--|
| Tweed River    | 12.12 | 9.89  | 0.55                                 | 0.30   |
| Richmond River | 10.71 | 8.78  | 0.41                                 | 0.17   |
| Clarence River | 21.19 | 16.32 | 0.58                                 | 0.34   |
| Nambucca River | 6.62  | 5.35  | 0.54                                 | 0.29   |
| Macleay River  | 22.06 | 17.69 | 0.65                                 | 0.42   |
| Camden Haven   | 12.40 | 9.76  | 0.61                                 | 0.37   |
| Wallis Lake    | 19.89 | 15.63 | 0.63                                 | 0.40   |
| Port Stephens  | 10.25 | 8.25  | 0.45                                 | 0.20   |

### Comparative importance of predictor variables

Variable importance indicated that both month and estuary were approximately 3–4 times more important than any other predictors of catch in our model (Figure 82). These were followed by net displacement of wind, the larval supply index and river flow, while climate indices and the mean EAC separation latitude were markedly less important (Figure 82). On a fishery-wide basis (i.e., all estuaries) very negative net wind displacement (i.e., offshore winds) in the previous spring–summer appeared to correlate with increased predicted daily catch by ~4 kg, while all other negative values had no effect (Figure 83a). Daily catch increased alongside positive wind displacement during the spawning/recruitment season, which supported the hypothesis put forward of south-easterly (i.e., onshore) winds having a larval retention effect. It should be noted that there were very few observations at the extremes of net wind displacement (Figure 84) and interpretation of the effect in this range of the covariate should be made cautiously. Predicted catch increased in a roughly linear fashion with our larval supply index before an apparent asymptote at very high values (Figure 83b). Conversely, predicted catch was lower when river flow in the preceding austral spring–summer was high, although the effect was small (i.e., ~1 kg; Figure 83c). Predicted catch increased by ~3 kg in an approximately linear fashion with the Tripole Index for the Interdecadal Pacific Oscillation (IPO) until it reached an asymptote at around 0 (Figure 83d). Predicted catches were highest when the mean Southern Oscillation Index (SOI) in the previous austral spring–summer was negative (indicative of El Niño conditions) and decreased by ~2 kg as the SOI became more positive (indicative of La Niña conditions; Figure 83e). The relationship between the Pacific Decadal Oscillation (PDO) Index and predicted catch approximated the inverse of the standard logistic function, increasing by 1.5 kg over the range of the covariate (Figure 83f). Finally, a weak dome-shaped relationship between predicted catch and the mean East Australian Current (EAC) separation latitude in the previous austral spring–summer was apparent, with a peak in predicted catch when the EAC separated around -33° (just south of Port Stephens; Figure 83g).

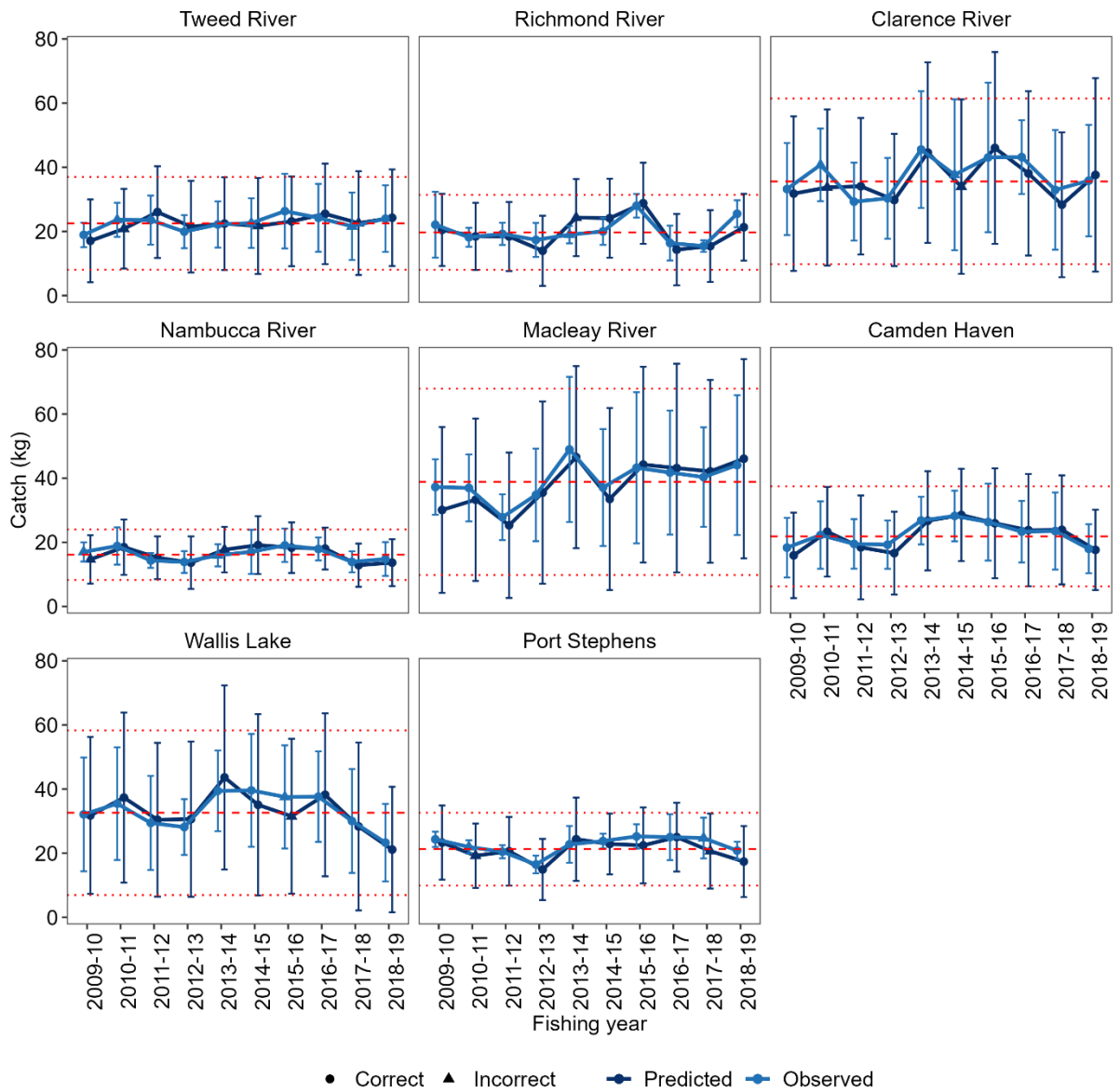


**Figure 81** Comparison between mean ( $\pm$  SD) observed and predicted daily catch (kg) in a fishing year. Dashed red line indicates the long-term mean ( $\pm$  SD, dotted lines).

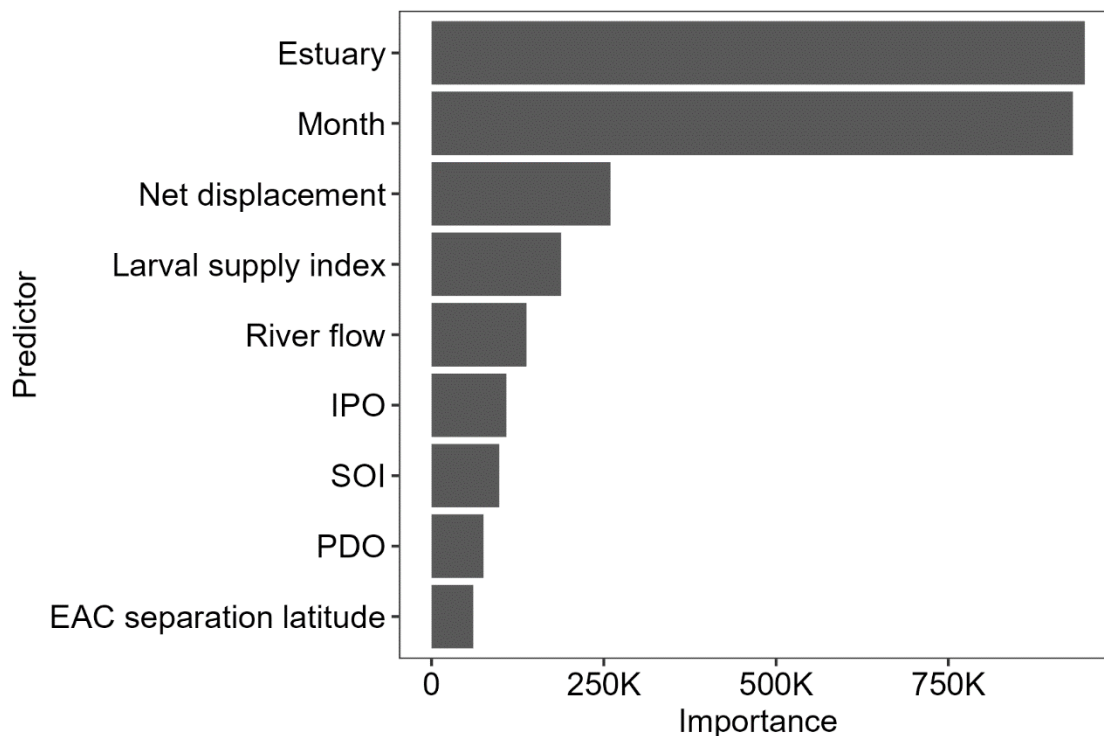


**Figure 82** Relative variable importance measured as the decrease in node impurity gained by inclusion of that variable.

## Conclusion and next steps

The variables and approach explored here shows promise for prediction of relative stock 'performance' for Giant Mud Crab in NSW. While only intended as a preliminary analysis, the approach performed well, correctly predicting above- or below-average catch years 86 % of the time. While estuary and month were most important in driving daily catch, variables representing various processes important in recruitment, such as larval supply and advection, were moderately influential as well.

Nonetheless, additional work is clearly required to further develop the tool for potential application in quota setting and quota management. In particular, this should include incorporation of a variable that captures the potential influence of freshwater flows on spawning migrations, which would provide an additional link between stock performance and larval supply. In addition to this, future simulations should further evaluate whether altering the variable lag improves model predictions. These enhancements will likely be incorporated as the preliminary modelling and findings presented here are further developed and refined for publication in the scientific literature.

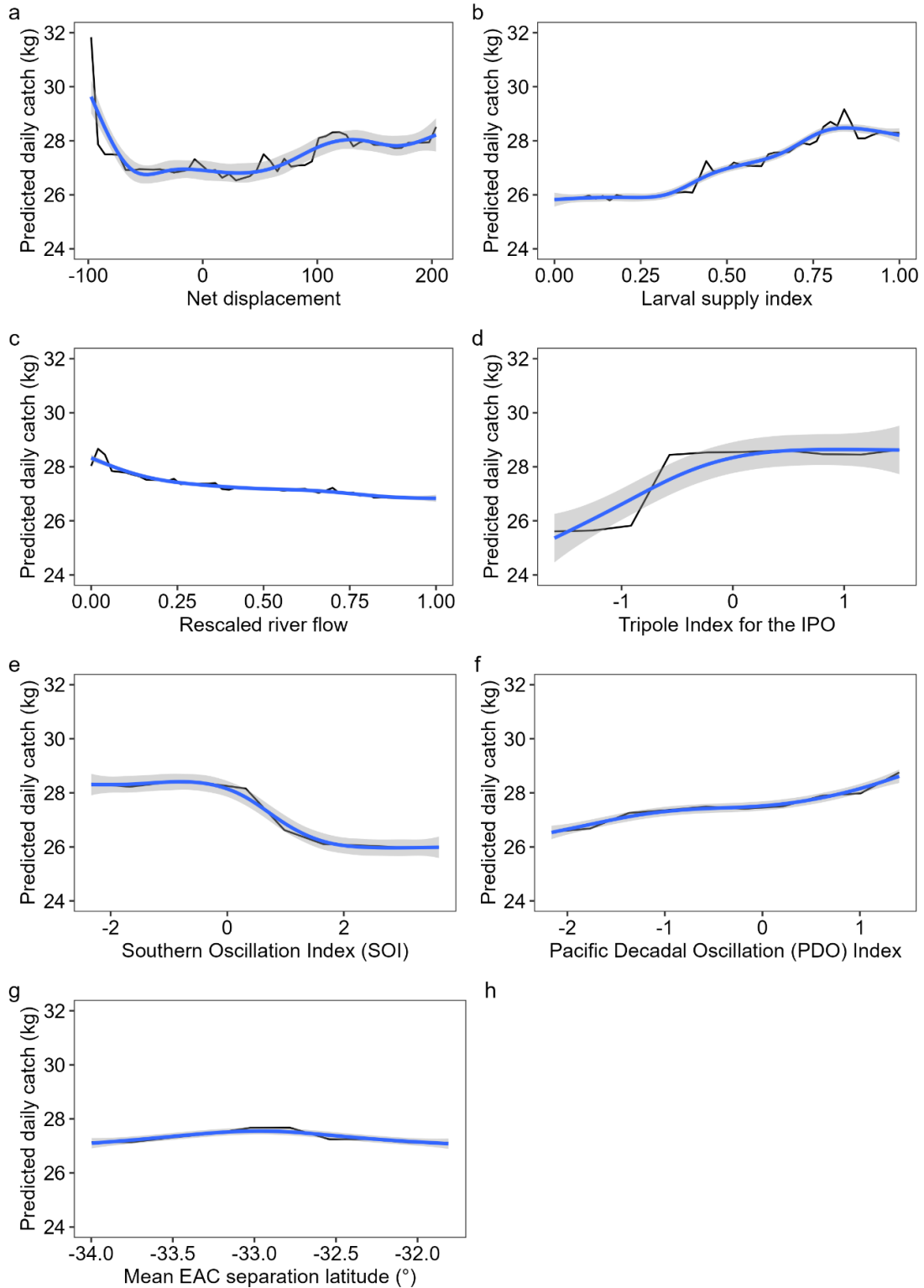


**Figure 83** Partial dependence between predicted daily catch (kg) and a) net wind displacement, b) larval supply index, c) rescaled river flow, d) Tripole Index for the Interdecadal Pacific Oscillation (IPO) e) Southern Oscillation Index (SOI), f) Pacific Decadal Oscillation (PDO) Index and g) mean East Australian Current (EAC) separation latitude ( $^{\circ}$ ). Note all variables reflect the environmental conditions in the previous austral spring–summer period (September–February) when settlement and recruitment is assumed to occur. Smoothed (blue) lines are overlaid to aid interpretation. Panels are ordered by variable importance (top left – bottom right).

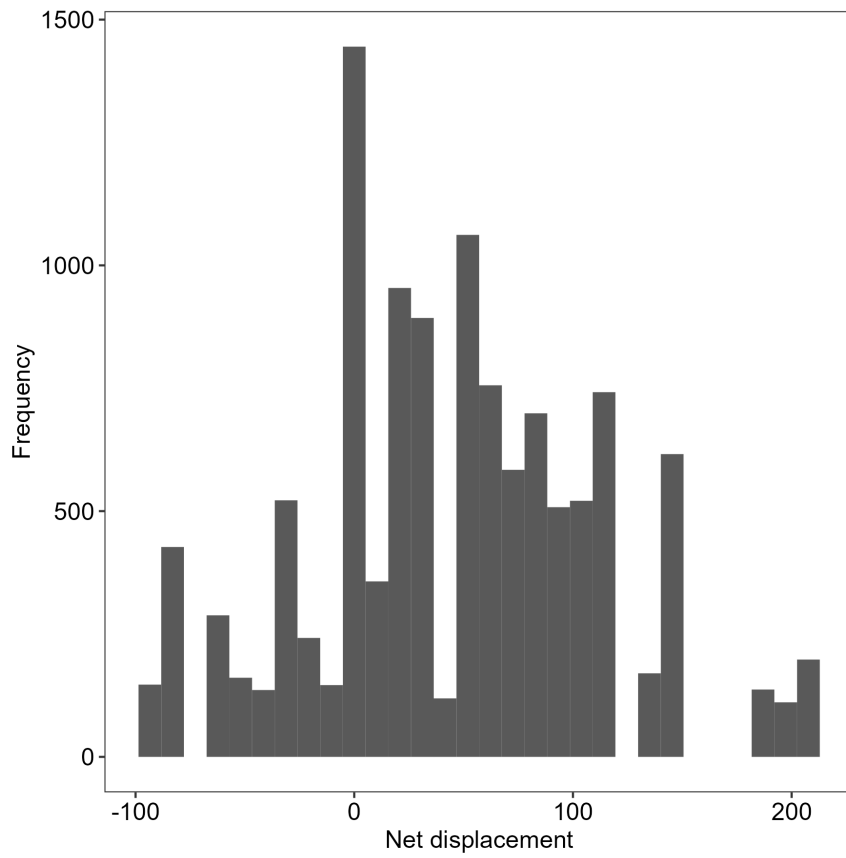


**Figure 84** Histogram of observations of net wind displacement in our training data

# General discussion and conclusions

## Blue Swimmer Crab

The data and analyses presented here represent one of the most comprehensive compendiums of research on south-eastern Australian Blue Swimmer Crab. The study period encapsulated a small number of freshwater inflow events in the study estuaries, which provided some insight in the response of Blue Swimmer Crab to associated physicochemical variation in the main commercially fished estuaries of NSW. The most obvious feature of the extended data set collected for Blue Swimmer Crab, is estuary-specific nuance on how the populations behave and respond to environmental variation. For these reasons, the discussion below is principally focussed on the main estuary for the fishery, Wallis Lake, with the key points of distinction for the other estuaries already highlighted in previous chapters.

Consistent with patterns in commercial catch, the greatest catch rates for Blue Swimmer Crab occurred in Wallis Lake, but across all estuaries the size structure in the majority of sampled months indicated the presence of only a single cohort. While there were instances where multiple cohorts were observed at the same time, these were rare, and were somewhat inconsistent between years. In Wallis Lake especially, size structures were chronically unimodal, with the exception of December samples when strong smaller modes were observed. While it remains possible that important nursery areas could have been missed in the survey, this evidence suggests that, at least for Wallis Lake, the bulk of the fishery within a season appears to be supported by a single recruitment event, with multiple batches of reproduction unlikely. This is supported by temporal trends in berried females in Wallis Lake, with only a single solid peak in egg-bearing females per spring/summer/autumn period, compared to other estuaries which had a more protracted peak. Taken together, these results point to a late-spring spawning within the estuary, and the progression of the resultant cohort through to the fishery by February, which supports catch through to the following spring (with the residue of the cohort contributing to some limited estuarine catch in the following summer). The presence of berried females at low levels throughout summer and autumn suggests that some additional low-level spawning may occur, but was not of sufficient magnitude to contribute noticeable peaks of recruits to the size structure during these seasons. The sharp decrease in size classes greater than the MLS suggests substantial fishing mortality within the estuary, however the presence of low abundance of larger crabs in inshore areas means that at least some crabs avoid the estuarine fishery and emigrate to sea, where they can spawn. The abundance of crabs inshore is the inverse of the estuary, meaning that there appears to be tight coupling of the estuarine-inshore distribution. Spawning could not be confirmed from our data however, as inshore waters were only sampled for a restricted window which did not coincide with late spring, and at low resolution. Dispersal modelling indicates that recruits from any spawning that does occur in inshore waters can recruit back into Wallis Lake, so ocean-spawned larvae are not 'lost' to this system.

Given the effect of low salinity on early life history stages, it was expected that survival and later recruitment to the estuary and fishery would be negatively impacted by heavy rains and estuary inflow during the spring, either through mortality, or a migratory response by estuarine crabs. Unfortunately, these conditions were comparatively infrequent during the period of the independent survey, and the influence on seasonal patterns in reproduction was difficult to convincingly model with only three recruitment seasons sampled. However, when this hypothesis was investigated through broader modelling of the commercial fisheries catch time-series, there was no evidence of a relationship between late spring/early summer estuary inflow and CPUE of exploitable size classes once the cohort had grown, nor was there much strong evidence that freshwater inflow led to emigration of crabs from the estuary to the sea.

Modelling of crab abundance in the independent survey revealed two key findings. Firstly, temperature positively influenced crab catch, which was as expected given crabs are ectotherms and growth and activity are tightly linked to this critical variable. Secondly, and more importantly, it appears that freshwater inflow to the estuary largely leads to a redistribution of crabs within the estuary. Within Wallis Lake, it is likely that this reflects a spatial consolidation of the population within the vast expanse of open water in the south of Wallis Lake (including movement of crabs from the north of estuary), to which there are no major tributaries and the physicochemical influence of freshwater inflow is somewhat dampened. We hypothesise that this geomorphological feature of Wallis Lake could provide a physicochemical 'refuge' in the lake which provides comparatively stable conditions, and coupled with substantial seagrass beds in this area, may largely explain why this particular estuary supports such considerable population of Blue Swimmer Crab (Raoult *et al.* 2022 confirms this through trophic modelling).

In the context of adaptive management, one of the most important findings of the study was the influence of both winter fishing mortality, and broad-scale climate indices, on Blue Swimmer Crab commercial catch. This is a key outcome, since it provides a means to predict, with reasonable certainty (~85 %), the relative strength of recruitment and catch in the fishing season prior to the season actually commencing. This provides an additional source of information to adaptively manage quota setting for the commercial fishery, based on expected recruitment strength. However, the incorporation of this additional variable would require some adjustment to the current 'fishing year' and the timing of the quota determination and implementation (possibly to December or January, once reporting for June-November period is completed), and will require some agility and speed in the process by which TAC is determined and implemented.

Despite the potential utility of this relationship as a tool to inform the setting of quota within a fishing year, unpacking this relationship raises a concerning attribute of the fishery which may require some consideration in the future—that the removal of pre-mated spawning females during the June-November period appears to adversely impact recruitment during the following fishing season. Mating in Blue Swimmer Crab coincides with the moulting period, which is in turn affected by temperature and growth. Consequently, it is likely that the final mating just prior to the onset of cooler temperatures (when both growth and activity slows) provides females with spermatophore(s) that are retained over winter and used to fertilise their eggs when the waters warm during the following spring. Winter catches in Wallis Lake are heavily dominated by females, probably because males enter a semi-hibernative state whereas females are more inclined to maintain their nutrition through the winter to support later egg development. While all berried females are required to be returned to the water, the fishing mortality of pre-mated (but non-ovigerous) females through the winter, and concomitant reduction in fecundity, could be responsible for a recruitment bottleneck which impacts population abundance in the following fishing season. While this variable provides a useful predictive tool at present, if any provisions were to be implemented to manage winter catch in the future, its utility could well be diminished.

The processes investigated and quantified here are also relevant to the design and implementation of fisheries enhancement measures for the species. Fisheries enhancement such as stocking is ideally implemented in response to perceived or actual (i.e., measured or predicted) recruitment bottlenecks. Prior to this project, it was hypothesised that excessive freshwater inflow to estuaries would drive emigration of Blue Swimmer Crab from estuaries, leading to coastal spawning and strong southward dispersal, creating a recruitment bottleneck in the estuary that experienced the flow in the first place. The research presented here provides evidence to support an adjusted hypothesis regarding recruitment bottlenecks for the species in south-eastern Australia. Firstly, modelling of Wallis Lake abundance shows that there is some negative influence of conductivities less than ~30 ms cm<sup>-1</sup>. If such conditions occur within the southern extent of the lake (although this will likely be rare), resultant emigration may lead to a reduction in estuarine spawning, although particle dispersal

patterns such there is a good chance of recruits returning to Wallis Lake where coastal spawning dominates. Secondly, relationships between temperature and reproductive indices suggest that GSI declines sharply at temperatures  $>24^{\circ}\text{C}$ , and egg mass is considerably greater at temperatures between  $22\text{-}24^{\circ}\text{C}$ , declining sharply outside of these bounds. If this is considered a reproductive optima, the deviation from these conditions during the main reproductive period (e.g., late spring), may well be considered to set the stage for a lower-than-average recruitment event. We could not test the influence of this over the extended time series of commercial catch, as estuarine temperature data was not available (only coastal SST), and during the course of the independent survey, late-spring water temperatures appeared to sit comfortably within this 'optimal' bracket. While conditions outside these bounds may lead to depressed spawning, this remains an area for future research and attention. Furthermore, whether or not such conditions eventuate in later recruitment limitation depends on a range of other processes, including density dependence, which also require further work and consideration. If this is the case, late-spring estuary temperature may provide a suitable means to inform adaptive management of release programs (and potentially quota setting as well), with stocking targeted to estuaries and periods when conditions are sub-optimal for reproduction.

With respect to fisheries enhancement, a final point to highlight is the potential use of hatchery releases to deal with depressed population abundances arising from fishing (or other factors). For certain estuaries, dispersal patterns suggest the estuary itself is the primary source of recruits (rather than another location acting as a source). Where this is the case, stocking may well prove to be a suitable response to depressed population abundances, but this would ideally be accompanied by other strategies aimed at dealing with the root cause of any decline.

## Giant Mud Crab

Research on spawning, dispersal and recruitment processes for Giant Mud Crab in NSW waters is almost non-existent. Existing work within this jurisdiction has principally dealt with broadscale modelling of patterns fishery-dependent data (e.g., Meynecke *et al.* 2012b), various investigations of gear configuration (e.g., Butcher *et al.* 2012; Rotherham *et al.* 2013; Broadhurst *et al.* 2018; Barnes *et al.* 2022), contamination (e.g., Taylor and Johnson 2016; Taylor *et al.* 2017b; Taylor *et al.* 2018b; Taylor 2019; Taylor *et al.* 2021), trophic ecology (e.g., Raoult *et al.* 2018; Raoult *et al.* 2022), and spatial management (Butcher *et al.* 2014). The lack of research on basic population processes has meant that there are significant gaps in knowledge which is otherwise essential for efficacious fisheries management. These knowledge gaps have also meant that previous work modelling fisheries dependent data (Meynecke *et al.* 2012b) could not effectively capture important source-sink relationships that were potentially a major factor in the broader relationships investigated, where biotic or abiotic conditions at a spatially separate location can ultimately affect productivity of a fishery elsewhere. Coupled with this, the combination of lagged and unlagged variables in these models meant that this earlier work was not altogether suitable for future catch prediction (which is necessary to support adaptive management).

The work captured in this report dealt with strategic questions that provide a foundation for a pipeline of research targeted at these fundamental knowledge gaps for Giant Mud Crab. Specifically, dispersal patterns following oceanic spawning are now better understood, which allowed the identification of source-sink dynamics and passive inter-estuarine connectivity, with implications for stock structure and management. Within important source estuaries, we have also now defined the particular conditions that promote spawning migrations, such that periods where suitable conditions did not occur can be identified, and used to reveal consequences for 'downstream sinks' of recruits, and the potential occurrence of supply (and later recruitment) bottlenecks. We have defined habitat

usage for Giant Mud Crab such that habitat bottlenecks can be identified, and also conducted basal analyses to improve modelling of fishery-dependent catch data, which will improve the quality and interpretation of future stock assessments, and models examining broadscale prediction of fisheries catch. Finally, we have proposed a numerical approach which uses variables that influence recruitment processes to predict future stock productivity. These new learnings have a range of implications for management of Giant Mud Crab, and provide a platform for a range of other critical research questions, both of which are summarised in *Implications* and *Recommendations and further development* (respectively) below.

For more detailed discussion of results and modelling outcomes, readers are referred to the individual chapters dealing with Giant Mud Crab. However, patterns in estuary-coast and inter-jurisdictional connectivity identified in this study reveal some interesting nuances in the NSW component of the Giant Mud Crab stock, which warrant further discussion.

While there are clear regulations within NSW that berried crabs must be released alive upon capture, anecdotal information from both fishers and fisheries compliance officers, as well as observer surveys over the years, and independent trapping work during this project, all point to a universal absence of berried Giant Mud Crab within estuarine systems, where the bulk of fishing pressure occurs. The source-sink relationships derived for the major commercially fished estuaries for Giant Mud Crab suggest that for estuaries within the EAC separation zone (in northern NSW), recruits may be largely sourced from spawning in Queensland (Figure 59), and consequently stock size and management arrangements in Queensland may have a substantial influence on the supply of recruits to these latitudes. In contrast to estuaries within the separation zone, estuaries south of this are likely to be impacted by stock size and management arrangements in both NSW, and Queensland. The protection of all female crabs from fishing mortality in Queensland source areas, and pre-spawning egression from NSW estuaries (where the fishing mortality occurs), suggests that females in spawning condition may be benefitting from substantial protection from fishing mortality. However, excessive estuarine harvest of female crabs prior to their egression from NSW estuaries could act to limit the supply of spawning females to oceanic waters, and in turn lead to supply bottlenecks for estuaries relying on recruits that come from spawning within NSW. Thus, despite the connection to Queensland where all females are protected, it is still essential to manage overall fishing mortality within NSW estuaries, as this is the principal source of recruits for a large number of estuaries on the mid-north coast of NSW. Such management would best account for interannual variations in stock size, drawing on the relationships presented in *Testing broad-scale environment-catch relationships for Giant Mud Crab*.

In spite of the research presented here, some of the mechanisms underpinning settlement and post-settlement processes (including recruitment into the estuary) are still unclear. This has been a longstanding knowledge gap that is yet to be entirely resolved for subtropical estuaries (despite targeted efforts by multiple researchers over several decades, whose conclusions largely disagree; Webley 2008; Alberts-Hubatsch *et al.* 2014), and is completely unknown for estuaries south of the Tweed River. Alberts-Hubatsch *et al.* (2014) had most success at capturing crabs smaller than 40 mm CW in subtropical estuaries, but after considerable efforts (~30 collectors/traps used for each of 31 sampling events over 3 months) only captured 149 crabs. During the pilot phase of the current study, a spatially extensive trial to capture early benthic stage Giant Mud Crab was undertaken using opera house traps (baited with prawn meat or diced pilchard) and fine mesh fyke nets around the mangrove fringe (following Alberts-Hubatsch *et al.* 2014) in Port Stephens estuary (Figure 85). Sampling did not yield any Giant Mud Crab of the target size class (<50 mm CL), despite the estuary supporting a strong Giant Mud Crab fishery, and the locations chosen for sampling reflecting habitats where others have previously observed juvenile Giant Mud Crab. While our efforts can only be considered to constitute a preliminary investigation, clearly additional effort is required to both develop efficacious means of capturing juvenile Giant Mud Crab, and further identifying important

early juvenile habitats, the densities of crabs within them, and fine-scale drivers of estuarine recruitment processes. Once these issues are dealt with, pre-recruit surveys for juvenile Giant Mud Crab may present a viable means to identify impacts of environmental variation on recruitment and settlement into estuarine nurseries, and provide additional insight into the strength of year-classes proceeding into the fishery.

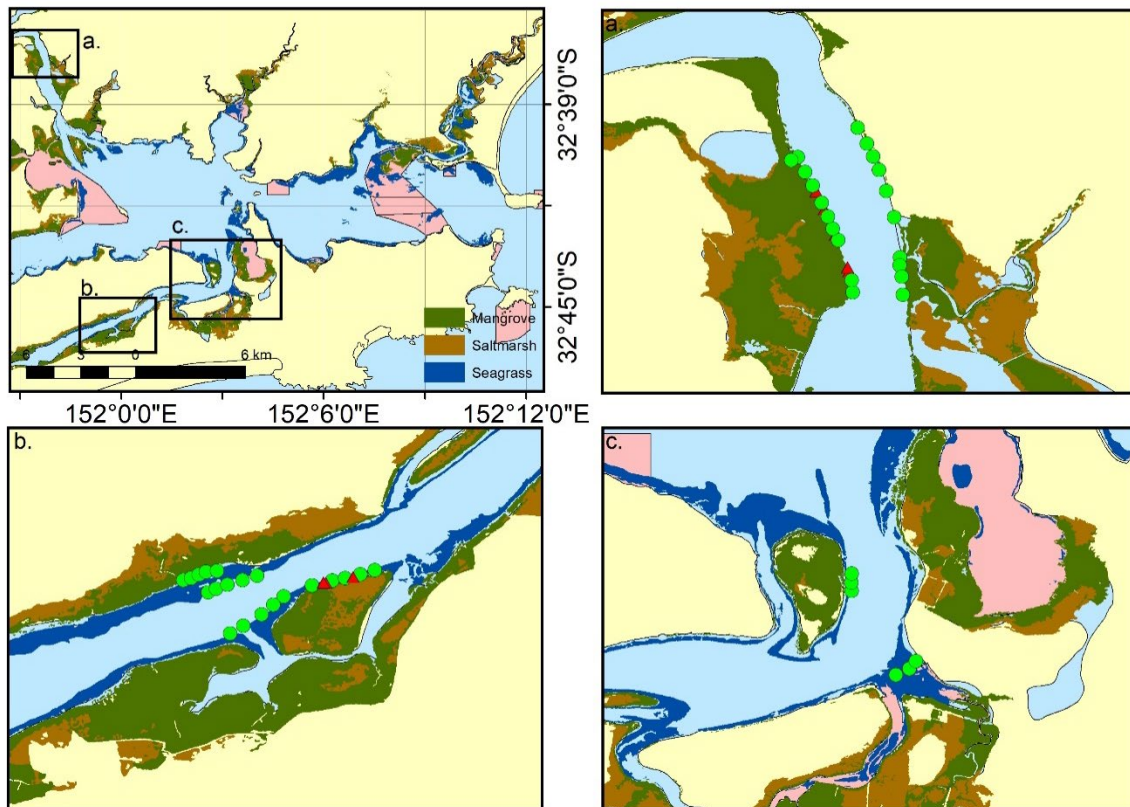


**Figure 85** Targeted sampling for early benthic stage Giant Mud Crab within Port Stephens using fyke nets (red triangles) and opera house traps (green circles) in inter-tidal mangrove habitats. Three locations within the estuary were sampled during the pilot phase of this project in 2018, which are indicated in each panel, with the upper left panel showing the position of these locations within the broader estuary.

The model presented in *Testing broad-scale environment-catch relationships for Giant Mud Crab* provides a platform from which adaptive management for the species can be built. The parameters included in this preliminary exploration provide an indication of how environmentally driven recruitment-level processes can influence fisheries harvest. Indices of stock biomass (as a proxy for larval supply) and environmental variables are comparatively easy to measure, and quantification of these variables in the period prior to the coming catch year can provide an indication to decision makers as to whether it is likely to be the 'better' or 'worse' recruitment year. While this is not a definitive predictor of stock biomass or productivity, this indicator, when considered alongside other factors, will certainly aid decision making surrounding suitable levels of catch, and allow quota levels to be adapted accordingly.

As discussed earlier for Blue Swimmer Crab, a second important outcome from this work was to provide new information to support development and adaptive management of fisheries

enhancement strategies for the species within NSW. The oceanic connectivity and habitat use data make two key contributions to the refinement of release strategies. Firstly, the broadscale connectivity that is demonstrated supports a model of panmictic stock structure within NSW, suggesting that broodstock collection does not need to be managed at a fine temporal scale. Secondly, if stock enhancement for Giant Mud Crab in south-eastern Australian estuaries proceeds in the future, environmental variables and their impact on recruitment provide useful indicators that can support decision making surrounding the potential need for releases to bolster natural recruitment in particular estuaries, in particular years.

# Implications

## Blue Swimmer Crab

As Blue Swimmer Crab are quota managed in NSW they require an ongoing process of performance reporting and stock assessment under the *Fisheries Management Act 1994*. Fundamentally, our results suggest populations of Blue Swimmer Crab in NSW and Queensland appear to constitute demographically separate stocks, supporting the current assessment and management at the state level. Many conventional stock assessment approaches and production-based models assume that an exploited population persists in a steady-state. Our findings demonstrate that environmental variability impacts abundance and reproductive biology of Blue Swimmer Crab, and the influence of this needs to be considered in the choice and application of future assessment approaches used to inform determination of stock status, and develop appropriate management provisions.

The scale and spatial structure of the fishery-independent monitoring program for Blue Swimmer Crab that was designed and implemented within the current project is appropriate to provide information on relative abundance, size structures, and variables that contribute to variations in abundance. Catch rates of both pre- and post-recruited crabs expressed as catch per unit of effort (CPUE) from fishery-independent surveys could be used as a primary biological performance indicator within a harvest strategy, to maintain Blue Swimmer Crab harvest within ecologically sustainable limits given the environmental conditions experienced at any particular point in time. Analysis of catch rate data from fishery-independent surveys conducted to date (2019-2021) can be used to inform limit, target and trigger reference points, and continued surveys will provide an ongoing data series against which the stock status and stock performance can be measured. Furthermore, fishery-independent estimates of relative abundance will also be used to validate commercial CPUE time series and provide insights into levels and direction of bias in commercial CPUE. A continuing environmental monitoring program similar to that applied in this project will be necessary to ensure environmental variability is incorporated into the assessment of indicators and associated decision rules within any harvest strategy framework employing indicators derived from independent surveys or commercial CPUE. However, the comparatively short period between spawning and recruitment to the fishery for Blue Swimmer Crab may create challenges for the incorporation of independent survey derived recruitment indices into decision making in time for the beginning of the TAC year.

The extensive reproduction data collected through the regular independent survey program reaffirms the current MLS for Blue Swimmer Crab in NSW (65 mm), as this exceeds estimates of the mean size at sexual maturity and the observed size of functional maturity (which indicates that a component of the spawning stock is continually protected from fishing pressure). However, the observed differences in the duration of the spawning period between estuaries has implications for the comparative reproductive potential of populations within individual estuaries. The short spawning period (1-2 months) and low proportion of female crabs berried in Wallis Lake (~50% lower), suggests spawning in adjacent ocean waters may be supporting recruitment to the most productive estuary for Blue Swimmer Crab. Where direct comparison could be made, key biological parameters estimated from the current study were generally similar to those previously reported for Blue Swimmer Crab in NSW. As southeast Australia is a global climate warming hotspot the population size structure, egg mass index, and batch fecundity derived from the current study across major estuaries may represent a useful proxy to understand the effects of further tropicalisation on reproduction of Blue Swimmer Crab, and flow-on effects for fisheries productivity in this region.

The regular independent survey program for Blue Swimmer Crab indicated that normally a single primary cohort moves through the Wallis Lake fishery each growth season, that originates from

spawning in spring and early summer. Our modelling indicates that winter harvest may directly influence abundance in the following season, due to the disproportionately high impact of this fishing on mated pre-spawning female crabs and concomitant impacts on egg production for the coming season. Future strategies to reduce winter fishing mortality may help to maximise egg production and support stronger recruitment to achieve improved economic and social outcomes from the fishery. Responsibility and obligations for the development of strategies to reduce winter fishing mortality should ideally be shared between the government, the commercial fishing industry, recreational fishers, Aboriginal traditional fishers, and other key stakeholders, under a co-management framework.

One of the most important findings of the study was the influence of both winter fishing mortality, and broad-scale climate indices, on Blue Swimmer Crab commercial catch in Wallis Lake. The ability to predict the relative strength of recruitment and catch in the fishing season prior to the season commencing, provides an additional source of information to support quota setting for the commercial fishery, and assists in identifying drivers of recent catch trends in the fishery. However, the influence of winter fishing mortality, and broad-scale climate indices on populations in other major estuaries, particularly Lake Macquarie where winter harvest by recreational anglers is difficult to quantify with high precision, remains poorly understood.

## **Giant Mud Crab**

In contrast to Blue Swimmer Crab, that appear to constitute demographically separate stocks, Giant Mud Crab maintain a comparatively high level of interjurisdictional connectivity, predominantly between Queensland and northern NSW. The male-only harvest policy implemented in Queensland likely provides a degree of stability in spawning biomass, which may support higher levels of recruitment for northern NSW estuaries that are well connected with spawning in Queensland waters. However, connectivity patterns suggest that estuaries within the mid-north coast of NSW may be demographically isolated from the rest of the stock where only ovigerous and female crabs less than current NSW minimum legal length are protected. Thus, fishing mortality, and environmental processes affecting recruitment, may contribute to catch rate variability in estuaries that source the majority of their larvae from within NSW.

The oceanic connectivity with Queensland means that stock structure issues need to be acknowledged, to accommodate potential changes in productivity, and their implications, in different parts of the stock. Our results show that environmental processes can influence catchability across a hierarchy of spatial and temporal scales which needs to be considered when interpreting estimates of stock size and fishing mortality rates from a stock assessment that currently does not explicitly model them. Inconsistent effects of temperature, the most influential environmental covariate on catch rates, across estuaries in the northern and central sections of NSW, suggests that the spatial scale for aggregation of commercial Giant Mud Crab catch and effort data may influence the outcomes of CPUE standardisation.

Our findings also highlight mechanistic linkages between estuarine variability and spawning migrations of Giant Mud Crab, the effects of which may contribute to interannual variation in spawning patterns, dispersal and recruitment processes, and ultimately impact productivity of Giant Mud Crab in different estuaries. The observed northward migration of female Giant Mud Crab, coupled with the predominant southward flow of the EAC, suggests that within a given estuary, new recruits may well have originated from the north, and variation in abundance may thus be influenced by spawning stock biomass and environmental conditions outside of the estuary where juvenile crabs settle.

Quantifying drivers of animal movement and response to environmental variation is often important for fisheries assessment. Although our results suggest that the tidal cycle is closely related to patterns in foraging, the duration of normal soak-times in the commercial fishery (typically 1 -2 days) means that it would be extremely difficult to capture the effects of the semidiurnal tidal cycle when standardizing and interpreting catch rates from the fishery. Our description of Giant Mud Crab behavioural dynamics are in close agreement with previous studies, and provide a mechanistic explanation of the observed distribution of the species across intertidal habitats.

## Recommendations and further development

Further to the ideas presented in the chapters above, the *General discussion and conclusions* and *Implications*, there are a few areas to consider for further analysis and development. For Blue Swimmer Crab, given the differences in the duration of the spawning period, proportion of mature crabs that are berried, the size structure of recorded catches of berried females between estuaries in our study, and reported variations in reproductive biology in response to environmental drivers elsewhere (e.g., Johnston and Yeoh 2021), there is a need for ongoing monitoring of the biology to support adaptive management of portunid fisheries in NSW. In addition, generating additional data on the relative abundance of berried female Blue Swimmer Crab in adjacent inshore ocean waters (outside of the small area and window sampled by the ‘inshore sub-program’) is an important future research priority. Linking putative ocean spawning events with the onshore wind analyses may identify a relationship between onshore winds and lagged catch rates.

While outside of the scope of this research project, data collected during the regular independent survey program, should also be used to evaluate the effectiveness of fishery-dependent monitoring programs in providing data for assessing and managing populations of Blue Swimmer Crab in NSW. Specifically, data collected from the independent survey program could be compared with data collected from observer-based surveys and fisher reported logbook data to inform a data monitoring plan for improved assessment and management. Finally, the extent to which small-scale temporal variations confound spatial comparisons of Blue Swimmer Crab populations sampled with traps, and the appropriate temporal scales for sampling, could be further examined using data from the regular independent survey program. This will help to quantify variability in populations across a hierarchy of temporal scales, yielding information that will help ensure that future sampling strategies provide the most representative results possible.

While much new knowledge on Giant Mud Crab in NSW is reported here, there is still a great deal that remains unknown. There is a need to collect local quantitative biological information on Giant Mud Crab to improve future assessments and evaluate the effectiveness of existing management controls. Future research should focus on estimating the size at functional maturity to ensure that the current minimum legal size is providing adequate protection to the reproductively mature component of populations in NSW. Research to understand the temporal dynamics of larval production (e.g., spawning and fecundity) may reduce uncertainty in larval dispersal models, and provide deeper insight to population connectivity in this region and the potential influence of climate change. Furthermore, the utility of targeted fishery-independent surveys, observer-based surveys, and fisher-collected data programs for assessing and managing populations of Giant Mud Crab in NSW needs to be further evaluated. Targeted fishery-independent surveys may be required in estuaries and/or areas of estuaries that are closed to commercial fishing, including recreational fishing havens, to fully assess stock status within NSW. Data collected from the recent observer program should be analysed to determine appropriate sample sizes required to estimate size structure and magnitude of retained and discarded catches for a desired precision and level of confidence, for each spatial/temporal stratum. A cost-effective environmental monitoring program needs to be implemented at an appropriate spatial scale to ensure environmental variability is incorporated into future assessments for both Giant Mud Crab and Blue Swimmer Crab. The future management objectives of the fishery, and magnitude of available funding, will provide guidance to the most appropriate survey type(s) for monitoring Giant Mud Crab in NSW in the future.

# Extension and adoption

## Communication and coverage

The communication and extension activities that occurred over the course of the project are summarised in Table 25.

**Table 25** Communication and coverage of project activities for the period from project commencement until the completion of the Final Report.

| Date       | Method               | Outlet   | Type         | Content  |
|------------|----------------------|--|--------------|--|
| 1/08/2018  | Direct communication | Wallis Lake Estuary Processes and Seafood Production Meeting | Face-to-face | Discussion of project objectives and design                            |
| 6/11/2018  | Direct communication | Letter to fishers  | Electronic   | Introductory letter  |
| 6/11/2018  | Direct communication | Letter to fishers  | Electronic   | Request for quote - Region 4 Estuary General                           |
| 14/11/2018 | Media                | 2SR  | Radio        | Interview and audio grabs  |
| 14/11/2018 | Media                | Macquarie Radio  | Radio        | Interview and audio grabs  |
| 19/02/2019 | Direct communication | Project signs deployed - Bellinger River                     | Signs        | Project information  |
| 28/02/2019 | Direct communication | Letter to Clarence Co-op                                     | Electronic   | Letter regarding research in Clarence River                            |
| 18/03/2019 | Direct communication | Project signs deployed - Clarence River                      | Signs        | Project information  |
| 16/04/2019 | Direct communication | Project flyer  | Flyer        | Project information  |
| 15/05/2019 | Direct communication | Letter to fishers  | Electronic   | Project information and request for quote - Zone 5 Ocean Trap and Line |
| 18/10/2019 | Direct communication | Project signs deployed – Port Stephens                       | Signs        | Project information  |

| Date       | Method               | Outlet  | Type                            | Content   |
|------------|----------------------|---|---------------------------------|---|
| 08/03/2021 | Direct communication | Gladstone Healthy Harbour Mud Crab Workshop           | Face-to-face (virtual)          | Presentation to interstate researchers/managers   |
| 29/04/2021 | Direct communication | International Conference on Shellfish Restoration     | Face-to-face                    | Presentation to scientists  |
| 16/06/2021 | Direct communication | Seafood Industry Field Day - Forster                  | Face-to-face (virtual)          | Presentation to industry stakeholders   |
| 17/06/2021 | Direct communication | Seafood Industry Field Day - Forster                  | Face-to-face (virtual)          | Presentation to industry stakeholders   |
| 19/10/2021 | Research papers      | <i>Fisheries Research</i>                             | Printed and online publications | <a href="https://doi.org/10.1016/j.fishres.2021.106140">https://doi.org/10.1016/j.fishres.2021.106140</a>                               |
| 02/12/2021 | Research papers      | <i>Marine and Freshwater Research</i>                 | Printed and online publications | <a href="https://www.publish.csiro.au/MF/MF21191">https://www.publish.csiro.au/MF/MF21191</a>   |
| 01/03/2022 | Research papers      | <i>Estuaries and Coasts</i>                           | Printed and online publications | <a href="https://link.springer.com/article/10.1007/s12237-022-01061-1">https://link.springer.com/article/10.1007/s12237-022-01061-1</a> |
| 09/03/2022 | Research papers      | <i>Marine and Freshwater Research</i>                 | Printed and online publications | <a href="https://www.publish.csiro.au/MF/ju-staccepted/MF21005">https://www.publish.csiro.au/MF/ju-staccepted/MF21005</a>               |
| 04/01/2023 | Research papers      | <i>Fisheries Research</i>                             | Printed and online publications | <a href="https://doi.org/10.1016/j.fishres.2022.106582">https://doi.org/10.1016/j.fishres.2022.106582</a>                               |
| 07/09/2022 | Research papers      | <i>Fisheries Oceanography</i>                         | Printed and online publications | <a href="https://doi.org/10.1111/fog.12608">https://doi.org/10.1111/fog.12608</a>   |
| 09/11/2022 | Direct communication | Australian Society for Fish Biology Annual Conference | Face-to-face                    | Presentation to scientists  |
| 07/04/2023 | Research papers      | <i>Movement Ecology</i>                               | Printed and online publications | <a href="https://movementecologyjournal.biomedcentral.com/articles">https://movementecologyjournal.biomedcentral.com/articles</a>       |
| 31/07/2023 | Direct communication | Project flyer   | Flyer                           | Information on project outcomes, distributed to fishers and posted online   |

## Adoption

### Blue Swimmer Crab

The independent survey that was commenced during this program continues to be carried out in two estuaries (Wallis Lake and Lake Macquarie) at the time that this report was finalised. Each survey represents a different component of adoption for the project. As NSW largest Blue Swimmer Crab fishery, the work in Wallis Lake is developing an ongoing time series to inform assessment, stock status reporting, and quota-setting processes for the NSW Blue Swimmer Crab stock. At present, the fishery is managed under an interim quota arrangement, however the data that is being generated through the ongoing independent survey will inform the review of quota in 2024/25. It is envisaged at this time that the application of the predictive tools outlined in *Long-term drivers of catch variability in Wallis Lake*, on an ongoing basis, will be considered.

The independent trap survey work in Lake Macquarie is continuing under a new project funded by the Recreational Fishing Saltwater Trust, and will be compared against the data collected and reported in *Fishery independent survey of Blue Swimmer Crab – Description and data summary*, *Latitudinal trends in the reproductive biology of female Blue Swimmer Crab in south-eastern Australia*, *Estuary-specific drivers of Blue Swimmer Crab abundance and distribution*, and *Reproductive cycles of Blue Swimmer Crab in relation to variation in temperature and conductivity*, to evaluate the potential impacts of recent regulation changes in this estuary to allow the use of round traps by recreational fishers for the capture of crabs.

The automated egg count methodology developed for Blue Swimmer Crab reported in *An automated image analysis system for estimating fecundity in portunid crabs* is currently being trialled for enumerating Eastern Rock Lobster eggs, to aid in stock assessment and population modelling for that species.

### Giant Mud Crab

The relationships identified in *Environmental drivers of variation in Giant Mud Crab harvest rates* continue to support catch-rate standardisation, stock assessment, and stock status reporting for Giant Mud Crab. Similar to Blue Swimmer Crab, Giant Mud Crab is managed under an interim quota arrangement, that will be reviewed in 2024/25. The relationships in all chapters, especially *Testing broad-scale environment-catch relationships for Giant Mud Crab* will inform the species assessment and quota-setting process from this point forward.

Furthermore, additional research on Giant Mud Crab in Queensland is building on the design and approach laid down in *Movement, habitat use, and behaviour of free-ranging Giant Mud Crab* and *Environmental influence on spawning migrations in Giant Mud Crab*.

At the time of this report, development and implementation of fisheries enhancement for both Blue Swimmer Crab and Giant Mud Crab continue to be a low priority in NSW. When planning commences for hatchery releases of these species, the findings of this report will be used to define recruitment limited niches in space and time, to which hatchery releases can be targeted.

# Project materials developed

Hanamseth, R., Hewitt, D.E., Johnson, D.D., Suthers, I.M., and Taylor, M.D. (2022) An automated image analysis system for estimating fecundity in portunid crabs. *Fisheries Research* **245**, 106140.

Hanamseth, R., Johnson, D.D., Suthers, I.M., and Taylor, M.D. (2022) Evaluation of a novel research trap for surveys of Blue Swimmer Crab populations. *Marine and Freshwater Research* **73**(6), 812-822.

Hewitt, D.E., Niella, Y., Johnson, D.D., Suthers, I.M., and Taylor, M.D. (2022) Crabs go with the flow: Declining conductivity and cooler temperatures trigger spawning migrations for female Giant Mud Crab (*Scylla serrata*) in subtropical estuaries. *Estuaries and Coasts* **45**, 2166-2180.

Hewitt, D.E., Schilling, H.T., Hanamseth, R., Everett, J.D., Li, J., Roughan, M., Johnson, D.D., Suthers, I.M., and Taylor, M.D. (2022) Mesoscale oceanographic features drive divergent patterns in connectivity for co-occurring estuarine portunid crabs. *Fisheries Oceanography* **31**(6), 587-600.

Hewitt, D.E., Johnson, D.D., Suthers, I.M., and Taylor, M.D. (2023) Crabs ride the tide: Incoming tides promote foraging of Giant Mud Crabs (*Scylla serrata*). *Movement Ecology* **11**, 10.1186/s40462-023-00384-3

Hewitt, D.E., Taylor, M.D., Suthers, I.M. and Johnson, D.D. (2023) Environmental drivers of variation in southeast Australian Giant Mud Crab (*Scylla serrata*) harvest rates. *Fisheries Research* **268**, 106850

Nolan, S.E.F., Johnson, D.D., Hanamseth, R., Suthers, I.M., and Taylor, M.D. (2022) Reproductive biology of female Blue Swimmer Crab in the temperate estuaries of south-eastern Australia. *Marine and Freshwater Research* **73**, 366-376.

Schilling, H., Johnson, D.D., Hanamseth, R., Suthers, I.M., and Taylor, M.D. (2023) Long-term drivers of catch variability in south-eastern Australia's largest portunid fishery. *Fisheries Research* **260**, 106582.

The information presented in chapters *Estuary-specific drivers of Blue Swimmer Crab abundance and distribution*, *Reproductive cycles of Blue Swimmer Crab in relation to variation in temperature and conductivity*, and *Testing broad-scale environment-catch relationships for Giant Mud Crab*, are either currently in review in the scientific literature, or will be submitted to the literature following the finalisation of the report.

# References

Addison, J.T., and Bell, M.C. (1997) Simulation modelling of capture processes in trap fisheries for clawed lobsters. *Marine and Freshwater Research* **48**(8), 1035-1044.

Alava, V.R., Qunitio, E.T., De Pedro, J.B., Priolo, F.M.P., Orozco, Z.G.A., and Wille, M. (2007) Lipids and fatty acids in wild and pond-reared mud crab *Scylla serrata* (Forsskål) during ovarian maturation and spawning. *Aquaculture Research* **38**(14), 1468-1477.

Alberts-Hubatsch, H., Yip Lee, S., Diele, K., Wolff, M., and Nordhaus, I. (2014) Microhabitat use of early benthic stage mud crabs, (Forsskål, 1775), in eastern Australia. *Journal of Crustacean Biology* **34**(5), 604-610.

Alberts-Hubatsch, H. (2015) Movement patterns and habitat use of the exploited swimming crab *Scylla serrata* (Forskål, 1775). Universität Bremen,

Alberts-Hubatsch, H., Lee, S.Y., Meynecke, J.O., Diele, K., Nordhaus, I., and Wolff, M. (2016) Life-history, movement, and habitat use of *Scylla serrata* (Decapoda, Portunidae): current knowledge and future challenges. *Hydrobiologia* **763**(1), 5-21.

Amin-Safwan, A., Muhd-Farouk, H., Mardhiyyah, M.P., Nadirah, M., and Ikhwanuddin, M. (2019) Does water salinity affect the level of 17 $\beta$ -estradiol and ovarian physiology of orange mud crab, *Scylla olivacea* (Herbst, 1796) in captivity? *Journal of King Saud University-Science* **31**(4), 827-835.

Andrade, L.S.d., Costa, R.C.d., Castilho, A.L., Frameschi, I.F., Sancinetti, G.S., and Fransozo, A. (2017) Reproductive and population traits of the swimming crab *Achelous spinimanus* (Crustacea: Decapoda) in an upwelling region in southeastern Brazil. *Nauplius* **25**, e2017004.

Archdale, M.V., Anasco, C.P., and Hiromori, S. (2006) Comparative fishing trials for invasive swimming crabs *Charybdis japonica* and *Portunus pelagicus* using collapsible pots. *Fisheries Research* **82**(1-3), 50-55.

Archdale, M.V., Añasco, C.P., Kawamura, Y., and Tomiki, S. (2007) Effect of two collapsible pot designs on escape rate and behavior of the invasive swimming crabs *Charybdis japonica* and *Portunus pelagicus*. *Fisheries Research* **85**(1-2), 202-209.

Archdale, M.V. (2012) Development of trapping gear and methods for swimming crabs. *Crabs: Anatomy, Habitat and Ecological Significance*, 27-47.

Archer, M.R., Roughan, M., Keating, S.R., and Schaeffer, A. (2017) On the variability of the East Australian Current: Jet structure, meandering, and influence on shelf circulation. *Journal of Geophysical Research: Oceans* **122**(11), 8464-8481.

- Asch, R.G., Stock, C.A., and Sarmiento, J.L. (2019) Climate change impacts on mismatches between phytoplankton blooms and fish spawning phenology. *Global Change Biology* **25**(8), 2544-2559.
- Bacheler, N.M., Schobernd, Z.H., Berrane, D.J., Schobernd, C.M., Mitchell, W.A., and Geraldi, N.R. (2013) When a trap is not a trap: converging entry and exit rates and their effect on trap saturation of black sea bass (*Centropristis striata*). *ICES Journal of Marine Science* **70**(4), 873-882.
- Bacheler, N.M., Michelot, T., Cheshire, R.T., and Shertzer, K.W. (2019) Fine-scale movement patterns and behavioral states of gray triggerfish *Balistes capriscus* determined from acoustic telemetry and hidden Markov models. *Fisheries Research* **215**, 76-89.
- Baliña, S., Temperoni, B., Lopez Greco, L.S., and Tropea, C. (2018) Losing reproduction: effect of high temperature on female biochemical composition and egg quality in a freshwater crustacean with direct development, the red cherry shrimp, *Neocaridina davidi* (Decapoda, Atyidae). *The Biological Bulletin* **234**(3), 139-151.
- Barnes, L., van der Meulen, D., Orchard, B., and Gray, C. (2013) Novel use of an ultrasonic cleaning device for fish reproductive studies. *Journal of Sea Research* **76**, 222-226.
- Barnes, T.C., Broadhurst, M.K., and Johnson, D.D. (2022) Disparity among recommended and adopted escape-gap designs and their utility for improving selection in an Australian portunid trap fishery. *Fisheries Research* **248**, 106219.
- Baylon, J.C. (2010) Effects of salinity and temperature on survival and development of larvae and juveniles of the Mud Crab, *Scylla serrata* (Crustacea: Decapoda: Portunidae). *Journal of the World Aquaculture Society* **41**(6), 858-873.
- Bellchambers, L.M., and de Lestang, S. (2005) Selectivity of different gear types for sampling the blue swimmer crab, *Portunus pelagicus* L. *Fisheries Research* **73**(1), 21-27.
- Bergshoeff, J.A., McKenzie, C.H., and Favaro, B. (2019) Improving the efficiency of the Fukui trap as a capture tool for the invasive European green crab (*Carcinus maenas*) in Newfoundland, Canada. *PeerJ* **7**, e6308.
- Biau, G., and Scornet, E. (2016) A random forest guided tour. *Test* **25**, 197-227.
- Biermann, J.L., North, E.W., and Boicourt, W.C. (2016) The distribution of blue crab (*Callinectes sapidus*) megalopae at the mouths of Chesapeake and Delaware Bays: Implications for larval ingress. *Estuaries and Coasts* **39**(1), 201-217.
- Breiman, L. (2001) Random forests. *Machine learning* **45**, 5-32.

- Brethes, J.-C., Bouchard, R., and Desrosiers, G. (1985) Determination of the area prospected by a baited trap from a tagging and recapture experiment with snow crabs (*Chionoecetes opilio*). *Journal of Northwest Atlantic Fishery Science* **6**(1), 37-42.
- Brick, R.W. (1974) Effects of water quality, antibiotics, phytoplankton and food on survival and development of larvae of *Scylla serrata* (Crustacea: Portunidae). *Aquaculture* **3**(3), 231-244.
- Broadhurst, M.K., Butcher, P.A., and Cullis, B.R. (2014) Effects of mesh size and escape gaps on discarding in an Australian giant mud crab (*Scylla serrata*) trap fishery. *PLoS One* **9**(9), e106414.
- Broadhurst, M.K., Millar, R.B., and Hughes, B. (2017) Performance of industry-developed escape gaps in Australian *Portunus pelagicus* traps. *Fisheries Research* **187**, 120-126.
- Broadhurst, M.K., Millar, R.B., and Hughes, B. (2018) Utility of multiple escape gaps in Australian *Scylla serrata* traps. *Fisheries Research* **204**, 88-94.
- Broadhurst, M.K., Smith, T.M., Millar, R.B., Hughes, B., Raoult, V., and Gaston, T.F. (2019) Cumulative selectivity benefits of increasing mesh size and using escape gaps in Australian *Portunus armatus* traps. *Fisheries Management and Ecology* **26**(4), 319-326.
- Broadhurst, M.K., Tolhurst, D.J., Hughes, B., Raoult, V., Smith, T.M., and Gaston, T.F. (2020) Optimising mesh size with escape gaps in a dual-species portunid-trap fishery. *Aquaculture and Fisheries* **5**(6), 308-316.
- Brodie, S., Ledee, E.J.I., Heupel, M.R., Babcock, R.C., Campbell, H.A., Gledhill, D.C., Hoenner, X., Huveneers, C., Jaine, F., Simpfendorfer, C., Taylor, M.D., Udyawer, V., and Harcourt, R.G. (2018a) Continental-scale animal tracking reveals functional movement classes across marine taxa. *Scientific Reports* **8**, 3717.
- Brodie, S., Litherland, L., Stewart, J., Schilling, H., Pepperell, J., and Suthers, I. (2018b) Citizen science records describe the distribution and migratory behaviour of a piscivorous predator, *Pomatomus saltatrix*. *ICES Journal of Marine Science* **75**(5), 1573-1582.
- Brooks, M.E., Kristensen, K., Van Benthem, K.J., Magnusson, A., Berg, C.W., Nielsen, A., Skaug, H.J., Machler, M., and Bolker, B.M. (2017) glmmTMB balances speed and flexibility among packages for zero-inflated generalized linear mixed modeling. *The R Journal* **9**(2), 378-400.
- Brooks, M.E., Melli, V., Savina, E., Santos, J., Millar, R., O'Neill, F.G., Veiga-Malta, T., Krag, L.A., and Feekings, J.P. (2022) Introducing selfisher: open source software for statistical analyses of fishing gear selectivity. *Canadian Journal of Fisheries and Aquatic Sciences* **99**(999), 1-9.
- Brownscombe, J.W., Lédée, E.J., Raby, G.D., Struthers, D.P., Gutowsky, L.F., Nguyen, V.M., Young, N., Stokesbury, M.J., Holbrook, C.M., and Brenden, T.O. (2019) Conducting and interpreting fish telemetry studies: considerations for researchers and resource managers. *Reviews in Fish Biology and Fisheries* **29**, 369-400.

Bryars, S.R., and Havenhand, J.N. (2004) Temporal and spatial distribution and abundance of blue swimmer crab (*Portunus pelagicus*) larvae in a temperate gulf. *Marine and Freshwater Research* **55**(8), 809-818.

Bryars, S.R., and Havenhand, J.N. (2006) Effects of constant and varying temperatures on the development of blue swimmer crab (*Portunus pelagicus*) larvae: Laboratory observations and field predictions for temperate coastal waters. *Journal of Experimental Marine Biology and Ecology* **329**(2), 218-229.

Burnham, K.P., and Anderson, D.R. (2002a) 'Model selection and multimodel inference: a practical information-theoretic approach.' (Springer-Verlag: New York) 488

Burnham, K.P., and Anderson, D.R. (2002b) 'Model Selection and Inference.' (Springer New York, NY) 355

Butcher, P.A., Leland, J.C., Broadhurst, M.K., Paterson, B.D., and Mayer, D.G. (2012) Giant mud crab (*Scylla serrata*): relative efficiencies of common baited traps and impacts on discards. *ICES Journal of Marine Science* **69**(8), 1511-1522.

Butcher, P.A., Boulton, A.J., Macbeth, W.G., and Malcolm, H.A. (2014) Long-term effects of marine park zoning on giant mud crab *Scylla serrata* populations in three Australian estuaries. *Marine Ecology Progress Series* **508**, 163-176.

Bycroft, B.L. (1986) A technique for separating and counting rock lobster eggs. *New Zealand Journal of Marine and Freshwater Research* **20**(4), 623-626.

Cadrin, S.X. (2020) Defining spatial structure for fishery stock assessment. *Fisheries Research* **221**, 105397.

Campbell, T.I., Tweedley, J.R., Johnston, D.J., and Loneragan, N.R. (2021) Crab diets differ between adjacent estuaries and habitats within a sheltered marine embayment. *Frontiers in Marine Science* **8**(80). [In English]

Caputi, N., de Lestang, S., Hart, A., Kangas, M., Johnston, D., and Penn, J. (2014) Catch predictions in stock assessment and management of invertebrate fisheries using pre-recruit abundance—case studies from Western Australia. *Reviews in Fisheries Science & Aquaculture* **22**(1), 36-54.

Caputi, N., Kangas, M., Denham, A., Feng, M., Pearce, A., Hetzel, Y., and Chandrapavan, A. (2016) Management adaptation of invertebrate fisheries to an extreme marine heat wave event at a global warming hot spot. *Ecology and Evolution* **6**(11), 3583-3593.

Carr, S.D., Tankersley, R.A., Hench, J.L., Forward Jr, R.B., and Luettich Jr, R.A. (2004) Movement patterns and trajectories of ovigerous blue crabs *Callinectes sapidus* during the spawning migration. *Estuarine, Coastal and Shelf Science* **60**(4), 567-579.

Carver, A.M., Wolcott, T.G., Wolcott, D.L., and Hines, A.H. (2005) Unnatural selection: effects of a male-focused size-selective fishery on reproductive potential of a blue crab population. *Journal of Experimental Marine Biology and Ecology* **319**(1-2), 29-41.

Cetina-Heredia, P., Roughan, M., Liggins, G., Coleman, M.A., and Jeffs, A. (2019) Mesoscale circulation determines broad spatio-temporal settlement patterns of lobster. *Plos One* **14**(2), e0211722.

Cetina-Heredia, P., Roughan, M., Van Sebille, E., and Coleman, M. (2014) Long-term trends in the East Australian Current separation latitude and eddy driven transport. *Journal of Geophysical Research: Oceans* **119**(7), 4351-4366.

Cetina-Heredia, P., Roughan, M., Sebille, E., Feng, M., and Coleman, M.A. (2015) Strengthened currents override the effect of warming on lobster larval dispersal and survival. *Global change biology* **21**(12), 4377-4386.

Champion, C., Broadhurst, M.K., Ewere, E.E., Benkendorff, K., Butcherine, P., Wolfe, K., and Coleman, M.A. (2020) Resilience to the interactive effects of climate change and discard stress in the commercially important blue swimmer crab (*Portunus armatus*). *Marine Environmental Research* **159**, 105009.

Chandrapavan, A., Caputi, N., and Kangas, M.I. (2019) The decline and recovery of a crab population from an extreme marine heatwave and a changing climate. *Frontiers in Marine Science* **6**, 510.

Chaplin, J., Yap, E., Sezmiş, E., and Potter, I. (2001) Genetic (microsatellite) determination of the stock structure of the blue swimmer crab in Australia. FRDC Project No. 98/118, Murdoch University, Murdoch.

Chassignet, E.P., Hurlburt, H.E., Smedstad, O.M., Halliwell, G.R., Hogan, P.J., Wallcraft, A.J., Baraille, R., and Bleck, R. (2007) The HYCOM (hybrid coordinate ocean model) data assimilative system. *Journal of Marine Systems* **65**(1-4), 60-83.

Chen, J.-C., and Chia, P.-G. (1996) Oxygen uptake and nitrogen excretion of juvenile *Scylla serrata* at different temperature and salinity levels. *Journal of Crustacean Biology* **16**(3), 437-442.

Ciannelli, L., Bailey, K., and Olsen, E.M. (2015) Evolutionary and ecological constraints of fish spawning habitats. *ICES Journal of Marine Science* **72**(2), 285-296.

CNES (2015) SSALTO/DUACS User Handbook: (M)SLA and (M)ADT Near-Real Time and Delayed Time Products. (AVISO Satellite Altimetry Data)

Coleman, M.A., Roughan, M., Macdonald, H.S., Connell, S.D., Gillanders, B.M., Kelaher, B.P., and Steinberg, P.D. (2011) Variation in the strength of continental boundary currents determines continent-wide connectivity in kelp. *Journal of Ecology* **99**(4), 1026-1032.

- Coleman, M.A., Cetina-Heredia, P., Roughan, M., Feng, M., van Sebille, E., and Kelaher, B.P. (2017) Anticipating changes to future connectivity within a network of marine protected areas. *Global Change Biology* **23**(9), 3533-3542.
- Comeau, M., Smith, M.D., and Mallet, M. (2009) Variability in trap catches for an American lobster, *Homarus americanus*, spring fishery. *New Zealand Journal of Marine and Freshwater Research* **43**(1), 401-410.
- Connolly, R.M., and Waltham, N.J. (2015) Spatial analysis of carbon isotopes reveals seagrass contribution to fishery food web. *Ecosphere* **6**(9), 1-12.
- Cooke, S.J., Martins, E.G., Struthers, D.P., Gutowsky, L.F., Power, M., Doka, S.E., Dettmers, J.M., Crook, D.A., Lucas, M.C., Holbrook, C.M., and Krueger, C.C. (2016) A moving target-incorporating knowledge of the spatial ecology of fish into the assessment and management of freshwater fish populations. *Environmental Monitoring and Assessment* **188**(4), 1-18.
- Coppens, A.B. (1981) Simple equations for the speed of sound in Neptunian waters. *The Journal of the Acoustical Society of America* **69**(3), 862-863.
- Cote, D., Nicolas, J.-M., Whoriskey, F., Cook, A.M., Broome, J., Regular, P.M., and Baker, D. (2019) Characterizing snow crab (*Chionoecetes opilio*) movements in the Sydney Bight (Nova Scotia, Canada): a collaborative approach using multiscale acoustic telemetry. *Canadian Journal of Fisheries and Aquatic Sciences* **76**(2), 334-346.
- Cote, D., Morris, C., Regular, P., and Piersiak, M. (2020) Effects of 2D Seismic on snow crab movement behavior. *Fisheries Research* **230**, 105661.
- Cowan, R.K., and Sponagle, S. (2009) Larval dispersal and marine population connectivity. *Annual Review of Marine Science* **1**, 443-466.
- Cowen, R.K., Gawarkiewicz, G., Pineda, J., Thorrold, S.R., and Werner, F.E. (2007) Population connectivity in marine systems an overview. *Oceanography* **20**(3), 14-21.
- Cowen, R.K., and Sponagle, S. (2009) Larval dispersal and marine population connectivity. *Annual review of marine science* **1**, 443-466.
- Creese, R.G., Glasby, T.M., West, G., and Gallen, C. (2009) Mapping the estuarine habitats of NSW. Port Stephens Fisheries Institute.
- Cury, P.M., Fromentin, J.-M., Figuet, S., and Bonhommeau, S. (2014) Resolving hjord's dilemma: how is recruitment related to spawning stock biomass in marine fish? *Oceanography* **27**(4), 42-47.
- Cutler, D.R., Edwards Jr, T.C., Beard, K.H., Cutler, A., Hess, K.T., Gibson, J., and Lawler, J.J. (2007) Random forests for classification in ecology. *Ecology* **88**(11), 2783-2792.

Das, T., and Stickle, W.B. (1994) Detection and avoidance of hypoxic water by juvenile *Callinectes sapidus* and *C. similis*. *Marine Biology* **120**(4), 593-600.

Davenport, J., and Wong, T. (1987) Responses of adult mud crabs (*Scylla serrata*) (Forsk.) to salinity and low oxygen tension. *Comparative Biochemistry and Physiology Part A: Physiology* **86**(1), 43-47.

Davis, T. (1984) Estimation of fecundity in barramundi, *Lates calcarifer* (Bloch), using an automatic particle counter. *Marine and Freshwater Research* **35**(1), 111-118.

de Lestang, S., Hall, N., and Potter, I.C. (2003a) Influence of a deep artificial entrance channel on the biological characteristics of the blue swimmer crab *Portunus pelagicus* in a large microtidal estuary. *Journal of Experimental Marine Biology and Ecology* **295**(1), 41-61.

de Lestang, S., Hall, N.G., and Potter, I.C. (2003b) Reproductive biology of the blue swimmer crab (*Portunus pelagicus*, Decapoda: Portunidae) in five bodies of water on the west coast of Australia. *Fishery Bulletin* **101**(4), 745-757.

de Lestang, S., Bellchambers, L.M., Caputi, N., Thomson, A.W., Pember, M.B., Johnston, D.J., and Harris, D.C. (2010) Stock–recruitment–environment relationship in a *Portunus pelagicus* fishery in Western Australia. In *Biology and Management of Exploited Crab Populations under Climate Change*. (Eds. GH Kruse, GL Eckert, R Foy, RN Lipcius, B Sainte-Marie, DL Stram and W D.) pp. 443-460. (Alaska Sea Grant, University of Alaska Fairbanks)

de Lestang, S., Caputi, N., How, J., Melville-Smith, R., Thomson, A., and Stephenson, P. (2012) Stock assessment for the west coast rock lobster fishery. Western Australia Fisheries Research REport Series vol. 217.

de Lestang, S., Caputi, N., Feng, M., Denham, A., Penn, J., Slawinski, D., Pearce, A., and How, J. (2015) What caused seven consecutive years of low puerulus settlement in the western rock lobster fishery of Western Australia? *ICES Journal of Marine Science* **72**(suppl\_1), i49-i58.

Delandmeter, P., and Van Sebille, E. (2019) The Parcels v2. 0 Lagrangian framework: new field interpolation schemes. *Geoscientific Model Development* **12**(8), 3571-3584.

DeMartini, E.E., DiNardo, G.T., and Williams, H.A. (2003) Temporal changes in population density, fecundity, and egg size of the Hawaiian spiny lobster (*Panulirus marginatus*) at Necker Bank, Northwestern Hawaiian Islands. *Fishery Bulletin* **101**, 22-31.

Demopoulos, A.W., Cormier, N., Ewel, K.C., and Fry, B. (2008) Use of multiple chemical tracers to define habitat use of Indo-Pacific mangrove crab, *Scylla serrata* (Decapoda: Portunidae). *Estuaries and Coasts* **31**(2), 371-381.

- DeRuiter, S.L., Langrock, R., Skirbutas, T., Goldbogen, J.A., Calambokidis, J., Friedlaender, A.S., and Southall, B.L. (2017) A multivariate mixed hidden Markov model for blue whale behaviour and responses to sound exposure.
- Doblin, M.A., and van Sebille, E. (2016) Drift in ocean currents impacts intergenerational microbial exposure to temperature. *Proceedings of the National Academy of Sciences*.
- Dodgshun, T. (1980) Simple, accurate method of counting fish eggs. *The Progressive Fish-Culturist* **42**(4), 237-238.
- Douma, J.C., and Weedon, J.T. (2019) Analysing continuous proportions in ecology and evolution: A practical introduction to beta and Dirichlet regression. *Methods in Ecology and Evolution* **10**(9), 1412-1430.
- Drinkwater, K.F., Tremblay, M.J., and Comeau, M. (2006) The influence of wind and temperature on the catch rate of the American lobster (*Homarus americanus*) during spring fisheries off eastern Canada. *Fisheries Oceanography* **15**(2), 150-165.
- Duan, J., An, J., and Yu, H. (2008) A new species and two new record species of genus *Allokepon* Markham, 1982 (Isopoda: Epicaridea: Bopyridae) from China. *Zootaxa* **1682**(1), 62–68-62–68.
- Egbert, G.D., and Erofeeva, S.Y. (2002) Efficient inverse modeling of barotropic ocean tides. *Journal of Atmospheric and Oceanic technology* **19**(2), 183-204.
- Emerson, L., Walker, M.G., and Witthames, P. (1990) A stereological method for estimating fish fecundity. *Journal of Fish Biology* **36**(5), 721-730.
- Espinoza, M., Farrugia, T.J., Webber, D.M., Smith, F., and Lowe, C.G. (2011) Testing a new acoustic telemetry technique to quantify long-term, fine-scale movements of aquatic animals. *Fisheries Research* **108**(2-3), 364-371.
- Everett, J., Macdonald, H., Baird, M., Humphries, J., Roughan, M., and Suthers, I. (2015) Cyclonic entrainment of preconditioned shelf waters into a frontal eddy. *Journal of Geophysical Research: Oceans* **120**(2), 677-691.
- Everett, J.D., Baird, M.E., Oke, P.R., and Suthers, I.M. (2012) An Avenue of Eddies: Quantifying the biophysical properties of mesoscale eddies in the Tasman Sea. *Geophysical Research Letters* **39**, L16608 doi:10.1029/2012GL053091
- Everett, J.D., van Sebille, E., Taylor, M.D., Suthers, I.M., Setio, C., Cetina-Heredia, P., and Smith, J.A. (2017) Dispersal of Eastern King Prawn larvae in a western boundary current: New insights from particle tracking. *Fisheries Oceanography* **26**(5), 513–525.

FAO (2018) The State of World Fisheries and Aquaculture: Meeting the Sustainable Development Goals. FAO, Rome.

Figueira, W.F., and Crowder, L.B. (2006) Defining patch contribution in source-sink metapopulations: the importance of including dispersal and its relevance to marine systems. *Population Ecology* **48**(3), 215-224.

Flávio, H., and Baktoft, H. (2021) actel: Standardised analysis of acoustic telemetry data from animals moving through receiver arrays. *Methods in Ecology and Evolution* **12**(1), 196-203.

Florko, K.R., Davidson, E.R., Lees, K.J., Hammer, L.J., Lavoie, M.-F., Lennox, R.J., Simard, É., Archambault, P., Auger-Méthé, M., and McKindsey, C.W. (2021) Tracking movements of decapod crustaceans: a review of a half-century of telemetry-based studies. *Marine Ecology Progress Series* **679**, 219-239.

Foo, S.A., and Byrne, M. (2017) Marine gametes in a changing ocean: impacts of climate change stressors on fecundity and the egg. *Marine Environmental Research* **128**, 12-24.

Foster, S.D., and Bravington, M.V. (2013) A Poisson–Gamma model for analysis of ecological non-negative continuous data. *Environmental and Ecological Statistics* **20**(4), 533-552.

Frederich, M., and Pörtner, H.O. (2000) Oxygen limitation of thermal tolerance defined by cardiac and ventilatory performance in spider crab, *Maja squinado*. *American Journal of Physiology-Regulatory, Integrative and Comparative Physiology* **279**(5), R1531-R1538.

Friedland, K., Ama-Abasi, D., Manning, M., Clarke, L., Kligys, G., and Chambers, R. (2005) Automated egg counting and sizing from scanned images: rapid sample processing and large data volumes for fecundity estimates. *Journal of Sea Research* **54**(4), 307-316.

Frusher, S.D., Hobday, A.J., Jennings, S.M., Creighton, C., D’Silva, D., Haward, M., Holbrook, N.J., Nursey-Bray, M., Pecl, G.T., and van Putten, E.I. (2014) The short history of research in a marine climate change hotspot: from anecdote to adaptation in south-east Australia. *Reviews in Fish Biology and Fisheries* **24**(2), 593-611.

Garcia, V., Schilling, H.T., Cruz, D.O., Hawes, S.M., Everett, J.D., Roughan, M., Miskiewicz, A.G., Pakhomov, E.A., Jeffs, A., and Suthers, I.M. (2022) Entrainment and development of larval fish assemblages in two contrasting cold core eddies of the East Australian Current system. *Marine Ecology Progress Series* **685**, 1-18.

Gaughan, D.J., and Potter, I.C. (1994) Relative abundance and seasonal changes in the macrozooplankton of the lower Swan Estuary in south-western Australia. *Records of the Western Australian Museum* **16**(4), 461-474.

Gervais, C.R., Champion, C., and Pecl, G.T. (2021) Species on the move around the Australian coastline: A continental-scale review of climate-driven species redistribution in marine systems. *Global Change Biology* **27**(14), 3200-3217.

Gibson, R., Barnes, M., and Atkinson, R. (2001) Selective tidal-stream transport of marine animals. *Oceanography and Marine Biology, an Annual Review* **39**, 305-353.

Gibson, R.N. (2003) Go with the flow: tidal migration in marine animals. *Hydrobiologia* **503**(1), 153-161.

Gillson, J. (2011) Freshwater flow and fisheries production in estuarine and coastal systems: Where a drop of rain is not lost. *Reviews in Fisheries Science* **19**(3), 168-186.

Gillson, J., Suthers, I., and Scandol, J. (2012) Effects of flood and drought events on multi-species, multi-method estuarine and coastal fisheries in eastern Australia. *Fisheries Management and Ecology* **19**(1), 54-68.

Glaister, J.P. (1978) Impact of river discharge on distribution and production of School Prawn *Metapenaeus macleayi* (Haswell) (Crustacea-Penaeidae) in Clarence River region, northern New South Wales. *Australian Journal of Marine and Freshwater Research* **29**(3), 311-323.

Glasby, T.M., and West, G. (2018) Dragging the chain: Quantifying continued losses of seagrasses from boat moorings. *Aquatic Conservation: Marine and Freshwater Ecosystems* **28**(2), 383-394.

Glennie, R., Adam, T., Leos-Barajas, V., Michelot, T., Photopoulou, T., and McClintock, B.T. (2023) Hidden Markov models: Pitfalls and opportunities in ecology. *Methods in Ecology and Evolution* **14**(1), 43-56.

Gopurenko, D., and Hughes, J.M. (2002) Regional patterns of genetic structure among Australian populations of the mud crab, *Scylla serrata* (Crustacea : Decapoda): evidence from mitochondrial DNA. *Marine and Freshwater Research* **53**(5), 849-857.

Gorsky, G., Ohman, M.D., Picheral, M., Gasparini, S., Stemmann, L., Romagnan, J.-B., Cawood, A., Pesant, S., García-Comas, C., and Prejger, F. (2010) Digital zooplankton image analysis using the ZooScan integrated system. *Journal of Plankton Research* **32**(3), 285-303.

Gray, C.A., and Barnes, L.M. (2015) Spawning, maturity, growth and movement of *Platycephalus fuscus* (Cuvier, 1829) (Platycephalidae): fishery management considerations. *Journal of Applied Ichthyology* **31**(3), 442-450.

Grazer, V.M., and Martin, O.Y. (2012) Investigating climate change and reproduction: experimental tools from evolutionary biology. *Biology* **1**(2), 411-438.

Green, B.S., Gardner, C., Hochmuth, J.D., and Linnane, A. (2014) Environmental effects on fished lobsters and crabs. *Reviews in Fish Biology and Fisheries* **24**, 613-638.

Griffen, B.D. (2018) The timing of energy allocation to reproduction in an important group of marine consumers. *PLoS One* **13**(6), e0199043.

Grothues, T.M., Able, K.W., and Pravatiner, J.H. (2012) Winter flounder (*Pseudopleuronectes americanus* Walbaum) burial in estuaries: acoustic telemetry triumph and tribulation. *Journal of Experimental Marine Biology and Ecology* **438**, 125-136.

Guillory, V., and Prejean, P. (1997) Blue crab, *Callinectes sapidus*, trap selectivity studies: mesh size. *Marine Fisheries Review* **59**, 29.

Guillory, V., and Prejean, P. (1998) Blue crab, *Callinectes sapidus*, retention rates in different trap meshes. *Marine Fisheries Review* **60**, 35-37.

Gurarie, E., Bracis, C., Delgado, M., Meckley, T.D., Kojola, I., and Wagner, C.M. (2016) What is the animal doing? Tools for exploring behavioural structure in animal movements. *Journal of Animal Ecology* **85**(1), 69-84.

Halsey, L.G., Matthews, P.G.D., Rezende, E.L., Chauvaud, L., and Robson, A.A. (2015) The interactions between temperature and activity levels in driving metabolic rate: Theory, with empirical validation from contrasting ectotherms. *Oecologia* **177**(4), 1117-1129.

Hamasaki, K. (2002) Effects of temperature on the survival, spawning and egg incubation period of overwintering mud crab broodstock, *Scylla paramamosain* (Brachyura: Portunidae). *Aquaculture Science* **50**(3), 301-308.

Hamasaki, K. (2003) Effects of temperature on the egg incubation period, survival and developmental period of larvae of the mud crab *Scylla serrata* (Forskål)(Brachyura: Portunidae) reared in the laboratory. *Aquaculture* **219**(1-4), 561-572.

Hamasaki, K., Ishii, M., and Dan, S. (2021) Seasonal variability in fecundity and egg size in the porcellanid crab *Petrolisthes japonicus* (Decapoda: Anomura: Porcellanidae). *Crustacean Research* **50**, 17-27.

Harris, D., Johnston, D., Sporer, E., Kangas, M., Felipe, N., and Caputi, N. (2012) Biology and management of a multi-sector blue swimmer crab fishery in a subtropical embayment – Shark Bay, Western Australia. *Marine and Freshwater Research* **63**(11), 1165-1179.

Hartig, F. (2020) DHARMA: Residual Diagnostics for Hierarchical (Multi-Level / Mixed) Regression Models. R package version 0.1.5. <http://florianhartig.github.io/DHARMA/>.

Hastie, T.J., and Tibshirani, R.J. (1990) Generalized additive models. *Statistical Science* **1**(3), 297-318.

Hay, T., Gribble, N., Vries, C.D., Danaher, K., Dunning, M., Hearnden, M., Caley, P., Wright, C., Brown, I., Bailey, S., and Phelan, M.J. (2005) Methods for Monitoring the Abundance and Habitat of the Northern Australian Mud Crab *Scylla serrata*: Final Report FRDC Project 2000/142. Department of Business, Industry and Resource Development, Darwin, Northern Territory.

- Hayes, C.T., Alford, S.B., Belgrad, B.A., Correia, K.M., Darnell, M.Z., Furman, B.T., Hall, M.O., Martin, C.W., McDonald, A.M., and Smeed, D.L. (2022) Regional variation in seagrass complexity drives blue crab *Callinectes sapidus* mortality and growth across the northern Gulf of Mexico. *Marine Ecology Progress Series* **693**, 141-155.
- Heasman, M.P. (1980) Aspects of the general biology and fishery of the mud crab *Scylla serrata* (Forsk.) in Moreton Bay, Queensland. PhD Thesis, University of Queensland,
- Heasman, M.P., and Fielder, D.R. (1983) Laboratory spawning and mass rearing of the mangrove crab, *Scylla serrata* (Forsk.), from first zoea to first crab stage. *Aquaculture* **34**(3), 303-316.
- Heasman, M.P., Fielder, D.R., and Shepherd, R.K. (1985) Mating and spawning in the mudcrab, *Scylla serrata* (Forsk.) (Decapoda: Portunidae), in Moreton Bay, Queensland. *Marine and Freshwater Research* **36**(6), 773-783.
- Henley, B.J., Gergis, J., Karoly, D.J., Power, S., Kennedy, J., and Folland, C.K. (2015) A tripole index for the interdecadal Pacific oscillation. *Climate Dynamics* **45**, 3077-3090.
- Hernández, C.M., Richardson, D.E., Rypina, I.I., Chen, K., Marancik, K.E., Shulzitski, K., and Llopiz, J.K. (2022) Support for the Slope Sea as a major spawning ground for Atlantic bluefin tuna: evidence from larval abundance, growth rates, and particle-tracking simulations. *Canadian Journal of Fisheries and Aquatic Sciences* **79**(5), 814-824.
- Herrmann, B., Sistiaga, M., Rindahl, L., and Tatone, I. (2017) Estimation of the effect of gear design changes on catch efficiency: methodology and a case study for a Spanish longline fishery targeting hake (*Merluccius merluccius*). *Fisheries Research* **185**, 153-160.
- Hertel, A.G., Niemelä, P.T., Dingemanse, N.J., and Mueller, T. (2020) A guide for studying among-individual behavioral variation from movement data in the wild. *Movement Ecology* **8**(1), 1-18.
- Hewitt, D.E., Niella, Y., Johnson, D.D., Suthers, I.M., and Taylor, M.D. (2022a) Crabs go with the flow: Declining conductivity and cooler temperatures trigger spawning migrations for female Giant Mud Crab (*Scylla serrata*) in subtropical estuaries. *Estuaries and Coasts*, 10.1007/s12237-022-01061-1.
- Hewitt, D.E., Schilling, H.T., Hanamseth, R., Everett, J.D., Li, J., Roughan, M., Johnson, D.D., Suthers, I.M., and Taylor, M.D. (2022b) Mesoscale oceanographic features drive divergent patterns in connectivity for co-occurring estuarine portunid crabs. *Fisheries Oceanography* **31**(6), 587-600.
- Hill, B.J. (1974) Salinity and temperature tolerance of zoeae of portunid crab *Scylla serrata*. *Marine Biology* **25**(1), 21-24.
- Hill, B.J. (1975) Abundance, breeding and growth of crab *Scylla serrata* in 2 South African estuaries. *Marine Biology* **32**(2), 119-126.

- Hill, B.J. (1976) Natural food, foregut clearance rate and activity of crab *Scylla serrata*. *Marine Biology* **34**(2), 109-116.
- Hill, B.J. (1978) Activity, track and speed of movement of crab *Scylla serrata* in an estuary. *Marine Biology* **47**(2), 135-141.
- Hill, B.J. (1979a) Biology of the crab *Scylla serrata* (Forsk.) in the St Lucia system. *Transactions of the Royal Society of South Africa* **44**(1), 55-62.
- Hill, B.J. (1979b) Aspects of the feeding strategy of the predatory crab *Scylla serrata*. *Marine Biology* **55**(3), 209-214.
- Hill, B.J. (1980) Effects of temperature on feeding and activity in the crab *Scylla serrata*. *Marine Biology* **59**(3), 189-192.
- Hill, B.J., Williams, M.J., and Dutton, P. (1982) Distribution of juvenile, subadult and adult *Scylla serrata* (Crustacea, Portunidae) on tidal flats in Australia. *Marine Biology* **69**(1), 117-120.
- Hill, B.J. (1994) Offshore spawning by the portunid crab *Scylla serrata* (Crustacea, Decapoda). *Marine Biology* **120**(3), 379-384.
- Hines, A.H., Jivoff, P.R., Bushmann, P.J., van Montfrans, J., Reed, S.A., Wolcott, D.L., and Wolcott, T.G. (2003) Evidence for sperm limitation in the blue crab, *Callinectes sapidus*. *Bulletin of Marine Science* **72**(2), 287-310.
- Hines, A.H., Johnson, E.G., Darnell, M.Z., Rittschof, D., Miller, T.J., Bauer, L.J., Rodgers, P., and Aguilar, R. (2010) Predicting effects of climate change on blue crabs in Chesapeake Bay. In *Biology and Management of Exploited Crab Populations under Climate Change*. (Eds. GH Kruse, GL Eckert, R Foy, RN Lipcius, B Sainte-Marie, DL Stram and W D.) pp. 109-128. (Alaska Sea Grant, University of Alaska Fairbanks)
- Hisam, F., Hajisamae, S., Ikhwanuddin, M., Aziz, N.A., Naimullah, M., and Hassan, M. (2018) Study on the reproductive biology of the blue swimming crab, *Portunus pelagicus* females from Pattani coastal waters, Thailand. *Aquaculture, Aquarium, Conservation & Legislation* **11**(6), 1776-1791.
- Hobday, A.J., and Pecl, G.T. (2014) Identification of global marine hotspots: sentinels for change and vanguards for adaptation action. *Reviews in Fish Biology and Fisheries* **24**(2), 415-425.
- Hooten, M.B., Johnson, D.S., McClintock, B.T., and Morales, J.M. (2017) 'Animal Movement: Statistical Models for Telemetry Data.' (CRC press)
- Huang, B., Thorne, P.W., Banzon, V.F., Boyer, T., Chepurin, G., Lawrimore, J.H., Menne, M.J., Smith, T.M., Vose, R.S., and Zhang, H. (2017) NOAA Extended Reconstructed Sea Surface Temperature (ERSST), Version 5. (Ed. NNCfE Information).

Huntingford, F., Taylor, A., Smith, I., and Thorpe, K. (1995) Behavioural and physiological studies of aggression in swimming crabs. *Journal of Experimental Marine Biology and Ecology* **193**(1-2), 21-39.

Hussey, N.E., Kessel, S.T., Aarestrup, K., Cooke, S.J., Cowley, P.D., Fisk, A.T., Harcourt, R.G., Holland, K.N., Iverson, S.J., and Kocik, J.F. (2015) Aquatic animal telemetry: a panoramic window into the underwater world. *Science* **348**(6240), 1255642.

Huveneers, C., Simpfendorfer, C.A., Kim, S., Semmens, J.M., Hobday, A.J., Pederson, H., Stieglitz, T., Vallee, R., Webber, D., Heupel, M.R., Peddemors, V., and Harcourt, R.G. (2016) The influence of environmental parameters on the performance and detection range of acoustic receivers. *Methods in Ecology and Evolution* **7**(7), 825-835.

Hyland, S.J., Hill, B.J., and Lee, C.P. (1984) Movement within and between different habitat by the portunid crab *Scylla serrata*. *Marine Biology* **80**(1), 57-61.

Isojunno, S., Sadykova, D., DeRuiter, S., Cure, C., Visser, F., Thomas, L., Miller, P.J.O.m., and Harris, C.M. (2017) Individual, ecological, and anthropogenic influences on activity budgets of long-finned pilot whales. *Ecosphere* **8**(12), e02044.

Jacox, M.G., Alexander, M.A., Amaya, D., Becker, E., Bograd, S.J., Brodie, S., Hazen, E.L., Pozo Buil, M., and Tommasi, D. (2022) Global seasonal forecasts of marine heatwaves. *Nature* **604**(7906), 486-490.

Jänes, H., Macreadie, P.I., Rizzari, J., Ierodionou, D., Reeves, S.E., Dwyer, P.G., and Carnell, P.E. (2022) The value of estuarine producers to fisheries: A case study of Richmond River Estuary. *Ambio* **51**(4), 875-887.

Jenkins, G.I., Michael, R., and Tweedley, J.R. (2017) Identifying future restocking options for Blue Swimmer Crabs (*Portunus armatus*).

Johnson, D., and London, J. (2018) crawl: an R package for fitting continuous-time correlated random walk models to animal movement data. *Zenodo doi* **10**, 10.

Johnson, D.D., Gray, C.A., and Macbeth, W.G. (2010) Reproductive biology of *Portunus pelagicus* in a south-east Australian estuary. *Journal of Crustacean Biology* **30**(2), 200-205.

Johnson, D.D. (2020a) NSW Stock Status Summary 2018/19 – Blue Swimmer Crab (*Portunus armatus*). NSW Department of Primary Industries - Fisheries, Port Stephens.

Johnson, D.D. (2020b) NSW Stock Status Summary 2018/19 – Giant Mud Crab (*Scylla serrata*). NSW Department of Primary Industries - Fisheries, Port Stephens.

Johnson, D.S., London, J.M., Lea, M.-A., and Durban, J.W. (2008) Continuous-time correlated random walk model for animal telemetry data. *Ecology* **89**(5), 1208-1215.

- Johnston, D., Harris, D., Caputi, N., and Thomson, A. (2011) Decline of a blue swimmer crab (*Portunus pelagicus*) fishery in Western Australia—History, contributing factors and future management strategy. *Fisheries Research* **109**(1), 119-130.
- Johnston, D., Yeoh, D., Harris, D., and Fisher, E. (2020) Blue Swimmer Crab (*Portunus armatus*) Resource in the West Coast Bioregion, Western Australia Part 1: Peel Harvey Estuary, Cockburn Sound and Swan Canning Estuary. Fisheries Research Report No. 307. Department of Primary Industries and Regional Development, Western Australia.
- Johnston, D., Chandrapavan, A., Walton, L., Beckmann, C., Johnson, D.D., and Garland, A. (2021a) Blue Swimmer Crab (*Portunus armatus*). In Status of Australian Fish Stocks 2020. pp. <https://fish.gov.au/report/299-Blue-Swimmer-Crab-2020> accessed 4 April 2022. (Fisheries Research and Development Corporation: Canberra)
- Johnston, D.J., and Yeoh, D.E. (2021) Temperature drives spatial and temporal variation in the reproductive biology of the blue swimmer crab *Portunus armatus* A. Milne-Edwards, 1861 (Decapoda: Brachyura: Portunidae). *Journal of Crustacean Biology* **41**(3).
- Johnston, D.J., Yeoh, D.E., and Harris, D.C. (2021b) Environmental drivers of commercial blue swimmer crab (*Portunus armatus*) catch rates in Western Australian fisheries. *Fisheries Research* **235**, 105827.
- Jonsen, I. (2016) Joint estimation over multiple individuals improves behavioural state inference from animal movement data. *Scientific Reports* **6**(1), 20625.
- Joo, R., Boone, M.E., Clay, T.A., Patrick, S.C., Clusella-Trullas, S., and Basille, M. (2020) Navigating through the R packages for movement. *Journal of Animal Ecology* **89**(1), 248-267.
- Josileen, J. (2013) Fecundity of the blue swimmer crab, *Portunus pelagicus* (Linnaeus, 1758) (Decapoda, Brachyura, Portunidae) along the coast of Mandapam, Tamil Nadu, India. *Crustaceana* **86**(1), 48-55.
- Jost, J.A., Podolski, S.M., and Frederich, M. (2012) Enhancing thermal tolerance by eliminating the pejus range: a comparative study with three decapod crustaceans. *Marine Ecology-Progress Series* **444**, 263-274.
- Junk, E.J., Smith, J.A., Suthers, I.M., and Taylor, M.D. (2021) Bioenergetics of blue swimmer crab (*Portunus armatus*) to inform estimation of release density for stock enhancement. *Marine and Freshwater Research*, <https://doi.org/10.1071/MF20363>.
- Kangas, M.I. (2000) Synopsis of the biology and exploitation of the blue swimmer crab, *Portunus pelagicus* Linnaeus, in Western Australia. Western Australian Department of Fisheries, Fisheries Research Report No. 121.

- Kell, L.T., Nash, R.D., Dickey-Collas, M., Mosqueira, I., and Szuwalski, C. (2016) Is spawning stock biomass a robust proxy for reproductive potential? *Fish and Fisheries* **17**(3), 596-616.
- Kerry, C., and Roughan, M. (2020) Downstream evolution of the East Australian Current system: Mean flow, seasonal, and intra-annual variability. *Journal of Geophysical Research: Oceans* **125**(5), e2019JC015227.
- Kerry, C., Roughan, M., and Powell, B. (2020) Predicting the submesoscale circulation inshore of the East Australian Current. *Journal of Marine Systems* **204**, 103286.
- Kingsford, M.J., and Suthers, I.M. (1994) Dynamic estuarine plumes and fronts: importance to small fish and plankton in coastal waters of NSW, Australia. *Continental Shelf Research* **14**(6), 655-672.
- Klibansky, N., and Juanes, F. (2008) Procedures for efficiently producing high-quality fecundity data on a small budget. *Fisheries Research* **89**(1), 84-89.
- Kramer, D.L., and Weary, D.M. (1991) Exploration versus exploitation: a field study of time allocation to environmental tracking by foraging chipmunks. *Animal Behaviour* **41**(3), 443-449.
- Kritzer, J.P., and Sale, P.F. (2004) Metapopulation ecology in the sea: from Levins' model to marine ecology and fisheries science. *Fish and Fisheries* **5**(2), 131-140.
- Kumar, M.S., Ferguson, G.J., Yongshun, X., Hooper, G., and Venema, S. (2000) Studies on reproductive biology and distribution of the blue swimmer crab (*Portunus pelagicus*) in South Australian Waters. South Australian Research and Development Institute, SARDI Research Report Series No. 47.
- Kumar, M.S., Xiao, Y.S., Venema, S., and Hooper, G. (2003) Reproductive cycle of the blue swimmer crab, *Portunus pelagicus*, off southern Australia. *Journal of the Marine Biological Association of the United Kingdom* **83**(5), 983-994.
- Lambert, Y. (2008) Why should we closely monitor fecundity in marine fish populations? *Journal of Northwest Atlantic Fishery Science* **41**.
- Lange, M., and van Sebille, E. (2017) Parcels v0. 9: prototyping a Lagrangian ocean analysis framework for the petascale age. *Geoscientific Model Development* **10**(11), 4175-4186.
- Langrock, R., King, R., Matthiopoulos, J., Thomas, L., Fortin, D., and Morales, J.M. (2012) Flexible and practical modeling of animal telemetry data: hidden Markov models and extensions. *Ecology* **93**(11), 2336-2342.
- Leis, J.M. (2021) Perspectives on larval behaviour in biophysical modelling of larval dispersal in marine, demersal fishes. *Oceans* **2**(1), 1-25.

Leland, J.C., Butcher, P.A., Broadhurst, M.K., Paterson, B.D., and Mayer, D.G. (2013) Relative trap efficiency for recreationally caught eastern Australian blue swimmer crab (*Portunus pelagicus*) and associated injury and mortality of discards. *Fisheries Research* **147**, 304-311.

Lenth, R.V. (2021) emmeans: Estimated Marginal Means, aka Least-Squares Means, R package version 1.6.2-1., <https://CRAN.R-project.org/package=emmeans>, accessed 6/10/2021.

Leos-Barajas, V., Photopoulou, T., Langrock, R., Patterson, T.A., Watanabe, Y.Y., Murgatroyd, M., and Papastamatiou, Y.P. (2017) Analysis of animal accelerometer data using hidden Markov models. *Methods in Ecology and Evolution* **8**(2), 161-173.

Li, J., Roughan, M., and Kerry, C. (2021) Dynamics of interannual eddy kinetic energy modulations in a Western Boundary Current. *Geophysical Research Letters* **48**(19), e2021GL094115.

Li, J., Roughan, M., and Kerry, C. (2022a) Drivers of ocean warming in the western boundary currents of the Southern Hemisphere. *Nature Climate Change* **12**(10), 901-909.

Li, J., Roughan, M., and Kerry, C. (2022b) Variability and drivers of ocean temperature extremes in a warming Western Boundary Current. *Journal of Climate* **35**(3), 1097-1111.

Li, M., and Bolker, B.M. (2017) Incorporating periodic variability in hidden Markov models for animal movement. *Movement ecology* **5**(1), 1-12.

Li, S., Wu, L., Yang, Y., Geng, T., Cai, W., Gan, B., Chen, Z., Jing, Z., Wang, G., and Ma, X. (2020) The Pacific Decadal Oscillation less predictable under greenhouse warming. *Nature Climate Change* **10**(1), 30-34.

Liu, Z., Wu, X., Wang, W., Yan, B., and Cheng, Y. (2014) Size distribution and monthly variation of ovarian development for the female blue swimmer crab, *Portunus pelagicus* in Beibu Gulf, off south China. *Scientia Marina* **78**(2), 257-268.

Loneragan, N.R., and Bunn, S.E. (1999) River flows and estuarine ecosystems: Implications for coastal fisheries from a review and a case study of the Logan River, southeast Queensland. *Australian Journal of Ecology* **24**(4), 431-440.

Long, X., Wu, X., Zhu, S., Ye, H., Cheng, Y., and Zeng, C. (2019) Salinity can change the lipid composition of adult Chinese mitten crab after long-term salinity adaptation. *PLoS One* **14**(7), e0219260.

Lunt, J., and Smee, D.L. (2014) Turbidity influences trophic interactions in estuaries. *Limnology and Oceanography* **59**(6), 2002-2012.

Madeira, D., Narciso, L., Cabral, H.N., and Vinagre, C. (2012) Thermal tolerance and potential impacts of climate change on coastal and estuarine organisms. *Journal of Sea Research* **70**, 32-41.

Malan, N., Archer, M., Roughan, M., Cetina-Heredia, P., Hemming, M., Rocha, C., Schaeffer, A., Suthers, I., and Queiroz, E. (2020) Eddy-driven cross-shelf transport in the East Australian Current separation zone. *Journal of Geophysical Research: Oceans* **125**(2), e2019JC015613.

Malan, N., Roughan, M., and Kerry, C. (2021) The rate of coastal temperature rise adjacent to a warming western boundary current is nonuniform with latitude. *Geophysical Research Letters* **48**(3), e2020GL090751.

Malan, N., Roughan, M., Hemming, M., and Schaeffer, A. (2023) Mesoscale circulation controls chlorophyll concentrations in the East Australian Current separation zone. *Journal of Geophysical Research: Oceans*, e2022JC019361.

Mantua, N. (1999) The Pacific Decadal Oscillation: a brief overview for non-specialists. *Encyclopedia of Environmental Change*.

Mantua, N.J., and Hare, S.R. (2002) The Pacific Decadal Oscillation. *Journal of Oceanography* **58**(1), 35-44.

Marks, R., Hesp, S.A., Johnston, D., Denham, A., and Loneragan, N. (2019) Temporal changes in the growth of a crustacean species, *Portunus armatus*, in a temperate marine embayment: evidence of density dependence. *ICES Journal of Marine Science* **77**(2), 773-790.

Marks, R., Hesp, S.A., Denham, A., Loneragan, N.R., Johnston, D., and Hall, N. (2021) Factors influencing the dynamics of a collapsed blue swimmer crab (*Portunus armatus*) population and its lack of recovery. *Fisheries Research* **242**, 106035.

Marra, G., and Wood, S.N. (2011) Practical variable selection for generalized additive models. *Computational Statistics & Data Analysis* **55**(7), 2372-2387.

Marriott, R.J., O'Neill, M.F., Newman, S.J., and Skepper, C.L. (2014) Abundance indices for long-lived tropical snappers: Estimating standardized catch rates from spatially and temporally coarse logbook data. *ICES Journal of Marine Science* **71**(3), 618-627.

Martínez-Moreno, J., Hogg, A.M., England, M.H., Constantinou, N.C., Kiss, A.E., and Morrison, A.K. (2021) Global changes in oceanic mesoscale currents over the satellite altimetry record. *Nature Climate Change* **11**(5), 397-403.

Maunder, M.N., and Punt, A.E. (2004) Standardizing catch and effort data: a review of recent approaches. *Fisheries Research* **70**(2-3), 141-159.

Maunder, M.N., Sibert, J.R., Fonteneau, A., Hampton, J., Kleiber, P., and Harley, S.J. (2006) Interpreting catch per unit effort data to assess the status of individual stocks and communities. *ICES Journal of Marine Science* **63**(8), 1373-1385.

McClatchie, S. (2012) Sardine biomass is poorly correlated with the Pacific Decadal Oscillation off California. *Geophysical Research Letters* **39**(13).

McClintock, B.T., Johnson, D.S., Hooten, M.B., Ver Hoef, J.M., and Morales, J.M. (2014) When to be discrete: the importance of time formulation in understanding animal movement. *Movement Ecology* **2**, 1-14.

McClintock, B.T., and Michelot, T. (2018) momentuHMM: R package for generalized hidden Markov models of animal movement. *Methods in Ecology and Evolution* **9**(6), 1518-1530.

McClintock, B.T., Langrock, R., Gimenez, O., Cam, E., Borchers, D.L., Glennie, R., and Patterson, T.A. (2020) Uncovering ecological state dynamics with hidden Markov models. *Ecology Letters* **23**(12), 1878-1903.

McClintock, B.T. (2021) Worth the effort? A practical examination of random effects in hidden Markov models for animal telemetry data. *Methods in Ecology and Evolution* **12**(8), 1475-1497.

McConnaughey, R.A., Hiddink, J.G., Jennings, S., Pitcher, C.R., Kaiser, M.J., Suuronen, P., Sciberras, M., Rijnsdorp, A.D., Collie, J.S., Mazor, T., Amoroso, R.O., Parma, A.M., and Hilborn, R. (2020) Choosing best practices for managing impacts of trawl fishing on seabed habitats and biota. *Fish and Fisheries* **21**(2), 319-337.

McEvoy, L., and McEvoy, J. (1992) Multiple spawning in several commercial fish species and its consequences for fisheries management, cultivation and experimentation. *Journal of Fish Biology* **41**, 125-136.

McKellar, A.E., Langrock, R., Walters, J.R., and Kesler, D.C. (2015) Using mixed hidden Markov models to examine behavioral states in a cooperatively breeding bird. *Behavioral Ecology* **26**(1), 148-157.

Meynecke, J.-O., and Richards, R.G. (2013) A full life cycle and spatially explicit individual-based model for the giant mud crab (*Scylla serrata*): a case study from a marine protected area. *ICES Journal of Marine Science* **71**(3), 484-498.

Meynecke, J.O., Lee, S.Y., Grubert, M., Brown, I.W., Montgomery, S., Gribble, N., Johnston, D., and Gillson, J. (2010) Evaluating the environmental drivers of mud crab (*Scylla serrata*) catches in Australia: Final Report FRDC Project 2008/012. Griffith University, Gold Coast, Queensland.

Meynecke, J.O., Grubert, M., Arthur, J.M., Boston, R., and Lee, S.Y. (2012a) The influence of the La Nina-El Nino cycle on giant mud crab (*Scylla serrata*) catches in Northern Australia. *Estuarine, Coastal and Shelf Science* **100**, 93-101.

Meynecke, J.O., Grubert, M., and Gillson, J. (2012b) Giant mud crab (*Scylla serrata*) catches and climate drivers in Australia - a large scale comparison. *Marine and Freshwater Research* **63**(1), 84-94.

- Michelot, T., Langrock, R., and Patterson, T.A. (2016) moveHMM: an R package for the statistical modelling of animal movement data using hidden Markov models. *Methods in Ecology and Evolution* **7**(11), 1308-1315.
- Middleton, J.H., Cox, D., and Tate, P. (1996) The oceanography of the Sydney region. *Marine Pollution Bulletin* **33**(7-12), 124-131.
- Miller, R.J. (1980) Design criteria for crab traps. *ICES Journal of Marine Science* **39**(2), 140-147.
- Monroy, P., Rossi, V., Ser-Giacomi, E., López, C., and Hernández-García, E. (2017) Sensitivity and robustness of larval connectivity diagnostics obtained from Lagrangian Flow Networks. *ICES Journal of Marine Science* **74**(6), 1763-1779.
- Montgomery, S.S. (1990) Movements of juvenile eastern king prawns, *Penaeus plebejus*, and identification of stock along the east-coast of Australia. *Fisheries Research* **9**(3), 189-208.
- Moore, A.B., Delargy, A.J., Cann, R.P., Heney, C., Le Vay, L., Lincoln, H., McCarthy, I.D., and Hold, N. (2022) Spatial and temporal variation of size at maturity in an intensive crustacean fishery with limited management. *Fisheries Research* **255**, 106450.
- Morgan, R., Andreassen, A.H., Åsheim, E.R., Finnøen, M.H., Dresler, G., Brembu, T., Loh, A., Miest, J.J., and Jutfelt, F. (2022) Reduced physiological plasticity in a fish adapted to stable temperatures. *Proceedings of the National Academy of Sciences* **119**(22), e2201919119.
- Muff, S., Nilsen, E.B., O'Hara, R.B., and Nater, C.R. (2022) Rewriting results sections in the language of evidence. *Trends in Ecology and Evolution* **37**(3), 203-210.
- Mullaney, T.J., Gillanders, B.M., Heagney, E.C., and Suthers, I.M. (2014) Entrainment and advection of larval sardine, *Sardinops sagax*, by the East Australian Current and retention in the western Tasman Front. *Fisheries Oceanography* **23**(6), 554-567.
- Myers, R., Rosenberg, A., Mace, P., Barrowman, N., and Restrepo, V. (1994) In search of thresholds for recruitment overfishing. *ICES Journal of Marine Science* **51**(2), 191-205.
- Nathan, R., Spiegel, O., Fortmann-Roe, S., Harel, R., Wikelski, M., and Getz, W.M. (2012) Using tri-axial acceleration data to identify behavioral modes of free-ranging animals: general concepts and tools illustrated for griffon vultures. *Journal of Experimental Biology* **215**(6), 986-996.
- Neuheimer, A.B., and Taggart, C.T. (2007) The growing degree-day and fish size-at-age: The overlooked metric. *Canadian Journal of Fisheries and Aquatic Sciences* **64**(2), 375-385.
- Niella, Y., Flávio, H., Smoothey, A.F., Aerestrup, K., Taylor, M.D., Peddemors, V., and Harcourt, R. (2020) Refined Shortest Paths (RSP): modelling fine scale space use of animals in estuarine areas using passive acoustic telemetry data. *Methods in Ecology and Evolution* **11**, 1733-1742.

Nolan, S.E.F., Johnson, D.D., Hanemseth, R., Suthers, I.M., and Taylor, M.D. (2022) Reproductive biology of female Blue Swimmer Crab in the temperate estuaries of south-eastern Australia. *Marine and Freshwater Research* **73**, 366-376.

Norman-Lopez, A., Pascoe, S., and Hobday, A.J. (2011) Potential economic impacts of climate change on Australian fisheries and the need for adaptive management. *Climate Change Economics* **2**(03), 209-235.

Norrie, C., Dunphy, B., Roughan, M., Weppe, S., and Lundquist, C. (2020) Spill-over from aquaculture may provide a larval subsidy for the restoration of mussel reefs. *Aquaculture Environment Interactions* **12**, 231-249.

North, E.W., Gallego, A., and Petitgas, P. (2009) Manual of recommended practices for modelling physical–biological interactions during fish early life. No. 1017-6195, ICES Cooperative Research Report No. 1017-6195.

NSW Department of Primary Industries (2014) The New South Wales Marine Fish Stocking Fishery Management Strategy. Port Stephens Fisheries Institute, Taylors Beach.

NSW DPIE (2021) Mallabula Point tide gauge. (Manly Hydraulics Laboratory, New South Wales Department of Planning, Industry and Environment)

Nurdiani, R., and Zeng, C. (2007) Effects of temperature and salinity on the survival and development of mud crab, *Scylla serrata* (Forsskål), larvae. *Aquaculture Research* **38**(14), 1529-1538.

Ochwada-Doyle, F., McLeod, J., Barrett, G., Clarke, G., and Gray, C. (2014) 'Assessment of recreational fishing in three recreational fishing havens in New South Wales.' (NSW Department of Primary Industries, Port Stephens)

Oke, P.R., Pilo, G.S., Ridgway, K., Kiss, A., and Rykova, T. (2019a) A search for the Tasman Front. *Journal of Marine Systems* **199**, 103217.

Oke, P.R., Roughan, M., Cetina-Heredia, P., Pilo, G.S., Ridgway, K.R., Rykova, T., Archer, M.R., Coleman, R.C., Kerry, C.G., and Rocha, C. (2019b) Revisiting the circulation of the East Australian Current: Its path, separation, and eddy field. *Progress in Oceanography* **176**, 102139.

Okubo, A. Oceanic diffusion diagrams. In 'Deep Sea Research and Oceanographic Abstracts', 1971, pp. 789-802

Oliver, E.C.J., Donat, M.G., Burrows, M.T., Moore, P.J., Smale, D.A., Alexander, L.V., Benthuisen, J.A., Feng, M., Sen Gupta, A., Hobday, A.J., Holbrook, N.J., Perkins-Kirkpatrick, S.E., Scannell, H.A., Straub, S.C., and Wernberg, T. (2018) Longer and more frequent marine heatwaves over the past century. *Nature Communications* **9**(1), 1324.

- Özgül, A., Lök, A., Ulaş, A., Düzbastılar, F.O., Tanrıkul, T.T., and Pelister, C. (2015) Preliminary study on the use of the Vemco Positioning System to determine fish movements in artificial reef areas: A case study on *Sciaena umbra* Linnaeus, 1758. *Journal of Applied Ichthyology* **31**(S3), 41-47.
- Pankhurst, N.W., and Munday, P.L. (2011) Effects of climate change on fish reproduction and early life history stages. *Marine and Freshwater Research* **62**(9), 1015-1026.
- Parker, L.M., Ross, P.M., O'Connor, W.A., Pörtner, H.O., Scanes, E., and Wright, J.M. (2013) Predicting the response of molluscs to the impact of ocean acidification. *Biology* **2**(2), 651-692.
- Patterson, R.G., Wolanski, E., Groom, R., Critchell, K., Playford, L., Grubert, M., Kennett, R., Tait, H., Udyawer, V., and Lambrechts, J. (2023) Improving certainty in marine ecosystems: A biophysical modelling approach in the remote, data-limited Gulf of Carpentaria. *Estuarine, Coastal and Shelf Science* **283**, 108254.
- Patterson, T.A., Basson, M., Bravington, M.V., and Gunn, J.S. (2009) Classifying movement behaviour in relation to environmental conditions using hidden Markov models. *Journal of Animal Ecology* **78**(6), 1113-1123.
- Patterson, T.A., Parton, A., Langrock, R., Blackwell, P.G., Thomas, L., and King, R. (2017) Statistical modelling of individual animal movement: an overview of key methods and a discussion of practical challenges. *AStA Advances in Statistical Analysis* **101**, 399-438.
- Payne, N.L., Taylor, M.D., Watanabe, Y., and Semmens, J.M. (2014) From physiology to physics: are we recognizing the flexibility of biologging tools? *Journal of Experimental Biology* **217**, 317-322.
- Payne, N.L., Smith, J.A., van der Meulen, D.E., Taylor, M.D., Watanabe, Y.Y., Takahashi, A., Marzullo, T.A., Gray, C.A., Cadiou, G., and Suthers, I.M. (2016) Temperature-dependence of fish performance in the wild: Links with species biogeography and physiological thermal tolerance. *Functional Ecology* **30**, 903-912.
- Pebesma, E.J. (2018) Simple features for R: standardized support for spatial vector data. *R Journal* **10**(1), 439.
- Pecl, G.T., Araújo, M.B., Bell, J.D., Blanchard, J., Bonebrake, T.C., Chen, I.-C., Clark, T.D., Colwell, R.K., Danielsen, F., Evengård, B., Falconi, L., Ferrier, S., Frusher, S., Garcia, R.A., Griffis, R.B., Hobday, A.J., Janion-Scheepers, C., Jarzyna, M.A., Jennings, S., Lenoir, J., Linnetved, H.I., Martin, V.Y., McCormack, P.C., McDonald, J., Mitchell, N.J., Mustonen, T., Pandolfi, J.M., Pettorelli, N., Popova, E., Robinson, S.A., Scheffers, B.R., Shaw, J.D., Sorte, C.J.B., Strugnell, J.M., Sunday, J.M., Tuanmu, M.-N., Vergés, A., Villanueva, C., Wernberg, T., Wapstra, E., and Williams, S.E. (2017) Biodiversity redistribution under climate change: Impacts on ecosystems and human well-being. *Science* **355**(6332), eaai9214.
- Pedersen, E.J., Miller, D.L., Simpson, G.L., and Ross, N. (2019) Hierarchical generalized additive models in ecology: an introduction with mgcv. *PeerJ* **7**, e6876.

Pohle, J., Langrock, R., Van Beest, F.M., and Schmidt, N.M. (2017) Selecting the number of states in hidden Markov models: pragmatic solutions illustrated using animal movement. *Journal of Agricultural, Biological and Environmental Statistics* **22**, 270-293.

Poore, G.C.B. (2004) 'Marine Decapod Crustacea of Southern Australia - A Guide to Identification.' (CSIRO Publishing: Collingwood)

Potter, I.C., Chrystal, P.J., and Loneragan, N.R. (1983) The biology of the blue manna crab *Portunus pelagicus* in an Australian estuary. *Marine Biology* **78**, 75-85.

Power, S., Casey, T., Folland, C., Colman, A., and Mehta, V. (1999) Inter-decadal modulation of the impact of ENSO on Australia. *Climate Dynamics* **15**(5), 319-324.

Power, S., Lengaigne, M., Capotondi, A., Khodri, M., Vialard, J., Jebri, B., Guilyardi, E., McGregor, S., Kug, J.-S., Newman, M., McPhaden, M.J., Meehl, G., Smith, D., Cole, J., Emile-Geay, J., Vimont, D., Wittenberg, A.T., Collins, M., Kim, G.-I., Cai, W., Okumura, Y., Chung, C., Cobb, K.M., Delage, F., Planton, Y.Y., Levine, A., Zhu, F., Sprintall, J., Di Lorenzo, E., Zhang, X., Luo, J.-J., Lin, X., Balmaseda, M., Wang, G., and Henley, B.J. (2021) Decadal climate variability in the tropical Pacific: Characteristics, causes, predictability, and prospects. *Science* **374**(6563), eaay9165.

Prasad, A.M., Iverson, L.R., and Liaw, A. (2006) Newer classification and regression tree techniques: bagging and random forests for ecological prediction. *Ecosystems* **9**, 181-199.

Punt, A.E., Walker, T.I., Taylor, B.L., and Pribac, F. (2000) Standardization of catch and effort data in a spatially-structured shark fishery. *Fisheries Research* **45**(2), 129-145.

Punt, A.E., Butterworth, D.S., de Moor, C.L., De Oliveira, J.A.A., and Haddon, M. (2016) Management strategy evaluation: Best practices. *Fish and Fisheries* **17**(2), 303-334.

Putman, N.F., and Naro-Maciel, E. (2013) Finding the 'lost years' in green turtles: insights from ocean circulation models and genetic analysis. *Proceedings of the Royal Society B: Biological Sciences* **280**(1768), 20131468.

Qasem, L., Cardew, A., Wilson, A., Griffiths, I., Halsey, L.G., Shepard, E.L.C., Gleiss, A.C., and Wilson, R. (2012) Tri-axial dynamic acceleration as a proxy for animal energy expenditure; Should we be summing values or calculating the vector? *PLoS ONE* **7**(2).

R Core Team (2022) R: A language and environment for statistical computing. (R Foundation for Statistical Computing: Vienna, Austria)

Ramirez-Llodra, E. (2002) Fecundity and life-history strategies in marine invertebrates. *Advances in Marine Biology* **43**, 87-170.

- Raoult, V., Gaston, T.F., and Taylor, M.D. (2018) Habitat–fishery linkages in two major south-eastern Australian estuaries show that the C4 saltmarsh plant *Sporobolus virginicus* is a significant contributor to fisheries productivity. *Hydrobiologia* **811**, 221–238.
- Raoult, V., Taylor, M.D., Schmidt, R.K., Cresswell, I.D., Ware, C., and Gaston, T.F. (2022) Valuing the contribution of estuarine habitats to commercial fisheries in a seagrass-dominated estuary. *Estuarine, Coastal and Shelf Science* **274**, 107927.
- Ravi, R., and Manisseri, M.K. (2013) Alterations in size, weight and morphology of the eggs of blue swimmer crab, *Portunus pelagicus* Linnaeus, 1758 (Decapoda, Brachyura, Portunidae) during incubation. *Turkish Journal of Fisheries and Aquatic Sciences* **13**(3).
- Reinfelds, I., Cohen, T., Batten, P., and Brierley, G. (2004) Assessment of downstream trends in channel gradient, total and specific stream power: a GIS approach. *Geomorphology* **60**(3-4), 403-416.
- Roberts, D.G., and Ayre, D.J. (2010) Panmictic population structure in the migratory marine sparid *Acanthopagrus australis* despite its close association with estuaries. *Marine Ecology Progress Series* **412**, 223-230.
- Robertson, W. (1989) Factors affecting catches of the crab *Scylla serrata* (Forskål)(Decapoda: Portunidae) in baited traps: soak time, time of day and accessibility of the bait. *Estuarine, Coastal and Shelf Science* **29**(2), 161-170.
- Robins, J.B., Halliday, I.A., Staunton-Smith, J., Mayer, D.G., and Sellin, M.J. (2005) Freshwater-flow requirements of estuarine fisheries in tropical Australia: A review of the state of knowledge and application of a suggested approach. *Marine and Freshwater Research* **56**(3), 343-360.
- Rogers, L.A., and Dougherty, A.B. (2019) Effects of climate and demography on reproductive phenology of a harvested marine fish population. *Global Change Biology* **25**(2), 708-720.
- Romine, J.G., Perry, R.W., Johnston, S.V., Fitzer, C.W., Pagliughi, S.W., and Blake, A.R. (2014) Identifying when tagged fishes have been consumed by piscivorous predators: application of multivariate mixture models to movement parameters of telemetered fishes. *Animal Biotelemetry* **2**, 1-13.
- Rose, N.L., Yang, H., Turner, S.D., and Simpson, G.L. (2012) An assessment of the mechanisms for the transfer of lead and mercury from atmospherically contaminated organic soils to lake sediments with particular reference to Scotland, UK. *Geochimica et Cosmochimica Acta* **82**, 113-135.
- Rotherham, D., Broadhurst, M.K., Gray, C.A., and Johnson, D.D. (2008) Developing a beam trawl for sampling estuarine fish and crustaceans: assessment of a codend cover and effects of different sizes of mesh in the body and codend. *ICES Journal of Marine Science: Journal du Conseil* **65**(4), 687-696.
- Rotherham, D., Johnson, D.D., Macbeth, W.G., and Gray, C.A. (2013) Escape gaps as a management strategy for reducing bycatch in net-covered traps for the giant mud crab *Scylla serrata*. *North American Journal of Fisheries Management* **33**(2), 307-317.

- Roughan, M., Mace, A.J., Largier, J.L., Morgan, S.G., Fisher, J.L., and Carter, M.L. (2005) Subsurface recirculation and larval retention in the lee of a small headland: a variation on the upwelling shadow theme. *Journal of Geophysical Research: Oceans* **110**, C10027.
- Roughan, M., Macdonald, H.S., Baird, M.E., and Glasby, T.M. (2011) Modelling coastal connectivity in a Western Boundary Current: Seasonal and inter-annual variability. *Deep Sea Research Part II: Topical Studies in Oceanography* **58**(5), 628-644.
- Roughan, M., Cetina-Heredia, P., Ribbat, N., and Suthers, I.M. (2022) Shelf transport pathways adjacent to the East Australian Current reveal sources of productivity for coastal reefs. *Frontiers in Marine Science*.
- Roy, P.S., Williams, R.J., Jones, A.R., Yassini, I., Gibbs, P.J., Coates, B., West, R.J., Scanes, P.R., Hudson, J.P., and Nichol, S. (2001) Structure and function of south-east Australian estuaries. *Estuarine, Coastal and Shelf Science* **53**(3), 351-384.
- Roy, R., Beguin, J., Argillier, C., Tissot, L., Smith, F., Smedbol, S., and De-Oliveira, E. (2014) Testing the VEMCO Positioning System: spatial distribution of the probability of location and the positioning error in a reservoir. *Animal Biotelemetry* **2**(1), 1-7.
- Rub, A.M.W., and Sandford, B.P. (2020) Evidence of a 'dinner bell' effect from acoustic transmitters in adult Chinook salmon. *Marine Ecology Progress Series* **641**, 1-11.
- Ruello, N.V. (1975) Geographical distribution, growth and breeding migration of eastern Australian King Prawn *Penaeus plebejus* Hess. *Australian Journal of Marine and Freshwater Research* **26**(3), 343-354.
- Ruscoe, I.M., Shelley, C.C., and Williams, G.R. (2004) The combined effects of temperature and salinity on growth and survival of juvenile mud crabs (*Scylla serrata* Forskål). *Aquaculture* **238**(1), 239-247.
- Sandery, P., Brassington, G., Colberg, F., Sakov, P., Herzfeld, M., Maes, C., and Tuteja, N. (2019) An ocean reanalysis of the western Coral Sea and Great Barrier Reef. *Ocean Modelling* **144**, 101495.
- Sandwell, D.T., Gille, S., and Smith, W. (2002) Bathymetry from space: Oceanography, geophysics, and climate. Geoscience Professional Services, Bethesda, Maryland.
- Saunders, T., Johnson, D.D., Johnston, D., and Walton, L. (2021) Mud Crabs. In Status of Australian Fish Stocks 2020. (<https://fish.gov.au/report/275-MUD-CRABS-2020#> accessed 6 March 2023: Canberra)
- Savina, E., Krag, L.A., Frandsen, R.P., and Madsen, N. (2017) Effect of fisher's soak tactic on catch pattern in the Danish gillnet plaice fishery. *Fisheries Research* **196**, 56-65.
- Scandol, J., and Kennelly, S. (2002) Using a fishery-independent survey to assess the status of a spanner crab *Ranina ranina* fishery: univariate analyses and biomass modelling. *Crustaceana* **75**(1), 13-39.

Scanes, E., Scanes, P.R., and Ross, P.M. (2020a) Climate change rapidly warms and acidifies Australian estuaries. *Nature communications* **11**(1), 1-11.

Scanes, E., Scanes, P.R., and Ross, P.M. (2020b) NSW estuary temperature, pH and salinity data. (Available at <https://datasets.seed.nsw.gov.au/dataset/nsw-estuary-temperature-ph-and-salinity-data>)

Schaeffer, A., Gramouille, A., Roughan, M., and Mantovanelli, A. (2017) Characterizing frontal eddies along the East Australian Current from HF radar observations. *Journal of Geophysical Research: Oceans* **122**(5), 3964-3980.

Schaeffer, A., and Roughan, M. (2017) Subsurface intensification of marine heatwaves off southeastern Australia: The role of stratification and local winds. *Geophysical Research Letters* **44**(10), 5025-5033.

Schilling, H., Johnson, D.D., Hanemseth, R., Suthers, I.M., and Taylor, M.D. (2023) Long-term drivers of catch variability in south-eastern Australia's largest portunid fishery. *Fisheries Research* **260**, 106582.

Schilling, H.T., Smith, J.A., Stewart, J., Everett, J.D., Hughes, J.M., and Suthers, I.M. (2019) Reduced exploitation is associated with an altered sex ratio and larger length at maturity in southwest Pacific (east Australian) *Pomatomus saltatrix*. *Marine Environmental Research* **147**, 72-79.

Schilling, H.T., Everett, J.D., Smith, J.A., Stewart, J., Hughes, J.M., Roughan, M., Kerry, C., and Suthers, I.M. (2020) Multiple spawning events promote increased larval dispersal of a predatory fish in a western boundary current. *Fisheries Oceanography* **29**(4), 309-323.

Schilling, H.T., Hewitt, D., Malan, N., Taylor, M.D., and Johnson, D.D. (2022a) Cross-jurisdictional larval supply essential for east Australian spanner crab (*Ranina ranina*) fishery. *Marine and Freshwater Research* **73**(11), 1352-1367.

Schilling, H.T., Hinchliffe, C., Gillson, J.P., Miskiewicz, A.G., and Suthers, I.M. (2022b) Coastal winds and larval fish abundance indicate a recruitment mechanism for southeast Australian estuarine fisheries. *Fisheries Oceanography* **31**(1), 40-55.

Sequeira, A.M., Heupel, M., Lea, M.A., Eguíluz, V.M., Duarte, C.M., Meekan, M.G., Thums, M., Calich, H., Carmichael, R., and Costa, D.P. (2019) The importance of sample size in marine megafauna tagging studies. *Ecological Applications* **29**(6), e01947.

Shelford, V.E. (1931) Some concepts of bioecology. *Ecology* **12**(3), 455-467.

Simons, R.D., Siegel, D.A., and Brown, K.S. (2013) Model sensitivity and robustness in the estimation of larval transport: a study of particle tracking parameters. *Journal of Marine Systems* **119**, 19-29.

Slesinger, E., Jensen, O.P., and Saba, G. (2021) Spawning phenology of a rapidly shifting marine fish species throughout its range. *ICES Journal of Marine Science* **78**(3), 1010-1022.

Smith, E.P. (2020) Ending reliance on statistical significance will improve environmental inference and communication. *Estuaries and Coasts* **43**(1), 1-6.

Smith, J.A., Eyre, B.J., Rosentreter, J., and Taylor, M.D. (2019) Modelling estuarine stocking density for crustaceans using net ecosystem metabolism. *Bulletin of Marine Science* **95**(2), 217-238.

Smith, K.D., Hall, N.G., de Lestang, S., and Potter, I.C. (2004) Potential bias in estimates of the size of maturity of crabs derived from trap samples. *ICES Journal of Marine Science* **61**(6), 906-912.

Smith, T.M., Hindell, J.S., Jenkins, G.P., and Connolly, R.M. (2008) Edge effects on fish associated with seagrass and sand patches. *Marine Ecology Progress Series* **359**, 203-213.

Smith, T.M., Hindell, J.S., Jenkins, G.P., Connolly, R.M., and Keough, M.J. (2011) Edge effects in patchy seagrass landscapes: the role of predation in determining fish distribution. *Journal of Experimental Marine Biology and Ecology* **399**(1), 8-16.

Spaet, J.L., Manica, A., Brand, C.P., Gallen, C., and Butcher, P.A. (2020) Environmental conditions are poor predictors of immature white shark *Carcharodon carcharias* occurrences on coastal beaches of eastern Australia. *Marine Ecology Progress Series* **653**, 167-179.

Spencer, D.M., Brown, I.W., Doubell, M.J., McGarvey, R., Lee, S.Y., and Lemckert, C.J. (2019) Bottom currents affect spanner crab catch rates in southern Queensland, Australia. *Marine and Coastal Fisheries* **11**(3), 248-257.

Steele, R.W., and Neuheimer, A.B. (2022) Assessing the ability of the growing degree-day metric to explain variation in size-at-age and duration-to-moult of lobsters and crabs. *Canadian Journal of Fisheries and Aquatic Sciences* **79**(5), 850-860.

Stevens, B.G., Miller, T.J., Lovrich, G., and Thiel, M. (2020) Crab fisheries. In *The Natural History of Crustacea Volume 9: Fisheries and Aquaculture*. (Eds. G Lovrich and M Thiel) pp. 21. (Oxford University Press, New York)

Stocks, J.R., Gray, C.A., and Taylor, M.D. (2014) Testing the effects of near-shore environmental variables on acoustic detections: Implications on telemetry array design and data interpretation. *Marine Technology Society Journal* **48**(1), 28-35.

Stoner, A. (2004) Effects of environmental variables on fish feeding ecology: Implications for the performance of baited fishing gear and stock assessment. *Journal of Fish Biology* **65**(6), 1445-1471.

Su, C.H., Eizenberg, N., Steinle, P., Jakob, D., Fox-Hughes, P., White, C.J., Rennie, S., Franklin, C., Dharssi, I., and Zhu, H. (2019) BARRA v1.0: the Bureau of Meteorology Atmospheric high-resolution Regional Reanalysis for Australia. *Geoscientific Model Development* **12**(5), 2049-2068.

- Sukumaran, K., and Neelakantan, B. (1997) Sex ratio, fecundity and reproductive potential in two marine portunid crabs, *Portunus (Portunus) sanguinolentus* (Herbst) and *Portunus (Portunus) pelagicus* (Linnaeus) along the Karnataka coast. *Indian Journal of Marine Sciences* **26**, 43-48.
- Sulkin, S.D., and Van Heukelem, W.F. (1986) Variability in the length of the megalopal stage and its consequence to dispersal and recruitment in the portunid crab *Callinectes sapidus* Rathbun. *Bulletin of Marine Science* **39**(2), 269-278.
- Sumpton, W., Gades, S., McLennan, M., Campbell, M.D., Tonks, M.L., Good, N., Hagedoorn, W., and Skilleter, G.A. (2003) Fisheries Biology and Assessment of the Blue Swimmer Crab (*Portunus pelagicus*) in Queensland. Queensland Department of Primary Industries, Deception Bay, Report to the Fisheries Research and Development Corporation, Project No. 98/117.
- Suthers, I.M., Young, J.W., Baird, M.E., Roughan, M., Everett, J.D., Brassington, G.B., Byrne, M., Condie, S.A., Hartog, J.R., Hassler, C.S., Hobday, A.J., Holbrook, N.J., Malcolm, H.A., Oke, P.R., Thompson, P.A., and Ridgway, K. (2011) The strengthening East Australian Current, its eddies and biological effects — an introduction and overview. *Deep Sea Research Part II: Topical Studies in Oceanography* **58**(5), 538-546.
- Swadling, D.S., Knott, N.A., Rees, M.J., Pederson, H., Adams, K.R., Taylor, M.D., and Davis, A.R. (2020) Seagrass canopies and the performance of acoustic telemetry: Implications for the interpretation of fish movements. *Animal Biotelemetry* **8**, 8.
- Swiney, K.M., Webb, J.B., Bishop, G.H., and Eckert, G.L. (2010) Temporal and spatial variability of Alaska red king crab fecundity, and accuracy of clutch fullness indices in estimating fecundity. In *Biology and Management of Exploited Crab Populations under Climate Change*. (Eds. GH Kruse, GL Eckert, R Foy, RN Lipcius, B Sainte-Marie, DL Stram and W D.) pp. 265-282. (Alaska Sea Grant, University of Alaska Fairbanks)
- Taylor, M.D., Baker, J., and Suthers, I.M. (2013a) Tidal currents, sampling effort and baited remote underwater video (BRUV) surveys: Are we drawing the right conclusions? *Fisheries Research* **140**, 96-104.
- Taylor, M.D., McPhan, L., van der Meulen, D.E., Gray, C.A., and Payne, N.L. (2013b) Interactive drivers of activity in a free-ranging estuarine predator. *PLoS ONE* **8**(11), e80962.
- Taylor, M.D., van der Meulen, D.E., Ives, M.C., Walsh, C.T., Reinfelds, I.V., and Gray, C.A. (2014) Shock, stress or signal? Implications of freshwater flows for a top-level estuarine predator. *PLoS ONE* **9**(4), e95680.
- Taylor, M.D., and Johnson, D.D. (2016) Preliminary investigation of perfluoroalkyl substances in exploited fishes of two contaminated estuaries. *Marine Pollution Bulletin* **111**, 509-513.
- Taylor, M.D., Babcock, R.C., Simpfendorfer, C.A., and Crook, D.A. (2017a) Where technology meets ecology: Acoustic telemetry in contemporary Australian aquatic research and management. *Marine and Freshwater Research* **68**(8), 1397-1402.

Taylor, M.D., Bowles, K.C., Johnson, D.D., and Moltschaniwskyj, N.A. (2017b) Depuration of perfluoroalkyl substances from the edible tissues of wild-caught invertebrate species. *Science of The Total Environment* **581**, 258-267.

Taylor, M.D., Chick, R.C., Lorenzen, K., Agnalt, A.L., Leber, K.M., Blankenship, H.L., Vander Haegen, G., and Loneragan, N.R. (2017c) Fisheries enhancement and restoration in a changing world. *Fisheries Research* **186**, 407–412.

Taylor, M.D., Fry, B., Becker, A., and Moltschaniwskyj, N.A. (2017d) Recruitment and connectivity influence the role of seagrass as a penaeid nursery habitat in a wave dominated estuary. *Science of The Total Environment* **584–585**, 622–630.

Taylor, M.D., Payne, N.L., Becker, A., and Lowry, M.B. (2017e) Feels like home: Homing of mature large-bodied fish following translocation from a power-station canal. *ICES Journal of Marine Science / Journal du Conseil* **74**(1), 301-310.

Taylor, M.D., Becker, A., Moltschaniwskyj, N.A., and Gaston, T. (2018a) Direct and indirect interactions between lower estuarine mangrove and saltmarsh habitats and a commercially important penaeid shrimp. *Estuaries and Coasts* **41**, 815-826.

Taylor, M.D., Beyer-Robson, J., Johnson, D.D., Knott, N.A., and Bowles, K.C. (2018b) Bioaccumulation of perfluoroalkyl substances in exploited fish and crustaceans: Spatial trends across two estuarine systems. *Marine Pollution Bulletin* **131**, 303-313.

Taylor, M.D. (2019) Survey design for quantifying perfluoroalkyl acid concentrations in fish, prawns and crabs to assess human health risks. *Science of The Total Environment* **652**, 59-65.

Taylor, M.D., and Johnson, D.D. (2021) Connectivity between a spatial management network and a multi-jurisdictional ocean trawl fishery. *Ocean & Coastal Management* **210**, 105691, <https://doi.org/10.1016/j.ocecoaman.2021.105691>.

Taylor, M.D., Johnson, D.D., Nilsson, S., Lin, C.-Y., Bräunig, J., Mueller, J.F., and Bowles, K.C. (2021) Trial of a novel experimental design to test depuration of PFASs from the edible tissues of Giant Mud Crab following exposure under natural conditions in the wild. *Science of the Total Environment* **758**, 143650.

Taylor, M.D., and Suthers, I.M. (2021) The socio-ecological system of urban fisheries in estuaries. *Estuaries and Coasts*, <https://doi.org/10.1007/s12237-021-00916-3>.

Thorsen, A., and Kjesbu, O. (2001) A rapid method for estimation of oocyte size and potential fecundity in Atlantic cod using a computer-aided particle analysis system. *Journal of Sea Research* **46**(3-4), 295-308.

Tilburg, C.E., Kernehan, C.D., Andon, A., and Epifanio, C.E. (2008) Modeling estuarine ingress of blue crab megalopae: Effects of temporal patterns in larval release. *Journal of Marine Research* **66**(3), 391-412.

- Tilburg, C.E., Dittel, A.I., and Epifanio, C.E. (2009) High concentrations of blue crab (*Callinectes sapidus*) larvae along the offshore edge of a coastal current: effects of convergent circulation. *Fisheries Oceanography* **18**(3), 135-146.
- Torrado, H., Mourre, B., Raventos, N., Carreras, C., Tintoré, J., Pascual, M., and Macpherson, E. (2021) Impact of individual early life traits in larval dispersal: A multispecies approach using backtracking models. *Progress in Oceanography* **192**, 102518.
- Towner, A.V., Leos-Barajas, V., Langrock, R., Schick, R.S., Smale, M.J., Kaschke, T., Jewell, O.J., and Papastamatiou, Y.P. (2016) Sex-specific and individual preferences for hunting strategies in white sharks. *Functional Ecology* **30**(8), 1397-1407.
- Tropea, C., Stumpf, L., and López Greco, L.S. (2015) Effect of temperature on biochemical composition, growth and reproduction of the ornamental red cherry shrimp *Neocaridina heteropoda* heteropoda (Decapoda, Caridea). *PLoS One* **10**(3), e0119468.
- Turner, H.V., Wolcott, D.L., Wolcott, T.G., and Hines, A.H. (2003) Post-mating behavior, intramolt growth, and onset of migration to Chesapeake Bay spawning grounds by adult female blue crabs, *Callinectes sapidus* Rathbun. *Journal of Experimental Marine Biology and Ecology* **295**(1), 107-130.
- Van Rossum, G., and Drake, F.L. (2009) Python 3 reference manual. (CreateSpace)
- Van Sebille, E., Griffies, S.M., Abernathey, R., Adams, T.P., Berloff, P., Biastoch, A., Blanke, B., Chassignet, E.P., Cheng, Y., and Cotter, C.J. (2018) Lagrangian ocean analysis: Fundamentals and practices. *Ocean Modelling* **121**, 49-75.
- Vergés, A., Steinberg, P.D., Hay, M.E., Poore, A.G., Campbell, A.H., Ballesteros, E., Heck Jr, K.L., Booth, D.J., Coleman, M.A., and Feary, D.A. (2014) The tropicalization of temperate marine ecosystems: climate-mediated changes in herbivory and community phase shifts. *Proceedings of the Royal Society B: Biological Sciences* **281**(1789), 20140846.
- Vergeynst, J., Vanwyck, T., Baeyens, R., De Mulder, T., Nopens, I., Mouton, A., and Pauwels, I. (2020) Acoustic positioning in a reflective environment: going beyond point-by-point algorithms. *Animal Biotelemetry* **8**(1), 1-17.
- Wall, D., Paterson, B., and Mohan, R. (2009) Behaviour of juvenile mud crabs *Scylla serrata* in aquaculture: response to odours of moulting or injured crabs. *Applied Animal Behaviour Science* **121**(1), 63-73.
- Walsh, C.T., Reinfelds, I.V., West, R.J., Gray, C.A., and van der Meulen, D.E. (2012) Distribution and movement of catadromous fish: design and implementation of a freshwater-estuarine acoustic telemetry array. *American Fisheries Society Symposium* **76**, 251-264.

Walters, C.J. (2007) Is adaptive management helping to solve fisheries problems? *AMBIO: A Journal of the Human Environment* **36**(4), 304-307.

Wang, W., Wu, X., Liu, Z., Zheng, H., and Cheng, Y. (2014) Insights into hepatopancreatic functions for nutrition metabolism and ovarian development in the crab *Portunus trituberculatus*: gene discovery in the comparative transcriptome of different hepatopancreas stages. *PloS one* **9**(1), e84921.

Wassenberg, T.J., and Hill, B.J. (1994) Laboratory study of the effect of light on the emergence behavior of 8 species of commercially important adult penaeid prawns. *Australian Journal of Marine and Freshwater Research* **45**(1), 43-50.

Webley, J.A., Connolly, R.M., and Young, R.A. (2009) Habitat selectivity of megalopae and juvenile mud crabs (*Scylla serrata*): implications for recruitment mechanism. *Marine Biology* **156**(5), 891.

Webley, J.A.C., and Connolly, R.M. (2007) Vertical movement of mud crab megalopae (*Scylla serrata*) in response to light: Doing it differently down under. *Journal of Experimental Marine Biology and Ecology* **341**(2), 196-203.

Webley, J.A.C. (2008) The ecology of Mud Crab (*Scylla serrata*): Their colonisation of estuaries and role as scavengers in ecosystem processes. PhD dissertation, Griffith University,

Wickham, H., Averick, M., Bryan, J., Chang, W., McGowan, L.D.A., François, R., Grolemund, G., Hayes, A., Henry, L., and Hester, J. (2019) Welcome to the Tidyverse. *Journal of Open Source Software* **4**(43), 1686.

Wijeratne, S., Pattiaratchi, C., and Proctor, R. (2018) Estimates of surface and subsurface boundary current transport around Australia. *Journal of Geophysical Research: Oceans* **123**(5), 3444-3466.

Williams, M.J., and Hill, B.J. (1982) Factors influencing pot catches and population estimates of the portunid crab *Scylla serrata*. *Marine Biology* **71**(2), 187-192.

Wilson, R.P., White, C.R., Quintana, F., Halsey, L.G., Liebsch, N., Martin, G.R., and Butler, P.J. (2006) Moving towards acceleration for estimates of activity-specific metabolic rate in free-living animals: the case of the cormorant. *Journal of Animal Ecology* **75**(5), 1081-1090.

Winger, P.D., and Walsh, P.J. (2011) Selectivity, efficiency, and underwater observations of modified trap designs for the snow crab (*Chionoecetes opilio*) fishery in Newfoundland and Labrador. *Fisheries Research* **109**(1), 107-113.

Witthames, P., and Walker, M.G. (1987) An automated method for counting and sizing fish eggs. *Journal of Fish Biology* **30**(3), 225-235.

Wood, S. (2011) Fast stable restricted maximum likelihood and marginal likelihood estimation of semiparametric generalised linear models. *Journal of the Royal Statistical Society (B)* **73**(1), 3-36.

Wood, S.N. (2003) Thin plate regression splines. *Journal of the Royal Statistical Society: Series B (Statistical Methodology)* **65**(1), 95-114.

Wood, S.N., and Fasiolo, M. (2017) A generalized Fellner-Schall method for smoothing parameter optimization with application to Tweedie location, scale and shape models. *Biometrics* **73**(4), 1071-1081.

Wu, L., Cai, W., Zhang, L., Nakamura, H., Timmermann, A., Joyce, T., McPhaden, M.J., Alexander, M., Qiu, B., Visbeck, M., Chang, P., and Giese, B. (2012) Enhanced warming over the global subtropical western boundary currents. *Nature Climate Change* **2**(3), 161-166.

Xiao, Y., and Kumar, M. (2004) Sex ratio, and probability of sexual maturity of females at size, of the blue swimmer crab, *Portunus pelagicus* Linnaeus, off southern Australia. *Fisheries Research* **68**(1), 271-282.

Yanagi, T., Tsukamoto, H., Igawa, S., and Shiota, K. (1995) Recruitment strategy of swimming crab, *Portunus trituberculatus*, in Hiuchi-Nada, Japan. *Fisheries Oceanography* **4**(3), 217-229.

Zhou, S., and Shirley, T.C. (1997) Performance of two red king crab pot designs. *Canadian Journal of Fisheries and Aquatic Sciences* **54**(8), 1858-1864.

Ziegler, P., Frusher, S., and Johnson, C. (2003) Space-time variation in catchability of southern rock lobster *Jasus edwardsii* in Tasmania explained by environmental, physiological and density-dependent processes. *Fisheries Research* **61**(1-3), 107-123.

Zucchini, W., MacDonald, I.L., and Langrock, R. (2017) 'Hidden Markov models for time series: an introduction using R.' (CRC press)